



UNIL | Université de Lausanne

Unicentre

CH-1015 Lausanne

<http://serval.unil.ch>

Year : 2013

Dibenzofuran degradation by *Sphingomonas wittichii* RW1 under environmental stresses

Coronado Martinez Edith Aimée

Coronado Martinez Edith Aimée, 2013, Dibenzofuran degradation by *Sphingomonas wittichii* RW1 under environmental stresses

Originally published at : Thesis, University of Lausanne

Posted at the University of Lausanne Open Archive.
<http://serval.unil.ch>

Droits d'auteur

L'Université de Lausanne attire expressément l'attention des utilisateurs sur le fait que tous les documents publiés dans l'Archive SERVAL sont protégés par le droit d'auteur, conformément à la loi fédérale sur le droit d'auteur et les droits voisins (LDA). A ce titre, il est indispensable d'obtenir le consentement préalable de l'auteur et/ou de l'éditeur avant toute utilisation d'une oeuvre ou d'une partie d'une oeuvre ne relevant pas d'une utilisation à des fins personnelles au sens de la LDA (art. 19, al. 1 lettre a). A défaut, tout contrevenant s'expose aux sanctions prévues par cette loi. Nous déclinons toute responsabilité en la matière.

Copyright

The University of Lausanne expressly draws the attention of users to the fact that all documents published in the SERVAL Archive are protected by copyright in accordance with federal law on copyright and similar rights (LDA). Accordingly it is indispensable to obtain prior consent from the author and/or publisher before any use of a work or part of a work for purposes other than



UNIL | Université de Lausanne

Faculté de biologie
et de médecine

Département de Microbiologie Fondamentale

Dibenzofuran degradation by *Sphingomonas wittichii* RW1 under environmental stresses

Thèse de Doctorat ès Sciences de la Vie (PhD)

Presente à la Faculté de Biologie et de Médecine
de l'Université de Lausanne par

Edith Aimée Coronado Martínez

Master en Biotechnologie diplômée par
l'Université National Autonome de Mexique

Prof. Alexandre Roulin, Président

Prof. Jan Roelof van der Meer, Directeur de thèse

Prof. Juan Ramos, Expert

Prof. Dirk Springael, Expert



UNIL | Université de Lausanne

Faculté de biologie
et de médecine

Ecole Doctorale

Doctorat ès sciences de la vie

Imprimatur

Vu le rapport présenté par le jury d'examen, composé de

<i>Président</i>	Monsieur Prof. Alexandre Roulin
<i>Directeur de thèse</i>	Monsieur Prof. Jan Roelof Van der Meer
<i>Experts</i>	Monsieur Prof. Dirk Springael
	Monsieur Prof. Juan L. Ramos

le Conseil de Faculté autorise l'impression de la thèse de

Madame Edith Coronado Martinez

Master en biotechnologie de l'Université Nationale Autonome du Mexique

intitulée

**Dibenzofuran degradation by *Sphingomonas wittichii* RW1
under environmental stresses**

Lausanne, le 15 février 2013

pour Le Doyen
de la Faculté de Biologie et de Médecine


Prof. Alexandre Roulin

TABLE OF CONTENTS

SUMMARY	vii
RÉSUMÉ	xi
GOALS	xv
OUTLINE.....	xvii
CHAPTER 1.....	1
General Introduction	
<i>Sphingomonas wittichii</i> RW1.....	2
DBF degradation by <i>S. wittichii</i> RW1.....	3
Bioremediation.....	6
Water Stress.....	8
References.....	11
CHAPTER 2.....	19
Genome-Wide Analysis of Salicylate and Dibenzofuran Metabolism in	
<i>Sphingomonas wittichii</i> RW1	
Introduction.....	21
Materials and methods.....	24
Results.....	29
Discussion.....	43
References.....	49
Supplementary information.....	55
CHAPTER 3.....	93
Development of Genetic Tools for Manipulations in <i>Sphingomonas wittichii</i> RW1	
Introduction.....	94
Materials and methods.....	96
Results.....	105
Discussion.....	115
References.....	118
Supplementary information.....	122

CHAPTER 4.....	123
Fluorescently tagged <i>Sphingomonas wittichii</i> RW1 for the detection of dibenzofuran in liquid cultures and soil	
Introduction.....	125
Materials and methods.....	128
Results.....	137
Discussion.....	147
References.....	152
Supplementary information.....	158
CHAPTER 5.....	161
Identification of water stress promoters in <i>Sphingomonas wittichii</i> RW1	
Introduction.....	163
Materials and methods.....	165
Results.....	175
Discussion.....	187
References.....	196
CHAPTER 6.....	201
General discussion	
Genetic manipulation of <i>S. wittichii</i> RW1.....	201
<i>S.wittichii</i> RW1 transposon mutant screening.....	202
Degradation and monitoring of DBF by RW1-based bioreporters.....	203
References.....	205
CURRICULUM VITAE.....	207
LIST OF PUBLICATIONS.....	221

SUMMARY

Sphingomonas wittichii is a gram-negative Alpha-proteobacterium, capable of degrading xenobiotic compounds such as dibenzofuran (DBF), dibenzo-*p*-dioxin, carbazole, 2-hydroxybiphenyl or nitro diphenyl ether herbicides. The metabolism of strain RW1 has been the subject of previous studies and a number of genes involved in DBF degradation have been characterized. It is known that RW1 possesses a unique initial DBF dioxygenase (encoded by the *dxnA1* gene) that catalyzes the first step in the degradation pathway. None of the organisms known to be able to degrade DBF have a similar dioxygenase, the closest match being the DBF dioxygenase from *Rhodococcus sp.* with an overall amino acid similarity of 45%. Genes participating in the conversion of the metabolite salicylate via the *ortho*-cleavage pathway to TCA cycle intermediates were identified as well. Apart from this scarce information, however, there is a lack of global knowledge on the genes that are involved in DBF degradation by strain RW1 and the influence of environmental stresses on DBF-dependent global gene expression. A global analysis is necessary, because it may help to better understand the behaviour of the strain under field conditions and suggest improvements for the current bioaugmentation practice.

Chapter 2 describes the results of whole-genome analysis to characterize the genes involved in DBF degradation by RW1. Micro-array analysis allowed us to detect differences in gene transcription when strain RW1 was exposed to DBF. This was complemented by ultra-high throughput sequencing of mutants no longer capable of growing on salicylate and DBF. Some of the genes of the *ortho*-cleavage pathway were induced 2 to 4 times in the presence of DBF, as well as the initial DBF dioxygenase. However two gene clusters, named 4925 and 5102 were induced up to 19 times in response to DBF induction. The cluster 4925

is putatively participating in a *meta*-cleavage pathway while the cluster 5102 might be part of a gentisate pathway. The three pathways, *ortho*-cleavage, *meta*-cleavage and gentisate pathway seem to be active in parallel when strain RW1 is exposed to DBF, presenting evidence for a redundancy of genes for DBF degradation in the genome of RW1.

Chapter 3 focuses on exploiting genetic tools to construct bioreporters representative for DBF degradation in RW1. A set of basic tools for genetic manipulation in *Sphingomonas wittichii* RW1 was tested and optimized. Both plasmids and mini-transposons were evaluated for their ability to be maintained in RW1 with or without antibiotic selection pressure, and for their ability to lead to fluorescent protein expression in strain RW1 from a constitutive promoter. Putative promoter regions of three of the previously found DBF-induced genes (Swit_4925, Swit_5102 and Swit_4897-*dxnA1*) were then used to construct *egfp*-bioreporters in RW1.

Chapter 4 describes the use of the constructed RW1-based bioreporter strains for examining the expression of the DBF degradation pathway genes under microcosm conditions. The bioreporter strains were first exposed to different carbon sources in liquid culture to calibrate the *egfp* induction. Contrary to our expectations from micro-array analysis only the construct with the promoter from gene cluster 4925 responded to DBF, whereas the other two constructs did not show specific induction with DBF. The response from the bioreporters was subsequently tested for sensitivity to water stress, given that this could have an important impact in soils. Exposure to liquid cultures with decreasing water potential, achieved by NaCl or PEG addition to the growth media, showed that eGFP expression in RW1 from the promoter regions 4925 and 5102 was not directly influenced by water stress, but only through an overall reduction in growth rate. In contrast, expression of eGFP from the

dxnA1 or an *uspA* promoter was also directly dependent on the extent of water stress. The RW1 with the 4925 construct was subsequently used in soil microcosms to evaluate DBF bioavailability to the cells in presence or absence of native microbiota or other contaminated material. We found that RW1 could grow on DBF added to soil, but bioreporter expression suggested that competition with native microbiota for DBF intermediates may limit its ability to proliferate to a maximum.

Chapter 5 describes the results from the experiments carried out to more specifically detect genes of RW1 that might be implicated in water stress resistance. Hereto we created transposon mutagenesis libraries in RW1, either with a classical mini-Tn5 or with a variant that would express *egfp* when the transposon would insert in a gene induced under water stress. Classical mutant libraries were screened by replica plating under high and low water stress conditions (achieved by adding NaCl to the agar medium). In addition, we screened for smaller microcolonies formed by mutants in agarose beads that could be analyzed with flow cytometry. A number of mutants impaired to grow on NaCl-supplemented media were recovered and the transposon insertion sites sequenced. In a second procedure we screened by flow cytometry for mutants with a higher eGFP production after exposure to growth medium with higher NaCl concentrations. Mutants from both libraries rarely overlapped. Discovered gene functions of the transposon insertions pointed to compatible solute synthesis (glutamate and proline), cell membrane synthesis and modification of cell membrane composition.

The results obtained in the present study give us a more complete picture of the mechanisms of DBF degradation by *S. wittichii* RW1, how it reacts to different DBF

availability and how the DBF catabolic activity may be affected by the conditions found in contaminated environments.

RÉSUMÉ

Sphingomonas wittichii est une alpha-protéobactérie gram-négative, capable de dégrader des composés xénobiotiques tels que le dibenzofurane (DBF), la dibenzo-*p*-dioxine, le carbazole, le 2-hydroxybiphényle ou les herbicides dérivés du nitro-diphényléther. Le métabolisme de la souche RW1 a fait l'objet d'études antérieures et un certain nombre de gènes impliqués dans la dégradation du DBF ont été caractérisés. Il est connu que RW1 possède une unique dioxygénase DBF initiale (codée par le gène *dxnA1*) qui catalyse la première étape de la voie de dégradation. Aucun des organismes connus pour être capables de dégrader le DBF n'a de dioxygénase similaire. L'enzyme la plus proche étant la DBF dioxygénase de *Rhodococcus sp.* avec 45% d'acides aminés conservés. Les gènes qui participent à la transformation du salicylate en métabolites intermédiaires du cycle de Krebs par la voie *ortho*-cleavage ont aussi été identifiés. Outre ces informations lacunaires, il y a un manque de connaissances sur l'ensemble des gènes impliqués dans la dégradation du DBF par la souche RW1 ainsi que l'effet des stress environnementaux sur l'expression génétique globale, en présence du DBF. Une analyse globale est nécessaire, car elle peut aider à mieux comprendre le comportement de la souche dans les conditions de terrain et de proposer des améliorations pour l'utilisation de la bio-augmentation comme technique de bio-remédiation.

Le chapitre 2 décrit les résultats de l'analyse du génome pour caractériser les gènes impliqués dans la dégradation du DBF par RW1. Une analyse de micro-arrays nous a permis de détecter des différences dans la transcription des gènes lorsque la souche RW1 a été exposée au DBF. L'analyse a été complétée par le criblage à ultra-haut débit de mutants qui n'étaient plus capables de croître avec le salicylate ou le DBF comme seule source de carbone. Certains des gènes de la voie *ortho*-cleavage, dont la DBF dioxygénase initiale, ont

été induits 2 à 4 fois, en présence du DBF. Cependant, deux groupes de gènes, nommés 4925 et 5102 ont été induits jusqu'à 19 fois en réponse au DBF. Le cluster 4925 participe probablement dans une voie de *meta*-cleavage tandis que le cluster 5102 pourrait faire partie d'une voie du gentisate. Les trois voies, *ortho*-cleavage, *meta*-cleavage et la voie du gentisate semblent être activées en parallèle lorsque la souche RW1 est exposée au DBF, ce qui représente une redondance de voies pour la dégradation du DBF dans le génome de RW1.

Le chapitre 3 se concentre sur l'exploitation des outils génétiques pour la construction de biorapporteurs de la dégradation du DBF par RW1. Un ensemble d'outils de base pour la manipulation génétique dans *Sphingomonas wittichii* RW1 a été testé et optimisé. Deux plasmides et mini-transposons ont été évalués pour leur capacité à être maintenu dans RW1 avec ou sans pression de sélection par des antibiotiques, et pour leur capacité à exprimer la protéine fluorescente verte (eGFP) dans la souche RW1. Les trois promoteurs des gènes Swit_4925, Swit_5102 et Swit_4897 (*dxnA1*), induits en réponse au DBF, ont ensuite été utilisés pour construire des biorapporteurs dans RW1.

Le chapitre 4 décrit l'utilisation des souches biorapportrices construites pour l'analyse de l'expression des gènes de la voie de dégradation du DBF dans des microcosmes avec différents types de sols. Les souches biorapportrices ont d'abord été exposées à différentes sources de carbone en cultures liquides afin de calibrer l'induction de la eGFP. La construction avec le promoteur du gène 4925 a permis une réponse au DBF. Mais contrairement à nos attentes, basées sur les résultats de l'analyse des micro-arrays, les deux autres constructions n'ont pas montré d'induction spécifique au DBF. La réponse des biorapporteurs a ensuite été testée pour la sensibilité au stress hydrique, étant donné que cela pourrait avoir un impact important dans les microcosmes. La diminution du potentiel

hydrique en culture liquide est obtenue par addition de NaCl ou de PEG au milieu de croissance. Nous avons montré que l'expression de la eGFP contrôlée par les promoteurs 4925 et 5102 n'était pas directement influencée par le stress hydrique, mais seulement par une réduction globale des taux de croissance. En revanche, l'expression de la eGFP dépendante des promoteurs *dxnA1* et *uspA* était aussi directement dépendante de l'ampleur du stress hydrique. La souche avec la construction 4925 a été utilisée par la suite dans des microcosmes avec différents types de sols pour évaluer la biodisponibilité du DBF en présence ou absence des microbes indigènes et d'autres composés contaminants. Nous avons constaté que RW1 pouvait se développer si le DBF a été ajouté au sol, mais l'expression de la eGFP par le biorapporteur suggère que la compétition avec la microbiota indigène pour les métabolites intermédiaires du DBF peut limiter sa capacité à proliférer de manière optimale.

Le chapitre 5 décrit les résultats des expériences réalisées afin de détecter spécifiquement les gènes de RW1 qui pourraient être impliqués dans la résistance au stress hydrique. Ici on a créé des bibliothèques de mutants de RW1 par transposon, soit avec un mini-Tn5 classique ou avec une variante qui exprime la eGFP lorsque le transposon s'insère dans un gène induit par le stress hydrique. Les bibliothèques de mutants ont été criblées par la méthode classique de repiquage sur boîtes, dans des conditions de stress hydrique élevé (obtenu par l'addition de NaCl dans les boîtes). En outre, nous avons criblé des micro-colonies dans des billes d'agarose qui ont pu être analysées par cytométrie de flux. Un certain nombre de mutants déficients à croître sur des milieux supplémentés avec du NaCl ont été isolés et les sites d'insertion du transposon séquencés. Dans une deuxième procédure nous avons criblé par cytométrie de flux des mutants avec une production de eGFP supérieure, après exposition à un milieu de croissance avec une concentration élevée de NaCl. Les mutants obtenus dans les deux bibliothèques n'étaient pas similaires. Les fonctions des gènes

où se trouvent les insertions de transposons sont impliqués dans la synthèse de solutés compatibles (glutamate et de la proline), dans la synthèse de la membrane cellulaire et dans la modification de la composition de la membrane cellulaire.

Les résultats obtenus dans la présente étude nous donnent une image plus complète des mécanismes de dégradation du DBF par *S. wittichii* RW1, comment cette souche réagit à la disponibilité du DBF et comment l'activité catabolique peut être affectée par les conditions rencontrées dans des environnements contaminés.

GOALS

The main objectives of the work presented here were to:

1. Develop genetic systems for introducing and manipulating recombinant DNA in *Sphingomonas wittichii* RW1, and for creating gene knockouts.
2. Determine the genes of strain RW1 involved in dibenzofuran degradation by genome-wide microarray and mutant analysis.
3. Produce reporter gene constructs based on RW1 responding to the presence of dibenzofuran and /or salicylate.
4. Monitor the influence of water stress on the performance of bioreporter constructs in strain RW1.
5. Screen for genes involved in resistance of RW1 to NaCl-induced stress.

OUTLINE

Chapter 1. General Introduction

This chapter describes the existing information on strain *Sphingomonas wittichii* RW1 and degradation of dibenzofuran (DBF) as far as enzymes and genes concerned. It also covers the general concepts of bioremediation and bioaugmentation, and the problems encountered when trying to implement it in the field. The framework of our study is then to improve our knowledge of DBF catabolism by *Sphingomonas wittichii* RW1 and to understand how this degradation capability can be affected by the conditions found in the environment.

Chapter 2. Genome-wide Analysis of Salicylate and Dibenzofuran Metabolism in *Sphingomonas wittichii* RW1

A description of the genes being differentially regulated in the presence of dibenzofuran and salicylate compared to phenylalanine is presented here. A genome-wide transcriptome analysis was used to detect differences in gene transcription under different growth conditions. This was complemented by ultra-high throughput sequencing of mutants no longer capable of growing on salicylate and dibenzofuran.

Chapter 3. Development of Genetic Tools for Manipulations in *Sphingomonas wittichii* RW1

The basic tools developed to perform genetic manipulation in *Sphingomonas wittichii* RW1 are described in this chapter. We optimized conditions for electrotransformation, conjugation and selection. A set of plasmid and transposons constructed were evaluated for their ability to be maintained and to express fluorescent protein in strain RW1 in the absence

and presence of antibiotic selection. The difference in transformation efficiency depending of the host used for plasmid replication is also explored. The capacity for transformation with linear DNA was investigated and the problems in finding consistent homologous recombination are discussed.

Chapter 4. Fluorescently Tagged *Sphingomonas wittichii* for the Detection of Dibenzofuran in Liquid Cultures and Soil

Using the transcriptome generated results, three genes were targeted for the construction of bioreporters for the detection of DBF. The RW1-based bioreporter strains were exposed to different carbon sources either in liquid culture or soil microcosms and the *egfp* induction was measured. One of the bioreporters reacted well to the presence of dibenzofuran in soil. Interestingly, the reporter signal in cells was lower in soils amended with dibenzofuran and PAH-contaminated material than in soils with dibenzofuran only. This suggested that indigenous bacteria present in the PAH-contaminated material remove part of the dibenzofuran metabolites produced by RW1, to which the reporter is reacting.

Chapter 5. Identification of Water Stress Promoters in *Sphingomonas wittichii* RW1

This chapter includes a screening of genes involved in water stress resistance by *Sphingomonas wittichii* RW1 using a transposon mutant library creation and selection under high NaCl conditions. NaCl-supplemented media was used to mimic the solute stress that the bacteria experience in the environment. Some clones were detected that were impaired to grow in NaCl-supplemented media as well as clones with a higher eGFP production in the presence of higher amount of NaCl compared to the control. The gene functions give us an indication of the mechanisms used by strain RW1 to cope with NaCl-induced stress.

CHAPTER 1

General Introduction

The viability of microorganisms introduced to polluted sites is usually lower than results from laboratory experiments suggest. As causes for this occurrence, some authors propose a low availability of carbon substrate, lack of nutrients, water stress, unfavorable environmental conditions (e.g., pH, toxic metals), or predation. However, there is a general lack of knowledge on how environmental conditions influence activity of introduced bacteria. *Sphingomonas wittichii* RW1 has the ability to degrade different polycyclic aromatic hydrocarbons and therefore, represents an interesting case for exploitation of its catabolic activities for the purpose of bioremediation. Several enzymes involved in degradation of dibenzofuran (DBF) have previously been characterized, but the complexity of the DBF pathway and the interplay of regulation of DBF degradation with environmental factors are largely unknown. The main goals of the underlying thesis work were thus to characterize the global regulation of the DBF degradation pathway, to identify key promoters representative for DBF degradation that could be used to develop bioreporters, and finally, to use such bioreporter strains to uncover the effects of environmental conditions on catabolic activity of strain RW1.

***Sphingomonas wittichii* RW1**

Sphingomonas wittichii RW1 (Figure 1A) is a gram negative α -proteobacterium, isolated from the Elbe River near Hamburg (Germany) for its ability to degrade dibenzofuran (DBF), dibenzo-*p*-dioxin (DBD) and chlorine substituted derivatives (Wittich *et al.*, 1992). DBF and DBD (Figure 1B and 1C) are poorly water soluble polycyclic aromatic hydrocarbons (PAH) that are formed as byproducts of coal tar industrial processes, during incineration, and in paper pulp bleaching. DBF, DBD and related compounds with chlorine substitutions are widely present at low concentrations in the environment and the food chain (Bowes *et al.*, 1973; Buser *et al.*, 1985; Beck *et al.*, 1994; Johansen *et al.*, 1996). Detrimental effects of exposure of fishes (Zitko *et al.*, 1973), rats (Yoshihara *et al.*, 1981), primates (McNulty, 1985), humans (Pluim *et al.*, 1993; Beck *et al.*, 1994; Soong and Ling, 1997) to DBF and DBD have been reported.

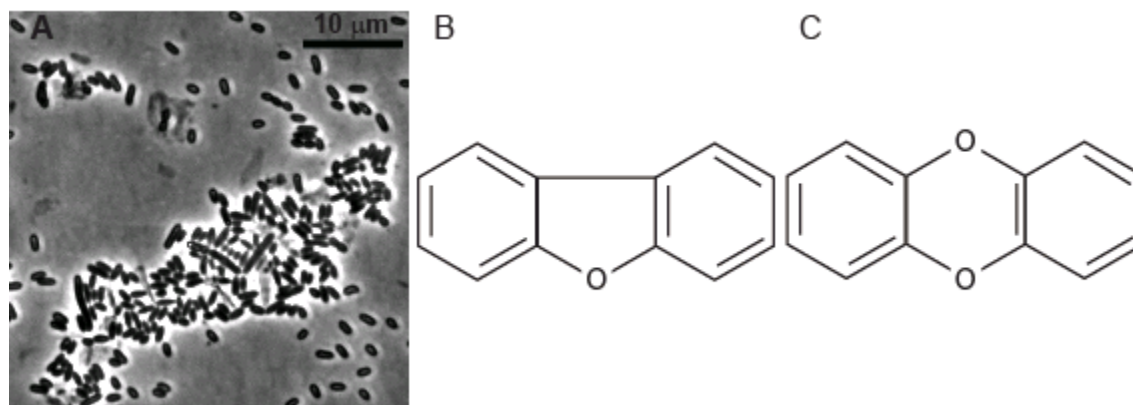


Figure 1. Phase contrast microscope image of *Sphingomonas wittichii* RW1 using a 1000x magnification (A). Structure of Dibenzofuran (B) and Dibenzo-*p*-dioxin (C).

A number of bacteria can use DBF and DBD as sole carbon and energy sources, including *Sphingomonas wittichii* RW1, *Staphylococcus auriculans* (Monna *et al.*, 1993),

Nocardioides aromaticivorans (Kubota *et al.*, 2005), *Rhodococcus sp.* HA01 (Aly *et al.*, 2008), *Pseudomonas putida* B6-2 (Li *et al.*, 2009), *Sphingomonas yanoikuyae* B1 (Cerniglia *et al.*, 1979), *Sphingomonas sp.* HH69 (Fortnagel *et al.*, 1990), *Sphingomonas sp.* XLDN2-5 (Gai *et al.*, 2007) and *Sphingomonas sp.* RW16 (Wittich *et al.*, 1999).

DBF degradation by *S. wittichii* RW1

Since the isolation of *Sphingomonas wittichii* RW1, several authors have explored the DBF and DBD degradation pathway and some of the enzymes involved have been purified and characterized. The genome of RW1 is fully sequenced (Miller *et al.*, 2010) and consists of one chromosome (5382 kb) and two megaplasmids, pSWIT01 (310 kb) and pSWIT02 (222 kb). The larger mega plasmid (pSWIT01) has been reported to be similar to pNL1 from *Novosphingobium aromaticivorans*, specifically in a 17 kb region coding for reverse transcriptase and a type4 pillus (Miller *et al.*, 2010), whereas the smaller (pSWIT02) contains genes implicated in DBF/DBD degradation (Bunz and Cook, 1993; Bunz *et al.*, 1993; Armengaud and Timmis, 1998; Armengaud *et al.*, 1998; 1999; 2000; Basta *et al.*, 2004; Miller *et al.*, 2010; Coronado *et al.*, 2012). Strain RW1 has an average GC content of 67% and several of its catabolic genes have been proposed to have been acquired by horizontal gene transfer (<http://genome.jgi-psf.org/sphwi/sphwi.home.html>).

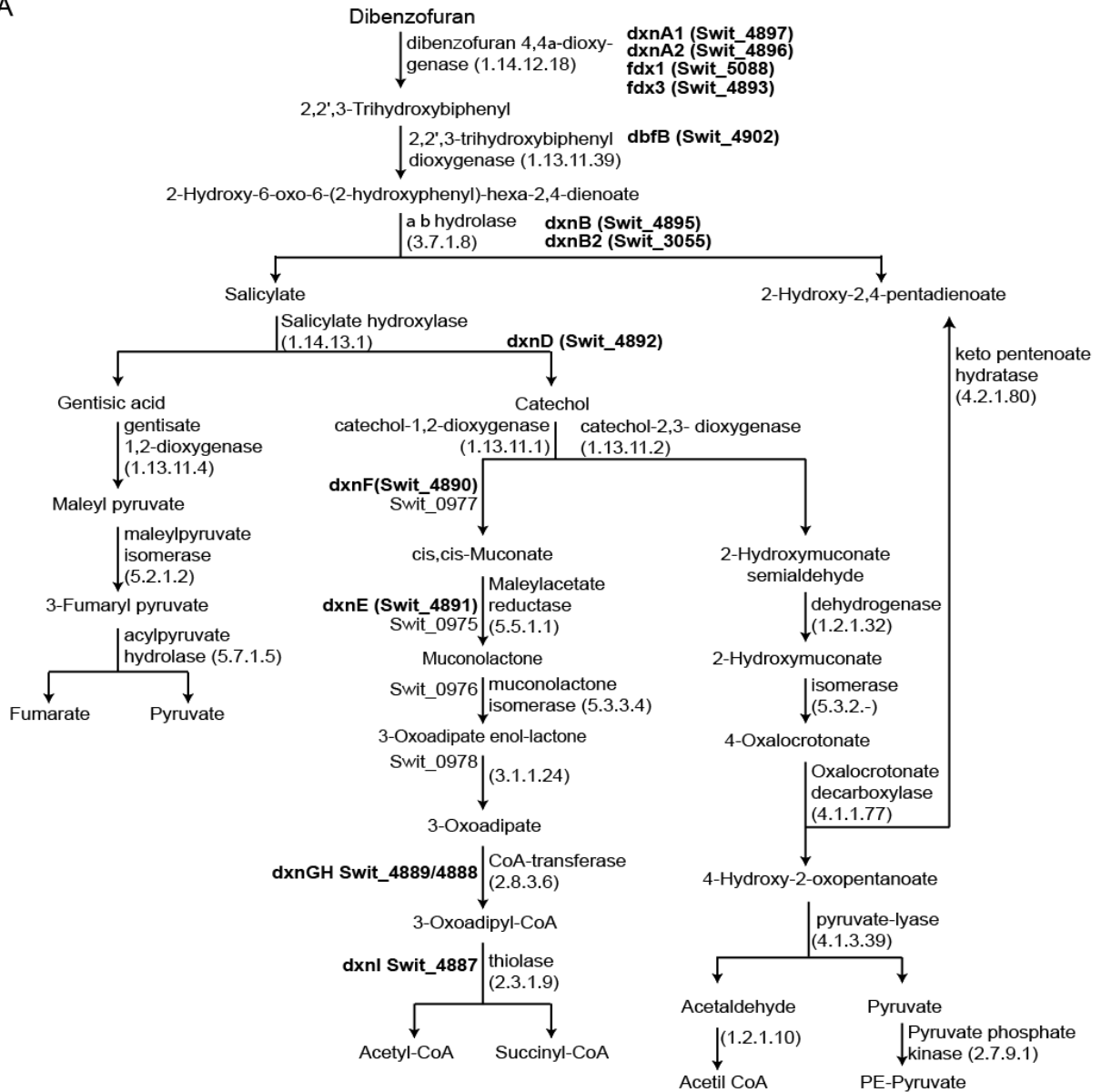
It is known that the initial step of DBF degradation in strain RW1 is an angular dioxygenation to produce 2,2',3-trihydroxybiphenyl. This reaction is catalyzed by a multicomponent DBF dioxygenase, which is composed of the terminal oxidase DxnA1A2 (Swit_4897 and Swit_4896), a reductase RedA2 (Swit_4920), and ferredoxins Fdx1 and

Fdx3 (Swit_5088 and Swit_4893) (Bunz and Cook, 1993; Armengaud and Timmis, 1997; Armengaud and Timmis, 1998; Armengaud *et al.*, 1998). The second step involves the catalytic activity of a 2,2',3-trihydroxybiphenyl dioxygenase DbfB (Swit_4902) (Happe *et al.*, 1993), producing a *meta* cleavage compound, which is subsequently transformed to salicylate and 2-hydroxy-2,4-pentadienoate by the $\alpha\beta$ hydrolase paralogues DxnB or DxnB2 (Swit_4895 and Swit_3055) (Bunz *et al.*, 1993; Seah *et al.*, 2007) (Figure 2A and 2B).

A number of genes encode possible lower pathway reactions, i.e., from salicylate to the TCA cycle intermediates acetyl-CoA and succinyl-CoA. Armengaud *et al.* (1999) characterized an *ortho*-cleavage pathway (beta-keto-adipate pathway). This operon was called the *dxn* cluster and includes the genes *dxnCDEFGHI* (Swit_4887 to Swit_4894). Similar as the *dxnA1A2B*, *dbfB* and *fdx* genes that form the upper pathway, the *dxnCDEFGHI* genes are encoded on pSWIT02. Two additional loci, Swit_0970 to Swit_0981 and Swit_3054 to Swit_3060, are putatively also participating in DBF degradation but are found on the chromosome (Armengaud *et al.*, 1998) (Figure 2B).

According to the KEGG (Kyoto Encyclopedia of Genes and Genomes) database, other alternative pathways for aromatic compound degradation besides the keto-adipate pathway are encoded on the RW1 chromosome, such as the gentisate pathway and a *meta*-cleavage pathway, which could direct DBF intermediates to the TCA cycle (Figure 2A). However, this assignment is based on a gene function prediction and no enzyme involved in these alternative pathways has been studied or characterized for strain RW1.

A



B

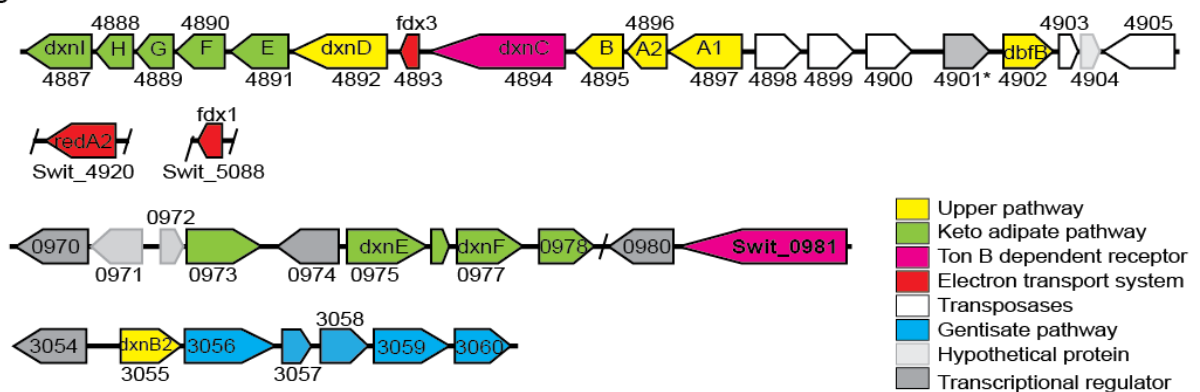


Figure 2. Schematic outline of the DBF degradation pathway (A) based on KEGG database information, and the published loci involved in DBF degradation (B) in *Spingomonas wittichii* RW1.

Bioremediation

Bioremediation refers to the use of microorganisms to degrade pollutants, as an alternative to the traditional physico-chemical processes (Scullion, 2006). Two approaches of bioremediation technology are the introduction of microorganisms to a contaminated site, called bioaugmentation, or the addition of nutrients to the site that will favour the activity of the native microorganisms, referred to as biostimulation (Vogel *et al.*, 1996; Gentry *et al.*, 2004; Tyagi *et al.*, 2011). Despite the numerous attempts to use bioaugmentation and bioremediation in contaminated sites, the results are usually disappointing when compared to the laboratory observations (Gentry *et al.*, 2004; El Fantroussi and Agatos, 2005; Thompson *et al.*, 2005; Scullion, 2006; Tyagi *et al.*, 2011). Several factors have been suggested to limit implementation of bioaugmentation and biostimulation. Some of those relate to the quality of the environment in which the strains are introduced, such as harsh growth conditions (Megharaj *et al.*, 1997; van Veen *et al.*, 1997; Chen *et al.*, 2008), oxidative stress (Givskov *et al.*, 1994), depletion of nutrients (Rosenberg *et al.*, 1992; Röling *et al.*, 2002; Ahn *et al.*, 2008), sudden changes in temperature (Steinle *et al.*, 2000), changes in pH (van der Gast and Thompson, 2004; Kim *et al.*, 2005), unavailability of the compound (Harms and Zehnder, 1995; Bosma *et al.*, 1996; Halden *et al.*, 1999; Johnsen and Karlson, 2004; Johnsen *et al.*, 2005; Wammer and Peters, 2005; Aso *et al.*, 2006; Das *et al.*, 2008; Rehmann *et al.*, 2008), or lack of water (Leahy and Colwell, 1990; Stark and Firestone, 1995). Other factors relate to the inherent qualities of the microorganisms themselves, such as general poor viability, low degrading activity when applied to contaminated sites (Gentry *et al.*, 2004; Thompson *et al.*, 2005; Tyagi *et al.*, 2011), sensitivity to toxic action of the compounds or subproducts (Coppotelli *et al.*, 2008, 2010) or competition with native microorganisms (Shi *et al.*, 2001; Kumar *et al.*, 2009; Morrison and Alexander, 1997). Many frequently found organic

pollutants such as polycyclic aromatic hydrocarbons or oil constituents have a low water solubility and high hydrophobicity. This favors their sorption to the organic matrix in soil, gradually leading to the process of *aging* by which the contaminants become less and less available for biota (Harms and Bosma, 1997).

On the basis of this, various propositions were made to possibly improve bioremediation efficiency of introduced strains. As examples, pretreatments may enhance the bioavailability of the pollutants to the degrading bacteria (Das *et al.*, 2008; Johnsen and Karlson, 2004), the use of genetically modified microorganism with enhanced degrading capacities (Ramos *et al.*, 1986, Pieper and Reineke, 2000) or enhanced compound uptake by altering the membrane pores (Aso *et al.*, 2006). Microorganisms can be pre-adapted to environmental conditions before actually introducing them on site (Megharaj *et al.*, 1997). Also immobilization has been used to increase cell viability and reduce toxic action (Obuekwe and Al-Murrawa, 2001; Moslemy *et al.*, 2002; Tao *et al.*, 2009; Wang *et al.*, 2010). Other techniques favor activation of cometabolic degradation by microorganisms that cannot fully mineralize a compound when they are used as pure cultures, because their genomes code for incomplete degradative pathways or the production of dead-end products (Wittich *et al.*, 1999; Kumar *et al.*, 2009; Li *et al.*, 2009; Hasan *et al.*, 2012; McGenity *et al.*, 2012).

Sphingomonas wittichii RW1 has a potential to be used for bioremediation of contaminated sites, due to its ability to metabolize a variety of toxic compounds. Two studies describe the DBF degradation by strain RW1 in sandy soils and soils containing organic matter artificially contaminated with DBF, DBD and 2-chlorodibenzo-*p*-dioxin (Megharaj *et al.*, 1997; Halden *et al.*, 1999). Megharaj *et al.* (1997) reported a 90% degradation of DBF

within 12 days, while no growth of RW1 was detected, maintaining around 10^5 CFU/gr soil during the whole duration of the experiment. Halden *et al.* (1999) showed an almost complete removal of DBF, DBD and 2-chlorodibenzo-*p*-dioxin. Similarly to the previous study, an exponential decrease of the RW1 population was observed, with a half-life of 7 days.

The pollutant degradation mechanisms by bacteria have been extensively studied (Leahy and Colwell, 1990; Fukuda *et al.*, 2002; Johnsen and Karlson, 2007; Peng *et al.*, 2008). However, a major constraint in the successful application of microorganisms for bioremediation is the lack of basic information on the environmental traits influencing the catabolic activity of microorganisms *in situ*. As part of this study, we aimed to more completely identify genes involved in DBF degradation by means of genome-wide microarrays in order to select target promoters and construct bioreporters strains. Such RW1 bioreporter strains would then perhaps better allow us to monitor the catabolic activity of RW1 as a function of environmental factors, prevailing at a polluted site.

Water Stress

It has been known for a long time that the water availability in the environment of cells has an impact on their metabolic activity, including compound biodegradation (Brown, 1976; Holden *et al.*, 1997). Water availability is therefore also an important factor in the control of bioremediation efficiency in the field (Leahy and Colwell, 1990; Stark and Firestone, 1995). A decrease in water availability for a microorganism that impairs its basic biochemical functions is considered as water stress (Brown, 1976).

A decrease in water activity is equivalent to a lowered water potential and this translates in an increase of the osmotic pressure (Potts, 1994). The osmotic potential, numerically equal to osmotic pressure but with a negative sign (Brown, 1976), has two components, the solute potential (SP) and matric potential (MP). SP increases linearly with increasing concentration of solutes and the MP describes the interaction of water with surfaces and interfaces (colloidal particles and solid particles from 0.002 to 1 μm diameter) (Potts, 1994). Under laboratory conditions the solute potential can be manipulated by adding to the culture media increasing amounts of permeable ionic solutes such as NaCl (Holden *et al.*, 1997; Mutnuri *et al.*, 2005; Chang *et al.*, 2007), urea (Reva *et al.*, 2006), Na₂SO₄ (Boch *et al.*, 1994), or KCl (Boch *et al.*, 1994; Axtell and Beattie, 2002). The matric potential can be modified by addition of non-permeating solutes that favor the flux of water molecules from the interior of the cell to the outside, such as PEG (Halverson and Firestone, 2000; Axtell and Beattie, 2002; Chang *et al.*, 2007), or glycerol (Boch *et al.*, 1994). Other ways to manipulate the matric potential include air dessication (Singh *et al.*, 2005; Cytryn *et al.*, 2007; LeBlanc *et al.*, 2008) or the Porous Surface Model (Dechesne *et al.*, 2008).

Microorganisms have different strategies to adapt to changes in water potential. As a consequence of hyperosmotic shock, bacteria stimulate the uptake of potassium and the synthesis of glutamate (Sleator and Hill, 2002). The secondary response is the accumulation of neutral osmoprotectants (compatible solutes), which in contrast to the ionic osmolytes of the primary response, can be accumulated to high intracellular concentration to counteract the outflow of water, without adversely affecting cellular processes (Boch *et al.*, 1994; Ogahara *et al.*, 1995; Kempf and Bremer, 1998; LeBlanc *et al.*, 2008; Poolman and Glaasker, 1998; Cytryn *et al.*, 2007; Brill *et al.*, 2011). Other strategies include the change in membrane fatty acid composition (Halverson and Firestone, 2000; Mutnuri *et al.*, 2005; Johnson *et al.*, 2011),

the up-regulation of proteins involved in stabilization of macromolecules and membrane structure (Hallsworth *et al.*, 2003; Cytryn *et al.*, 2007; LeBlanc *et al.*, 2008), the production of exopolysaccharides (Chang *et al.*, 2007; Gülez *et al.*, 2012), overproduction of transmembrane transporters (Lucht and Bremer, 1994; Reva *et al.*, 2006; Cytryn *et al.*, 2007) or to enter physiological states of low growth or stationary phase (Holden *et al.*, 1997; Wright and Beattie, 2004; Singh *et al.*, 2005).

Knowing that bacteria undergo different changes in order to adapt to a water stress condition, is thus important to understand the impact that a decreased water potential could have on its degrading capacity. One of the goals of this study is therefore to monitor the catabolic activity of *S. wittichii* RW1 when inoculated in liquid media with a decreased water potential as well as when inoculated in soil microcosms, by following bioreporters responding to DBF.

References

- Ahn Y-B, Liu F, Fennell DE and Häggblom MM** (2008) Biostimulation and bioaugmentation to enhance dechlorination of polychlorinated dibenzo-*p*-dioxins in contaminated sediments. *FEMS Microbiology Ecology* 66: 271-281.
- Aly HAH, Huu NB, Wray V, Junca H and Pieper DH** (2008) Two angular dioxygenases contribute to the metabolic versatility of dibenzofuran-degrading *Rhodococcus sp.* Strain HA01. *Applied and Environmental Microbiology* 74: 3812-3822.
- Armengaud J and Timmis KN** (1997) Molecular characterization of *fdx1*, a *putidaredoxin*-type [2Fe-2S] ferredoxin able to transfer electrons to the dioxin dioxygenase of *Sphingomonas sp.* RW1. *European Journal of Biochemistry* 247: 833-842.
- Armengaud J and Timmis KN** (1998) The reductase RedA2 of the multi-component dioxin dioxygenase system of *Sphingomonas sp.* RW1 is related to class-I cytochrome P450-type reductases. *European Journal of Biochemistry* 253: 437-444.
- Armengaud J, Happe B and Timmis KN** (1998) Genetic analysis of dioxin dioxygenase of *Sphingomonas sp.* strain RW1: catabolic genes dispersed on the genome. *Journal of Bacteriology* 180: 3954-3966.
- Armengaud J, Timmis KN and Wittich R-M** (1999) A functional 4-hydroxysalicylate/hydroxyquinol degradative pathway gene cluster is linked to the initial Dibenzo-*p*-dioxin pathway genes in *Sphingomonas sp.* strain RW1. *Journal of Bacteriology* 181: 3452-3461.
- Armengaud J, Gaillard J and Timmis KN** (2000) A second [2Fe-2S] ferredoxin from *Sphingomonas sp.* strain RW1 can function as an electron donor for the dioxin dioxygenase. *Journal of Bacteriology* 182: 2238-2244.
- Aso Y, Miyamoto Y, Mine Harada K, Momma, K, Kawai S, Hashimoto W, Mikami B, Murata K** (2006) Engineered membrane superchannel improves bioremediation potential of dioxin-degrading bacteria. *Nature Biotechnology* 24: 188-189.
- Axtell CA and Beattie GA** (2002) Construction and characterization of a proU-gfp transcriptional fusion that measures water availability in a microbial Habitat. *Applied and Environmental Microbiology* 68: 4604-4612.
- Basta T, Keck A, Klein J and Stolz A** (2004) Detection and characterization of conjugative degradative plasmids in xenobiotic-degrading *Sphingomonas* strains. *Journal of Bacteriology*. 186: 3862-3872.

- Beck H, Dross A and Mathar W** (1994) PCDD and PCDF exposure and levels in humans in Germany. *Environmental Health Perspectives* 102: 173-185.
- Boch J, Kempf B and Bremer E** (1994) Osmoregulation in *Bacillus subtilis*: synthesis of the osmoprotectant glycine betaine from exogenously provided choline. *Journal of Bacteriology* 176: 5364-5371.
- Bosma TNP, Middeldorp PJM, Schraa G and Zehnder AJB** (1996) Mass transfer limitation of biotransformation: quantifying bioavailability. *Environmental Science and Technology* 31: 248-252.
- Bowes GW, Simoneit BR, Burlingame AL, de Lappe BW and Risebrough RW** (1973) The search for chlorinated dibenzofurans and chlorinated dibenzodioxins in wildlife populations showing elevated levels of embryonic death. *Environmental Health Perspectives* 5: 191-198.
- Brill J, Hoffmann T, Bleisteiner M and Bremer E** (2011) osmotically controlled synthesis of the compatible solute proline is critical for cellular defense of *Bacillus subtilis* against high osmolarity. *Journal of Bacteriology* 193: 5335-5346.
- Brown AD** (1976) Microbial water stress. *Bacteriological Reviews* 40: 803-846.
- Bunz PV and Cook AM** (1993) Dibenzofuran 4,4a-dioxygenase from *Sphingomonas sp.* strain RW1: angular dioxygenation by a three-component enzyme system. *Journal of Bacteriology* 175: 6467-6475.
- Bünz PV, Falchetto R and Cook AM** (1993) Purification of two isofunctional hydrolases (EC 3.7.1.8) in the degradative pathway for dibenzofuran in *Sphingomonas sp.* strain RW1. *Biodegradation* 4: 171-178.
- Buser H-R, Rappe C and Bergqvist P-A** (1985) Analysis of polychlorinated dibenzofurans, dioxins and related compounds in environmental samples. *Environmental Health Perspectives* 60: 293-302.
- Cerniglia CE, Morgan JC and Gibson DT** (1979) Bacterial and fungal oxidation of dibenzofuran. *Biochemical Journal* 180: 175-170.
- Chang, WS, van de Mortel M, Niesen L, Nino de Guzman G, Li X and Halverson H** (2007) Alginate production by *Pseudomonas putida* creates a hydrated microenvironment and contributes to biofilm architecture and stress tolerance under water-limiting conditions. *Journal of Bacteriology* 189: 8290-8299
- Chen J, Wong MH, Wong YS and Tam NFY** (2008) Multi-factors on biodegradation kinetics of polycyclic aromatic hydrocarbons (PAHs) by *Sphingomonas sp.* a bacterial strain isolated from mangrove sediment. *Marine Pollution Bulletin* 57: 695-702.
- Coppotelli B, Ibarrolaza A, Del Panno M and Morelli I** (2008) Effects of the inoculant strain *Sphingomonas paucimobilis* 20006FA on soil bacterial community and biodegradation in phenanthrene-contaminated soil. *Microbial Ecology* 55: 173-183.

- Coppotelli B, Ibarrolaza A, Dias R, Panno M, Berthe-Corti L and Morelli I** (2010) Study of the degradation activity and the strategies to promote the bioavailability of phenanthrene by *Sphingomonas paucimobilis* strain 20006FA. *Microbial Ecology* 59: 266-276.
- Coronado E, Roggo C, Johnson DR and van der Meer JR** (2012) Genome-wide analysis of salicylate and dibenzofuran metabolism in *Sphingomonas wittichii* RW1. *Frontiers in Microbiology* 3.
- Cytryn EJ, Sangurdekar DP, Streeter JG, Franck WL, Chang W-S, Stacey G, Emerich DW, Joshi T, Xu D and Sadowsky MJ** (2007) Transcriptional and physiological responses of *Bradyrhizobium japonicum* to desiccation-induced stress. *Journal of Bacteriology* 189: 6751-6762.
- Das P, Mukherjee S and Sen R** (2008) Improved bioavailability and biodegradation of a model polyaromatic hydrocarbon by a biosurfactant producing bacterium of marine origin. *Chemosphere* 72: 1229-1234.
- Dechesne A, Or D, Gulez G and Smets BF** (2008) The porous surface model, a novel experimental system for online quantitative observation of microbial processes under unsaturated conditions. *Applied and Environmental Microbiology* 74: 5195-5200.
- El Fantroussi S and Agathos SN** (2005) Is bioaugmentation a feasible strategy for pollutant removal and site remediation? *Current Opinion in Microbiology* 8: 268-275.
- Fortnagel P, Harms H, Wittich RM, Krohn, S, Meyer H, Sinnwell V, Wilkes H and Francke W** (1990) Metabolism of dibenzofuran by *Pseudomonas sp.* strain HH69 and the mixed culture HH27. *Applied and Environmental Microbiology* 56: 1148-1156.
- Fukuda K, Nagata S and Taniguchi H** (2002) Isolation and characterization of dibenzofuran-degrading bacteria. *FEMS Microbiology Letters* 208: 179-185.
- Gai Z, Yu B, Li L, Wang Y, Ma C, Feng J, Deng Z and Xu P** (2007) Cometabolic degradation of dibenzofuran and dibenzothiophene by a newly isolated carbazole-degrading *Sphingomonas sp.* strain. *Applied and Environmental Microbiology* 73: 2832-2838.
- Gentry T, Rensing C and Pepper IAN** (2004) New approaches for bioaugmentation as a remediation technology. *Critical Reviews in Environmental Science and Technology* 34: 447-494.
- Givskov M, Eberl L, Møller S, Poulsen LK and Molin S** (1994) Responses to nutrient starvation in *Pseudomonas putida* KT2442: analysis of general cross-protection, cell shape, and macromolecular content. *Journal of Bacteriology* 176: 7-14.
- Gülez G, Dechesne A, Workman CT and Smets BF** (2012) Transcriptome dynamics of *Pseudomonas putida* KT2440 under water stress. *Applied and Environmental Microbiology* 78: 676-683.

- Halden RU, Halden BG and Dwyer DF** (1999) Removal of dibenzofuran, dibenzo-*p*-dioxin, and 2-Chlorodibenzo-*p*-dioxin from soils inoculated with *Sphingomonas sp.* strain RW1. Applied and Environmental Microbiology 65: 2246-2249.
- Hallsworth J, Heim S and Timmis KN** (2003) Chaotropic solutes cause water stress in *Pseudomonas putida*. Environmental Microbiology 5: 1270-1280.
- Halverson LJ and Firestone MK** (2000) Differential effects of permeating and nonpermeating solutes on the fatty acid composition of *Pseudomonas putida*. Applied and Environmental Microbiology 66: 2414-2421.
- Happe B, Eltis LD, Poth H, Hedderich R and Timmis KN** (1993) Characterization of 2,2',3-trihydroxybiphenyl dioxygenase, an extradiol dioxygenase from the dibenzofuran- and dibenzo-*p*-dioxin-degrading bacterium *Sphingomonas sp.* strain RW1. Journal of Bacteriology 175: 7313-7320.
- Harms H and Bosma TNP** (1997) Mass transfer limitation of microbial growth and pollutant degradation. Journal of Industrial Microbiology and Biotechnology 18: 97-105.
- Harms H and Zehnder A** (1995) Bioavailability of sorbed 3-Chlorodibenzofuran. Applied and Environmental Microbiology 61:27-33
- Hasan S, Wietzes P and Janssen D** (2012) Biodegradation kinetics of 4-fluorocinnamic acid by a consortium of *Arthrobacter* and *Ralstonia* strains. Biodegradation 23: 117-125.
- Holden PA, Halverson LJ and Firestone MK** (1997) Water stress effects on toluene biodegradation by *Pseudomonas putida*. Biodegradation 8: 143-151.
- Johansen HR, Alexander J, Rosslund OJ, Planting S, Lovik M, Gaarder PI, Gdynia W, Bjerve KS and Becher G.** (1996) PCDDs, PCDFs, and PCBs in human blood in relation to consumption of crabs from a contaminated Fjord area in Norway. Environmental Health Perspectives 104: 756-764.
- Johnsen AR and Karlson U** (2004) Evaluation of bacterial strategies to promote the bioavailability of polycyclic aromatic hydrocarbons. Applied Microbiology and Biotechnology 63: 452-459.
- Johnsen A and Karlson U** (2007) Diffuse PAH contamination of surface soils: environmental occurrence, bioavailability, and microbial degradation. Applied Microbiology and Biotechnology 76: 533-543.
- Johnsen AR, Wick LY and Harms H** (2005) Principles of microbial PAH-degradation in soil. Environmental Pollution 133: 71-84.
- Johnson D, Coronado E, Moreno-Forero S, Heipieper H and van der Meer J** (2011) Transcriptome and membrane fatty acid analyses reveal different strategies for responding to permeating and non-permeating solutes in the bacterium *Sphingomonas wittichii*. BMC Microbiology 11: 250.

Kempf B and Bremer E (1998) Uptake and synthesis of compatible solutes as microbial stress responses to high-osmolality environments. *Archives of Microbiology* 170: 319-330.

Kim Y-H, Freeman JP, Moody JD, Engesser K-H and Cerniglia CE (2005) Effects of pH on the degradation of phenanthrene and pyrene by *Mycobacterium vanbaalenii* PYR-1. *Applied Microbiology and Biotechnology* 67: 275-285.

Kubota M, Kawahara K, Sekiya K, Uchida T, Hattori Y, Futamata H and Hiraishi A (2005) *Nocardioides aromaticivorans* sp. nov., a dibenzofuran-degrading bacterium isolated from dioxin-polluted environments. *Systematic and Applied Microbiology* 28: 165-174.

Kumar M, Wu P-C, Tsai J-C and Lin J-G (2009) Biodegradation of soil-applied polycyclic aromatic hydrocarbons by sulfate-reducing bacterial consortium. *Journal of Environmental Science and Health, Part A* 44: 12 - 20.

Leahy JG and Colwell RR (1990) Microbial degradation of hydrocarbons in the environment. *Microbiological Reviews* 54: 305-315.

LeBlanc JC, Gonçalves ER and Mohn WW (2008) Global response to desiccation stress in the soil actinomycete *Rhodococcus jostii* RHA1. *Applied and Environmental Microbiology* 74: 2627-2636.

Li Q, Wang X, Yin G, Gai Z, Tang H, Ma C, Deng Z and Xu P (2009) New metabolites in dibenzofuran cometabolic degradation by a biphenyl-cultivated *Pseudomonas putida* strain B6-2. *Environmental Science and Technology* 43: 8635-8642.

Lucht JM and Bremer E (1994) Adaptation of *Escherichia coli* to high osmolarity environments: Osmoregulation of the high-affinity glycine betaine transport system ProU. *FEMS Microbiology Reviews* 14: 3-20.

McGenity TJ, Folwell BD, McKew BA and Sanni GO (2012) Marine crude-oil biodegradation: a central role for interspecies interactions. *Aquatic Biosystems* 8: 10-29.

McNulty WP (1985) Toxicity and fetotoxicity of TCDD, TCDF and PCB isomers in *Rhesus Macaques* (*Macaca mulatta*). *Environmental Health Perspectives* 60: 77-88.

Megharaj M, Wittich RM, Blasco R, Pieper DH and Timmis KN (1997) Superior survival and degradation of dibenzo-*p*-dioxin and dibenzofuran in soil by soil-adapted *Sphingomonas* sp. strain RW1. *Applied Microbiology and Biotechnology* 48: 109-114.

Miller TR, Delcher AL, Salzberg SL, Saunders E, Detter JC and Halden RU (2010) Genome sequence of the dioxin-mineralizing bacterium *Sphingomonas wittichii* RW1. *Journal of Bacteriology* 192: 6101-6102.

- Monna L, Omori T and Kodama T** (1993) Microbial degradation of dibenzofuran, fluorene, and dibenzo-*p*-dioxin by *Staphylococcus auriculans* DBF63. *Applied and Environmental Microbiology* 59: 285-289.
- Morrison DE and Alexander M** (1997) Biodegradability of nonaqueous-phase liquids affects the mineralization of phenanthrene in soil because of microbial competition. *Environmental Toxicology and Chemistry* 16: 1561-1567.
- Moslemy P, Neufeld RJ and Guiot SR** (2002) Biodegradation of gasoline by gellan gum-encapsulated bacterial cells. *Biotechnology and Bioengineering* 80: 175-184.
- Mutnuri S, Vasudevan N, Kastner M and Heipieper H** (2005) Changes in fatty acid composition of *Chromohalobacter israelensis* with varying salt concentrations. *Current Microbiology* 50: 151-154.
- Obuekwe CO and Al-Muttawa E** (2001) Self-immobilized bacterial cultures with potential for application as ready-to-use seeds for petroleum bioremediation. *Biotechnology Letters* 23: 1025-1032.
- Ogahara T, Ohno M, Takayama M, Igarashi K and Kobayashi H** (1995) Accumulation of glutamate by osmotically stressed *Escherichia coli* is dependent on pH. *Journal of Bacteriology* 177: 5987-5990.
- Peng R-H, Xiong A-S, Xue Y, Fu X-Y, Gao F, Zhao W, Tian Y-S and Yao Q-H** (2008) Microbial biodegradation of polyaromatic hydrocarbons. *FEMS Microbiology Reviews* 32: 927-955.
- Pieper DH and Reineke W** (2000) Engineering bacteria for bioremediation. *Current Opinion in Biotechnology* 11: 262-270.
- Pluim HJ, Vijlder JJMd, Olie K, Kok, JH, Vulsma T, van Tijn D A, van der Slikke JW and Koppe JG** (1993) Effects of pre- and postnatal exposure to chlorinated dioxins and furans on human neonatal thyroid hormone concentrations. *Environmental Health Perspectives* 101: 504-508.
- Poolman B and Glaasker E** (1998) Regulation of compatible solute accumulation in bacteria. *Molecular Microbiology* 29: 397-407.
- Potts M** (1994) Desiccation tolerance of prokaryotes. *Microbiology and Molecular Biology Reviews* 58: 755-805.
- Ramos JL, Stolz A, Reineke W and Timmis KN** (1986) Altered effector specificities in regulators of gene expression: TOL plasmid *xyIS* mutants and their use to engineer expansion of the range of aromatics degraded by bacteria. *Proceedings of the National Academy of Sciences* 83: 8467-8471.
- Rehmann L, Prpich GP and Daugulis AJ** (2008) Remediation of PAH contaminated soils: Application of a solid-liquid two-phase partitioning bioreactor. *Chemosphere* 73: 798-804.

Reva ON, Weinel C, Weinel M, Bohm K, Stjepandic D, Hoheisel JD and Tummeler B (2006) Functional genomics of stress response in *Pseudomonas putida* KT2440. *Journal of Bacteriology* 188: 4079-4092.

Röling WFM, Milner MG, Jones DM, Lee K, Daniel F, Swannell RJP and Head IM (2002) Robust hydrocarbon degradation and dynamics of bacterial communities during nutrient-enhanced oil spill bioremediation. *Applied and Environmental Microbiology* 68: 5537-5548.

Rosenberg E, Legmann R, Kushmaro A, Taube R, Adler E and Ron EZ (1992) Petroleum bioremediation — a multiphase problem. *Biodegradation* 3: 337-350.

Scullion J (2006) Remediating polluted soils. *Naturwissenschaften* 93: 51-65.

Seah SYK, Ke J, Denis G, Horsman GP, Fortin PD, Whiting CJ and Eltis LD (2007) Characterization of a C-C bond hydrolase from *Sphingomonas wittichii* RW1 with novel specificities towards polychlorinated biphenyl metabolites. *Journal of Bacteriology* 189: 4038-4045.

Shi T, Fredrickson JK and Balkwill DL (2001) Biodegradation of polycyclic aromatic hydrocarbons by *Sphingomonas* strains isolated from the terrestrial subsurface. *Journal of Industrial Microbiology and Biotechnology* 26: 283-289.

Singh J, Kumar D, Ramakrishnan N, Singhal V, Jervis J, Garst JF, Slaughter SM, DeSantis AM, Potts M and Helm RF (2005) Transcriptional response of *Saccharomyces cerevisiae* to desiccation and rehydration. *Applied and Environmental Microbiology* 71: 8752-8763.

Sleator RD and Hill C (2002) Bacterial osmoadaptation: the role of osmolytes in bacterial stress and virulence. *FEMS Microbiology Reviews* 26: 49-71.

Soong D-K and Ling Y-C (1997) Reassessment of PCDD/DFs and Co-PCBs toxicity in contaminated rice-bran oil responsible for the disease “Yu-Cheng”. *Chemosphere* 34: 1579-1586.

Stark JM and Firestone MK (1995) Mechanisms for soil moisture effects on activity of nitrifying bacteria. *Applied and Environmental Microbiology* 61: 218-221.

Steinle P, Thalmann P, Höhener P, Hanselmann KW and Stucki G (2000) Effect of environmental factors on the degradation of 2,6-dichlorophenol in soil. *Environmental Science and Technology* 34: 771-775.

Tao X-Q, Lu G-N, Liu J-P, Li T and Yang L-N (2009) Rapid degradation of Phenanthrene by using *Sphingomonas sp.* GY2B immobilized in calcium alginate gel beads. *International Journal of Environmental Research and Public Health* 6: 2470-2480.

Thompson IP, Van Der Gast CJ, Ciric L and Singer AC (2005) Bioaugmentation for bioremediation: the challenge of strain selection. *Environmental Microbiology* 7: 909-915.

- Tyagi M, da Fonseca M and de Carvalho C** (2011) Bioaugmentation and biostimulation strategies to improve the effectiveness of bioremediation processes. *Biodegradation* 22: 231-241.
- van der Gast CJ and Thompson IP** (2005) Effects of pH amendment on metal working fluid wastewater biological treatment using a defined bacterial consortium. *Biotechnology and Bioengineering* 89: 357-366.
- van Veen JA, van Overbeek LS and van Elsas JD** (1997) Fate and activity of microorganisms introduced into soil. *Microbiology and Molecular Biology Reviews* 61: 121-135.
- Vogel TM** (1996) Bioaugmentation as a soil bioremediation approach. *Current Opinion in Biotechnology* 7: 311-316.
- Wammer KH and Peters CA** (2005) Polycyclic Aromatic Hydrocarbon biodegradation rates: a structure-based study. *Environmental Science and Technology* 39: 2571-2578.
- Wang Q, Mueller AP, Leong CR, Matsumoto Ki, Taguchi S and Nomura CT** (2010) Quick and efficient method for genetic transformation of biopolymer-producing bacteria. *Journal of Chemical Technology and Biotechnology* 85: 775-778.
- Wittich RM, Wilkes H, Sinnwell V, Francke W and Fortnagel P** (1992) Metabolism of dibenzo-*p*-dioxin by *Sphingomonas sp.* strain RW1. *Applied and Environmental Microbiology* 58: 1005-1010.
- Wittich RM, Strömpl C, Moore ERB, Blasco R and Timmis KN** (1999) Interaction of *Sphingomonas* and *Pseudomonas* strains in the degradation of chlorinated dibenzofurans. *Journal of Industrial Microbiology and Biotechnology* 23: 353-358.
- Wright CA and Beattie GA** (2004) *Pseudomonas syringae pv.* tomato cells encounter inhibitory levels of water stress during the hypersensitive response of *Arabidopsis thaliana*. *Proceedings of the National Academy of Sciences* 101: 3269-3274.
- Yoshihara Si, Nagata K, Yoshimura H, Kuroki H and Masuda Y** (1981) Inductive effect on hepatic enzymes and acute toxicity of individual polychlorinated dibenzofuran congeners in rats. *Toxicology and Applied Pharmacology* 59: 580-588.
- Zitko V, Wildish DJ, Hutzinger O and Choi PM** (1973) Acute and chronic oral toxicity of chlorinated dibenzofurans to salmonid fishes. *Environmental Health Perspectives* 5: 187-189.

CHAPTER 2

Genome-Wide Analysis of Salicylate and Dibenzofuran

Metabolism in *Sphingomonas wittichii* RW1

Abstract

Sphingomonas wittichii RW1 is a bacterium isolated for its ability to degrade the xenobiotic compounds dibenzo-*p*-dioxin and dibenzofuran (DBF). A number of genes involved in DBF degradation have been previously characterized, such as the *dxn* cluster, *dbfB*, and the electron transfer components *fdx1*, *fdx3* and *redA2*. Here we use a combination of whole genome transcriptome analysis and transposon library screening to characterize RW1 catabolic and other genes implicated in the reaction to or degradation of DBF. To detect differentially expressed genes upon exposure to DBF, we applied three different growth exposure experiments, using either short DBF exposures to actively growing cells or growing them with DBF as sole carbon and energy source. Genome-wide gene expression was examined using a custom-made microarray. In addition, proportional abundance determination of transposon insertions in RW1 libraries grown on salicylate or DBF by ultra-high throughput sequencing was used to infer genes whose interruption caused a fitness loss for growth on DBF. Expression patterns showed that batch and chemostat growth conditions, and short or long exposure of cells to DBF produced very different responses. Numerous other uncharacterized catabolic gene clusters putatively involved in aromatic compound metabolism increased expression in response to DBF. In addition, only very few transposon

insertions completely abolished growth on DBF. Some of those (e.g., in *dxnAI*) were expected, whereas others (in a gene cluster for phenylacetate degradation) were not. Both transcriptomic data and transposon screening suggest operation of multiple redundant and parallel aromatic pathways, depending on DBF exposure. In addition, increased expression of other non-catabolic genes suggests that during initial exposure, *S. wittichii* RW1 perceives DBF as a stressor, whereas after longer exposure, the compound is recognized as a carbon source and metabolized using several pathways in parallel.

This chapter was previously published in the journal *Frontiers in Microbiology* (2012) issue 3 page 300 as part of research topic Biodegradation and Bioremediation of Polynuclear aromatic hydrocarbons (PAH) by Edith Coronado, Clémence Roggo, David R. Johnson and Jan Roelof van der Meer.

Introduction

Dibenzofuran (DBF) and dibenzo-*p*-dioxin (DBD) are poorly water-soluble polycyclic aromatic hydrocarbons (PAH) that are formed as byproducts of coal tar industrial processes, during incineration, and in paper pulp bleaching. DBF, DBD and related compounds with chlorine substitutions are widely present at low concentrations in the environment and the food chain (Bowes *et al.*, 1973; Buser *et al.*, 1985; Beck *et al.*, 1994; Johansen *et al.*, 1996), and detrimental effects of exposure have been reported (Zitko *et al.*, 1973; Yoshihara *et al.*, 1981; McNulty, 1985; Pluim *et al.*, 1993; Soong and Ling, 1997). A number of bacteria can use DBF and DBD as sole carbon and energy sources, including *Staphylococcus auriculans* (Monna *et al.*, 1993), *Nocardioides aromaticivorans* (Kubota *et al.*, 2005), *Rhodococcus sp.* HA01 (Aly *et al.*, 2008), *Pseudomonas putida* B6-2 (Li *et al.*, 2009), *Sphingomonas yanoikuyae* B1 (Cerniglia *et al.*, 1979), *Sphingomonas sp.* HH69 (Fortnagel *et al.*, 1990), *Sphingomonas sp.* XLDN2-5 (Gai *et al.*, 2007), *Sphingomonas sp.* RW16 (Wittich *et al.*, 1999) or *Sphingomonas wittichii* RW1 (Wittich *et al.*, 1992, Wilkes *et al.*, 1996). Consequently, there has been an interest to apply such isolates for bioaugmentation of DBF/DBD-contaminated sites. Megharaj *et al.* (1997) and Halden *et al.* (1999) observed DBF and DBD degradation by *S. wittichii* RW1 applied to inoculated soil microcosms, while Aso *et al.* (2006) reported increased DBF degradation rates by inoculating a modified strain of *S. wittichii* RW1 in contaminated soil.

Despite such anecdotal reports, bioaugmentation with strains such as RW1 have not consistently resulted in accelerated pollutant degradation rates. Possible reasons that have been put forward to explain the limited success of bioaugmentation include the lack of essential nutrients in the soil, the creation of toxic dead-end products (Halden *et al.*, 1999),

the low availability of the hydrocarbons (Aso *et al.*, 2006), and the poor ability of the bacteria to adapt to the soil environment (Megharaj *et al.*, 1997). However, the cellular responses of bacteria such as RW1 to different conditions have not been extensively studied, and perhaps DBF/DBD metabolism is regulated in a complex manner depending on the types of exposure.

To address this knowledge gap, we systematically explored gene transcription of *S. wittichii* RW1 at a genome-wide level in batch and chemostat cultures, with and without exposure to DBF or salicylate (SAL) under different cellular growth and environmental conditions. *S. wittichii* RW1 (Wittich *et al.*, 1992) is a gram-negative α -*Proteobacterium*, with a genome consisting of one chromosome and two mega plasmids, named pSWIT01 and pSWIT02 (Miller *et al.*, 2010). The larger mega plasmid pSWIT01 has been reported to be similar to pNL1 from *Novosphingobium aromaticivorans*, whereas the smaller pSWIT02 contains a number of genes previously implicated in DBF/DBD degradation (Bunz and Cook, 1993; Bunz *et al.*, 1993; Armengaud and Timmis, 1998; Armengaud *et al.*, 1998; 1999; 2000; Basta *et al.*, 2004; Miller *et al.*, 2010). Several enzymes participating in DBF degradation have been purified and characterized, notably the initial multicomponent DBF dioxygenase, which is composed of the terminal oxidase DxnA1, a reductase (RedA2), and a ferredoxin (Fdx1) (Bunz and Cook, 1993). In addition, a 2,2',3-trihydroxybiphenyl dioxygenase activity (DbfB) and its corresponding gene (Swit_4902) were characterized (Happe *et al.*, 1993), and two hydrolases, DxnB and DxnB2, (Swit_4895 and Swit_3055) were described (Bunz *et al.*, 1993; Seah *et al.*, 2007). Several of the genes for the above-mentioned enzymes were cloned and characterized, such as *fdx1* (Swit_5088, Armengaud and Timmis, 1997), *redA2* (Swit_4920, Armengaud and Timmis, 1998), and *dxnA1A2B* (Swit_4897 and Swit_4896, Armengaud *et al.*, 1998). The expression of *dxnA1* in RW1 was reported to be higher in DBF-grown than in LB-grown cells (Armengaud *et al.*, 1998), while Bunz and Cook (1993)

observed that DxnA1 was constitutively synthesized in RW1 cells growing on acetate, benzoate, or salicylate as sole carbon and energy source. Finally, a number of other genes, notably the gene *fdx3* (Swit_4893) and a cluster of genes named *dxCDEFGHI* (Swit_4887 to Swit_4894) were cloned and overexpressed in *Escherichia coli*. Their enzyme activities were determined, suggesting that they are involved in DBF degradation by RW1 (Armengaud *et al.*, 1999).

The main objective of the study presented here was to study RW1 gene transcription at the genome-wide level during exposure to DBF. Our hypothesis was that we would clearly see the expression of the abovementioned genes in DBF degradation, but perhaps would also detect other genes for catabolic functions specifically induced or repressed during exposure to DBF. Secondly, we were interested to study how the expression of RW1 genes would change under different growth conditions and exposures to DBF, which might give us clues about how expression in the DBF degradation pathway changes under environmental conditions. Because DBF is poorly water soluble (~5 mg/L) we followed pathway induction by exposing RW1 cells in batch culture to carbon substrate exchange or by transiting stably chemostat-growing cultures from medium without to medium with saturating DBF levels. Finally, we cultured cells in batch culture with DBF, SAL, or phenylalanine (PHE) as sole carbon and energy source. A custom-made RW1 microarray (Johnson *et al.*, 2011) was used to analyze differences in genome-wide gene expression under different conditions. In addition, we used genome-wide transposon screening (Langridge *et al.*, 2009) to further identify genes necessary for growth on DBF as sole carbon and energy source.

Materials and methods

1. Bacterial cultivation

A stock of *S. wittichii* RW1 was kept at -80°C and a small aliquot was plated on minimal medium agar (1.5% w/v) with 5 mM SAL, or by placing DBF crystals in the lid of a Petri dish. Liquid cultures were always prepared from an isolated colony of RW1 from a plate. Minimal media (MM) were based on DSM457 media (Johnson *et al.*, 2011) amended with 5 mM SAL, 5 mM PHE, or with DBF crystals in a dosage of 5 μmol per ml as carbon source. All cultures were incubated at 30°C with rotary shaking at 180 rpm. Batch cultures of strain RW1 were prepared in 50 ml Erlenmeyer flasks containing 15 ml of MM. The cultures were started at an initial culture turbidity of 0.005 (at 600 nm, OD_{600}) for all carbon sources evaluated. Carbon-limited continuous culturing of *S. wittichii* RW1 was carried out in triplicate 500-ml working volume reactors (Infors-HT), containing 400 ml MM and 5 mM PHE as carbon and energy source. Reactors were inoculated with 100 ml of a preculture of *S. wittichii* RW1, which was prepared by inoculating a single colony into a 1 L Erlenmeyer flask with 300 ml of MM plus 5 mM PHE and streptomycin (Sm), and grown until stationary phase ($\text{OD}_{600} \sim 1$). Streptomycin was added (at 50 $\mu\text{g}/\text{ml}$) to the growth media to avoid culture contamination, since strain RW1 is naturally resistant to Sm. The triplicate fermentors were then first operated in batch mode at 30°C and with a stirring speed of 200 rpm. The pH and partial oxygen pressure (pO_2) were monitored online and were maintained at 7 and $\sim 90\%$, respectively. When the culture turbidity reached a steady value of $\text{OD}_{600} = 1$ (the maximum OD obtained with 5 mM PHE), the inflow of fresh MM with 5 mM PHE was started. The flow rate was set to 23.8 ml/h, giving a dilution rate of 0.05 h^{-1} , which corresponds to a doubling time of 14.6 h. The culture turbidity was measured at regular time intervals and

culture samples were plated on LB agar without Sm to verify culture purity. Silicon based antifoam suspension (Antifoam-B emulsion, Sigma-Aldrich) was added at a rate of 0.025 ml/h to avoid excessive culture foaming. The continuous culture was considered in equilibrium after five reactor volume changes and when the measured parameters (culture turbidity and pO₂) were stable.

2. Genome-wide transposon screening

A transposon insertion library was constructed by conjugating plasmid pRL27 from *E. coli* BW20767 to *S. wittichii* RW1 as described by Larsen *et al.* (2002). RW1 transconjugants were selected on MM+SAL plates in the presence of 50 µg/ml kanamycin. RW1 kanamycin-resistant colonies were pooled and stored in aliquots at -80°C in the presence of 15% (v/v) glycerol. Individual aliquots of the library were then grown for five passages in batch culture on MM with 5 mM SAL or with DBF crystals (approximately 50 generations). After five subsequent transfers the total genomic DNA was extracted from the cultures and from the initial library. Aliquots of 5 µg DNA were fragmented and used for Illumina library preparation, during which specifically DNA fragments containing the transposon DNA were amplified, as described in Langridge *et al.* (2009). Samples were then sequenced on an Illumina HiSeq2000 machine at the Lausanne Genomic Technologies Facility (University of Lausanne). Transposon containing sequences were filtered, trimmed and mapped on the *S. wittichii* genome using the *Xpression* pipeline, which was developed by the Harwood lab at the University of Washington (for download: <https://depts.washington.edu/cshlab/html/rnaseq.html>). Genes without any transposon insertions were scored and compared between the two conditions and the starting library.

3. Short exposure of *S. wittichii* RW1 to DBF in batch cultures

S. wittichii RW1 was grown in MM+PHE to stationary phase and this culture was used to inoculate 8 identical 100 ml Erlenmeyer flasks with 20 ml of MM+PHE. These cultures were then grown to exponential phase ($OD_{600} \sim 0.2$), upon which the cells were transferred to 50 ml glass centrifuge tubes and centrifuged at 6,000 rpm for 2 min. The supernatant was discarded and 20 ml of preheated (30°C) MM+PHE was added to four of the tubes, whereas 20 ml of preheated (30°C) MM+DBF (presaturated) was added to the other four tubes. Cells were resuspended immediately and the tubes were incubated in a rotary shaker at 150 rpm for 30 min at 30°C. After this period, the cells were collected by filtering the cultures over a 0.2 μm Millipore filter, which were then transferred into 2 ml tubes and immediately frozen in liquid N_2 . The cells on filters were stored at -80°C until further processing for RNA isolation.

4. Long exposure of *S. wittichii* RW1 to DBF in batch cultures

Secondly, we tested continuous exposure of *S. wittichii* RW1 in batch culture to DBF compared to PHE. A single stationary phase preculture grown in MM+PHE was used as inoculum for two sets of four replicate cultures in 100 ml Erlenmeyer flasks with 20 ml of either MM plus 5 mM PHE or MM plus saturating DBF (dosage of 5 μmol per ml). Cultures were grown until an OD_{600} of 0.2, after which the cells were collected on 0.2 μm filters (Millipore), immediately transferred into 2 ml tubes and frozen in liquid N_2 . The filters were kept at -80°C until further processing for RNA isolation.

5. Transient exposure of *S. wittichii* RW1 to DBF in continuous culture

In order to achieve an immediate pulse addition of DBF to *S. wittichii* RW1 cells which otherwise experienced carbon-limited conditions, we used cells growing continuously on MM+PHE. Triplicate fermentors with stably growing RW1 cultures on MM+PHE were induced with DBF by injecting a volume of 1 ml DBF dissolved in 2,2',4,4',6,8,8'-heptamethylnonane (HMN, at 2.5 mg/ml) into each fermentor (500 ml culture volume) and subsequently changing immediately the inflow medium to MM plus 5 mM PHE plus saturated amounts of DBF (crystals visible in the stirred medium). Addition of HMN to exponentially growing cultures on PHE did not cause any growth rate retardation (not shown). Culture samples (4 x 2 ml) were taken, transferred to 2 ml centrifuge tubes with screw cap and centrifuged at 13,000 rpm for one min at room temperature. The supernatant was quickly removed by decanting and the cell pellets were frozen with liquid N₂. Control samples (T₀) were taken immediately before the transition. Further samples were taken 30 min, 1 h, 2 h, and 6 h after the transition to medium with DBF. The cell pellets were stored at -80°C until further processing for RNA isolation.

6. RNA processing, microarray hybridization and analysis

RNA was extracted and purified from the frozen cells on the filters or cell pellets by hot-phenol extraction as described elsewhere (Johnson *et al.*, 2008). cDNA was labeled from the total RNA pool using reverse transcription in the presence of cyanine-3-dCTP. A total of 60 ng of cDNA were used to hybridize to an Agilent 8 X 15K custom *S. wittichii* RW1 microarray (Johnson *et al.*, 2011). The microarray contains a total of 12,873 50-mer probes that cover >99% of the predicted protein coding genes (5323 out of 5345) within the genome of strain RW1. The cDNA samples were loaded randomly onto the microarray slide to eliminate slide-to-slide variations. Slides were hybridized and scanned following the One-

color Microarray-Based Gene Expression Analysis Manual (Agilent Technologies, Santa Clara, CA) protocols. Signals were extracted using Agilent Feature Extraction software 10.5.1.1 (Agilent). Microarray data were normalized and globally scaled using GENESPRING GX software (version 11). The difference between the signals in treatment and control samples was tested as described elsewhere (Johnson *et al.*, 2008; 2011). All microarray datasets have been deposited as a single file in the NCBI Gene Expression Omnibus under accession number GSE37328 according to MIAME standards (<http://www.ncbi.nlm.nih.gov/pubmed/11726920>).

Results

Genes implicated in DBF degradation

In order to discover specific genes of RW1 that could be implicated in the response to exposure to DBF, we used a combination of genome-wide expression and transposon insertion screening approaches. An estimated 42,000 independent transposon mutants of RW1 were tested as a library for growth in batch on SAL or DBF medium. After five medium passages, corresponding to 50 generations, the distribution and abundance of transposon insertions in the genome was analyzed by Illumina sequencing and compared to that in the starting library. One hundred and thirty nine genes were specifically absent in the library grown on DBF, but were present by at least 30 transposon reads in the starting library (Table S1). Less stringently, 589 genes were covered by transposon insertions at one-tenth or less in the DBF compared to initial library (Table S1). Among a global annotation of putative catabolic genes in aromatic compound metabolism there were 17 genes missing in the DBF library, 5 of which were not simultaneously absent in the SAL library (Table 1, Table S2), suggesting their unique implication in DBF degradation. One of those was previously recognized (Swit_4896 or *dxnA2*), whereas others have not so far been identified as such (i.e., Swit_1643 for FMN-dependent alpha-hydroxy acid dehydrogenase, Swit_1684 for FAD-binding monooxygenase, Swit_1757 for a putative Rieske-motif containing protein, and Swit_1861 for a putative dioxygenase). Transposon insertions in the previously identified genes Swit_4895 (*dxnB*) and Swit_4897 (*dxnA1*) were 10-fold or more underrepresented in the DBF-grown library but not completely absent (Table S2). None of the other genes previously implicated in DBF degradation were absent from the DBF transposon library, suggesting they code for redundant functions. In contrast, transposon insertions were absent

in several genes in a cluster for phenylacetate degradation (*paa*, Swit_750 to Swit_758) in both DBF and SAL-libraries, although these genes are actually expressed to a lower level under such growth conditions (see below). Apart from this cluster, no transposon insertions were detected in a number of other putative catabolic genes after both DBF and SAL growth, e.g., Swit_311 carboxymuconolactone decarboxylase, Swit_893 ferredoxin, Swit_1639-1642 part of enzymes for a *meta*-cleavage pathway, Swit_1759 ferredoxin, Swit_2113 acetaldehyde dehydrogenase, Swit_2251 ferredoxin, or Swit_2292 putative extradiol cleavage enzyme (table S2). Two of those (Swit_1640, Swit_1641) are 100 and 96% identical, respectively, to Swit_2112 and Swit_2113, and may therefore have been missed because the transposon insertion sites cannot be uniquely mapped to one region on the chromosome.

Interestingly, some fifty transposon insertions were at least 10-fold or more abundant in the DBF library compared to time 0, where they were present with at least 30 reads (Table S3), suggesting a small fitness increase of such mutants under those growth conditions. Although this list is still quite long and cannot be interpreted succinctly, it is interesting to find a number of putative catabolic genes, regulatory factors and stress response factors (Table S3).

Table 1. RW1 gene cluster representatives for putative aromatic compound metabolism with significantly changed expression levels or proportional abundances in transposon libraries. For expanded version, see Table S2.

Cluster ¹	Swit Locus	Name or gene name	Strand	Tn library ²			Expression, fold change ³							
				TN01	SAL	DBF	SAL/PHE	SAL/DBF	DBF/PHE	DBF shock	30 m	Chemostat shift		
												1 h	2 h	6 h
310-312	311	carboxymuconolactone decarboxylase	<	-(+)	-(±)	-			1.21	1.93	2.81	2.51	2.03	1.25
748-749	749	<i>paaB?</i>	<	-(-)	-(-)	+	0.04		0.72	0.12	0.31	0.35	0.35	0.31
750-758	750	3-hydroxyacyl-CoA dehydrogenase	>	+(-)	-(-)	-	0.07		0.53	0.11	0.48	0.47	0.38	0.48
	753	<i>paaA</i>	>	+(+)	-(±)	+	0.04		0.50	0.04	0.24	0.15	0.14	0.16
	754	<i>paaB</i>	>	+(+)	-(±)	±	0.02		0.24	0.05	0.14	0.07	0.05	0.05
	755	<i>paal</i>	>	-(-)	-(-)	-	0.02		0.19	0.05	0.17	0.10	0.05	0.06
	756	<i>paaJ</i>	>	+(+)	-(±)	-			1.06	1.66	1.72	1.51	1.45	1.01
975-978	975	muconate cycloisomerase	>	±(+)	+(+)	±	8.36		1.72	1.06	0.74	0.58	0.46	1.95
	978	3-oxoadipate enol-lactonase	>	+(+)	+(+)	±	2.26	2.20	1.02	1.56	1.33	1.05	0.60	1.04
1639-1644	1639	4-oxalocrotonate decarboxylase	>	+(-)	-(-)	-			1.68	1.17	0.99	1.13	1.47	1.83
	1643	FMN-dependent alpha-hydroxy acid dehydrogenase	>	±(+)	±(±)	-			1.27	0.92	1.13	1.08	1.10	1.05
1754-1760	1757	Rieske-type protein; beta subunit	>	-(+)	±(±)	-			0.95	0.74	0.96	0.86	0.81	0.80
	1759	ferredoxin	>	±(±)	-(-)	-			1.04	2.03	1.09	1.01	1.62	1.99
1825-1830	1827	alpha/beta hydrolase fold protein	<	±(+)	+(+)	+			1.05	4.63	1.36	1.71	1.54	1.61
	1828	acyl-CoA dehydrogenase type 2	<	+(+)	±(±)	+			1.04	14.83	4.63	4.56	2.87	1.71
	1829	Rieske-type protein	<	+(+)	-(±)	±			1.13	6.11	2.04	1.95	2.27	2.08
1847-1852	1848	putative extradiol dioxygenase	>	-(+)	±(±)	±	3.39		3.23	28.64	2.75	3.05	3.14	2.79
1860-1861	1861	dioxygenase motif	>	-(±)	±(±)	-			1.54	6.29	2.50	3.54	0.77	1.69
2634-2636	2634	benzoate 1,2-dioxygenase; alpha	>	+	+	+	28.8		5.06	2.36	1.42	1.87	2.07	3.05
3055-3066	3055	alpha/beta hydrolase fold protein (<i>dxnB2</i>)	>	±(±)	-(-)	+			2.60	1.65	0.68	0.64	0.85	0.90
	3056	Rieske-type protein; alpha subunit (putative salicylate 5 hydroxylase)	>	+(+)	+(+)	+	2.44		2.31	2.19	0.78	0.59	0.73	0.82
	3057	Rieske; beta subunit	>	+(-)	-(±)	+			2.35	1.07	0.64	0.51	0.57	0.57
	3058	maleylacetoacetate isomerase"	>	+(+)	+(+)	+	2.42		2.48	0.74	0.55	0.41	0.38	0.45
3083-3084	3084	5-oxopent-3-ene-1,2,5-tricarboxylate decarboxylase	<	+(+)	+(+)	+	3.88	2.74	1.35	1.46	1.06	1.26	1.39	1.19
3085-3086	3086	gentisate 1,2-dioxygenase like protein	>	+(+)	+(+)	+	3.92		1.49	2.03	1.32	1.51	1.53	1.07
3087-3096	3087	2,4-dihydroxyhept-2-ene-1,7-dioic acid aldolase	<	±(+)	±(+)	±	16.9	17.71	0.98	1.01	0.93	2.06	1.03	1.53
	3094	putative extradiol dioxygenase	>	+(+)	+(+)	+	5.33	2.79	1.85	1.72	1.28	0.96	0.93	1.10
3416-3418	3418	putative extradiol dioxygenase	>	+(-)	-(±)	+			1.13	2.95	1.96	2.62	2.95	1.82
3863-3865	3865	4-hydroxyphenylpyruvate dioxygenase	<	+(+)	+(+)	+	7.99		1.73	1.40	1.60	2.17	2.48	3.23
4273	4273	vanillate monooxygenase	>	+(+)	+(+)	+			1.13	1.20	1.25	1.87	2.20	2.51

4278	4278	Rieske-type protein; alpha subunit	<	+(+)	+(+)	+		1.54	2.33	1.89	1.84	2.04	1.84
4887-4897	4890	hydroxyquinol 1,2 dioxygenase (<i>dxnF</i>)	<	+(+)	+(+)	+		2.87	1.17	1.26	0.92	0.88	0.85
	4895	alpha/beta hydrolase fold	<	+(-)	+(±)	±		1.29	0.90	1.16	0.93	1.34	1.40
	4896	aromatic-ring-hydroxylating dioxygenase (<i>dxnA2</i>)	<	+(±)	+(±)	-		1.85	0.69	1.46	1.61	1.24	2.10
	4897	ring hydroxylating dioxygenase (<i>dxnA1</i>)	<	+(-)	+(±)	±	0.48	2.93	1.52	1.32	1.72	1.39	2.53
4902	4902	<i>dbfB</i> extradiol dioxygenase	>	+(+)	+(+)	+	0.37	4.41	2.35	0.79	0.46	0.46	0.67
4922-4925	4923	4-hydroxy-2-ketovaleate aldolase	<	+(+)	+(+)	+	0.13	11.47	0.84	0.93	0.57	0.61	0.55
5101-5102	5101	monooxygenase, FAD binding	<	+(+)	+(+)	+	56.05	17.27	0.80	0.94	0.68	0.52	1.10
	5102	gentisate 1,2-dioxygenase	<	+(+)	+(+)	+	41.98	11.31	0.82	1.19	1.16	1.19	1.16

1) Numbering according to Swit-annotation. Genbank Accession Nrs: NC_009511, NC_009507, NC_009508

2) +(+) , present in two replicate libraries; -(-), absent in two replicate libraries; ±, present at less then one-tenth of the abundance in the starting library.

3) Bold-type setting: statistically significant change (P<0.05) compared to control condition.

Specific gene expression in presence of DBF

In order to further discover genes for DBF metabolism, we used microarray analyses to examine RW1 genome-wide gene expression in the presence or absence of DBF and under a variety of cellular growth conditions. Comparison of all probe signals across all growth conditions showed two broad clusters of expression patterns, roughly representing the differences (almost opposite behavior) of growing in chemostat and in batch culture (Figure 1A). In comparison to PHE-grown cells, 525 RW1 genes were differentially expressed during short exposure to DBF in batch (Figure 1B, *SI file 1*), 920 genes in at least one time point of the transient exposure in chemostat (*SI file 1*) and 474 genes in the long exposure in batch cultures (*SI file 1*). A higher number of genes were shared between the short and transient DBF exposures (205 genes) than among the other conditions. A total of 109 genes were commonly differentially expressed to all the conditions of DBF exposure, among which 18% with increased, and 78% with decreased expression in DBF compared to control (Table S4). Globally speaking, the COG distribution of differentially expressed genes between the three growth conditions with DBF was similar, with notable exceptions of COG-C (*Energy production and conversion*), COG-K (*Transcription*), and COG-N to COG-Q being more abundant in DBF-grown cells (Figure 2).

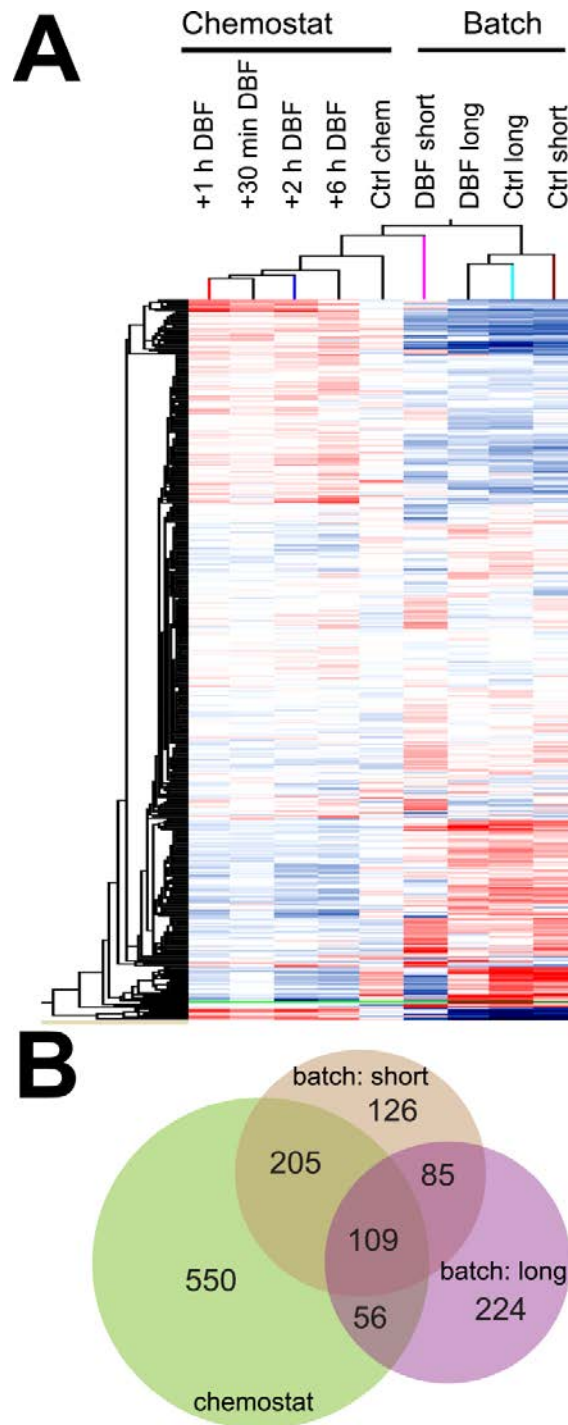


Figure 1. (A) Hierarchical clustering of RW1 gene expression over all conditions generated by GENESPRING GX. *Short* refers to the short DBF exposure in batch cultures, *Long* to cells grown in batch cultures on DBF, and *Chemostat* refers to the transient exposure to DBF in continuously grown cultures. (B) Venn diagram (Hulsen *et al.*, 2008) grouping the genes differentially expressed in the DBF exposure experiments compared to PHE-control conditions. Numbers represent genes exclusive for one condition, while the numbers in the intersections represent those occurring between two or more conditions.

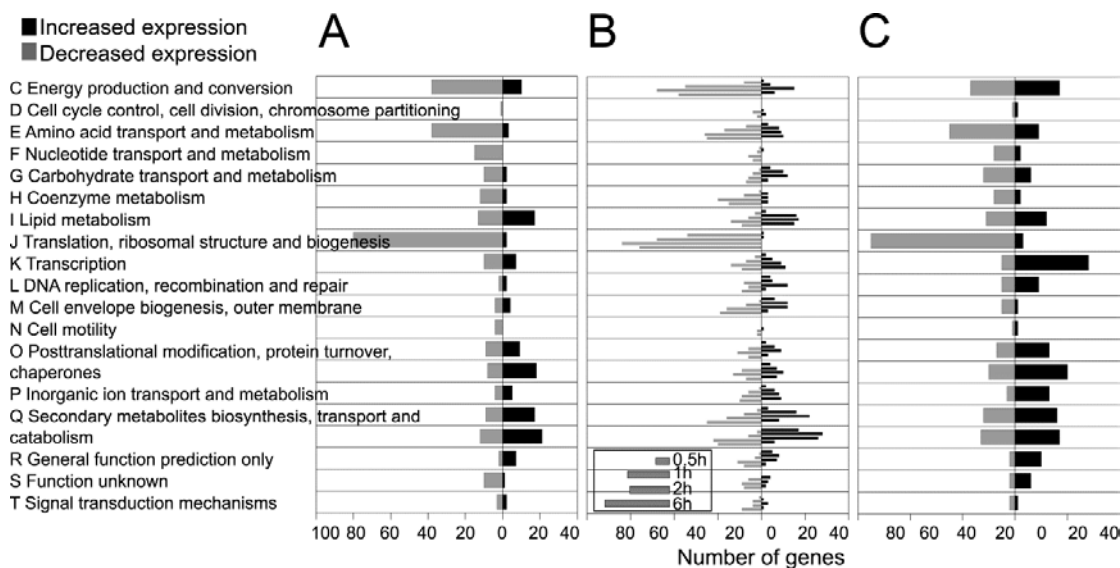


Figure 2. Proportional abundances of differentially expressed genes in conditions of DBF exposure compared to PHE, categorized per COG. (A) Short exposure to DBF in PHE-grown batch cultures, (B), transient exposure to DBF in chemostats, and (C) growth on DBF in batch culture.

Long exposure to DBF in batch cultures

Maximum specific growth rates of RW1 in batch culture were different on PHE, SAL or DBF, with $0.24 \pm 0.09 \text{ h}^{-1}$, $0.16 \pm 0.01 \text{ h}^{-1}$ and $0.20 \pm 0.03 \text{ h}^{-1}$, respectively (Figure 3). In comparison, 474 genes were differentially expressed between growth on PHE and DBF (8.6% of the whole genome), with 52% having increased and 48% decreased expression (*SI* file 1). Exponentially growing cells on SAL showed 231 differentially expressed genes compared to PHE (168 increased and 83 decreased), and 167 between SAL and DBF (87 up and 80 down). Among genes putatively involved in aromatic compound metabolism, most strikingly, the *paa* gene cluster (Swit_748 to Swit_762) was much lower expressed both during SAL and DBF growth compared to PHE (Table 1, Table S2). Conversely, a set of four closely located gene clusters showed increased expression in SAL (Swit_3083 to Swit_3094), but not in PHE or DBF. The Swit_3083-Swit_3094 clusters may thus constitute the pathway genes

specifically expressed during growth on SAL, although none of them appeared to be essential in the transposon scanning (Table S2). By contrast, the plasmid located *dxn* catabolic genes (between Swit_4897 and Swit_4930) had a decreased expression in SAL compared to DBF, but were overall higher expressed in DBF- than PHE-grown cells. This confirms that they are specifically expressed during growth on DBF. Of these, only Swit_4896 (*dxnA2*) and to a lesser extent Swit_4895 (*dxnB*) and Swit_4897(*dxnA1*) were essential for growth on DBF (Table S2). Finally, the two plasmid-located genes Swit_5101 and Swit_5102 (coding for a monooxygenase and gentisate 1,2-dioxygenase) had a strongly increased expression during growth on SAL and DBF, compared to growth on PHE. However, again these two genes are not essential for growth on SAL or DBF (Table 1, Table S2).

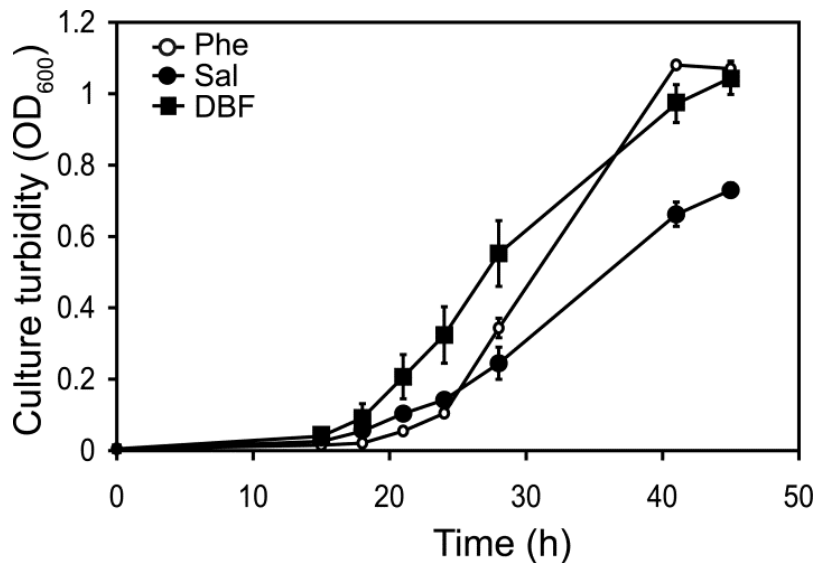


Figure 3. Growth of *S. wittichii* RW1 on minimal media (MM) with PHE (open circles), SAL (closed circles) or DBF (closed squares) as sole carbon and energy source.

Other notable differentially expressed genes included those for putative transport functions, such as aquaporin Z (Swit_0028) and a number of TonB-dependent like receptors. For example, the TonB-dependent like receptor DxnC (Swit_4894) was up to 6 times higher

expressed in DBF-grown cells as compared to PHE-grown cells. A putative efflux system encoded by Swit_3219-3222 was expressed up to 50 times higher in SAL- than DBF- or PHE-grown cells (SI file 1).

Short exposure to DBF in batch cultures

When RW1 cells were exponentially grown on PHE, after which they were exposed for 30 min to medium with DBF, 525 genes were differentially expressed compared to the control (9% of the whole genome). Sixty three percent of those had decreased and 37% displayed increased expression. A large proportion of differentially expressed genes (171 of 525) consisted of genes grouped in COG-E (*Amino acid metabolism*), COG-C (*Energy production and conversion*) and COG-J (*Translation, ribosomal structure and biogenesis*, Figure 2A). The expression of most of those (91%) decreased in DBF- compared to PHE-exposed cells, including genes for ribosomal proteins, tricarboxylic acid cycle (TCA), oxidative phosphorylation, tRNA-synthetases and elongation factors. This suggests temporary growth arrest and a major reconfiguration of the catabolic pathways.

The expression of 17 genes participating in lipid metabolism, including genes from the fatty acid metabolism pathway, were 2- to 16-fold higher in DBF- than PHE-exposed cells. Also, between 13- to 31-fold higher expression was detected of two genes coding for OmpA-domain containing proteins (Swit_1172 and Swit_2322) and of two genes for putative efflux pumps (Swit_3724 and Swit_3725). Four genes involved in cell motility (Swit_1264, Swit_1268, Swit_1270 and Swit_1458) were 2 to 5-fold lower expressed in the presence of DBF (Table 2).

Expression of genes involved in aromatic compound metabolism was clearly different during immediate exposure to DBF as compared to exponential growth on DBF (Table 1, Table S2). Several genes were not as highly expressed as during growth on DBF as sole carbon and energy source, such as Swit_2634-2636 (benzoate dioxygenase), the Swit_3055-3066 cluster, the plasmid-located Swit_4887-4897 cluster (with *dxnF*, *dxnC*, *dxnA1A2*) or Swit_4902 (*dbfB*). More strikingly, expression of Swit_4923, Swit_5101 and Swit_5102 was not detectable at all, whereas these genes were up to 17-fold higher expressed during growth on DBF. In contrast, expression of other genes appeared more clearly after immediate exposure to DBF, such as that of Swit_4278 (uncharacterized aromatic ring dioxygenase), Swit_3418 (putative extradiol dioxygenase), Swit_3086 (putative gentisate 1,2-dioxygenase), Swit_1827-1829, Swit_1848 (putative extradiol dioxygenase) and Swit_1861 (uncharacterized dioxygenase). Also expression of Swit_3793 (membrane transporter for aromatic hydrocarbons) was 21-fold higher in immediate response to DBF. Conversely, and in agreement with growth on DBF alone, expression of the *paa* pathway genes (Swit_748-758) was again much lower than in cells exposed to PHE.

Interestingly, several genes putatively involved in stress response displayed from 18- to 109-fold increased expression immediately after contact to DBF but not during growth on DBF, such as a catalase (Swit_3730) and two 1-cys-peroxiredoxin genes (Swit_3741 and Swit_3743). Also, and this more consistently throughout all growth conditions with DBF, an alternative ECF sigma 24 factor showed up to 10-fold higher expression (Swit_3924, Table 2).

Transient exposure to DBF in continuous cultures

To avoid the sudden starvation of cells upon transient exposure to DBF as in the batch shock exposure experiment, we grew RW1 in continuous culture with 5 mM PHE and under carbon-limited conditions. A sudden transition to DBF exposure was achieved by spiking the reactor medium instantaneously with saturating DBF amounts (5 mg/L) and simultaneously changing the medium inflow to one containing MM plus 5 mM PHE and saturating DBF. Under these conditions, a total of 920 genes was found to be differentially expressed in at least one time point evaluated (17% of the whole genome) with 154 genes appearing 30 min after exposure to DBF (53% with increased and 47% with decreased expression), 415 at 1 h (51% increased and 49% decreased), 663 at 2 h (38% up and 62% down) and then decreasing to 465 at 6 h (28% up and 72% down). A set of 48 genes expressed similarly across all time points, with 2 with increased and 46 with decreased expression (*SI file 1*).

A large proportion of differentially expressed genes (204) grouped in COG-C (*Energy production and conversion*), COG-E (*Amino acid transport and metabolism*), and COG-J (*Translation, ribosomal structure and biogenesis*). 81% of these displayed decreased and 19% increased expression (Figure 2B), suggesting again partial growth arrest but not as severe as in the batch shock exposure (*SI file 1*). Interestingly, a clear transition and an adaptive effect could be seen from the abundance of differentially expressed genes in the different COG categories over time after the start of exposure to DBF (Figure 2B). Among the COG-I (*Lipid metabolism*), 37 out of 54 genes increased expression, as well as three genes coding for OmpA-domain containing proteins (Swit_0853, Swit_2278 and Swit_2322). A cluster comprising three genes involved in trehalose synthesis (Swit_3608 to Swit_3610) temporarily increased expression in response to DBF. Again, several stress response genes, such as for a redoxin, catalases, 1-cys peroxiredoxins or DNA repair proteins transcribed up

to 13 times higher in response to DBF induction in chemostat (Table 2), as well as genes for three putative ECF sigma 24 factors (Swit_3924, Swit_3972 and Swit_4736).

Compared to the transient batch DBF shock and growth on DBF, the shift exposure to DBF in chemostat caused again a somewhat different transcription pattern of genes involved in aromatic compound metabolism (Table 1, Table S2). As examples, increased transcription of the cluster Swit_1827-1830 was detectable but this leveled out from early (30 min) to late transition (6 h). Cluster Swit_1848-1852 and Swit_1861 expressed more like batch growth on DBF but less than after batch shock exposure. Expression of the benzoate dioxygenase (Swit_2634-2636) increased similarly as during batch growth on DBF or after DBF shock. In contrast, expression of the cluster Swit_3055-3066 and of the *dxn* gene cluster (Swit_4887-4897) was no longer increased in chemostat (except *dxnA1* after 6 h). In contrast, expression of Swit_3863-3865 was higher in chemostat but not in the two other DBF exposure conditions. Consistently with the other two growth conditions with DBF, expression of the *paa* cluster was lower in chemostat-grown cells exposed to DBF compared to PHE, which was already detectable after 30 min.

Table 2. RW1 gene cluster representatives with significantly changed expression levels or proportional abundances in transposon libraries.

Swit Locus	Name	Tn library ¹			Expression, fold change ²					Chemostat shift		
		TN01	SAL	DBF	SAL/ PHE	SAL/ DBF	DBF shock	DBF /PHE	30 m	1 h	2 h	6 h
	Stress response											
0016	Redoxin domain-containing protein	+	+	+			0.99	1.75	2.51	5.13	3.76	2.69
0847	Glutathione S-transferase domain-containing protein	±	+	+			2.50	1.82	1.89	2.57	2.23	1.34
2245	Glutathione S-transferase domain-containing protein	+	+	+			3.10	1.56	3.16	4.72	4.11	2.28
3730	Catalase	+	+	+			206.50	1.87	1.16	2.73	10.6	4.89
3741	1-Cys peroxiredoxin	-	-	-			28.84	1.60	2.33	5.46	8.06	1.67
3743	1-Cys peroxiredoxin	+	+	+			102.54	1.83	1.44	2.89	12.7	3.12
3979	ATP-dependent DNA ligase	+	+	+			2.46	1.35	2.39	3.61	2.45	1.53
3982	DNA ligase D	+	+	+			3.25	1.05	3.56	7.31	5.43	2.68
4092	DNA repair protein Rada	±	-	±			1.22	0.89	1.39	1.72	2.20	2.31
4209	Glutathione-dependent formaldehyde-activating, GFA	+	-	+			3.56	1.82	3.05	5.54	4.32	2.41
5282	DNA ligase D	+	+	+			2.20	1.12	2.89	4.17	3.48	1.93
5311	Catalase	+	±	±			2.91	1.27	4.56	6.41	4.53	2.23
	DNA metabolic process											
0001	Chromosomal replication initiator protein DnaA	-	-	-			0.25	0.68	0.40	0.30	0.23	0.31
2767=3050=4 905=5124	IS4 family transposase	ND	ND	ND			4.24	4.44	1.21	0.90	1.04	1.26
4903	Transposase IS3/IS911 family protein	ND	ND	ND		0.17	1.26	10.50	0.83	0.51	0.36	0.52
4930	Transposase Tn3 family protein	+	+	+		0.46	1.96	1.89	0.95	0.93	1.16	0.96
5075	Transposase Tn3 family protein	+	+	+			2.50	2.00	1.47	1.33	1.19	1.23
5078	Transposase IS66	ND	ND	ND	2.14		2.48	2.33	0.97	1.05	1.34	1.46
5109	IS4 family transposase	+	+	+			2.64	1.99	1.16	1.24	1.16	1.30
	Transcription and translation											
0431	RNA polymerase sigma factor RpoD	-	-	-			0.29	0.54	0.62	0.65	0.63	0.85
1325	Ribosomal protein L17	+	-	+			0.09	0.53	0.35	0.25	0.19	0.13
1358	Ribosomal protein S12	-	-	-			0.02	0.27	0.47	0.34	0.23	0.20
3924	ECF subfamily RNA polymerase sigma 24 factor	+	+	+			10.36	2.26	4.27	4.28	2.58	1.16
3972	ECF subfamily RNA polymerase sigma 24 factor	-	-	-			1.54	1.17	0.92	1.09	1.47	2.57
4736	ECF subfamily RNA polymerase sigma 24 factor	±	-	+			1.27	0.94	1.27	1.42	1.49	2.25

1) +, present in the library; -, absent in the library; ±, present at less than one-tenth compared to the starting library; ND, no reads assignable (duplicated genes).

2) Bold-type setting: statistically significant change (P<0.05) compared to control condition.

Discussion

The major objective of this work was to study the global response of *S. wittichii* to exposure to DBF. Although DBF functions as a carbon and energy source for *S. wittichii* its behavior is complex, most of all because of the properties of DBF itself and secondly, because of numerous redundancies in aromatic compound catabolic pathways. In order to study this question, we used two different techniques: microarray analysis of genome-wide gene expression (Johnson *et al.*, 2008; 2011) and genome-wide transposon screening (Langridge *et al.*, 2009). At the low aqueous solubility of DBF we expected that the magnitude of direct gene expression difference would be quite small, as normally the compound's concentration or more precisely, the compound flux, determines the promoter response (Leveau *et al.*, 1999, Tecon and van der Meer, 2006). Moreover, gene induction magnitudes of catabolic pathways have been shown to be maximal during transition phases but level out when cells reach a new equilibrium (Leveau *et al.*, 1999). Finally, the inductive response of a carbon source is dependent on the simultaneous presence of other (possibly more preferred) carbon sources (Duetz *et al.*, 1994). We thus designed three different types of exposure of cells to DBF, all of which necessarily compromised one or other aspect of cellular physiology. In the first (named short exposure in batch) RW1 was grown on PHE as sole carbon and energy source into exponential phase in order to have actively growing cells. At the time of exposure, the cells were rapidly harvested and resuspended in the same medium with PHE or with DBF in order to maximize their potential response to the new carbon source. Although numerous genes including catabolic pathway genes increased expression during exposure to DBF compared to PHE, the cells clearly completely changed their physiology and went through a period of growth delay. Gene expression for central metabolic pathways, such as the TCA cycle, amino acid metabolism, but also for ribosomal

proteins, elongation factors, tRNA-synthetases and cell division was immediately declining. This suggests that the cells exposed to DBF during a short period cannot immediately gain sufficient energy from the available DBF in solution and go through a period of starvation and stress response. However, this experimental condition is still important, because it mimicks what might happen when cells are inoculated from laboratory-grown culture into a bioremediation site.

In the second type of experiment (transient exposure in chemostat) RW1 cells were growing continuously under carbon limiting conditions with PHE, in order to make sure they would not suffer energy losses during transition. As a consequence of maintaining carbon limiting conditions, the actual PHE concentration in the medium is very low and the cells were expected to react instantaneously to a newly added carbon source (DBF). Indeed, we observed a clear transient response (Figure 2B) implicating a large number of genes, surprising given the controlled conditions of chemostat operation. Even during these controlled growth conditions, the cells experienced DBF not just as a new carbon substrate but rather as a stress factor, necessitating the immediate differential regulation of specific stress-response genes. We detected increased expression of genes for catalases, peroxiredoxins and glutathione-s-transferases, which form a known strategy for the detoxification of xenobiotics and reactive oxygen species (Domínguez-Cuevas *et al.*, 2006, Dayer *et al.*, 2008). Genes implicated in DNA repair, chaperones and OmpA-domain containing proteins, a putative sensor of membrane integrity (Wang, 2002), also increased expression. These responses are similar to what has been observed when exposing *Pseudomonas putida* KT2440, or *P. putida* DOT-T1E to the aromatic hydrocarbons toluene and pentachlorophenol (Segura *et al.*, 2005, Domínguez-Cuevas *et al.*, 2006, Muller *et al.*, 2007). Both the short exposure to DBF in batch cultures and in chemostat also led to specific

differential expression of the RpoD sigma factor and of alternative ECF factors (Table 2). ECF sigma 24 factors have been implicated in the response of cells to perturbations such as extracytoplasmic protein miss folding, heat shock, oxidative or solvent stress (Mecenas *et al.*, 1993; de las Peñas *et al.*, 1997; Testerman *et al.*, 2002; Domínguez-Cuevas *et al.*, 2006), and could play an important role in the adaptability of *S. wittichii*, the genome of which codes for 14 different putative ECF sigma 24 factors. Previously, Johnson *et al.* (2011) reported an increase in expression of two ECF sigma 24 genes (Swit_3836 and Swit_3924) in RW1 upon exposure to water potential decrease by NaCl, the expression of one of which (Swit_3924) also increased during shock exposures of cells to DBF (Table 2). In a similar way, *B. xenovorans* LB400 and *P. putida* KT2440 have been found to induce ECF sigma 24 in response to hydrocarbons such as benzoate and toluene (Denef *et al.*, 2006; Domínguez-Cuevas *et al.*, 2006).

In the third experiment (long exposure in batch) RW1 cells are grown in batch either on PHE, SAL or on DBF as sole carbon source, and in all cases harvested at the same culture turbidity in exponential phase. Stress response gene transcription under those conditions was not different between DBF or PHE-grown cells, indicating that the cells adapt after a while to metabolize DBF without stress.

Perhaps surprisingly, in the light of typical linear pathway thinking from work on catabolic pathways in pseudomonads, expression of pathways for aromatic compound metabolism even with a single compound (DBF) involved a myriad of possibilities. This suggests, first of all, that *S. wittichii* has an extreme redundancy in its use of aromatic compound metabolism (Figure 4). This was evident from the finding that actually very few transposon insertions completely abolished growth on DBF (Table 1, Table S2). Secondly,

the pathways seem to operate under distinct growth conditions and, not unlikely, in temporarily different stages (Table 1, Table S2). Among the few exceptions to this were two clusters (Swit_1847-1852, Swit_1860-1861), to a lesser extent Swit_2634-2636 (benzoate dioxygenase), and Swit_3864-3866 (homogentisate dioxygenase) that were always expressed higher in presence of DBF, irrespective of the growth conditions. In contrast, increased expression of the typical *dxn* genes discovered so far was only detectable during growth on DBF, but not in the two other conditions. This situation of pathway parallelism is analogous to the existence of three different pathways for benzoate metabolism in *Burkholderia xenovorans*, that can operate under different conditions in degradation of (polychlorinated) biphenyls and chlorobenzoates (Denef *et al.*, 2006).

Which genes can we finally conclude are 'implicated' in DBF degradation? Although salicylate has been postulated as an intermediate for DBF degradation, the pathway that is most highly and specifically expressed during SAL growth (Swit_3086-3095) is not particularly induced during DBF growth (Table 1, Table S2, Figure 4). More likely are two pathway branches that would lead to gentisate from salicylate (Swit_5101/5102) or to catechol (Swit_3056/3057, Figure 4). Both these gene groups are induced on DBF, although their precise function cannot be sufficiently predicted from sequence comparisons only. The other major metabolite formed from DBF is 2-hydroxy-2,4-pentadienoate, which could be further processed to acetyl-CoA through activity of the enzymes encoded by the Swit_4923-4925 cluster (Figure 4). Although Swit_4923-4925 were higher transcribed on DBF but not on SAL, they do not seem to be essential for growth on DBF, since transposon insertions were detected in all of them. At least three alternative pathways seem to be encoded on the RW1 genome (Figure 4), and, interestingly, transposon insertions in one of those genes (Swit_1639) were never recovered. This suggests that the Swit_1639-1641 pathway is somehow important, although the genes are not specifically transcribed to higher levels

during growth on DBF compared to SAL or PHE. It is also possible that bioinformatic functionality predictions here are incorrect because of confusion and close sequence homology between the paralogous enzymes 4-oxalocrotonate-decarboxylase and 2-hydroxy-2,4-pentadienoate hydratase (Figure 4). Growth on SAL alone leads to increased expression of a different set of metabolic pathway genes than on DBF, suggesting different intermediate processing via homoprotocatechuate and/or 4-hydroxyphenylpyruvate (Figure 4). Such pathways, however, are currently incomplete with no known links between salicylate and homoprotocatechuate.

In conclusion, we find that the DBF 'metabolome' in *S. wittichii* is surprisingly complex with numerous parallel and redundant branches. The strategy of parallelism and redundancy may have specific ecological advantages in certain niches with perhaps multiple structurally similar substrates, but may be too costly to maintain competitively in environments with abundance of singular substrates that may favor bacteria with single pathway induction. Possibly, the parallelism and redundancy suggested by our 'population' data suggest are in reality split across individual cells with a high degree of metabolic heterogeneity.

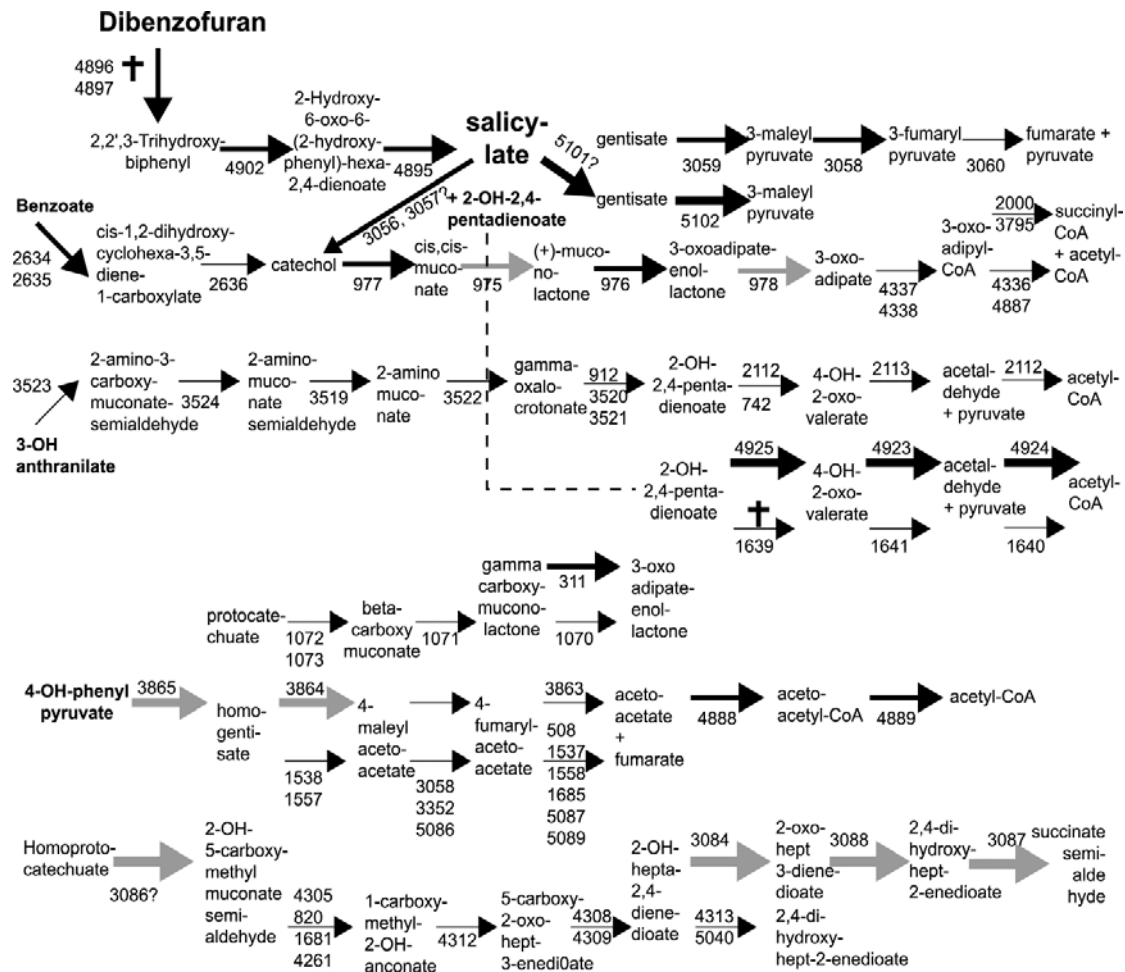


Figure 4. Compilation of possible encoded aromatic compound degradation pathways in *S. wittichii* RW1 with relevance to either DBF or SAL metabolism. Numbers below arrows correspond to gene names (e.g., Swit_5101). Thick arrows indicate gene induction during growth on SAL or DBF compared to PHE. Grey arrows point to induction on SAL only. Crosses indicate genes in which no transposon insertions were found after 50 generations growth on DBF. Pathway predictions were done using KEGG and NCBI.

Acknowledgments

This work was supported by grant KBBE-211684 from the European Commission within the FP7 Framework Programme. The authors thank Caroline Harwood and Somsak Phattarasukoi from the University of Washington for sharing the Xpression Pipeline, and their generous instructions.

References

- Aly HAH, Huu NB, Wray V, Junca H and Pieper DH** (2008) Two angular dioxygenases contribute to the metabolic versatility of dibenzofuran-degrading *Rhodococcus sp.* Strain HA01. *Applied and Environmental Microbiology* 74: 3812-3822.
- Armengaud J and Timmis KN** (1997) Molecular characterization of *fdx1*, a *putidaredoxin*-type [2Fe-2S] ferredoxin able to transfer electrons to the dioxin dioxygenase of *Sphingomonas sp.* RW1. *European Journal of Biochemistry* 247: 833-842.
- Armengaud J and Timmis KN** (1998) The reductase RedA2 of the multi-component dioxin dioxygenase system of *Sphingomonas sp.* RW1 is related to class-I cytochrome P450-type reductases. *European Journal of Biochemistry* 253: 437-444.
- Armengaud J, Gaillard J and Timmis KN** (2000) A second [2Fe-2S] ferredoxin from *Sphingomonas sp.* strain RW1 can function as an electron donor for the dioxin dioxygenase. *Journal of Bacteriology* 182: 2238-2244.
- Armengaud J, Happe B and Timmis KN** (1998) Genetic analysis of dioxin dioxygenase of *Sphingomonas sp.* strain RW1: catabolic genes dispersed on the genome. *Journal of Bacteriology* 180: 3954-3966.
- Armengaud J, Timmis KN and Wittich R-M** (1999) A functional 4-hydroxysalicylate/hydroxyquinol degradative pathway gene cluster is linked to the initial Dibenzo-*p*-dioxin pathway genes in *Sphingomonas sp.* strain RW1. *Journal of Bacteriology* 181: 3452-3461.
- Aso Y, Miyamoto Y, Mine Harada K, Momma, K, Kawai S, Hashimoto W, Mikami B, Murata K** (2006) Engineered membrane superchannel improves bioremediation potential of dioxin-degrading bacteria. *Nature Biotechnology* 24: 188-189.
- Basta T, Keck A, Klein J and Stolz A** (2004) detection and characterization of conjugative degradative plasmids in xenobiotic-degrading *Sphingomonas* Strains. *Journal of Bacteriology*. 186: 3862-3872.
- Beck H, Dross A and Mathar W** (1994) PCDD and PCDF exposure and levels in humans in Germany. *Environmental Health Perspectives* 102: 173-185.
- Bowes GW, Simoneit BR, Burlingame AL, de Lappe BW and Risebrough RW** (1973) The search for chlorinated dibenzofurans and chlorinated dibenzodioxins in wildlife populations showing elevated levels of embryonic death. *Environmental Health Perspectives* 5: 191-198.

- Bunz PV and Cook AM** (1993) Dibenzofuran 4,4a-dioxygenase from *Sphingomonas sp.* strain RW1: angular dioxygenation by a three-component enzyme system. *Journal of Bacteriology* 175: 6467-6475.
- Bünz PV, Falchetto R and Cook AM** (1993) Purification of two isofunctional hydrolases (EC 3.7.1.8) in the degradative pathway for dibenzofuran in *Sphingomonas sp.* strain RW1. *Biodegradation* 4: 171-178.
- Buser H-R, Rappe C and Bergqvist P-A** (1985) Analysis of polychlorinated Dibenzofurans, Dioxins and related compounds in environmental samples. *Environmental Health Perspectives* 60: 293-302.
- Cerniglia CE, Morgan JC and Gibson DT** (1979) Bacterial and fungal oxidation of dibenzofuran. *Biochemical Journal* 180: 175-170.
- Dayer Rg, Fischer BB, Eggen RIL and Lemaire SpD** (2008) The peroxiredoxin and glutathione peroxidase families in *Chlamydomonas reinhardtii*. *Genetics* 179: 41-57.
- De Las Peñas A, Connolly L and Gross CA** (1997) SigmaE is an essential sigma factor in *Escherichia coli*. *Journal of Bacteriology* 179: 6862-6864.
- Denef VJ, Klappenbach JA, Patrauchan MA, Patrauchan MA, Florizone C, Rodrigues JLM, Tsoi TV, Verstraete W, Eltis LD and Tiedje JM** (2006) Genetic and genomic insights into the role of benzoate-catabolic pathway redundancy in *Burkholderia xenovorans* LB400. *Applied and Environmental Microbiology* 72: 585-595.
- Domínguez-Cuevas P, Gonzalez-Pastor J-E, Marques S, Ramos JL and de Lorenzo V** (2006) Transcriptional tradeoff between metabolic and stress-response programs in *Pseudomonas putida* KT2440 cells exposed to toluene. *Journal of Biological Chemistry* 281: 11981-11991.
- Duetz WA, Marques S, de Jong C, Ramos JL and van Andel JG** (1994) Inducibility of the TOL catabolic pathway in *Pseudomonas putida* (pWW0) growing on succinate in continuous culture: evidence of carbon catabolite repression control. *Journal of Bacteriology* 176: 2354-2361.
- Fortnagel P, Harms H, Wittich RM, Krohn, S, Meyer H, Sinnwell V, Wilkes H and Francke W** (1990) Metabolism of dibenzofuran by *Pseudomonas sp.* strain HH69 and the mixed culture HH27. *Applied and Environmental Microbiology* 56: 1148-1156.
- Gai Z, Yu B, Li L, Wang Y, Ma C, Feng J, Deng Z and Xu P** (2007) Cometabolic degradation of dibenzofuran and dibenzothiophene by a newly isolated carbazole-degrading *Sphingomonas sp.* strain. *Applied and Environmental Microbiology* 73: 2832-2838.

Halden RU, Halden BG and Dwyer DF (1999) Removal of Dibenzofuran, Dibenzo-*p*-dioxin, and 2-Chlorodibenzo-*p*-dioxin from soils inoculated with *Sphingomonas sp.* strain RW1. Applied and Environmental Microbiology 65: 2246-2249.

Happe B, Eltis LD, Poth H, Hedderich R and Timmis KN (1993) Characterization of 2,2',3-trihydroxybiphenyl dioxygenase, an extradiol dioxygenase from the dibenzofuran- and dibenzo-*p*-dioxin-degrading bacterium *Sphingomonas sp.* strain RW1. Journal of Bacteriology 175: 7313-7320.

Hulsen T, de Vlieg J and Alkema W (2008) BioVenn - a web application for the comparison and visualization of biological lists using area-proportional Venn diagrams.

Johansen HR, Alexander J, Rosslund OJ, Planting S, Lovik M, Gaarder PI, Gdynia W, Bjerve KS and Becher G (1996) PCDDs, PCDFs, and PCBs in human blood in relation to consumption of crabs from a contaminated Fjord area in Norway. Environmental health perspectives 104: 756-764.

Johnson D, Coronado E, Moreno-Forero S, Heipieper H and van der Meer J (2011) Transcriptome and membrane fatty acid analyses reveal different strategies for responding to permeating and non-permeating solutes in the bacterium *Sphingomonas wittichii*. BMC Microbiology 11: 250.

Johnson DR, Brodie EL, Hubbard AE, Andersen GL, Zinder SH and Alvarez-Cohen L (2008) Temporal transcriptomic microarray analysis of "*Dehalococcoides ethenogenes*" strain 195 during the transition into stationary phase. Applied and Environmental Microbiology 74: 2864-2872.

Kubota M, Kawahara K, Sekiya K, Uchida T, Hattori Y, Futamata H and Hiraishi A (2005) *Nocardioides aromaticivorans sp. nov.*, a dibenzofuran-degrading bacterium isolated from dioxin-polluted environments. Systematic and Applied Microbiology 28: 165-174.

Langridge GC, Phan MD, Turner DJ, Perkins TT, Parts L, Haase J, Charles I, Maskell DJ, Peters SE, Dougan G, Wain J, Parkhill J and Turner AK (2009) Simultaneous assay of every *Salmonella* Typhi gene using one million transposon mutants. Genome Research 19: 2308-2316.

Larsen R, Wilson M, Guss A and Metcalf W (2002) Genetic analysis of pigment biosynthesis in *Xanthobacter autotrophicus* Py2 using a new, highly efficient transposon mutagenesis system that is functional in a wide variety of bacteria. Archives of Microbiology 178: 193-201.

Leveau JHJ, König F, Fuchsli H, Werlen C and Van Der Meer JR (1999) Dynamics of multigene expression during catabolic adaptation of *Ralstonia eutropha* JMP134 (pJP4) to the herbicide 2,4-dichlorophenoxyacetate. Molecular Microbiology 33: 396-406.

- Li Q, Wang X, Yin G, Gai Z, Tang H, Ma C, Deng Z and Xu P** (2009) New metabolites in dibenzofuran cometabolic degradation by a biphenyl-cultivated *Pseudomonas putida* strain B6-2. *Environmental Science and Technology* 43: 8635-8642.
- McNulty WP** (1985) Toxicity and fetotoxicity of TCDD, TCDF and PCB isomers in *Rhesus Macaques* (*Macaca mulatta*). *Environmental Health Perspectives* 60: 77-88.
- Mecas J, Rouviere PE, Erickson JW, Donohue TJ and Gross CA** (1993) The activity of sigma E, an *Escherichia coli* heat-inducible sigma-factor, is modulated by expression of outer membrane proteins. *Genes and Development* 7: 2618-2628.
- Megharaj M, Wittich RM, Blasco R, Pieper DH and Timmis KN** (1997) Superior survival and degradation of dibenzo-*p*-dioxin and dibenzofuran in soil by soil-adapted *Sphingomonas sp.* strain RW1. *Applied Microbiology and Biotechnology* 48: 109-114.
- Miller TR, Delcher AL, Salzberg SL, Saunders E, Detter JC and Halden RU** (2010) Genome sequence of the Dioxin-Mineralizing bacterium *Sphingomonas wittichii* RW1. *Journal of Bacteriology* 192: 6101-6102.
- Monna L, Omori T and Kodama T** (1993) Microbial degradation of dibenzofuran, fluorene, and dibenzo-*p*-dioxin by *Staphylococcus auriculans* DBF63. *Applied and Environmental Microbiology* 59: 285-289.
- Muller JF, Stevens AM, Craig J and Love NG** (2007) transcriptome analysis reveals that multidrug efflux genes are upregulated to protect *Pseudomonas aeruginosa* from pentachlorophenol stress. *Applied and Environmental Microbiology* 73: 4550-4558.
- Müller TA, Byrde SM, Werlen C, van der Meer JR and Kohler HP** (2004) Genetic analysis of phenoxyalkanoic acid degradation in *Sphingomonas herbicidovorans* MH. *Applied and Environmental Microbiology* 70: 6066-6075.
- Pluim HJ, Vijlder JJMd, Olie K, Kok, JH, Vulsma T, van Tijn D A, van der Slikke JW and Koppe JG** (1993) Effects of pre- and postnatal exposure to chlorinated dioxins and furans on human neonatal thyroid hormone concentrations. *Environmental Health Perspectives* 101: 504-508.
- Seah SYK, Ke J, Denis G, Horsman GP, Fortin PD, Whiting CJ and Eltis LD** (2007) Characterization of a C-C bond hydrolase from *Sphingomonas wittichii* RW1 with novel specificities towards polychlorinated biphenyl metabolites. *Journal of Bacteriology* 189: 4038-4045.
- Segura A, Godoy P, van Dillewijn P, Hurtado A, Arroyo N, Santacruz S and Ramos JL** (2005) Proteomic analysis reveals the participation of energy- and stress-related proteins in the response of *Pseudomonas putida* DOT-T1E to Toluene. *Journal of Bacteriology* 187: 5937-5945.

- Soong D-K and Ling Y-C** (1997) Reassessment of PCDD/DFs and Co-PCBs toxicity in contaminated rice-bran oil responsible for the disease “Yu-Cheng”. *Chemosphere* 34: 1579-1586.
- Tecon R, Wells M and Van Der Meer JR** (2006) A new green fluorescent protein-based bacterial biosensor for analysing phenanthrene fluxes. *Environmental Microbiology* 8: 697-708.
- Testerman TL, Vazquez-Torres A, Xu Y, Jones-Carson J, Libby SJ and Fang FC** (2002) The alternative sigma factor σ E controls antioxidant defenses required for *Salmonella* virulence and stationary-phase survival. *Molecular Microbiology* 43: 771-782.
- Wang Y** (2002) The Function of OmpA in *Escherichia coli*. *Biochemical and Biophysical Research Communications*, 29: 396-401.
- Wilkes H, Wittich R, Timmis KN, Fortnagel P and Francke W** (1996) Degradation of chlorinated Dibenzofurans and Dibenzo-*p*-dioxins by *Sphingomonas sp.* strain RW1. *Applied and Environmental Microbiology* 62: 367-371.
- Wittich RM, Strömpl C, Moore ERB, Blasco R and Timmis KN** (1999) Interaction of *Sphingomonas* and *Pseudomonas* strains in the degradation of chlorinated dibenzofurans. *Journal of Industrial Microbiology and Biotechnology* 23: 353-358.
- Wittich RM, Wilkes H, Sinnwell V, Francke W and Fortnagel P** (1992) Metabolism of dibenzo-*p*-dioxin by *Sphingomonas sp.* strain RW1. *Applied and Environmental Microbiology* 58: 1005-1010.
- Yoshihara Si, Nagata K, Yoshimura H, Kuroki H and Masuda Y** (1981) Inductive effect on hepatic enzymes and acute toxicity of individual polychlorinated dibenzofuran congeners in rats. *Toxicology and Applied Pharmacology* 59: 580-588.
- Zitko V, Wildish DJ, Hutzinger O and Choi PM** (1973) Acute and chronic oral toxicity of chlorinated dibenzofurans to salmonid fishes. *Environmental Health Perspectives* 5: 187-189.

Supplementary information

Table S1. Genes without any detectable, or with one-tenth or less transposon insertions in the DBF-library compared to time 0 (TN0), but with at least 30 reads in TN0.

locus ¹	product	COG category	Log2 Expression ratio compared to PHE-grown cells ²					Tn RATIO DBF /TN0	
			DBF shock	DBF batch	Chemostat 30 m	1 h	2 h		6 h
Swit_0033	Phosphoribosylglycinamide formyltransferase	F	0.398					0.000	
Swit_0037	Polyphosphate kinase	P		2.187				0.000	
Swit_0039	Ppx/gppa phosphatase	FP	2.065					0.000	
Swit_0166	Hypothetical protein	S						0.000	
Swit_0169	P-type conjugative transfer protein trbg	U						0.000	
Swit_0179	Hypothetical protein	S						0.000	
Swit_0203	Endonuclease III / DNA-(apurinic or apyrimidinic site) lyase	L	0.445				2.090	0.000	
Swit_0207	NAD-dependent deacetylase	K						0.000	
Swit_0222	Phage integrase family protein	L						0.000	
Swit_0276	Hypothetical protein	X23						0.000	
Swit_0284	Xylose isomerase domain-containing protein	G						0.000	
Swit_0291	NADH:flavin oxidoreductase	C				2.267		0.000	
Swit_0371	Hypothetical protein	I						0.000	
Swit_0444	Hypothetical protein	X34	2.491		2.465	3.090		0.000	
Swit_0449	Polysaccharide biosynthesis protein	R						0.000	
Swit_0614	NUDIX hydrolase	F						0.000	
Swit_0641	XRE family transcriptional regulator	K						0.000	
Swit_0651	Excinuclease ABC subunit C	L						0.000	
Swit_0658	Hypothetical protein	X48					4.006	0.000	
Swit_0671	Hypothetical protein	X49						0.000	
Swit_0739	Hypothetical protein	S						0.000	
Swit_0750	3-hydroxyacyl-coa dehydrogenase	I	0.112		0.475	0.465	0.378	0.476	0.000
Swit_0756	Phenylacetate-coa oxygenase subunit paaj	R							0.000
Swit_0760	Tetr family transcriptional regulator	K	0.114	0.222	0.202	0.129	0.103	0.134	0.000
Swit_0814	Hypothetical protein	S							0.000
Swit_0842	FAD-binding molybdopterin dehydrogenase	C							0.000
Swit_0855	XRE family transcriptional regulator	K							0.000
Swit_0880	hypothetical protein	S					3.606	0.000	
Swit_0923	ECF subfamily RNA polymerase sigma-24 factor	K						0.000	

Swit_0949	Sulfite dehydrogenase (cytochrome) subunit sora apoprotein	R							0.000
Swit_1020	Hypothetical protein	X67							0.000
Swit_1110	DGPFAETKE family protein	S					2.299		0.000
Swit_1154	RND efflux system outer membrane lipoprotein	MU							0.000
Swit_1165	Asnc family transcriptional regulator	K	2.300						0.000
Swit_1213	Hypothetical protein	S							0.000
Swit_1309	Nucleotidyl transferase	M	0.497	0.443					0.000
Swit_1389	GTP-dependent nucleic acid-binding protein engd	J	0.171	0.331		0.406	0.389	0.244	0.000
Swit_1508	17 kda surface antigen	X112	3.230	2.008					0.000
Swit_1519	Diguanylate cyclase/phosphodiesterase	T							0.000
Swit_1579	Hypothetical protein	X118							0.000
Swit_1594	Hypothetical protein	X121							0.000
Swit_1614	Hypothetical protein	S							0.000
Swit_1639	4-oxalocrotonate decarboxylase	Q							0.000
Swit_1684	FAD-binding monooxygenase	HC							0.000
Swit_1704	Nitrate/sulfonate/bicarbonate ABC transporter periplasmic component-like protein	P							0.000
Swit_1716	Peptidyl-prolyl cis-trans isomerase	O							0.000
Swit_1720	Cupin	S				2.033			0.000
Swit_1732	Tetr family transcriptional regulator	K	3.147						0.000
Swit_1759	Ferredoxin	C	2.029						0.000
Swit_1760	L-carnitine dehydratase/bile acid-inducible protein F	C							0.000
Swit_1766	Isochorismatase hydrolase	Q					2.133	2.065	0.000
Swit_1786	Hypothetical protein	X128		2.009					0.000
Swit_1795	Cbb3-type cytochrome oxidase maturation protein	P							0.000
Swit_1915	Hypothetical protein	S				2.252			0.000
Swit_1953	RND family efflux transporter MFP subunit	M							0.000
Swit_1967	Phzf family phenazine biosynthesis protein	R							0.000
Swit_1975	Arac family transcriptional regulator	K							0.000
Swit_2017	Protein tyrosine/serine phosphatase	T							0.000
Swit_2134	Hypothetical protein	S							0.000
Swit_2200	Hypothetical protein	X166							0.000
Swit_2213	Hypothetical protein	X177							0.000
Swit_2214	Hypothetical protein	X178						2.025	0.000
Swit_2457	Cytidylate kinase	F	0.193	0.415					0.000
Swit_2649	IS4 family transposase	L					0.476		0.000
Swit_2680	Double-strand break repair protein addb	L							0.000
Swit_2681	Double-strand break repair helicase adda	L							0.000
Swit_2709	Camphor resistance protein crcb	D							0.000

Swit_2710	Ribosomal large subunit pseudouridine synthase C	J							0.000
Swit_2722	NADPH-glutathione reductase	C	0.406						0.000
Swit_2723	Glucose-6-phosphate isomerase	G							0.000
Swit_2785	Glycerophosphoryl diester phosphodiesterase	C						0.423	0.000
Swit_2813	Hypothetical protein	S	0.164			0.400	0.420		0.000
Swit_2835	Transcription termination factor Rho	K	0.187		0.461	0.376	0.275		0.000
Swit_2878	Hypothetical protein	S	0.386						0.000
Swit_2913	Iron-sulfur cluster assembly accessory protein	S							0.000
Swit_2929	Miab-like trna modifying enzyme	J	0.478						0.000
Swit_2982	NADH-ubiquinone/plastoquinone oxidoreductase subunit 3	C	0.097	0.444	0.441	0.360	0.287	0.255	0.000
Swit_2984	NADH (or F420H2) dehydrogenase subunit C	C	0.143	0.471		0.453	0.407	0.360	0.000
Swit_3011	Hypothetical protein	S							0.000
Swit_3174	Hypothetical protein	P					2.120	2.022	0.000
Swit_3342	Bifunctional sulfate adenylyltransferase subunit 1/adenylylsulfate kinase	P	4.717						0.000
Swit_3461	Hypothetical protein	S							0.000
Swit_3588	Lysr family transcriptional regulator	K							0.000
Swit_3679	Hypothetical protein	K							0.000
Swit_3684	Hypothetical protein	S						2.843	0.000
Swit_3744	Beta-lactamase domain-containing protein	R	6.056				4.384		0.000
Swit_3797	Acyl-coa dehydrogenase domain-containing protein	I	11.591		2.845	2.900	3.022	3.705	0.000
Swit_3819	Transcription elongation factor nusa	K	0.319						0.000
Swit_3848	Rnase E	J				0.495	0.417	0.409	0.000
Swit_3879	Cytochrome C oxidase assembly protein	O	0.172				0.349	0.217	0.000
Swit_3913	Peptidase M23B	M	0.368		0.234	0.108	0.153	0.143	0.000
Swit_3954	Hypothetical protein	S							0.000
Swit_3962	Hypothetical protein	X304	0.260						0.000
Swit_3988	Heme exporter protein ccmc	O							0.000
Swit_3991	Periplasmic protein thiol--disulfide oxidoreductase dsbe	CO						0.444	0.000
Swit_4030	Orn/DAP/Arg decarboxylase 2	E							0.000
Swit_4041	Trna pseudouridine synthase A	J					2.443		0.000
Swit_4050	Deoxycytidine triphosphate deaminase	F	0.422			0.417	0.382	0.444	0.000
Swit_4117	Metal-dependent amidase/aminoacylase/carboxypeptidase-like protein	R							0.000
Swit_4152	Hypothetical protein	S							0.000
Swit_4163	Glutathione S-transferase domain-containing protein	O							0.000
Swit_4164	3-oxoacid coa-transferase subunit A	I	2.247						0.000
Swit_4177	Helix-turn-helix domain-containing protein	K							0.000
Swit_4182	Glyoxalase/bleomycin resistance protein/dioxygenase	R							0.000
Swit_4218	Tetr family transcriptional regulator	K					0.397	0.412	0.000

Swit_4250	Glutathione S-transferase domain-containing protein	O								0.000
Swit_4270	Dioic acid aldolase	G		0.362						0.000
Swit_4385	Hypothetical protein	X330	8.277		2.705	3.083	2.799	2.426		0.000
Swit_4391	Transglutaminase domain-containing protein	E			2.608	4.961	4.017	2.237		0.000
Swit_4449	Hypothetical protein	350								0.000
Swit_4463	Hypothetical protein	X357								0.000
Swit_4481	Hypothetical protein	S								0.000
Swit_4518	Glucose-methanol-choline oxidoreductase	E								0.000
Swit_4529	Hypothetical protein	S	3.798							0.000
Swit_4533	Glycoside hydrolase family protein	G	3.122							0.000
Swit_4547	Hypothetical protein	S						2.448		0.000
Swit_4596	Cytochrome oxidase assembly	O								0.000
Swit_4622	Hypothetical protein	R	3.265							0.000
Swit_4653	Hypothetical protein	X379					2.119			0.000
Swit_4666	UDP-N-acetylglucosamine 2-epimerase	M					0.445	0.460		0.000
Swit_4685	D-3-phosphoglycerate dehydrogenase	HE	0.076	0.301		0.408	0.296	0.255		0.000
Swit_4687	Class I cytochrome c	C	0.182		0.484	0.412	0.323	0.324		0.000
Swit_4704	Antibiotic biosynthesis monooxygenase	S	4.903			2.048				0.000
Swit_4799	Integral membrane sensor signal transduction histidine kinase	T								0.000
Swit_4808	Limonene-1	R								0.000
Swit_4827	Surface antigen (D15)	M								0.000
Swit_4844	Grea/greb family elongation factor	K			2.824	3.605	2.954			0.000
Swit_4872	Hypothetical protein	X399	3.010							0.000
Swit_4896	Aromatic-ring-hydroxylating dioxygenase	Q						2.096		0.000
Swit_5016	Hypothetical protein	L						2.126		0.000
Swit_5148	Hypothetical protein	S				0.432				0.000
Swit_5164	Hypothetical protein	X424								0.000
Swit_5165	Hypothetical protein	X425								0.000
Swit_5178	Hypothetical protein	S	2.161							0.000
Swit_5230	Hypothetical protein	Z								0.000
Swit_5296	Response regulator receiver protein	T								0.000
Swit_5312	Short-chain dehydrogenase/reductase SDR	R								0.000
Swit_5316	Hypothetical protein	X462	0.285		0.418	0.358	0.343	0.302		0.000
Swit_5395	Hypothetical protein	X482								0.000
<u>Less than tenfold present in the transposon library DBF versus time 0</u>										
Swit_0303	Hypothetical protein	X25								0.001
Swit_0011	Phage integrase family protein	L								0.001
Swit_0016	Redoxin domain-containing protein	O			2.506	5.136	3.767	2.687		0.095
Swit_0019	Group 1 glycosyl transferase	M								0.047

Swit_0044	Hypothetical protein	S	2.302	3.387	2.248	0.007
Swit_0070	N-acetylmuramoyl-L-alanine amidase	V				0.020
Swit_0143	Polysaccharide biosynthesis protein	R				0.001
Swit_0144	Hypothetical protein	S				0.054
Swit_0159	Hypothetical protein	X10			0.467	0.003
Swit_0161	P-type conjugative transfer atpase trbb	U				0.086
Swit_0175	Luxr family transcriptional regulator	TK				0.022
Swit_0176	ECF subfamily RNA polymerase sigma-24 factor	K				0.002
Swit_0178	Conjugal transfer relaxase traA	L				0.011
Swit_0182	Type IV secretory pathway protease traf-like protein	OU				0.007
Swit_0190	Hypothetical protein	S				0.074
Swit_0199	AAA atpase	R				0.005
Swit_0242	Cyclase/dehydrase	I			0.491	0.007
Swit_0245	Nifr3 family TIM-barrel protein	J	0.299			0.063
Swit_0247	Fis family nitrogen metabolism transcriptional regulator ntrC	T		0.405	0.289	0.407
Swit_0270	Binding-protein-dependent transport system inner membrane protein	P				0.013
Swit_0307	Hypothetical protein	S				0.004
Swit_0316	Alcohol dehydrogenase	CR				0.006
Swit_0325	3-ketosteroid-delta-1-dehydrogenase	C				0.012
Swit_0344	Enoyl-coa hydratase	I				0.051
Swit_0349	Hypothetical protein	S				0.002
Swit_0353	Hypothetical protein	S				0.012
Swit_0354	Transcriptional regulator	K				0.027
Swit_0359	Cytochrome P450	Q				0.010
Swit_0372	Hypothetical protein	S				0.029
Swit_0374	Marr family transcriptional regulator	K				0.023
Swit_0375	Acyl-coa dehydrogenase domain-containing protein	I				0.003
Swit_0397	Phosphotransferase system	G				0.018
Swit_0433	Hypothetical protein	S	0.276	0.481		0.033
Swit_0488	Beta-lactamase domain-containing protein	R	0.388		0.367	0.002
Swit_0571	Uroporphyrin-III C/tetrapyrrole methyltransferase	R				0.084
Swit_0650	Acyl-coa dehydrogenase domain-containing protein	I				0.009
Swit_0669	AMP-dependent synthetase and ligase	I				0.013
Swit_0673	TonB-dependent receptor	P				0.058
Swit_0676	Hypothetical protein	S	2.225	2.019		0.079
Swit_0695	Hypothetical protein	S	3.852		2.379	0.017
Swit_0700	Hypothetical protein	S				0.069
Swit_0704	Luciferase family protein	C				0.006

Swit_0708	Hypothetical protein	S							0.076
Swit_0724	Methylenetetrahydromethanopterin reductase	C							0.023
Swit_0725	Tonb-dependent receptor	P							0.081
Swit_0730	Tonb-dependent receptor	P							0.005
Swit_0731	Amidase	J							0.035
Swit_0745	Hypothetical protein	S							0.002
Swit_0752	Beta-ketoadipyl coa thiolase	I		0.352					0.070
Swit_0754	Phenylacetate-coa oxygenase subunit paab	Q	0.048	0.236	0.143	0.072	0.050	0.047	0.003
Swit_0763	Aromatic amino acid aminotransferase	E	0.042	0.440	0.139	0.120	0.114	0.148	0.007
Swit_0790	Thiolase	I							0.039
Swit_0800	Hypothetical protein	S	4.387		2.904	2.974	2.064	2.241	0.004
Swit_0802	TPR repeat-containing protein	NU							0.053
Swit_0819	Gentisate 1	Q							0.095
Swit_0820	5-carboxymethyl-2-hydroxymuconate delta-isomerase	Q							0.065
Swit_0826	Short-chain dehydrogenase/reductase SDR	IQR							0.090
Swit_0831	Asp/Glu racemase	Q							0.002
Swit_0838	Tonb-dependent receptor	P							0.084
Swit_0843	Acyl-coa synthetase	IQ							0.030
Swit_0857	Marr family transcriptional regulator	K							0.087
Swit_0865	Hypothetical protein	S							0.073
Swit_0922	Anti-feci sigma factor fecr	PT						0.456	0.001
Swit_0924	Tonb-dependent receptor	P							0.003
Swit_0930	Peptidase S15	R							0.013
Swit_0931	Tonb-dependent receptor	P							0.005
Swit_0932	Rieske (2Fe-2S) domain-containing protein	PR						2.022	0.070
Swit_0936	Peptidase S15	R							0.067
Swit_0942	Sarcosine oxidase subunit gamma	E			2.551	2.964	2.877	2.208	0.002
Swit_0950	Hypothetical protein	S							0.014
Swit_0953	CRP/FNR family transcriptional regulator	T	2.495		4.305	5.176	3.648		0.008
Swit_0955	CRP/FNR family transcriptional regulator	T				2.056			0.051
Swit_0962	Rieske (2Fe-2S) domain-containing protein	PR							0.009
Swit_0966	Rieske (2Fe-2S) domain-containing protein	PR							0.071
Swit_0968	Hypothetical protein	X65				2.354	2.782	2.157	0.003
Swit_0971	Asp/Glu racemase	E					2.030		0.003
Swit_0978	3-oxoadipate enol-lactonase	R							0.033
Swit_1011	Enoyl-coa hydratase	I							0.083
Swit_1012	Enoyl-coa hydratase	I							0.100
Swit_1014	Enoyl-coa hydratase/isomerase	I							0.008
Swit_1018	Enoyl-coa hydratase/isomerase	I							0.018

Swit_1039	Transketolase	C							0.098
Swit_1045	Short-chain dehydrogenase/reductase SDR	R							0.064
Swit_1057	Pyruvate dehydrogenase	C							0.026
Swit_1059	Hypothetical protein	X70				2.495			0.006
Swit_1073	Protocatechuate 3	Q							0.002
Swit_1074	L-threonine aldolase	E							0.019
Swit_1077	Tonb-dependent receptor	P							0.070
Swit_1082	Peptidase S10	E							0.072
Swit_1170	Type B carboxylesterase	I							0.042
Swit_1201	UDP-glucose/GDP-mannose dehydrogenase	M				0.442	0.439		0.002
Swit_1209	Major facilitator transporter	EGPR					0.432		0.075
Swit_1223	Addiction module antitoxin	L							0.076
Swit_1303	Thioesterase superfamily protein	Q				0.457	0.457		0.002
Swit_1325	50S ribosomal protein L17	J	0.087		0.352	0.248	0.188	0.132	0.061
Swit_1382	Hypothetical protein	S							0.003
Swit_1394	Cytochrome c1	C	0.063		0.339	0.200	0.140	0.138	0.002
Swit_1422	Cytochrome c-type biogenesis protein ccmb	O							0.075
Swit_1425	Amino acid aldolase-like protein	E			2.710	0.419		0.454	0.017
Swit_1427	Major facilitator transporter	R			2.044				0.084
Swit_1445	Alpha/beta hydrolase fold protein	R							0.003
Swit_1446	Response regulator receiver protein	TK	3.019						0.023
Swit_1523	Hypothetical protein	S	2.018						0.010
Swit_1526	Thiamine pyrophosphate binding domain-containing protein	EH							0.004
Swit_1529	Thiolase	I							0.005
Swit_1535	Lysr family transcriptional regulator	K							0.018
Swit_1537	Fumarylacetoacetate (FAA) hydrolase	Q							0.012
Swit_1542	Rieske (2Fe-2S) domain-containing protein	PR							0.008
Swit_1544	Ethyl tert-butyl ether degradation ethd	-					0.395	0.475	0.017
Swit_1554	Major facilitator transporter	EGPR							0.081
Swit_1561	Hypothetical protein	HC	2.062						0.082
Swit_1566	Ornithine cyclodeaminase	E							0.024
Swit_1572	Alpha/beta hydrolase fold protein	R							0.023
Swit_1573	Tonb-dependent receptor	P							0.085
Swit_1575	Hypothetical protein	X116							0.005
Swit_1578	DNA methylase N-4/N-6 domain-containing protein	L						2.013	0.001
Swit_1580	Hypothetical protein	L	0.455						0.002
Swit_1583	Tonb-dependent receptor	P							0.009
Swit_1585	Arac family transcriptional regulator	K	2.241	2.084					0.076
Swit_1587	Aldehyde dehydrogenase	C							0.004

Swit_1590	Ornithine cyclodeaminase	E						0.010
Swit_1591	Endoribonuclease L-PSP	J						0.001
Swit_1598	Acyl-coa dehydrogenase domain-containing protein	I						0.009
Swit_1600	AMP-dependent synthetase and ligase	IQ						0.001
Swit_1602	Short-chain dehydrogenase/reductase SDR	IQR						0.070
Swit_1605	Aldehyde dehydrogenase	C				2.148		0.064
Swit_1606	L-carnitine dehydratase/bile acid-inducible protein F	C						0.011
Swit_1608	Dehydratase	I						0.009
Swit_1611	Lipid-transfer protein	I						0.013
Swit_1616	Glyoxalase/bleomycin resistance protein/dioxygenase	E						0.003
Swit_1632	Glucose-methanol-choline oxidoreductase	E						0.047
Swit_1635	Xylose isomerase domain-containing protein	G						0.095
Swit_1645	Type 11 methyltransferase	H						0.001
Swit_1646	Glutathione S-transferase domain-containing protein	O						0.005
Swit_1649	Amidase	J						0.083
Swit_1650	5-carboxymethyl-2-hydroxyruconate delta-isomerase	Q						0.043
Swit_1655	Major facilitator transporter	EGPR						0.001
Swit_1657	Alcohol dehydrogenase	CR				2.300		0.039
Swit_1658	Short-chain dehydrogenase/reductase SDR	IQR						0.001
Swit_1659	Hypothetical protein	S						0.001
Swit_1661	Short-chain dehydrogenase/reductase SDR	IQR						0.001
Swit_1663	Hydroxyacylglutathione hydrolase	R						0.059
Swit_1664	Glutathione S-transferase domain-containing protein	O						0.054
Swit_1667	Glutamine synthetase	E						0.060
Swit_1669	Short-chain dehydrogenase/reductase SDR	IQR						0.006
Swit_1670	Alpha/beta hydrolase domain-containing protein	I						0.007
Swit_1678	Tetr family transcriptional regulator	K						0.004
Swit_1687	Vanillate monooxygenase	PR						0.072
Swit_1697	Hypothetical protein	S						0.005
Swit_1730	AMP-dependent synthetase and ligase	IQ						0.001
Swit_1731	Acyl-coa dehydrogenase domain-containing protein	I	3.002		2.354	2.844	2.792	0.003
Swit_1738	Amidohydrolase 3	Q	2.053			2.082	3.307	0.015
Swit_1739	Glucose-methanol-choline oxidoreductase	E						0.003
Swit_1741	Epoxide hydrolase domain-containing protein	R						0.046
Swit_1743	Cytochrome P450	Q						0.092
Swit_1745	Aldehyde dehydrogenase	C						0.001
Swit_1749	Amidohydrolase 2	R						0.005
Swit_1752	Acyl-coa dehydrogenase domain-containing protein	I	3.073					0.005
Swit_1753	Amidohydrolase 2	R	0.395					0.017

Swit_1754	Alpha/beta hydrolase fold protein	R						0.028
Swit_1755	Short-chain dehydrogenase/reductase SDR	IQR		2.606	4.197	5.083	2.808	0.009
Swit_1762	Oxidoreductase domain-containing protein	R						0.004
Swit_1763	Long-chain-fatty-acid--coa ligase	IQ						0.045
Swit_1771	Acetyl-coa acetyltransferase	I						0.003
Swit_1777	Lysr family transcriptional regulator	K			2.134			0.093
Swit_1782	Intradiol ring-cleavage dioxygenase	Q						0.062
Swit_1790	Multicopper oxidase	Q						0.009
Swit_1793	Multicopper oxidase	Q						0.043
Swit_1816	Hypothetical protein	O	2.367		0.492	0.385	0.279	0.067
Swit_1818	Beta-lactamase	V						0.033
Swit_1825	Tetr family transcriptional regulator	K					0.316	0.024
Swit_1829	Rieske (2Fe-2S) domain-containing protein	PR	6.097	2.036		2.266	2.092	0.004
Swit_1830	Fumarate reductase/succinate dehydrogenase flavoprotein domain-containing protein	C	2.585					0.070
Swit_1832	Dehydratase	I		2.451	4.422	4.090	4.212	0.004
Swit_1845	Tetr family transcriptional regulator	K	9.020					0.006
Swit_1854	Short-chain dehydrogenase/reductase SDR	IQR	2.007	3.182	2.803		3.056	0.022
Swit_1865	N-acetyltransferase GCN5	J						0.024
Swit_1877	Short chain dehydrogenase	IQR						0.042
Swit_1878	FAD dependent oxidoreductase	Q						0.086
Swit_1897	Hypothetical protein	X131				0.494		0.037
Swit_1908	Extracellular ligand-binding receptor	E					2.215	0.047
Swit_1916	Endonuclease/exonuclease/phosphatase	R	3.489	4.312	6.873	5.118		0.084
Swit_1926	ABC transporter-like protein	V	0.246	0.457	0.335	0.282	0.234	0.018
Swit_1947	Hypothetical protein	E						0.079
Swit_1951	RND efflux system outer membrane lipoprotein	MU	6.305					0.010
Swit_1954	Two component transcriptional regulator	TK	3.448				2.244	0.008
Swit_1990	Lactoylglutathione lyase	E						0.035
Swit_1995	Cytochrome P450	Q						0.002
Swit_1996	Hypothetical protein	S						0.003
Swit_2009	Ethyl tert-butyl ether degradation ethd	X138						0.004
Swit_2030	Hypothetical protein	MG						0.071
Swit_2039	Arac family transcriptional regulator	K						0.055
Swit_2044	Glucose-methanol-choline oxidoreductase	E						0.036
Swit_2050	Aminoglycoside phosphotransferase	R						0.005
Swit_2052	Hypothetical protein	X143	3.245					0.007
Swit_2058	Regulatory protein luxr	K						0.096
Swit_2079	Major facilitator transporter	EGPR						0.045

Swit_2121	Tonb-dependent receptor	P						0.056
Swit_2128	Hypothetical protein	V	0.375					0.071
Swit_2133	Translocation protein tolB	U						0.003
Swit_2142	Hypothetical protein	S	0.108	0.350		0.378	0.426	0.005
Swit_2172	Hypothetical protein	X152					2.007	0.014
Swit_2175	Hypothetical protein	S						0.048
Swit_2327	Hypothetical protein	S						0.090
Swit_2331	Hydrogenobyrinic acid a	R				0.434	0.360	0.088
Swit_2376	Group 1 glycosyl transferase	M						0.049
Swit_2415	Ornithine cyclodeaminase	E						0.068
Swit_2453	Capsule polysaccharide biosynthesis protein	M	0.427					0.001
Swit_2454	Capsule polysaccharide biosynthesis protein	M						0.003
Swit_2468	Dimethylmenaquinone methyltransferase	H						0.049
Swit_2644	Degt/dnrj/eryc1/strs aminotransferase	M					0.375	0.015
Swit_2666	Alpha/beta hydrolase fold protein	R					0.484	0.009
Swit_2671	Group 1 glycosyl transferase	M						0.088
Swit_2695	Glycine cleavage system protein H	E						0.007
Swit_2731	Aconitase	C	0.220		0.393	0.272	0.218	0.008
Swit_2732	Bifunctional aconitate hydratase 2/2-methylisocitrate dehydratase	C	0.206		0.438	0.439		0.075
Swit_2789	Atpase mipz	D						0.004
Swit_2826	PTS transporter subunit IIA-like nitrogen-regulatory protein ptsn	GT						0.001
Swit_2874	Hypothetical protein	S				0.411	0.349	0.006
Swit_2876	Glycosyl transferase family protein	M	0.299		0.487	0.363	0.447	0.007
Swit_2877	Type 12 methyltransferase	O						0.041
Swit_2958	Badm/Rrf2 family transcriptional regulator	K				2.355		0.076
Swit_2973	Signal transduction histidine kinase lyts	T						0.002
Swit_3013	Cell division ATP-binding protein fitse	D						0.034
Swit_3060	Fumarylacetoacetate (FAA) hydrolase	Q			0.419	0.344	0.362	0.013
Swit_3071	Glutathione S-transferase domain-containing protein	O						0.077
Swit_3081	Gntr family transcriptional regulator	K						0.066
Swit_3241	Tonb-dependent receptor	P	17.642	0.304			5.409	0.012
Swit_3244	Metal dependent phosphohydrolase	R	5.073					0.046
Swit_3279	Short-chain dehydrogenase/reductase SDR	IQR	2.596		2.341	3.467	2.978	0.013
Swit_3325	Ethyl tert-butyl ether degradation ethd	X256						0.096
Swit_3328	Hypothetical protein	S						0.003
Swit_3338	Alpha/beta hydrolase fold protein	R						0.064
Swit_3351	Hypothetical protein	S	0.408	0.394			0.483	0.003
Swit_3355	Short-chain dehydrogenase/reductase SDR	IQR						0.009
Swit_3364	Short-chain dehydrogenase/reductase SDR	IQR						0.006

Swit_3367	Cytochrome P450-like protein	Q							0.065
Swit_3381	Hpr(Ser) kinase/phosphatase	-							0.028
Swit_3401	Acetyl-coa acetyltransferase-like protein	I							0.076
Swit_3403	Short-chain dehydrogenase/reductase SDR	IQR							0.016
Swit_3410	Rieske (2Fe-2S) domain-containing protein	PR							0.008
Swit_3415	Hypothetical protein	S							0.077
Swit_3433	Hypothetical protein	S		2.266					0.049
Swit_3450	ETC complex I subunit	C	0.433						0.082
Swit_3491	Group 1 glycosyl transferase	M		0.499					0.005
Swit_3492	Group 1 glycosyl transferase	M							0.001
Swit_3493	ABC transporter-like protein	GM							0.005
Swit_3494	Polysaccharide export protein	M							0.016
Swit_3587	Alkyl hydroperoxide reductase	O		3.207					0.009
Swit_3595	Major facilitator transporter	EGPR	0.381						0.004
Swit_3621	Regulatory protein iclr	K							0.077
Swit_3629	Acyl-coa dehydrogenase domain-containing protein	I							0.054
Swit_3645	Amidohydrolase 2	R							0.063
Swit_3667	Thioredoxin domain-containing protein	O							0.010
Swit_3681	Hypothetical protein	S							0.034
Swit_3686	Hypothetical protein	S							0.002
Swit_3689	Conjugal transfer coupling protein trag	U							0.048
Swit_3691	P-type conjugative transfer atpase trbb	U							0.060
Swit_3698	Conjugal transfer protein trbf	U					2.085		0.032
Swit_3713	RND family efflux transporter MFP subunit	C					2.883		0.004
Swit_3716	Cytochrome B561	C			4.534	7.383			0.012
Swit_3732	Dps family ferritin	P	22.901		2.772				0.003
Swit_3760	Cobalamin synthesis protein	R							0.067
Swit_3762	Endoribonuclease L-PSP	J							0.061
Swit_3788	Exodeoxyribonuclease III Xth	L	0.371			0.470			0.006
Swit_3880	Cytochrome c oxidase subunit III	C	0.238		0.465	0.389			0.006
Swit_3882	Hypothetical protein	S	0.334						0.030
Swit_3926	Signal transduction histidine kinase	T	2.935						0.051
Swit_3934	Sporulation domain-containing protein	S							0.094
Swit_3958	Cysteine synthase A	E				0.437			0.079
Swit_3964	3-deoxy-manno-octulosonate cytidyltransferase	M				0.458			0.001
Swit_3965	Kpsf/gutq family protein	M	0.305						0.100
Swit_3966	Hypothetical protein	S							0.008
Swit_4006	Hlyd family type I secretion membrane fusion protein	V	0.114	0.419	0.350	0.313	0.225		0.003
Swit_4008	Tolc family type I secretion outer membrane protein	MU	0.387	0.495	0.454	0.459	0.336		0.004

Swit_4015	ABC-2 type transporter	M	0.463	0.490	0.410	0.371	0.310	0.001
Swit_4016	Group 1 glycosyl transferase	M						0.002
Swit_4039	Asparagine synthase	E						0.047
Swit_4092	DNA repair protein rada	O				2.198	2.311	0.039
Swit_4119	Lipid-transfer protein	I						0.100
Swit_4128	Hypothetical protein	X321						0.002
Swit_4132	FAD dependent oxidoreductase	P						0.080
Swit_4141	Major facilitator transporter	G						0.004
Swit_4143	5-oxoprolinase	Q						0.060
Swit_4151	Tonb-dependent receptor	P						0.002
Swit_4155	Amine oxidase	E						0.029
Swit_4158	Succinate semialdehyde dehydrogenase	C				2.049		0.008
Swit_4166	Lysr family transcriptional regulator	K						0.009
Swit_4167	4-aminobutyrate aminotransferase	E						0.068
Swit_4169	Amidase	J						0.024
Swit_4172	Aminotransferase	E						0.002
Swit_4180	2-nitropropane dioxygenase	R						0.072
Swit_4184	Acyl-coa dehydrogenase type 2	I						0.003
Swit_4187	Amidase	J						0.040
Swit_4195	Hypothetical protein	S						0.053
Swit_4207	Putative esterase	R						0.062
Swit_4209	Glutathione-dependent formaldehyde-activating protein	S	3.549	3.055	5.530	4.310	2.410	0.022
Swit_4215	Alpha/beta hydrolase fold protein	R						0.004
Swit_4219	Major intrinsic protein	G	2.783					0.006
Swit_4222	Hypothetical protein	S						0.093
Swit_4232	L-carnitine dehydratase/bile acid-inducible protein F	C						0.008
Swit_4235	Alpha/beta hydrolase fold protein	R						0.010
Swit_4236	Alpha/beta hydrolase fold protein	R						0.007
Swit_4244	Peptidase S15	E						0.004
Swit_4252	2OG-Fe(II) oxygenase	R						0.017
Swit_4253	Tonb-dependent receptor	P	2.196					0.078
Swit_4257	Tonb-dependent receptor	P						0.090
Swit_4260	Luciferase family protein	C		2.596				0.018
Swit_4263	Gentisate 1 2-dioxygenase-like protein	Q						0.003
Swit_4266	Type B carboxylesterase	I						0.006
Swit_4274	Tonb-dependent receptor	P						0.006
Swit_4275	Isochorismatase hydrolase	Q						0.007
Swit_4277	Glucose-methanol-choline oxidoreductase	E						0.070
Swit_4278	Rieske (2Fe-2S) domain-containing protein	PR	2.337			2.044		0.002

Swit_4279	2-hydroxy-3-oxopropionate reductase	I						0.008
Swit_4282	Tonb-dependent receptor	P						0.015
Swit_4290	Hypothetical protein	-	3.480	0.344				0.014
Swit_4295	Acyl-coa dehydrogenase type 2	I	2.590			2.193	2.118	0.010
Swit_4301	Major facilitator transporter	G						0.022
Swit_4302	Tonb-dependent receptor	P						0.059
Swit_4306	Succinate semialdehyde dehydrogenase	C				2.101		0.049
Swit_4314	2-dehydro-3-deoxyglucarate aldolase	G						0.002
Swit_4316	Marr family transcriptional regulator	KK						0.008
Swit_4320	Lysr family transcriptional regulator	K						0.041
Swit_4326	3-isopropylmalate dehydratase small subunit	E						0.001
Swit_4329	Major facilitator transporter	G						0.019
Swit_4331	Tetr family transcriptional regulator	K						0.041
Swit_4332	Tonb-dependent receptor	P						0.061
Swit_4334	Luciferase family protein	C						0.001
Swit_4360	Hypothetical protein	R					2.906	0.006
Swit_4364	Methylamine dehydrogenase accessory protein maud	C		2.103				0.047
Swit_4373	Hypothetical protein	X328				0.479	0.356	0.059
Swit_4376	ATP-dependent protease peptidase subunit	O	0.424			0.486		0.006
Swit_4377	ATP-dependent protease ATP-binding subunit hslu	O	0.371					0.072
Swit_4420	Serine O-acetyltransferase	E				2.402	2.522	0.002
Swit_4428	Sell domain-containing protein	R						0.016
Swit_4434	Hypothetical protein	X340						0.021
Swit_4435	Hypothetical protein	S						0.087
Swit_4436	Bacteriophage terminase large (atpase) subunit-like protein	R						0.013
Swit_4441	Hypothetical protein	X344						0.001
Swit_4447	Hypothetical protein	X348						0.001
Swit_4451	Hypothetical protein	X351						0.001
Swit_4456	Hypothetical protein	S						0.011
Swit_4457	Hypothetical protein	S						0.017
Swit_4475	Hypothetical protein	X361	7.030		4.322	6.132	4.748	2.788
Swit_4491	Excinuclease ABC subunit C	L						0.002
Swit_4505	Phosphoenolpyruvate-protein phosphotransferase ptsp	T	0.474					0.006
Swit_4522	Acyltransferase 3	R						0.009
Swit_4532	Sugar transferase	M	9.898					0.016
Swit_4534	UDP-glucose 6-dehydrogenase	M					0.476	0.006
Swit_4538	Hypothetical protein	X366						0.002
Swit_4542	Dtdp-4-dehydrorhamnose 3	M						0.003
Swit_4560	Hypothetical protein	S						0.001

Swit_4568	Histidine kinase	T							0.005
Swit_4581	ABC-2 type transporter	V							0.098
Swit_4587	Glyoxalase/bleomycin resistance protein/dioxygenase	R							0.098
Swit_4606	Hypothetical protein	R							0.081
Swit_4612	Beta-lactamase	V							0.004
Swit_4619	Hypothetical protein	S							0.004
Swit_4644	Cold-shock DNA-binding protein family protein	K							0.015
Swit_4695	GDSL family lipase	E							0.003
Swit_4706	Beta-lactamase	V	0.461				0.453		0.032
Swit_4729	DNA repair protein recn	L							0.007
Swit_4767	Heat shock protein dnaj domain-containing protein	O							0.064
Swit_4821	Group 1 glycosyl transferase	M					0.427		0.008
Swit_4859	Pyruvate phosphate dikinase	G	0.148		0.461	0.316	0.314	0.296	0.005
Swit_4885	Formamidopyrimidine-DNA glycosylase	L							0.015
Swit_4894	Tonb-dependent receptor	P		2.091					0.002
Swit_4895	Alpha/beta hydrolase fold	R							0.001
Swit_4897	Ring hydroxylating dioxygenase	PR		2.923				2.530	0.000
Swit_4902	Glyoxalase/bleomycin resistance protein/dioxygenase	E	2.344	4.416		0.459	0.463		0.008
Swit_4910	Dehydrogenase	IQR							0.001
Swit_4912	Hypothetical protein	R	2.402						0.006
Swit_4915	Transposase IS3/IS911 family protein	L							0.022
Swit_4916	IS66 Orf2 family protein	L							0.003
Swit_4944	Hypothetical protein	S							0.070
Swit_4955	Cobyrinic acid a	D				0.455	0.498	0.458	0.001
Swit_4959	Hypothetical protein	S							0.089
Swit_4976	Hypothetical protein	X411							0.002
Swit_5001	P-type DNA transfer atpase virb11	NU							0.036
Swit_5003	P-type conjugative transfer protein virb9	U							0.002
Swit_5006	Type IV secretion system family protein	U							0.003
Swit_5008	Type IV secretory pathway	U							0.054
Swit_5017	Methylmalonate-semialdehyde dehydrogenase [acylating]	C							0.076
Swit_5020	3-oxoadipate enol-lactonase	R							0.056
Swit_5021	Acyl coa:acetate/3-ketoacid coa transferase beta subunit-like protein	I							0.025
Swit_5023	3-oxoacid coa-transferase	I							0.018
Swit_5047	Benzoylformate decarboxylase	EH							0.017
Swit_5079	IS66 Orf2 family protein	L							0.084
Swit_5088	Ferredoxin	C					0.453	0.381	0.031
Swit_5096	Hypothetical protein	L		2.761					0.004

Swit_5105	Hypothetical protein	L							0.050
Swit_5123	Transposase	L							0.073
Swit_5126	Hypothetical protein	G							0.071
Swit_5138	Istb ATP binding domain-containing protein	L							0.093
Swit_5163	Hypothetical protein	X423	0.250		0.473		0.495		0.022
Swit_5168	Hypothetical protein	X427							0.002
Swit_5185	Hypothetical protein	S							0.024
Swit_5189	Hypothetical protein	X433							0.001
Swit_5198	Hypothetical protein	X436							0.013
Swit_5201	Hypothetical protein	S							0.006
Swit_5203	Nitric oxide dioxygenase	C					2.100		0.004
Swit_5204	CRP/FNR family transcriptional regulator	T							0.014
Swit_5206	Hypothetical protein	S							0.052
Swit_5218	Hypothetical protein	X439							0.002
Swit_5220	Hypothetical protein	S							0.020
Swit_5221	Hypothetical protein	S							0.021
Swit_5228	Hypothetical protein	X443							0.016
Swit_5231	Limonene-1	Q							0.073
Swit_5235	Citrate transporter	P							0.001
Swit_5239	Hypothetical protein	X447							0.007
Swit_5240	Hypothetical protein	S	2.270						0.037
Swit_5252	Hypothetical protein	X450							0.036
Swit_5257	Hypothetical protein	J							0.096
Swit_5259	Hypothetical protein	S							0.049
Swit_5263	Hypothetical protein	X454							0.002
Swit_5272	Spermidine synthase-like protein	E			0.466		0.442	0.406	0.006
Swit_5273	Hypothetical protein	S			0.411	0.412	0.389	0.432	0.033
Swit_5285	Putative DNA topoisomerase I	L	4.492		4.208	4.487	2.233		0.001
Swit_5290	Mscs mechanosensitive ion channel	M		2.045	2.943	5.760	4.831		0.017
Swit_5298	Hypothetical protein	P							0.018
Swit_5300	Periplasmic sensor diguanylate cyclase/phosphodiesterase	T							0.050
Swit_5302	Hypothetical protein	S							0.020
Swit_5303	Hypothetical protein	S					2.123		0.020
Swit_5308	Hypothetical protein	X460							0.007
Swit_5309	Acetyl-coa acetyltransferase	I							0.069
Swit_5310	Hypothetical protein	X461	2.615		3.595	6.344	4.666	2.649	0.057
Swit_5311	Catalase	P	2.908		4.572	6.406	4.538	2.237	0.017
Swit_5313	2Fe-2S iron-sulfur cluster binding domain-containing protein	C	6.562		5.273	6.389	5.051	2.296	0.003
Swit_5314	Molybdopterin dehydrogenase	C	3.529		2.429	3.436	2.791		0.085

Swit_5315	Xanthine dehydrogenase	C	9.224		4.166	6.823	5.400	2.991	0.017
Swit_5319	Cell cycle transcriptional regulator ctra	TK	0.406						0.010
Swit_5330	Hypothetical protein	X466							0.005
Swit_5337	Grea/greb family elongation factor	K					2.216	5.117	0.076
Swit_5344	Cyclase/dehydrase	S	22.537		5.836	10.006	6.161	2.955	0.007
Swit_5348	Hypothetical protein	S	26.025	3.226	2.865	3.052	2.248		0.056
Swit_5350	Hypothetical protein	X350		3.165					0.005
Swit_5358	Hypothetical protein	X474			2.053	2.103	2.287		0.008
Swit_5360	Hypothetical protein	S							0.070
Swit_5361	Lytic transglycosylase	M	2.166						0.003
Swit_5365	Type IV conjugative transfer system protein tral	-				2.176	2.212		0.002
Swit_5366	Trae family protein	U							0.005
Swit_5367	Hypothetical protein	S							0.033
Swit_5369	Hypothetical protein	O							0.002
Swit_5377	Trau family protein	-							0.002
Swit_5378	Type-F conjugative transfer system pilin assembly protein trbc	S							0.029
Swit_5381	Traf-like protein	CO							0.059
Swit_5382	Trah family protein	-							0.038
Swit_5383	Trag domain-containing protein	-							0.047
Swit_5385	Hypothetical protein	R		2.150				3.614	0.045

1) Black characters, chromosome; blue characters, pSWIT02; red characters, pSWIT01.

2) Only values that are significantly different ($P < 0.05$) from the control are shown.

Table S2. Clustering, essentiality and fold-expression change of *Sphingomonas wittichii* RW1 genes coding for putative functions in aromatic compound metabolism.

Expanded version from Table 1. For legend, see Table 1.

Locus	Name	Strand	Tn library			Expression, fold change							
			TN01	SAL	DBF	SAL/PHE	SAL/DBF	DBF/PHE	DBF shock	30 m	Chemostat shift		
											1 h	2 h	6 h
310	AMP-dependent synthetase and ligase	<	+(+)	+(+)	+			0.98	0.96	0.73	0.77	0.85	0.92
311	carboxymuconolactone decarboxylase	<	-(+)	-(±)	-			1.21	1.93	2.81	2.51	2.03	1.25
312	amidohydrolase 3	<	+(+)	+(+)	+			1.06	0.68	0.75	0.75	0.73	0.99
742	2-keto-4-pentenoate hydratase	<	+(+)	+(+)	+			0.76	0.72	0.73	0.93	1.04	1.00
743	ARD-beta	<	-(±)	-(+)	+			0.73	1.10	1.39	1.29	1.39	1.97
744	ARD-alpha	<	+(+)	+(+)	+			0.78	1.06	1.23	1.21	1.14	1.68
745	hypothetical protein	<	+(+)	-(±)	±			0.84	1.28	1.02	0.93	1.46	1.78
746	amidase	<	±(±)	±(-)	+			0.98	1.54	1.10	1.26	1.49	1.74
747	MarR family transcriptional regulator	>	+(+)	-(+)	+			1.16	1.53	1.05	0.99	1.31	1.39
748		<	+(+)	±(+)	+	0.11		0.28	0.15	0.36	0.40	0.34	0.38
749	paaB?	<	-(-)	-(-)	+	0.04		0.72	0.12	0.31	0.35	0.35	0.31
750	3-hydroxyacyl-CoA dehydrogenase	>	+(-)	-(-)	-	0.07		0.53	0.11	0.48	0.47	0.38	0.48
751	paaD	>	+(+)	+(+)	+	0.05		0.37	0.15	0.27	0.44	0.27	0.13
752	beta-ketoadipyl CoA thiolase	>	+(+)	+(+)	+	0.19		0.35	0.57	0.71	0.64	1.15	0.62
753	paaA	>	+(+)	-(±)	+	0.04		0.50	0.04	0.24	0.15	0.14	0.16
754	paaB	>	+(+)	-(±)	±	0.02		0.24	0.05	0.14	0.07	0.05	0.05
755	paaI	>	-(-)	-(-)	-	0.02		0.19	0.05	0.17	0.10	0.05	0.06
756	paaJ	>	+(+)	-(±)	-			1.06	1.66	1.72	1.51	1.45	1.01
757	paaK	>	+(+)	+(+)	+	0.02		0.09	0.08	0.34	0.34	0.40	0.37
758	enoyl-CoA hydratase/isomerase	>	+(+)	+(-)	+	0.03		0.76	0.72	0.73	0.93	1.04	1.00
819	gentisate 1,2-diox	>	+(+)	±(±)	+			1.21	1.27	1.08	1.37	1.27	1.88
820	5-carboxymethyl-2-hydroxy-3-oxo-2-oxopentanoate delta-isomerase	>	+(+)	±(±)	±			0.84	1.91	1.09	1.13	1.22	1.19
892		<	+(+)	+(+)	+			1.15	0.49	0.92	0.70	0.67	0.78
893	ferredoxin	<	-(-)	-(-)	-			1.16	0.59	0.64	0.46	0.68	1.37
894	EDO	<	+(+)	±(+)	+			1.11	0.79	0.98	1.01	1.10	1.09

1553	TetR repressor	>	-(+)	±(+)	-	0.84	0.33	0.70	0.65	0.66	0.95
1557	homogentisate 1,2-dioxygenase	>	+(+)	+ (±)	+	0.80	1.68	1.13	1.14	1.68	1.55
1558	fumarylacetoacetase	>	+(+)	±(±)	+	1.40	0.83	1.48	2.07	2.11	1.38
1559	ARD-alpha	<	+(+)	±(±)	+	0.98	0.77	0.93	0.75	0.75	0.90
1639	4-oxalocrotonate decarboxylase	>	+(-)	-(-)	-	1.68	1.17	0.99	1.13	1.47	1.83
1640=2112	acetaldehyde dehydrogenase	>	-(-)	-(-)	-						
1641	4-hydroxy-2-ketovalerate aldolase	>	+(+)	- (±)	+	1.08	1.24	1.18	1.21	1.39	1.17
1642	NAD-binding D-isomer specific 2-hydroxyacid dehydrogenase	>	-(+)	-(-)	-	1.13	0.97	0.75	0.66	0.99	0.69
1643	FMN-dependent alpha-hydroxy acid dehydrogenase	>	±(+)	±(±)	-	1.27	0.92	1.13	1.08	1.10	1.05
1644	methionine aminopeptidase	>	+(+)	±(+)	+	0.78	0.70	0.82	0.88	1.01	1.61
1679	hypothetical protein	>	+(+)	+(+)	+	1.09	1.30	1.17	1.28	1.64	1.39
1680	EDO	>	+(+)	- (±)	+	1.42	1.00	1.23	1.16	1.41	1.72
1681	5-carboxymethyl-2-hydroxy muconate delta-isomerase	>	+(+)	±(±)	+	0.98	2.16	1.45	1.60	1.39	1.53
1682	hypothetical	>	-(+)	+ (±)	+	1.20	1.30	1.06	1.62	1.69	1.29
1683	amidohydrolase 2	>	+(+)	+(+)	+	0.95	0.53	1.06	1.10	0.99	0.75
1684	FAD-binding monooxygenase	>	+(+)	±(±)	-	0.98	1.08	1.30	1.22	1.26	1.39
1685	fumarylacetoacetase	>	+(+)	+ (±)	+	1.00	0.55	1.43	1.88	1.27	0.94
1686	ARD-alpha	>	+(+)	+(+)	+	1.24	1.25	1.13	1.11	1.43	1.74
1687	vanillate monooxygenase	>	+(+)	- (±)	+	1.13	1.37	0.88	1.01	1.18	1.17
1728	major facilitator protein	<	+(+)	+ (±)	+	1.20	1.61	1.21	1.83	1.54	1.77
1729	dioxygenase motif	<	- (±)	- (±)	±	1.29	1.54	1.38	0.75	0.95	0.68
1754	alpha/beta hydrolase fold protein	>	+(+)	+(+)	+	1.45	1.92	1.45	1.42	1.39	1.67
1755	short-chain dehydrogenase/reductase SDR	>	+(+)	+(+)	±	1.14	1.33	2.60	4.20	5.10	2.81
1756	EDO	>	+(+)	+(+)	+	1.09	1.14	1.44	1.26	1.64	1.74
1757	ARD-beta	>	-(+)	±(±)	-	0.95	0.74	0.96	0.86	0.81	0.80

0.45

1758	ARD-alpha	>	+(+)	+(±)	+		1.66	1.62	1.11	1.13	1.72	2.16	
1759	ferredoxin	>	+(±)	-(-)	-		1.04	2.03	1.09	1.01	1.62	1.99	
1760	L-carnitine dehydratase	>	+(±)	-(±)	-		0.79	1.65	1.40	1.73	1.83	1.68	
1825	TetR family transcriptional regulator	<	+(+)	-(+)	±		1.09	0.75	0.81	0.66	0.53	0.32	
1826	EDO	<	+(+)	+(+)	+		1.05	3.92	1.75	1.64	1.78	1.21	
1827	alpha/beta hydrolase fold protein	<	±(+)	+(+)	+		1.05	4.63	1.36	1.71	1.54	1.61	
1828	acyl-CoA dehydrogenase type2	<	+(+)	±(±)	+		1.04	14.83	4.63	4.56	2.87	1.71	
1829	ARD	<	+(+)	-(±)	±		1.13	6.11	2.04	1.95	2.27	2.08	
1830	hypothetical	<	+(+)	+(±)	+		0.92	2.58	1.11	1.28	1.37	1.27	
1845	TetR regulator	>	+(+)	±(±)	±		1.09	0.75	0.81	0.66	0.53	0.32	
1846	Enoyl-CoA dehydratase	<	+(+)	-(±)	+		1.05	3.92	1.75	1.64	1.78	1.21	
1847	cytochrome P450-like protein	>	+(+)	+(±)	+		1.39	7.57	1.48	1.88	2.06	1.89	
1848	EDO	>	-(+)	±(±)	±	3.39	3.23	28.64	2.75	3.05	3.14	2.79	
1849	hypothetical	>	+(±)	-(±)	+		1.59	25.11	3.58	4.23	2.60	3.92	
1850	acyl CoA domain	>	+(+)	+(+)	+		1.34	11.88	2.83	2.53	1.75	1.66	
1851	acyl CoA domain	>	+(+)	+(+)	+		1.45	7.84	1.58	1.26	1.66	1.09	
1852	hypothetical	>	±(+)	-(±)	-		0.95	1.99	1.16	1.39	1.48	1.32	
1860	3-ketosteroid delta4-dehydrogenase	>	+(+)	+(±)	+		1.39	7.57	1.48	1.88	2.06	1.89	
1861	dioxygenase motif	>		-(±)	±(±)	-		1.54	6.29	2.50	3.54	0.77	1.69
2112=1640	4-oxalocrotonate decarboxylase	>	+(-)	+(-)	+								
2113	acetaldehyde dehydrogenase	>		-(-)	-								
2114	4-hydroxy-2-ketovalerate aldolase	>	-(+)	-(+)	+		1.39	0.94	1.01	1.01	0.71	1.22	
2250	NAD(P)H dehydrogenase (quinone)	<	+(+)	-(-)	+		0.81	0.76	0.77	0.74	0.49	0.95	
2251	ferredoxin	<		-(-)	-		1.09	0.80	0.70	0.78	0.74	0.61	
2252	acyl-CoA dehydrogenase domain-containing protein	<	+(+)	+(+)	+		1.00	1.01	0.88	1.20	1.06	0.96	
2253	ARD-alpha	<	+(+)	+(+)	+		1.11	0.77	1.06	1.11	1.06	1.38	
2283		<	+(+)	±(±)	+		1.77	1.35	1.16	1.14	1.29	1.68	
2284	EDO	<		-(-)	-	0.45	1.42	1.75	0.86	0.90	1.21	1.39	
2285	ARD-alpha	<	+(+)	+(+)	+		1.89	1.82	0.90	0.82	1.22	1.65	

2292	EDO	>	-(-)	-(-)	-		1.43	0.61	0.98	1.02	0.80	0.72
2293	GntR transcriptional regulator	>	+(+)	+(+)	+		1.77	1.35	1.16	1.14	1.29	1.68
2310	ARD-alpha (vanillate?)	>	+(+)	+(+)	+		0.98	1.06	1.13	1.05	1.31	1.17
2311	EDO	>	+(±)	+(±)	+		1.10	2.51	1.71	2.06	2.68	2.07
2312	acyl-CoA dehydrogenase type 2	>	+(+)	+(+)	+		1.22	0.93	0.84	1.13	0.93	1.16
2634	benzoate 1,2-diox alpha	>	+	+	+	28.8	5.06	2.36	1.42	1.87	2.07	3.05
2635	benzoate 1,2-diox beta	>	+	+	+	5.37	2.91	1.34	1.22	1.30	1.30	1.62
2636	benD	>	+	+	+		1.09	1.32	1.16	0.85	0.97	0.73
3022	GntR regulator	<	-(±)	-(±)	-		0.75	1.20	0.87	1.25	1.39	1.42
3023	ARD (vanillate?)	<	+(+)	+(+)	+		0.97	1.13	0.97	0.87	0.73	0.55
3024	cytochrome P450	<	+(+)	+(+)	+		1.01	1.24	1.26	1.04	1.12	1.22
3025	cupin-like	<	±(+)	±(+)	+		1.08	1.34	1.58	1.41	1.71	2.25
3026	TonB receptor	<	+(-)	+(±)	+		0.96	1.39	0.86	1.06	0.81	0.68
3055	alpha/beta hydrolase fold protein	>	+(±)	-(-)	+		2.60	1.65	0.68	0.64	0.85	0.90
3056	ARD-alpha (putative salicylate 5 hydroxylase)	>	+(+)	+(+)	+	2.44	2.31	2.19	0.78	0.59	0.73	0.82
3057	ARD-beta	>	+(-)	-(±)	+		2.35	1.07	0.64	0.51	0.57	0.57
3058	maleylacetoacetate isomerase"	>	+(+)	+(+)	+	2.42	2.48	0.74	0.55	0.41	0.38	0.45
3059	gentisate 1,2-dioxygenase	>	+(+)	+(+)	+		1.68	1.91	0.90	0.72	0.66	0.72
3060	fumarylacetoacetate (FAA) hydrolase	>	+(+)	+(+)	+		1.46	1.16	0.62	0.42	0.34	0.36
3061	hypothetical protein"	>	+(+)	+(±)	+		1.00	0.69	0.57	0.41	0.38	0.38
3062	phthalate 4,5-dioxygenase	>	+(+)	+	+		1.00	1.05	0.74	0.64	0.59	0.49
3063	amidohydrolase 2	>	+(+)	-(-)	+		1.16	0.94	0.75	0.53	0.50	0.45
3064	protocatechuate 4,5-dioxygenase	>	+(+)	+(+)	+		1.64	1.42	0.81	0.71	0.66	0.64
3065	demethylmenaquinone methyltransferase-like protein	>	+(+)	+(+)	+		1.17	1.75	0.98	0.59	0.43	0.59
3066	dimethylmenaquinone methyltransferase	>	+(-)	+(±)	+	0.44	1.00	1.01	0.75	0.65	0.64	0.59
3067	succinate semialdehyde dehydrogenase	>	+(+)	+(+)	+	0.45	2.58	2.22	0.93	0.86	0.88	1.25
3068	short-chain dehydrogenase/reductase SDR"	>	+(+)	+(+)	+	0.46	2.04	1.48	0.90	0.88	0.81	0.91

3083	ornithine cyclodeaminase	<	+	+	+	2.88	2.08	1.38	1.06	1.17	1.03	1.13	1.00
3084	5-oxopent-3-ene-1,2,5-tricarboxylate decarboxylase	<	+	+	+	3.88	2.74	1.35	1.46	1.06	1.26	1.39	1.19
3085	LysR regulator	>	+(+)	+(+)	+			2.48	1.23	1.10	1.22	1.06	1.14
3086	gentisate 1,2-dioxygenase like protein	>	+(+)	+(+)	+	3.92		1.49	2.03	1.32	1.51	1.53	1.07
3087	2,4-dihydroxyhept-2-ene-1,7-dioic acid aldolase	<	±	±	±	16.9	17.71	0.98	1.01	0.93	2.06	1.03	1.53
3088	2-oxo-hepta-3-ene-1,7-dioic acid hydratase	<	+	+	+	8.46	7.38	1.12	1.24	0.94	0.79	0.99	0.99
3089	pseudogene	>				14.69	9.01	1.44	0.74	0.71	2.10	1.18	0.99
3090	acyl-CoA dehydrogenase type 2	>	+	+	+	4.63	3.02	1.41	1.38	1.17	1.13	1.30	1.87
3091	TonB-dependent receptor	>	+	+	+	5.29	4.56	1.13	0.86	0.82	0.60	0.69	0.87
3092	hypothetical protein	>	+	+	+	8.78	4.67	1.67	1.35	1.09	0.91	0.80	0.93
3093	hypothetical protein	>	±	+	+	6.59	4.66	1.33	1.11	0.97	0.45	0.80	0.94
3094	putative extradiol dioxygenase	>	+	+	+	5.33	2.79	1.85	1.72	1.28	0.96	0.93	1.10
3095	hypothetical protein	>	+	-	+	7.96	4.01	1.82	1.29	1.06	0.89	0.84	0.85
3096	ferredoxin:cytochrome p450:oxidoreductase	>	+	+	+			0.92	0.73	0.97	0.86	0.82	0.86
3263	TonB receptor protein	>	+(+)	+(+)	+			1.00	1.16	1.14	1.65	1.58	1.91
3264	ARD- iron sulfur	>	+(+)	-(+)	+			0.81	1.54	1.29	1.42	2.07	2.30
3265	ferredoxin oxidoreductase	>	+(+)	+(+)	+			1.16	0.78	1.49	1.43	1.33	1.51
3266	ARD-alpha	>	+(+)	-(+)	+			1.05	1.01	1.01	1.21	1.25	1.47
3267	hydroxypyruvate isomerase	>	+(+)	+(+)	+			0.84	1.11	1.00	0.88	1.23	0.89
3395	TonB-dependent receptor	>	+(+)	+(±)	+			1.49	0.78	1.01	0.88	0.99	1.16
3396	ARD (vanillate?)	>	+(+)	+(±)	+			0.95	1.87	1.61	1.79	1.68	1.25
3407	EDO	>	±(+)	-(±)	±			1.12	0.62	0.78	0.84	0.85	0.84
3408	Hypothetical protein	>	+(+)	+(+)	+			0.98	1.05	1.13	1.39	0.90	0.81
3409	ARD-alpha	>	+(+)	+(±)	+			1.11	1.20	1.09	0.82	0.93	1.09
3410	ARD-alpha	>	+(+)	+(±)	±			0.99	1.02	0.87	0.91	1.15	1.09
3411	LuxR family protein	>	+(+)	±(±)	+			1.54	1.92	0.96	0.95	1.04	1.12
3416	vanillate monooxygenase		+	+	+			1.37	1.26	1.22	1.14	1.24	1.38
3417	FAD-binding monooxygenase		+	+	+			0.91	0.62	0.88	1.12	1.13	1.22
3418	putative extradiol dioxygenase		+	-	+			1.13	2.95	1.96	2.62	2.95	1.82

3519	aminomuconate-semialdehyde dehydrogenase	>	+(+)	+(+)	+		0.93	0.76	1.00	0.92	1.26	1.13
3520	4-oxalocrotonate decarboxylase	>	+(+)	+(±)	+		0.95	1.58	1.27	1.13	1.40	1.73
3521	4-oxalocrotonate decarboxylase	>	-(+)	-(±)	+		0.78	1.85	1.13	1.23	1.69	1.41
3522	2-aminomuconate deaminase	>	+(+)	+(+)	+		1.89	0.82	0.97	1.02	0.30	0.95
3523	3-hydroxyanthranilate 3,4-dioxygenase	>	+(+)	+(+)	+		0.84	1.04	1.23	1.28	1.15	1.19
3524	aminocarboxymuconate-semialdehyde decarboxylase	>	+(+)	+(+)	+		0.99	1.95	1.04	0.83	1.05	0.82
3525	hypothetical	>	+(±)	+(±)	+		0.86	1.31	0.99	1.23	1.34	1.57
3863	fumarylacetoacetate hydrolase	<	+(+)	+(+)	+		1.05	0.91	1.25	1.69	1.65	1.26
3864	homogentisate 1,2-dioxygenase	<	+(+)	+(+)	+	3.81	1.44	1.69	1.66	2.06	2.08	2.23
3865	4-hydroxyphenylpyruvate dioxygenase	<	+(+)	+(+)	+	7.99	1.73	1.40	1.60	2.17	2.48	3.23
4258	gentisate-1,2 dioxygenase like	>	+(+)	+(+)	+		1.01	0.71	0.91	1.00	0.83	0.95
4261	5-carboxymethyl-2-hydroxymuconate delta-isomerase	>	+(+)	+(±)	+		0.86	0.90	1.74	1.09	1.71	1.37
4262	ornithine cyclodeaminase	>	+(+)	+(±)	+		0.93	1.22	1.46	1.57	1.74	2.33
4263	gentisate 1 2-dioxygenase-like protein	>	+(+)	+(+)	±		1.20	0.90	0.99	0.84	1.12	0.85
4264	hypothetical protein	>	-(+)	+(±)	±		0.86	1.33	0.85	0.91	0.81	0.71
4265	LysR family transcriptional regulator	>	+(+)	+(+)	+		2.01	2.58	1.35	1.06	1.19	1.38
4269	vanillate monooxygenase	>	+(+)	+(±)	+		0.80	1.01	1.20	1.13	1.27	1.75
4273	vanillate monooxygenase	>	+(+)	+(+)	+		1.13	1.20	1.25	1.87	2.20	2.51
4278	ARD-alpha	<	+(+)	+(+)	+		1.54	2.33	1.89	1.84	2.04	1.84
4280	ARD-alpha	>	+(+)	+(+)	+		0.90	0.78	1.03	0.85	1.07	1.38
4281	ARD-beta	>	+(+)	+(+)	+		0.78	0.71	0.68	0.73	0.86	1.03

4336	beta-ketoacyl CoA thiolase	<	+(+)	+(+)	+		0.75	0.88	1.06	1.02	2.07	1.39
4337	butyryl-CoA:acetate CoA transferase	<	+(+)	+(+)	+	0.42	0.70	0.60	1.09	1.09	1.18	1.89
4338	3-oxoacid CoA-transferase subunit A	<	+(+)	-(+)	+		1.16	1.40	1.04	1.04	1.31	1.53
4339	beta-ketoadipate pathway transcriptional regulator	>	+(+)	-(+)	+		0.91	1.13	1.18	1.33	1.24	1.96
4887	beta-ketoacyl CoA thiolase	<	+(+)	+(+)	+		1.54	0.92	0.79	0.92	0.78	0.98
4888	butyryl-CoA:acetate CoA transferase	<	+(+)	+(+)	+		2.14	0.55	0.93	0.66	0.59	0.91
4889	3-oxoacid CoA-transferase	<	+(+)	+(+)	+		2.79	1.10	1.27	1.31	0.92	1.24
4890	hydroxyquinol 1,2 dioxygenase	<	+(+)	+(+)	+		2.87	1.17	1.26	0.92	0.88	0.85
4891	iron-containing alcohol dehydrogenase	<	+(+)	+(+)	+		2.35	0.99	0.95	1.27	1.44	1.79
4892	hypothetical protein	<	+(+)	+(+)	+		2.50	1.01	0.82	0.61	0.81	0.95
4893	ferredoxin	<	+(±)	+(±)	+		2.64	3.61	1.35	0.46	0.56	0.79
4894	TonB-dependent receptor	<	+(+)	+(+)	+		2.08	0.93	1.52	1.61	0.99	1.15
4895	alpha/beta hydrolase fold	<	+(-)	+(±)	±		1.29	0.90	1.16	0.93	1.34	1.40
4896	aromatic-ring-hydroxylating dioxygenase	<	+(±)	+(±)	-		1.85	0.69	1.46	1.61	1.24	2.10
4897	ring hydroxylating dioxygenase	<	+(-)	+(±)	±	0.48	2.93	1.52	1.32	1.72	1.39	2.53
4902	DbfB EDO	>	+(+)	+(+)	+	0.37	4.41	2.35	0.79	0.46	0.46	0.67
4922	pyruvate	<	+(+)	+(+)	+	0.13	10.13	0.55	0.81	0.55	0.51	0.46
4923	4-hydroxy-2-ketovalerate aldolase	<	+(+)	+(+)	+	0.13	11.47	0.84	0.93	0.57	0.61	0.55
4924	acetaldehyde dehydrogenase	<	+(+)	+(+)	+	0.11	12.55	0.47	0.93	0.72	0.62	0.69
4925	4-oxalocrotonate decarboxylase	<	+(+)	+(+)	+		13.45	0.67	0.80	0.62	0.63	0.67
5020	3-oxoadipate enol-lactonase		+(+)	+(+)	±		0.24	-0.23	-0.15	-0.17	-0.04	0.44
5021	Acyl CoA:acetate/3-ketoacid CoA transferase beta subunit-like protein		+(+)	±(±)	±		0.75	-0.21	0.01	0.07	0.23	0.53
5023	3-oxoacid CoA-transferase		+(+)	+(±)	±		0.67	0.55	0.98	0.87	0.80	0.12
5040	2-oxo-hepta-3-ene-1,7-dioic acid hydratase	<	+(+)	+(+)	+		0.77	0.99	0.85	0.67	0.54	0.53
5041	intradiol ring-cleavage	<	+(+)	+(+)	+		0.86	1.41	0.93	0.75	0.64	0.48

5042	dioxygenase Hypothetical	<	+(+)	+(+)	+		1.02	1.21	1.27	1.10	0.84	0.45
5043	monooxygenase, FAD- binding	<	+(+)	+(+)	+		1.08	1.58	1.77	1.59	1.10	0.91
5044	major facilitator transporter	<	+(+)	+(+)	+		0.89	1.49	1.22	1.00	1.01	0.80
5045	TonB-dependent receptor	<	+(+)	+(+)	+		1.16	2.13	1.53	1.04	0.97	0.65
5046	Aldehyde dehydrogenase	<	+(+)	+(+)	+		1.52	1.61	1.41	1.57	1.34	1.34
5047	Benzoylformate decarboxylase	<	+(+)	+(+)	+		1.14	1.14	0.75	1.01	1.12	1.26
5084	hypothetical protein	<	-(+)	-(±)	+		1.01	0.77	0.72	0.42	0.27	0.18
5085	hypothetical protein	<	+(+)	+(+)	+		0.97	0.54	0.52	0.27	0.18	0.12
5086	maleylacetoacetate isomerase	<	+(+)	+(+)	+		1.30	0.83	0.60	0.29	0.23	0.18
5087	fumarylacetoacetate (FAA) hydrolase	<	+(+)	+(+)	+		1.39	0.97	0.51	0.25	0.20	0.15
5088	ferredoxin	<	+(+)	+(+)	+		1.60	0.94	0.75	0.58	0.45	0.38
5089	fumarylacetoacetate (FAA) hydrolase	<	+(+)	+(+)	+		1.47	1.10	0.69	0.44	0.40	0.43
5101	Monooxygenase, FAD binding	<	+(+)	+(+)	+	56.05	17.27	0.80	0.94	0.68	0.52	1.10
5102	gentisate 1,2-dioxygenase	<	+(+)	+(+)	+	41.98	11.31	0.82	1.19	1.16	1.19	1.16

Table S3. *Spingomonas wittichii* genes with tenfold or more transposon insertions after 50 generations DBF growth compared to the starting library.

locus	product	COG _cat	log Ratio	log Ratio	chemostat	chemostat	chemostat	chemostat	RATIO Tn
			DBF short/ctrl	DBF long/ctrl	log ratio 30m	log ratio 1h	log ratio 2h	log ratio 6h	abundance DBF/TN0
Swit_0155	hypothetical protein	S						1.004	18.104
Swit_0265	glutamate synthase (NADH) large subunit	E							9.978
Swit_0652	methylmalonate-semialdehyde dehydrogenase	C							11.617
Swit_1290	FliI/YscN family ATPase	NU							21.653
Swit_1532	aromatic-ring-hydroxylating dioxygenase subunit beta	Q							11.737
Swit_1533	helix-turn-helix domain-containing protein	F	1.172	1.515					28.894
Swit_2055	FAD-dependent pyridine nucleotide-disulfide oxidoreductase	C							30.951
Swit_2338	sodium:dicarboxylate symporter	C							12.476
Swit_2339	hypothetical protein	S	2.015	1.088				1.114	12.550
Swit_2362	4-hydroxybenzoate polyprenyltransferase	H							15.820
Swit_2373	glycosyl transferase family protein	M							163.299
Swit_2557	cold-shock DNA-binding protein family protein	K	-1.451		-1.079	-1.685	-1.757		48.619
Swit_2574	hypothetical protein	S						-1.921	13.203
Swit_2724	methyl-accepting chemotaxis sensory transducer	NT				1.076	1.279		12.728
Swit_2819	hypothetical protein	S	-1.248						10.882
Swit_2840	hypothetical protein	S							16.503
Swit_2858	CorA family protein Mg ²⁺ transporter protein	P							10.970
Swit_2894	carboxyl transferase	I	-1.206				1.271	1.923	15.959
Swit_2907	RNA polymerase factor sigma-54	K							70.940
Swit_2978	UDP-galactose 4-epimerase	M	1.022						74.466
Swit_3024	vanillate monooxygenase	PR							11.423
Swit_3033	major facilitator transporter	G							17.943
Swit_3044	TonB-dependent receptor	P	1.467	1.499		-1.249	-1.495	-1.277	28.696
Swit_3045	FAD-binding monooxygenase	HC							50.412
Swit_3067	succinate semialdehyde dehydrogenase	C	1.151	1.366					10.870
Swit_3113	peptidase M14	E							16.894
Swit_3200	lycopene cyclase	S					-1.432	-1.522	19.995

Swit_3258	AsnC family transcriptional regulator	K							10.006
Swit_3455	large conductance mechanosensitive channel protein	M		1.091		1.116			10.755
Swit_3529	type 12 methyltransferase	I				1.160			19.543
Swit_3606	hypothetical protein	P							24.734
Swit_3755	ketosteroid isomerase-like protein	R							12.567
Swit_3853	4-phytase	E							12.239
Swit_3976	molybdopterin binding aldehyde oxidase and xanthine dehydrogenase	C						1.100	14.851
Swit_4355	aminoglycoside phosphotransferase	R							11.414
Swit_4378	arsenate reductase-like protein	P	-1.201		-1.097	-1.704	-1.956	-1.914	14.199
Swit_4417	molybdate ABC transporter inner membrane subunit	P	-1.252						13.930
Swit_4602	extradiol cleavage dioxygenase	R							11.966
Swit_4697	arsenate reductase	P	-2.194			-1.129	-1.045	-1.326	9.972
Swit_4728	hypothetical protein	S		1.147		-1.113	-1.222	-1.493	13.386
Swit_4822	hypothetical protein	X396							11.500
Swit_4889	3-oxoacid CoA-transferase	I		1.484					13.048
Swit_5149	hypothetical protein	X420							12.033
Swit_5305	camphor resistance protein CrcB	D							13.557

Table S4. Commonly expressed RW1 genes with at least 4-fold expression difference.

Locus	product	COG _cat	Ratio DBF short/ctr	Ratio DBF long/ctrl	Ratio Chem 30m/ctrl	Ratio Chem 1h/ctrl	Ratio Chem 2h/ctrl	Ratio Chem 6h/ctrl	RATIO Tn abun-dance DBF/TN0
Swit_0028	Aquaporin Z	G	6.27	2.83	1.94	2.51	2.23	2.49	2.07
Swit_0045	Histone family protein DNA-binding protein	L	4.06	4.63	0.77	0.55	0.49	0.63	3.83
Swit_0063	Hypothetical protein	S	0.52	1.10	0.43	0.31	0.29	0.23	1.38
Swit_0072	Hypothetical protein	X6	4.99	1.13	7.92	11.14	7.64	2.88	1.04
Swit_0083	50S ribosomal protein L9	J	0.02	0.30	0.34	0.30	0.14	0.18	49.79
Swit_0085	Pseudo		0.02	0.31	0.36	0.24	0.19	0.17	
Swit_0090	Aminodeoxychorismate lyase	R	0.36	0.74	0.68	0.48	0.29	0.23	0.13
Swit_0097	Marr family transcriptional regulator	K	24.31	4.91	2.48	2.94	2.86	1.98	24.73
Swit_0101	K+ potassium transporter	P	0.21	0.44	0.66	0.59	0.47	0.39	7.77
Swit_0114	Short-chain dehydrogenase/reductase SDR	IQR	0.29	0.68	0.53	0.35	0.31	0.22	0.22
Swit_0117	Tonb family protein	M	0.14	1.16	0.60	0.38	0.24	0.28	0.00
Swit_0118	Mota/tolq/exbb proton channel	U	0.20	0.92	0.53	0.26	0.19	0.19	0.24
Swit_0133	Queueine trna-ribosyltransferase	J	0.21	0.42	0.80	0.64	0.52	0.59	0.23
Swit_0137	Sapc family protein	S	0.09	0.33	0.53	0.43	0.42	0.34	2.54
Swit_0140	DEAD/DEAH box helicase	LKJ	0.15	0.35	0.52	0.43	0.35	0.44	5.39
Swit_0145	Glutathione S-transferase domain-containing protein	O	4.27	1.62	1.51	1.17	1.79	1.63	17.49
Swit_0230	Hypothetical protein	S	4.47	1.17	1.61	1.95	1.57	1.99	2.67
Swit_0239	Hypothetical protein	X21	18.21	2.00	4.14	7.16	6.90	3.54	1.15
Swit_0262	GTP-binding protein typa	T	0.06	0.32	0.37	0.32	0.22	0.25	0.00
Swit_0387	Hypothetical protein	X28	4.01	1.79	1.01	0.91	0.96	1.10	140.63
Swit_0389	Hypothetical protein	S	0.24	0.41	0.59	0.53	0.52	0.63	0.03
Swit_0429	Periplasmic-like protein	S	0.58	0.89	0.38	0.35	0.12	0.18	1.33
Swit_0436	Hypothetical protein	X31	0.19	0.32	0.50	0.49	0.39	0.39	0.17
Swit_0461	Elongation factor Ts	J	0.19	0.68	0.59	0.45	0.33	0.26	0.00
Swit_0490	Hypothetical protein	S	16.62	1.96	1.44	1.59	1.58	1.14	1.03
Swit_0535	Tonb-dependent receptor	P	10.17	2.66	2.31	1.54	1.37	1.35	1.47
Swit_0545	Hypothetical protein	X37	10.13	2.31	3.95	8.04	6.80	3.38	3.71
Swit_0578	Amidophosphoribosyltransferase	F	0.23	0.72	0.65	0.68	0.60	0.70	1.01
Swit_0594	Trigger factor	O	0.06	0.36	0.53	0.48	0.31	0.29	0.44
Swit_0630	Polyhydroxyalkonate synthesis repressor phar	S	0.13	0.78	0.31	0.15	0.15	0.14	4.68
Swit_0632	Acetyl-coa acetyltransferase	I	0.21	0.49	0.47	0.33	0.36	0.26	3.06
Swit_0635	Trar/dksa family transcriptional regulator	T	0.22	0.68	0.58	0.57	0.41	0.34	193.95
Swit_0642	Ribosomal protein S12 methylthiotransferase	J	0.08	0.28	0.59	0.51	0.43	0.40	2.86
Swit_0654	CRP/FNR family transcriptional regulator	T	50.82	3.39	4.27	6.53	4.49	2.49	0.15

Swit_0655	Hypothetical protein	X46	11.05	3.61	3.28	4.65	3.97	2.08	1.47
Swit_0658	Hypothetical protein	X48	0.82	1.03	1.94	1.47	1.50	4.01	0.00
Swit_0687	Tonb-dependent receptor	P	3.64	4.80	0.72	0.42	0.59	1.11	0.92
Swit_0689	Hypothetical protein	S	2.52	9.99	0.38	0.12	0.19	0.40	1.07
Swit_0690	YVTN beta-propeller repeat-containing protein	S	4.25	5.58	0.46	0.34	0.61	0.90	15.79
Swit_0691	Hypothetical protein	C	3.98	4.60	0.27	0.30	0.39	0.64	0.28
Swit_0692	Extracellular solute-binding protein	ET	5.69	6.06	0.28	0.25	0.35	0.70	0.40
Swit_0693	Pyrrolo-quinoline quinone	G	8.64	6.69	0.39	0.35	0.45	0.90	1.74
Swit_0694	Two component luxr family transcriptional regulator	TK	3.37	4.06	0.61	0.36	0.45	0.83	14.65
Swit_0703	Aldehyde dehydrogenase	C	15.85	10.28	0.36	0.30	0.42	0.89	0.47
Swit_0714	Tonb-dependent receptor	P	0.33	0.10	0.45	0.24	0.18	0.33	0.32
Swit_0748	Bifunctional aldehyde dehydrogenase/enoyl-coa hydratase	C	0.15	0.28	0.36	0.40	0.34	0.38	2.09
Swit_0750	3-hydroxyacyl-coa dehydrogenase	I	0.11	0.53	0.48	0.47	0.38	0.48	0.00
Swit_0751	Phenylacetic acid degradation protein paad	Q	0.15	0.37	0.27	0.43	0.27	0.13	1.94
Swit_0753	Phenylacetate-coa oxygenase subunit paaa	S	0.04	0.50	0.24	0.16	0.14	0.16	1.87
Swit_0754	Phenylacetate-coa oxygenase subunit paab	Q	0.05	0.24	0.14	0.07	0.05	0.05	0.00
Swit_0757	Phenylacetate-coa oxygenase/reductase subunit paak	C	0.08	0.09	0.34	0.34	0.39	0.37	0.57
Swit_0758	Enoyl-coa hydratase/isomerase	I	0.04	0.09	0.33	0.30	0.26	0.25	0.14
Swit_0760	Tetr family transcriptional regulator	K	0.11	0.22	0.20	0.13	0.10	0.13	0.00
Swit_0761	Dehydrogenase catalytic domain-containing protein	C	0.08	0.12	0.17	0.12	0.13	0.11	0.00
Swit_0762	Transketolase domain-containing protein	C	0.04	0.17	0.10	0.08	0.07	0.07	0.18
Swit_0763	Aromatic amino acid aminotransferase	E	0.04	0.44	0.14	0.12	0.11	0.15	0.01
Swit_0772	Hypothetical protein	X50	0.18	0.37	0.56	0.53	0.46	0.32	38.35
Swit_0784	Hypothetical protein	S	10.23	1.35	3.06	3.66	2.51	1.26	0.26
Swit_0785	Hypothetical protein	S	18.53	1.63	4.68	6.35	3.64	1.78	0.45
Swit_0800	Hypothetical protein	S	4.39	0.92	2.90	2.97	2.06	2.24	0.00
Swit_0812	Tonb-dependent receptor	P	4.15	1.09	1.47	1.91	1.88	1.86	0.15
Swit_0858	Hemerythrin HHE cation binding domain-containing protein	S	33.06	2.23	4.53	7.38	5.50	3.09	0.59
Swit_0862	Phasin family protein	S	0.04	0.30	0.34	0.34	0.32	0.24	1.08
Swit_0878	Hypothetical protein	S	8.41	2.85	3.62	5.46	5.55	2.62	55.40
Swit_0879	Group 1 glycosyl transferase	M	0.15	0.43	0.55	0.47	0.48	0.38	22.44
Swit_0916	Peptidase dimerisation domain-containing protein	E	0.19	0.56	0.85	0.51	0.52	0.44	0.67
Swit_0941	Formyltetrahydrofolate deformylase	F	0.17	0.43	0.54	0.59	0.53	1.23	24.36
Swit_0958	Butyryl-coa:acetate coa transferase	I	7.11	2.36	6.63	2.42	1.24	0.54	5.07
Swit_0959	3-oxoacid coa-transferase subunit A	I	6.52	2.75	3.64	1.38	0.72	0.27	9.58
Swit_0981	Tonb-dependent receptor	P	8.00	2.64	1.42	1.07	1.24	1.15	0.31
Swit_0995	PRC-barrel domain-containing protein	S	37.74	2.05	3.05	5.25	5.24	3.29	96.39
Swit_1052	Ornithine cyclodeaminase	E	1.44	1.43	1.58	1.11	1.36	6.28	0.57

Swit_1090	Diacylglycerol kinase catalytic subunit	IR	4.93	1.72	4.05	5.26	3.59	1.69	0.65
Swit_1116	Tonb-dependent receptor	P	0.11	0.27	0.84	0.62	0.47	0.66	2.05
Swit_1146	ATP-dependent protease La	O	4.79	2.10	2.79	4.00	3.12	2.10	5.27
Swit_1147	Molecular chaperone (small heat shock protein)-like protein	O	7.47	2.01	4.13	6.04	5.15	3.11	0.69
Swit_1148	Type B carboxylesterase	I	2.72	1.13	1.55	2.59	2.77	6.04	1.04
Swit_1181	NAD(P)(+) transhydrogenase	C	0.13	0.89	0.36	0.33	0.24	0.30	1.56
Swit_1182	NAD/NADP transhydrogenase subunit alpha-like protein	C	0.14	0.85	0.25	0.15	0.16	0.13	75.86
Swit_1183	NAD(P) transhydrogenase subunit alpha	C	0.23	0.61	0.49	0.34	0.26	0.26	6.06
Swit_1219	Hypothetical protein	S	0.17	1.44	0.79	0.70	0.40	0.58	5.21
Swit_1247	Hypothetical protein	X87	23.26	2.60	7.83	7.75	5.76	2.45	14.24
Swit_1268	Flagellar basal body flae domain-containing protein	N	0.17	1.25	1.23	1.19	1.15	1.15	1.07
Swit_1270	Flagellar basal-body rod protein flgc	N	0.10	1.35	0.86	1.05	0.88	0.92	36.42
Swit_1286	Flagellar hook-basal body complex subunit flie	NU	0.24	2.33	1.41	1.21	1.13	0.69	37.85
Swit_1293	Flagellar basal body-associated protein flil	N	0.14	1.43	1.11	1.06	0.94	0.78	2.97
Swit_1295	Hypothetical protein	S	4.70	1.10	3.20	7.53	6.80	4.79	4.12
Swit_1320	DGPFAETKE family protein	S	2.38	1.19	4.76	9.41	7.71	4.00	0.00
Swit_1325	50S ribosomal protein L17	J	0.09	0.53	0.35	0.25	0.19	0.13	0.06
Swit_1361	Hypothetical protein	S	14.11	2.29	4.08	8.18	7.26	4.36	30.38
Swit_1377	50S ribosomal protein L25/general stress protein Ctc	J	0.06	0.40	0.33	0.26	0.16	0.13	2.08
Swit_1388	Hypothetical protein	X99	4.21	2.67	1.04	1.22	1.07	1.31	0.21
Swit_1389	GTP-dependent nucleic acid-binding protein engd	J	0.17	0.33	0.56	0.41	0.39	0.24	0.00
Swit_1390	Dehydratase	I	0.17	0.38	0.35	0.21	0.17	0.13	2.35
Swit_1394	Cytochrome c1	C	0.06	0.77	0.34	0.20	0.14	0.14	0.00
Swit_1449	Phenylacetate-coa ligase	H	0.11	0.38	0.65	0.67	0.73	0.81	0.38
Swit_1457	DNA uptake lipoprotein-like protein	R	0.35	0.86	0.48	0.39	0.27	0.25	0.00
Swit_1458	Flagellar motor switch protein flim	N	0.21	0.97	0.72	0.76	0.79	1.44	1.91
Swit_1507	17 kda surface antigen	X111	83.33	4.67	6.05	7.99	6.97	3.75	0.76
Swit_1509	17 kda surface antigen	M	10.17	2.43	2.45	3.11	2.71	1.99	0.37
Swit_1547	Fumarylacetoacetate (FAA) hydrolase	Q	1.15	1.33	0.85	0.95	1.15	5.58	1.79
Swit_1827	Alpha/beta hydrolase fold protein	R	4.61	1.05	1.35	1.70	1.54	1.61	1.93
Swit_1828	Acyl-coa dehydrogenase type 2	I	14.82	1.04	4.62	4.57	2.88	1.71	0.72
Swit_1829	Rieske (2Fe-2S) domain-containing protein	PR	6.10	1.13	2.04	1.95	2.27	2.09	0.00
Swit_1831	Enoyl-coa hydratase/isomerase	I	4.67	1.10	2.51	3.55	2.31	1.91	27.81
Swit_1832	Dehydratase	I	1.43	0.85	2.45	4.42	4.09	4.21	0.00
Swit_1836	Acyl-coa dehydrogenase domain-containing protein	I	8.32	1.10	3.12	3.39	2.43	1.91	0.50
Swit_1840	Enoyl-coa hydratase/isomerase	I	5.05	0.74	2.55	2.98	2.36	3.00	1.66
Swit_1845	Tetr family transcriptional regulator	K	9.02	1.82	1.54	1.52	1.53	1.65	0.01
Swit_1846	Enoyl-coa hydratase	I	14.00	1.14	2.71	2.88	2.76	2.75	1.92

Swit_1847	Cytochrome P450-like protein	Q	7.57	1.40	1.48	1.88	2.06	1.89	0.27
Swit_1849	Glyoxalase/bleomycin resistance protein/dioxygenase	Q	25.18	1.60	3.57	4.21	2.61	3.91	0.31
Swit_1850	Acyl-coa dehydrogenase domain-containing protein	I	11.88	1.34	2.83	2.53	1.75	1.66	1.36
Swit_1851	Acyl-coa dehydrogenase domain-containing protein	I	7.83	1.46	1.58	1.26	1.66	1.09	0.61
Swit_1858	Sulfatase	P	6.58	1.37	2.59	2.33	2.74	3.39	0.35
Swit_1859	Tonb-dependent receptor	P	8.35	1.16	2.38	2.16	1.85	1.66	0.39
Swit_1860	Hypothetical protein	C	4.89	0.91	1.25	1.40	1.10	1.00	0.18
Swit_1926	ABC transporter-like protein	V	0.25	0.65	0.46	0.34	0.28	0.23	0.02
Swit_1945	Crp/FNR family transcriptional regulator	T	1.32	4.02	1.40	1.39	1.52	3.05	0.03
Swit_1951	RND efflux system outer membrane lipoprotein	MU	6.31	0.75	0.96	1.08	1.10	0.94	0.01
Swit_1952	Hydrophobe/amphiphile efflux-1 (HAE1) family protein	V	5.21	0.62	1.15	1.32	1.22	0.93	0.19
Swit_1955	Integral membrane sensor signal transduction histidine kinase	T	5.62	0.76	1.17	1.48	2.33	1.72	0.26
Swit_2047	Arac family transcriptional regulator	K	1.43	4.10	0.97	1.25	1.43	2.55	0.66
Swit_2123	Hypothetical protein	S	1.99	0.92	0.93	0.65	0.56	0.23	1.77
Swit_2142	Hypothetical protein	S	0.11	0.35	0.65	0.52	0.38	0.43	0.01
Swit_2228	Hypothetical protein	R	0.66	0.48	0.24	0.52	0.17	0.13	1.35
Swit_2278	Ompa/motb domain-containing protein	M	7.79	1.32	2.50	3.02	2.37	2.08	1.48
Swit_2322	Ompa/motb domain-containing protein	M	25.01	1.91	5.18	6.10	2.98	1.75	117.41
Swit_2324	Hypothetical protein	S	16.31	2.31	5.70	13.29	8.93	4.76	0.25
Swit_2335	Hypothetical protein	S	4.15	1.50	2.58	3.16	2.47	1.74	11.03
Swit_2339	Hypothetical protein	S	4.04	2.13	1.10	1.53	1.87	2.17	12.55
Swit_2341	Cytochrome c peroxidase-like protein	P	3.03	4.50	1.84	1.92	1.85	2.68	2.02
Swit_2383	Ribosomal-protein-alanine acetyltransferase	R	0.54	1.33	0.46	0.31	0.20	0.25	0.00
Swit_2399	Methionine synthase	E	0.14	0.70	0.25	0.17	0.16	0.19	2.58
Swit_2400	Methionine synthase	E	0.03	0.67	0.19	0.10	0.10	0.11	3.78
Swit_2401	5,10-Methylene tetrahydrofolate reductase	E	0.03	0.54	0.15	0.10	0.10	0.13	0.47
Swit_2402	Arsr family transcriptional regulator	H	0.07	0.40	0.26	0.17	0.13	0.24	0.30
Swit_2403	Vacj family lipoprotein	M	0.23	1.05	0.47	0.34	0.24	0.28	3.41
Swit_2422	Transglycosylase-associated protein	S	40.28	3.70	2.94	5.68	5.18	2.81	0.19
Swit_2431	50S ribosomal protein L20	J	0.07	0.36	0.41	0.36	0.26	0.22	8.54
Swit_2433	Asma family protein	M	4.71	1.42	2.58	3.90	3.64	1.95	1.69
Swit_2438	Ribose-phosphate pyrophosphokinase	FE	0.12	0.46	1.34	1.52	1.24	1.10	0.25
Swit_2448	Hypothetical protein	GER	0.10	0.44	0.63	0.50	0.52	0.53	1.86
Swit_2457	Cytidylate kinase	F	0.19	0.41	0.71	0.82	0.61	0.70	0.00
Swit_2526	Signal-transduction protein	T	7.05	3.22	1.41	1.35	1.95	3.05	6.56
Swit_2532	Inorganic diphosphatase	C	0.03	0.36	0.58	0.55	0.66	1.11	1.33
Swit_2559	Hypothetical protein	X205	0.04	0.22	0.43	0.38	0.30	0.15	1.02
Swit_2634	Benzoate 1,2.dioxygenase α	PR	2.36	5.06	1.42	1.87	2.07	3.05	2.30

Swit_2640	Sugar transferase	M	0.40	0.92	0.51	0.36	0.25	0.22	56.02
Swit_2651	Hypothetical protein	HJ	1.02	1.45	0.51	0.20	0.16	0.14	6.92
Swit_2652	Polysaccharide biosynthesis protein	R	0.45	1.50	0.42	0.19	0.17	0.16	2.91
Swit_2653	Serine acetyltransferase-like protein	E	0.34	1.54	0.40	0.20	0.18	0.21	1.77
Swit_2654	Hypothetical protein	R	0.76	1.49	0.46	0.20	0.18	0.15	62.98
Swit_2659	Hypothetical protein	X218	0.16	0.30	0.48	0.58	0.64	0.55	12.03
Swit_2664	Aspartate-semialdehyde dehydrogenase	E	0.21	0.34	0.56	0.49	0.44	0.42	4.68
Swit_2679	Hypothetical protein	S	5.36	4.98	0.86	0.59	0.57	0.65	11.44
Swit_2687	Preprotein translocase subunit seca	U	0.19	0.70	0.62	0.60	0.48	0.61	34.71
Swit_2702	Class II aldolase/adducin family protein	G	0.10	0.38	0.75	0.54	0.54	0.59	1.88
Swit_2703	Tetr family transcriptional regulator	K	0.15	0.61	0.90	0.54	0.32	0.34	86.01
Swit_2731	Aconitase	C	0.22	0.81	0.56	0.39	0.27	0.22	0.01
Swit_2732	Bifunctional aconitate hydratase 2/2-methylisocitrate dehydratase	C	0.21	0.69	0.61	0.44	0.44	0.57	0.07
Swit_2738	CHAP domain-containing protein	R	1.08	2.21	0.36	0.21	0.23	0.23	5.56
Swit_2779	Dps family ferritin	P	5.66	2.88	2.54	3.26	2.15	1.40	0.25
Swit_2796	Glutaminase	E	0.77	1.58	0.56	0.48	0.25	0.20	82.54
Swit_2810	Trpr binding protein wrba	R	6.75	1.59	1.19	1.12	0.93	0.93	5.76
Swit_2813	Hypothetical protein	S	0.16	0.58	0.56	0.52	0.40	0.42	0.00
Swit_2815	Hypothetical protein	S	1.58	0.76	1.24	2.10	2.85	4.14	2.44
Swit_2820	Electron transport protein SCO1/senc	R	0.20	0.71	0.71	0.55	0.44	0.75	0.28
Swit_2827	30S ribosomal protein S30P	J	6.32	3.88	1.43	0.87	0.99	1.09	1.45
Swit_2835	Transcription termination factor Rho	K	0.19	0.51	0.55	0.46	0.38	0.28	0.00
Swit_2900	Methionine-R-sulfoxide reductase	O	6.96	1.30	2.07	2.33	2.06	2.11	190.08
Swit_2926	Isocitrate lyase	C	0.05	0.16	0.50	0.33	0.26	0.18	1.83
Swit_2960	Hypothetical protein	X227	0.24	0.60	0.79	0.71	0.84	0.71	8.14
Swit_2970	Hypothetical protein	S	0.06	0.33	0.44	0.34	0.31	0.21	1.10
Swit_2980	Elongation factor P	J	0.10	0.36	0.45	0.35	0.23	0.19	6.98
Swit_2982	NADH-ubiquinone/plastoquinone oxidoreductase subunit 3	C	0.10	0.44	0.44	0.36	0.29	0.26	0.00
Swit_2984	NADH (or F420H2) dehydrogenase subunit C	C	0.14	0.47	0.50	0.45	0.41	0.36	0.00
Swit_2990	Hypothetical protein	X232	0.13	0.88	0.52	0.32	0.19	0.16	0.00
Swit_3008	Hypothetical protein	M	0.27	1.14	0.28	0.20	0.11	0.17	2.32
Swit_3103	Tonb-dependent receptor	P	6.93	1.54	1.26	1.11	1.28	1.97	0.83
Swit_3111	HNH endonuclease	V	5.17	3.34	1.42	1.04	0.87	0.92	0.49
Swit_3114	Hypothetical protein	S	4.11	3.47	1.99	2.78	2.15	1.43	1.23
Swit_3116	HAD family hydrolase	R	0.09	0.25	0.49	0.53	0.42	0.30	7.83
Swit_3189	Tonb-dependent receptor	H	0.16	0.80	1.15	0.64	0.72	1.01	0.57
Swit_3212	Histidine kinase	T	0.16	0.87	0.51	0.32	0.25	0.24	145.34
Swit_3236	Pyruvate flavodoxin/ferredoxin oxidoreductase domain-	C	4.67	2.19	1.27	1.14	1.08	1.05	3.20

	containing protein								
Swit_3240	Aldehyde dehydrogenase	C	6.10	0.43	1.09	1.24	1.43	3.50	2.25
Swit_3241	Tonb-dependent receptor	P	17.64	0.30	1.59	1.44	1.77	5.41	0.01
Swit_3242	Amidohydrolase 3	R	8.49	0.49	1.61	1.78	1.69	3.39	0.68
Swit_3243	Amidohydrolase 3	R	13.10	0.60	1.15	1.39	1.43	2.32	0.61
Swit_3244	Metal dependent phosphohydrolase	R	5.07	0.60	1.09	1.02	1.41	1.58	0.05
Swit_3246	Amidohydrolase 3	R	10.68	0.83	0.96	0.76	0.53	1.94	0.32
Swit_3250	Hypothetical protein	C	6.12	0.52	1.31	1.41	1.52	2.08	1.27
Swit_3251	Amine dehydrogenase	Q	4.41	0.92	1.12	1.28	1.41	1.49	57.75
Swit_3252	Methylamine dehydrogenase accessory protein maud	C	4.38	0.78	1.20	1.17	1.40	1.67	1.26
Swit_3254	Amine dehydrogenase	C	11.83	0.78	1.75	1.61	2.23	3.29	0.26
Swit_3256	Tonb-dependent receptor	P	16.33	0.65	1.72	1.96	2.71	4.99	7.82
Swit_3259	Hypothetical protein	S	5.13	0.75	3.41	3.37	3.92	4.94	0.14
Swit_3342	Bifunctional sulfate adenylyltransferase subunit 1/adenylylsulfate kinase	P	4.72	0.54	0.98	1.10	1.20	0.79	0.00
Swit_3430	Hypothetical protein	S	4.76	1.16	3.62	7.70	7.51	4.73	1.41
Swit_3448	Polyprenyl synthetase	H	0.23	0.39	0.91	0.83	0.83	0.76	2.60
Swit_3463	Cell wall hydrolase sleb	M	0.19	0.27	0.24	0.20	0.22	0.15	0.17
Swit_3467	DNA-directed RNA polymerase subunit beta'	K	0.16	0.83	0.63	0.42	0.29	0.39	0.00
Swit_3480	ABC transporter-like protein	R	0.17	0.37	0.67	0.64	0.47	0.77	2.02
Swit_3503	Parb-like partition protein	K	4.82	2.24	1.24	1.30	1.47	1.52	5.40
Swit_3504	Response regulator receiver protein	T	7.23	3.23	1.01	0.95	0.83	1.08	1.04
Swit_3531	Cyclophilin type peptidyl-prolyl cis-trans isomerase	O	0.23	0.66	0.61	0.51	0.35	0.34	4.37
Swit_3596	Hypothetical protein	X279	55.46	1.54	3.89	6.49	5.67	3.42	0.52
Swit_3601	Short-chain dehydrogenase/reductase SDR	IQR	3.15	1.44	1.04	1.33	2.63	4.89	1.73
Swit_3602	Acetyl-coa acetyltransferase	I	2.17	1.30	1.22	1.64	2.81	4.32	0.88
Swit_3603	Acyl-coa dehydrogenase domain-containing protein	I	2.65	1.09	1.28	2.02	5.80	10.05	2.00
Swit_3604	Tetr family transcriptional regulator	K	1.85	1.10	1.25	1.35	3.40	4.56	2.53
Swit_3605	Phosphate transporter	P	0.16	0.70	0.54	0.58	0.41	0.28	1.47
Swit_3609	Glycoside hydrolase 15-like protein	G	5.95	1.62	3.30	5.38	3.59	1.58	1.24
Swit_3613	Hypothetical protein	X281	7.61	1.46	2.60	3.48	2.82	1.60	196.81
Swit_3617	Putative inner membrane protein translocase component ydc	U	0.18	0.57	0.70	0.61	0.71	0.68	0.13
Swit_3716	Cytochrome B561	C	1.33	1.11	1.31	1.80	4.53	7.38	0.01
Swit_3717	Hypothetical protein	S	1.57	1.28	1.17	1.60	2.98	4.14	0.37
Swit_3719			22.48	0.84	1.06	1.47	7.83	3.64	
Swit_3720	Tolc family type I secretion outer membrane protein	MU	18.13	1.23	1.23	2.09	6.93	4.03	0.30
Swit_3721	Hypothetical protein	S	124.82	1.63	1.45	2.87	12.21	7.38	0.67
Swit_3722	FAD-dependent pyridine nucleotide-disulfide oxidoreductase	C	156.95	3.55	1.22	2.05	7.97	5.01	4.04

Swit_3724	RND family efflux transporter MFP subunit	-	40.04	1.81	1.38	2.27	8.09	4.72	0.69
Swit_3725	Acriflavin resistance protein	V	27.32	1.25	1.60	2.49	9.00	4.94	1.54
Swit_3726	Arsr family transcriptional regulator	K	4.30	1.00	0.89	1.07	2.77	1.92	1.05
Swit_3727	Hypothetical protein	S	7.18	0.76	0.98	1.68	4.85	2.71	40.03
Swit_3728	Hypothetical protein	S	9.42	0.87	0.79	1.09	4.78	2.65	0.57
Swit_3730	Catalase	P	205.98	1.87	1.17	2.73	10.61	4.90	0.81
Swit_3732	Dps family ferritin	P	22.90	0.97	0.82	1.10	2.77	1.27	0.00
Swit_3733	Redoxin domain-containing protein	CO	6.23	0.79	0.96	1.44	3.24	1.39	0.71
Swit_3735	Cytochrome d ubiquinol oxidase subunit II	C	19.63	1.34	1.02	2.83	8.52	3.40	0.25
Swit_3736	Cytochrome bd ubiquinol oxidase subunit I	C	7.68	1.19	1.20	2.66	5.68	2.45	0.39
Swit_3737	Cysteine ABC transporter permease/ATP-binding protein	CO	7.64	1.39	0.89	1.53	3.46	0.87	28.41
Swit_3738	ABC transporter-like protein	CO	8.84	1.06	1.00	1.19	1.99	1.47	0.16
Swit_3739	Chloride channel core protein	P	14.89	0.95	1.47	3.20	3.09	1.67	1.33
Swit_3742	Thioredoxin	O	6.01	1.11	1.05	1.76	3.30	1.56	30.61
Swit_3743	1-Cys peroxiredoxin	O	102.84	1.82	1.45	2.88	12.72	3.11	0.57
Swit_3744	Beta-lactamase domain-containing protein	R	6.06	0.75	0.96	1.49	4.38	1.68	0.00
Swit_3745	Hypothetical protein	R	7.08	1.39	1.65	3.16	7.22	2.23	2.42
Swit_3746	Type 11 methyltransferase	H	10.38	1.02	1.40	1.99	4.55	1.69	0.30
Swit_3747	Hypothetical protein	X291	6.73	1.11	1.12	1.11	2.28	0.78	112.37
Swit_3774	7-cyano-7-deazaguanine reductase	R	0.25	0.43	0.61	0.53	0.46	0.53	5.18
Swit_3778	Hypothetical protein	S	0.08	0.55	0.17	0.13	0.13	0.15	13.12
Swit_3791	Merr family transcriptional regulator	K	5.53	0.88	2.11	2.72	2.51	1.88	0.80
Swit_3792	AMP-dependent synthetase and ligase	IQ	4.81	1.95	2.48	3.28	3.22	3.08	1.85
Swit_3793	Aromatic hydrocarbon degradation membrane protein	I	26.50	1.95	4.44	5.76	5.06	5.26	1.74
Swit_3794	Hypothetical protein	S	16.31	3.74	2.87	3.16	3.65	3.77	1.48
Swit_3795	Acetyl-coa acetyltransferase	I	9.06	2.43	1.85	1.64	1.67	1.95	0.61
Swit_3796	3-hydroxyacyl-coa dehydrogenase	I	7.72	1.91	2.84	2.83	2.81	3.34	0.99
Swit_3797	Acyl-coa dehydrogenase domain-containing protein	I	11.59	1.31	2.84	2.90	3.02	3.71	0.00
Swit_3798	DEAD/DEAH box helicase	KJ	0.17	0.35	0.55	0.51	0.89	0.76	1.62
Swit_3803	Erfk/ybis/ycfs/ynhg family protein	S	11.61	1.32	4.77	5.95	4.19	2.05	0.17
Swit_3808	Trna pseudouridine synthase B	J	0.23	0.27	0.68	0.88	0.78	0.94	0.21
Swit_3810	Polynucleotide phosphorylase/polyadenylase	J	0.09	0.39	0.53	0.37	0.24	0.28	45.17
Swit_3829	Protein translocase subunit secb	U	0.19	0.53	0.52	0.47	0.37	0.32	1.26
Swit_3838	Malate synthase G	C	0.58	0.15	0.67	0.41	0.26	0.30	3.25
Swit_3867	Hypothetical protein	S	4.43	1.63	1.16	1.43	1.73	2.45	1.19
Swit_3876	Cytochrome c oxidase subunit I	C	0.16	0.86	0.53	0.33	0.25	0.24	25.23
Swit_3879	Cytochrome C oxidase assembly protein	O	0.17	0.51	0.65	0.51	0.35	0.22	0.00
Swit_3880	Cytochrome c oxidase subunit III	C	0.24	0.70	0.68	0.56	0.47	0.39	0.01
Swit_3909	Lysine exporter protein lyse/ygga	E	0.17	0.57	0.57	0.23	0.37	0.27	0.65

Swit_3913	Peptidase M23B	M	0.37	0.92	0.23	0.11	0.15	0.14	0.00
Swit_3924	ECF subfamily RNA polymerase sigma-24 factor	K	10.36	2.26	4.27	4.28	2.58	1.16	0.23
Swit_3927	Entericidin ecnab	S	52.18	6.04	2.56	3.77	2.73	1.54	1.07
Swit_3960	Hypothetical protein	S	0.24	0.62	0.40	0.31	0.25	0.18	1.15
Swit_3961	Ybak/prolyl-trna synthetase associated domain-containing protein	S	0.24	0.57	0.56	0.86	0.79	0.21	5.53
Swit_3981	Ku family containing protein	S	10.47	2.01	5.27	7.69	6.58	3.85	0.77
Swit_4005	Sulfotransferase	R	0.17	0.63	0.38	0.39	0.26	0.38	36.11
Swit_4006	Hlyd family type I secretion membrane fusion protein	V	0.11	0.59	0.42	0.35	0.31	0.23	0.00
Swit_4044	Hypothetical protein	X310	4.52	2.14	1.03	1.18	1.75	2.19	52.48
Swit_4060	Uroporphyrinogen-III C-methyltransferase	H	0.15	0.55	0.43	0.34	0.38	0.41	0.00
Swit_4080	Transporter DMT superfamily protein	R	0.21	0.53	0.90	0.71	0.54	0.51	1.44
Swit_4096	Hemerythrin HHE cation binding domain-containing protein	X320	6.22	2.06	3.43	5.62	5.78	3.69	80.24
Swit_4103	Hypothetical protein	S	0.02	0.26	0.39	0.27	0.25	0.22	1.01
Swit_4110	Translation initiation factor IF-1	J	0.11	0.45	0.58	0.52	0.35	0.34	3.25
Swit_4111	Maf protein	D	0.25	0.56	0.60	0.61	0.59	0.58	35.32
Swit_4113	Hypothetical protein	S	0.25	0.97	0.65	0.44	0.46	0.61	0.17
Swit_4363	Methylamine dehydrogenase heavy subunit	Q	7.36	2.15	1.05	1.16	1.53	1.96	0.65
Swit_4375	Hypothetical protein	S	0.25	0.75	0.53	0.57	0.58	0.65	6.31
Swit_4381	Endoribonuclease L-PSP	J	0.22	0.57	0.59	0.89	0.63	0.83	2.83
Swit_4385	Hypothetical protein	X330	8.28	1.22	2.70	3.08	2.80	2.43	0.00
Swit_4386	Hypothetical protein	S	7.88	1.12	1.84	1.75	1.71	1.35	0.26
Swit_4402	Hypothetical protein	S	0.25	0.62	0.56	0.50	0.40	0.35	5.31
Swit_4432	PAS/PAC sensor hybrid histidine kinase	T	9.22	3.09	3.15	2.96	2.14	1.13	0.29
Swit_4475	Hypothetical protein	X361	7.03	1.64	4.32	6.13	4.75	2.79	0.00
Swit_4483	FOF1 ATP synthase subunit A	C	0.02	0.22	0.26	0.21	0.14	0.11	0.17
Swit_4504	2-nitropropane dioxygenase	R	0.20	0.48	0.42	0.44	0.45	0.28	0.00
Swit_4532	Sugar transferase	M	9.90	1.27	1.15	0.95	1.08	1.16	0.02
Swit_4564	Hypothetical protein	X368	5.76	1.06	3.22	6.33	5.61	3.20	1.28
Swit_4582	Hypothetical protein	X370	21.21	2.76	1.11	1.95	1.85	2.24	1.38
Swit_4590	Hypothetical protein	X371	4.67	1.42	2.39	2.49	2.09	1.28	0.14
Swit_4591	Hypothetical protein	X372	30.71	5.65	1.96	3.23	2.79	2.30	1.08
Swit_4594	30S ribosomal protein S9	J	0.09	0.40	0.51	0.35	0.22	0.20	0.06
Swit_4663	Deoxyhypusine synthase-like protein	O	0.14	0.48	0.61	0.49	0.41	0.43	0.11
Swit_4685	D-3-phosphoglycerate dehydrogenase	HE	0.08	0.30	0.57	0.41	0.30	0.25	0.00
Swit_4687	Class I cytochrome c	C	0.18	0.55	0.48	0.41	0.32	0.32	0.00
Swit_4696	Tonb-dependent receptor	P	0.02	0.17	0.62	0.75	0.54	0.53	2.58
Swit_4697	Arsenate reductase	P	0.22	0.56	0.63	0.46	0.48	0.40	9.97
Swit_4704	Antibiotic biosynthesis monooxygenase	S	4.90	1.76	1.39	2.05	1.98	1.94	0.00

Swit_4730	Alpha/beta hydrolase domain-containing protein	I	0.98	0.64	1.98	6.40	7.08	5.01	0.70
Swit_4746	Hypothetical protein	S	4.12	1.43	1.55	2.04	1.67	0.99	0.19
Swit_4749	Transglycosylase-associated protein	X385	23.11	1.62	4.19	6.60	6.18	5.00	0.72
Swit_4773	Hypothetical protein	S	5.11	1.75	1.28	1.83	1.68	1.52	0.11
Swit_4779	Hypothetical protein	X391	37.72	2.92	1.29	0.99	0.94	0.98	0.29
Swit_4780	Glyoxalase/bleomycin resistance protein/dioxygenase	Q	4.24	1.15	0.98	0.96	0.82	0.81	0.85
Swit_4781	Tonb-dependent receptor	P	5.49	1.32	0.96	0.85	0.97	1.14	2.75
Swit_4790	Methylcitrate synthase	C	1.31	1.95	1.58	1.42	2.15	4.00	0.33
Swit_4801	Type IV secretory pathway virj component-like protein	U	4.28	0.85	1.64	2.09	2.70	1.98	5.11
Swit_4812	Metallophosphoesterase	G	0.20	0.50	0.42	0.44	0.17	0.15	4.10
Swit_4830	Bcr/cfla subfamily drug resistance transporter	G	0.16	0.47	0.60	0.65	0.52	0.66	2.41
Swit_4859	Pyruvate phosphate dikinase	G	0.15	0.50	0.46	0.32	0.31	0.30	0.00
Swit_4863	Hypothetical protein	S	14.77	4.06	2.07	2.28	1.98	1.13	0.15
Swit_4877	Hypothetical protein	X401	0.78	1.13	0.50	0.27	0.34	0.23	0.44
Swit_4902	Glyoxalase/bleomycin resistance protein/dioxygenase	E	2.34	4.42	0.79	0.46	0.46	0.67	0.01
Swit_4904/ 5096	Hypothetical protein	L	6.23	7.73	0.71	0.36	0.37	0.33	2.33
Swit_4919	Hypothetical protein	L	0.67	1.03	0.84	0.62	0.59	0.24	44.56
Swit_4922	Pyruvate	G	0.56	10.12	0.80	0.55	0.52	0.46	4.97
Swit_4923	4-hydroxy-2-ketovalerate aldolase	E	0.84	11.48	0.93	0.58	0.61	0.55	2.46
Swit_4924	Acetaldehyde dehydrogenase	Q	0.47	12.56	0.92	0.72	0.62	0.69	2.96
Swit_4925	4-oxalocrotonate decarboxylase	Q	0.67	13.44	0.80	0.62	0.63	0.67	3.01
Swit_5012	Regulatory protein	TK	4.01	2.04	1.05	0.98	1.22	0.81	1.27
Swit_5030	Hypothetical protein	S	0.60	1.11	0.43	0.24	0.30	0.17	1.50
Swit_5058	Cyclase family protein	R	8.32	2.97	0.88	0.82	1.06	2.05	1.33
Swit_5085	Hypothetical protein	X415	0.54	0.97	0.52	0.27	0.18	0.12	3.99
Swit_5086	Maleylacetoacetate isomerase	O	0.83	1.30	0.60	0.29	0.23	0.18	5.60
Swit_5087	Fumarylacetoacetate (FAA) hydrolase	Q	0.97	1.39	0.51	0.25	0.20	0.15	4.81
Swit_5101	Monoxygenase	HC	0.80	17.33	0.94	0.68	0.52	1.10	2.73
Swit_5102	Gentisate 1	Q	0.82	11.30	1.19	1.15	1.19	1.16	2.08
Swit_5134	AMP-binding protein	IQ	0.88	1.17	0.40	0.23	0.28	0.24	2.12
Swit_5163	Hypothetical protein	X423	0.25	0.64	0.47	0.57	0.49	0.57	0.02
Swit_5269	Transcriptional regulator	K	0.24	0.57	0.47	0.49	0.28	0.25	20.85
Swit_5275	Hypothetical protein	X455	8.63	2.56	1.04	1.03	1.18	1.53	1.48
Swit_5285	Putative DNA topoisomerase I	L	4.49	1.77	4.21	4.49	2.23	1.11	0.00
Swit_5287	Hypothetical protein	S	4.94	1.51	4.12	5.71	4.77	2.72	0.12
Swit_5291	Short-chain dehydrogenase/reductase SDR	IQR	8.75	1.95	7.64	9.38	5.94	2.32	0.92
Swit_5313	2Fe-2S iron-sulfur cluster binding domain-containing protein	C	6.56	1.42	5.27	6.39	5.05	2.30	0.00
Swit_5315	Xanthine dehydrogenase	C	9.22	1.32	4.17	6.82	5.40	2.99	0.02

Swit_5323	Histidine kinase	T	0.66	1.06	0.70	0.29	0.21	0.19	1.85
Swit_5324	Hypothetical protein	X464	0.76	1.01	0.67	0.37	0.21	0.22	0.78
Swit_5337	Grea/greb family elongation factor	K	1.03	0.62	1.11	1.48	2.22	5.12	0.08
Swit_5344	Cyclase/dehydrase	S	22.54	1.80	5.84	10.01	6.16	2.95	0.01
Swit_5345	Alcohol dehydrogenase	ER	25.06	2.12	6.84	10.63	6.71	2.26	0.93
Swit_5348	Hypothetical protein	S	26.03	3.23	2.87	3.05	2.25	1.52	0.06
Swit_5354	Chemotaxis protein cher	NT	0.21	0.96	0.42	0.29	0.28	0.42	1.21

CHAPTER 3

Development of Genetic Tools for Manipulations in *Sphingomonas wittichii* RW1

Abstract

Sphingomonas wittichii RW1 is a bacterium isolated for its ability to degrade dibenzofuran and dibenzo-*p*-dioxin, two toxic polyaromatic compounds. In order to better understand and characterize the genes involved in dibenzofuran degradation and environmental survival of RW1, we attempted to test and develop a set of genetic tools for manipulation of RW1, such as transformation, mini-transposon insertion and homologous recombination by marker replacement. The applied methods were analogous to tools more commonly used for organisms such as *E. coli*, *P. putida* and other sphingomonads. Electrotransformation and biparental conjugation allowed us to introduce plasmids, transposons and linear DNA into RW1 cells. A much higher transformation efficiency was obtained when the plasmids were extracted from RW1 than from *E. coli*. Unfortunately, genetic rearrangements of the transposon constructs introduced in RW1 occurred frequently, and transformed linear DNA inserted in unknown locations rather than by homologous recombination. Using a suicide plasmid we attempted to obtain deletion mutants to characterize gene functions, but we were unable to obtain single recombinants. On the other hand, transposon insertion mutants were obtained with frequencies sufficiently high to allow genetic screenings.

Introduction

Sphingomonas wittichii RW1 is a gram-negative α -proteobacterium, isolated from the Elbe River (Hamburg) for its ability to degrade dibenzofuran (DBF), dibenzo-*p*-dioxin (DBD), substituted DBFs and DBDs, and carbazole (Wittich *et al.*, 1992 Wilkes *et al.*, 1996; Halden *et al.*, 1999; Nam *et al.*, 2005). The genome of RW1 has been fully sequenced (Miller *et al.*, 2010) and consists of one chromosome and two megaplasmids, pSWIT01 and pSWIT02. The larger mega plasmid (T01) has been reported to be similar to pNL1 from *Novosphingobium (Sphingomonas) aromaticivorans* (Miller *et al.*, 2010), whereas the smaller (T02) contains the genes implicated in DBF/DBD degradation (Bunz and Cook, 1993; Bunz *et al.*, 1993; Armengaud and Timmis, 1998; Armengaud *et al.*, 1998; 1999; 2000; Basta *et al.*, 2004; Miller *et al.*, 2010; Coronado *et al.*, 2012).

In contrast to pseudomonads, where catabolic genes are often clustered in large operons, many species in the genus *Sphingomonas* show a scattered gene organization for the degradation of aromatic compounds and in some sphingomonads catabolic genes are encoded on plasmids. Some examples are the degradative genes for phenoxyalkanoic acid in *Sphingomonas herbicidovorans* (Muller *et al.*, 2004), for naphthalene/biphenyl/toluene in *S. aromaticivorans* F199 and B0695, *S. stygia*, *Sphingomonas subterranea*, *Sphingomonas xenophaga* BN6 (Basta *et al.*, 2005), for pentachlorophenol in *Sphingomonas (Sphingobium) chlorophenolicum* (Cai and Xun, 2002) or DBF and DBD in *S. wittichii* RW1 (Armengaud *et al.*, 1998; Basta *et al.*, 2004). Also, in many cases insertion sequences, transposons and/or transposase genes are widely distributed in their genomes, in some cases close to xenobiotic degrading operons as for *Sphingomonas yanoikuyae* XLDN2-5 (Gai *et al.*, 2010), *Sphingomonas paucimobilis* (Dogra *et al.*, 2004), *S. herbicidovorans* (Muller *et al.*, 2004)

Sphingomonas sp. LB126 (Wattiau *et al.*, 2001) and *S. wittichii* RW1 (Armengaud *et al.*, 1999). The chromosome of strain RW1 codes for at least 29 different transposase genes. The presence of such insertion elements has been suggested to be responsible for the genetic 'flexibility' of this genus (Gai *et al.*, 2010). Indeed, plasmid and genomic rearrangements have been observed in *Sphingomonas sp.* HH69, *Sphingomonas sp.* SS3 (Basta *et al.*, 2004), *S. herbicidovorans* (Muller *et al.*, 2004) and *S. wittichii* RW1 (Basta *et al.*, 2004).

In contrast to many other genera, genetic tools for sphingomonads are not very well developed. Notable exceptions include the pWB-derived suicide plasmids developed for *Sphingomonas sp.* LB126 (Wattiau *et al.*, 2001), which were successfully used for directed mutagenesis. In the case of *S. wittichii* RW1 very few attempts were made for genetic manipulations, and the genetic tools so far were only partially successful due to the very low transformation efficiencies (Armengaud *et al.*, 1998), as well as to genetic rearrangements in the introduced plasmids (Basta *et al.*, 2004).

Much of the planned research in this thesis relied heavily on the development of suitable genetic systems for RW1. For example, to test in situ expression of DBF pathway genes it was necessary to be able to produce stable and inducible reporter gene fusions in RW1, and to study specific gene functions picked up by microarray analysis, it would be nice to be able to knock them out by homologous recombination and marker replacement. The main goals of this chapter were therefore to test and where possible develop suitable genetic systems for manipulation of strain RW1. In particular, we determined the conditions and efficiency for DNA delivery into RW1 (transformation and conjugation), we tested stability of plasmid and transposon-based constructs in RW1 and we examined the efficiencies of transposon mutagenesis and the possibilities for homologous recombination and gene

knockout via marker replacement. For some experiments, we compared the efficiency in RW1 with that in another *Sphingomonas* sp. strain LH128, a phenanthrene degrader (Bastiaens *et al.*, 2000)

Materials and methods

1. Bacteria cultivation

A stock of *S. wittichii* RW1 (Wittich *et al.*, 1992) was kept at -80°C and a small aliquot was plated on agar with 5 mM salicylate (SAL) and incubated at 30°C. Liquid cultures were always prepared from an isolated colony of RW1 from a plate that was not stored longer than 7 days at room temperature. If necessary, colonies were tested by PCR for the presence of the *dxnA1* gene (4,4a-Dibenzofuran dioxygenase, Swit_4897), using primers PdxnA1-fw and PdxnA1-rev (Table 1). Minimal media (MM) were based on DSM457 amended with 5 mM salicylate (MM+SAL), 5 mM phenylalanine (PHE) or DBF (dosage of 5 µmol per ml). Agar plates were prepared with MM+SAL supplemented with 1.5% bacteriological agar No.1 (Oxoid). Antibiotic usage for RW1 included kanamycin (Km, at 50 µg per ml), tetracycline (Tc, at 20 µg per ml) or gentamicin (Gm, at 8 µg per ml) to select for the presence of plasmids or transposon insertions. RW1 was grown in 50 ml Erlenmeyer flasks containing 15 ml of MM+SAL and incubated at 30°C in a rotary shaker (180 rpm). *Sphingomonas* sp. LH128 (Bastiaens *et al.*, 2000) was grown on R₂A media (Reasoner and Geldreich, 1985), and incubated at 30°C. *Escherichia coli* strains were grown at 37°C in Lysogeny Broth (LB) with antibiotics as appropriate. The strains used are listed in Table 1.

Table 1. Strains, plasmids and primers used.

c	Description	Reference
Strains		
<i>Sphingomonas wittichii</i> RW1	Dibenzofuran degrader	Wittich <i>et al.</i> , 1992
<i>Sphingomonas sp.</i> LH128	Phenanthrene degrader	Bastiaens <i>et al.</i> , 2000
<i>Escherichia coli</i> DH5 α	Host for propagation of plasmids	Hanahan <i>et al.</i> , 1985
<i>E. coli</i> DH5 α pir	Host for propagation of plasmids with R6K origin of replication	de Lorenzo and Timmis, 1994
<i>E. coli</i> S17-1 λ pir	For replication and mobilization of plasmids with oriR6K.	de Lorenzo and Timmis, 1994
<i>E. coli</i> CC118 λ pir	For replication of pir-dependent plasmids	Herrero <i>et al.</i> , 1990
Plasmids		
pPROBE'- <i>egfp</i>	Broad-host range coding for a <i>egfp</i> gene	Miller <i>et al.</i> , 2000
pPROBE'-P _{Tac} - <i>egfp</i>	Constitutive <i>egfp</i> expression	This study
pPROBE'-P _{dxnA1} - <i>egfp</i>	Contains a <i>egfp</i> fused to the upstream region of Swit_4897 (<i>dxnA1</i> -promoter)	This study
pME6012	Shuttle vector	Heeb <i>et al.</i> , 2000
pME6012-P _{Tac} - <i>egfp</i>	pME6012 with a constitutively expressed <i>egfp</i> gene	This study
pUC18-miniTn7-Gm	Template for amplification of gentamicin resistance gene	Choi <i>et al.</i> , 2005
pJP5603-ISceIv2	Suicide plasmid containing I-SceI sites, R6Kori	Wong and Mekalanos, 2000
pJAMA23	Vector coding for a promoterless <i>egfp</i> gene	Jaspers <i>et al.</i> , 2001
pBAM1	All synthetic plasmid bearing R6k <i>oriV</i> , <i>oriT</i> sequence, with a hyperactive transposase and a miniTn5	Martinez-García <i>et al.</i> , 2011
Primers		Sequence
PdxnA1-rev	Amplification of upstream region of gene <i>dxnA1</i> (SmaI)	gccttcagcacaccgggtcg cgatca
PdxnA1-fw	Amplification of upstream region of gene <i>dxnA1</i> (Sall)	ggggtcgcacatgcctgtctcc
<i>egfp</i> -out	Annealing in <i>egfp</i> 70 nucleotides towards its start	tcaacaagaattgggacaactc cag
npt-fw	Forward primer for the amplification of the Km resistance gene	atcgtggctggccacgacggg
npt-rev	Reverse primer for the amplification of the Km resistance gene	ctgatagcgggccccacacc
Gfp-fw	Amplification of internal fragment of <i>egfp</i> , forward	ggctctgaagtcaagtttgaag
Gfp-rev	Amplification of internal fragment of <i>egfp</i> , reverse	caagaaggaccatgtggt
Ter	Anneals to terminator sequence in pJAMA23	caggaaatttcgagggatgc
4898-rev	Anneals to Swit_4898	aatccgtctggtatcgcttcg
up-Swit_3836 fw	Fw primer of the upstream region of Swit_3836 (SmaI)	tgatagccccgggtggactggac
up-Swit_3836 rev	Rev primer of the upstream region of Swit_3836 (SpeI)	gcacgttcgaactgattcacatc
gm-fw	Forward primer for amplification of Gm resistance gene	gcagtcgcctaaacaaa
gm-rev	Reverse primer for amplification of Gm resistance gene	cacttctcccgtatgcccaact
Gm-down	For amplification of downstream of Gm resistance gene	tcgaccaagtaccgccac
RW4210751	Anneals to Swit_3835 towards Swit_3836	gacgaggtcagggcgat
RW4212785	Anneals to Swit_3837 towards Swit_3836	ccatatttcagcattgcaac
PSwit4925-rev	Amplification of the upstream region of gene Swit_4925 (BamHI)	caattgtgatccatggcgc
Swit_3836 fw	Anneals to the start of gene Swit_3836	gatctgctcccgcattgcgac
Swit_3836 rev	Anneals to the end of gene Swit_3836	ccagccgcgaggtgatcg
PSwit4925-fw	Amplification of the upstream region of gene Swit_4925 (PstI)	cggtgtgctcagcaagcgg
PSwit5102-rev	Amplification of the upstream region of gene Swit_5102 (BamHI)	tacgcgcggatccgccttt
PSwit5102-fw	Amplification of the upstream region of gene Swit_5102 (PstI)	gagtgatctcagagccggg

2. Plasmid and transposon construction

Plasmid pPROBE'-P_{Tac}-*egfp* was constructed with the broad host plasmid pPROBE'-tagless (Miller *et al.*, 2000), and has the *egfp* gene under control of the hybrid Tac promoter (de Boer *et al.*, 1983). The plasmid was produced by ligating the SmaI-EcoRI fragment of pPROBE'-tagless with the P_{Tac} (SmaI/EcoRI) fragment coming from the plasmid pME3280::miniTn7-P_{Tac}-*mche* (Rochat *et al.*, 2010). A highly concentrated preparation of the plasmid (around 1 µg/µl) coming from *E. coli* DH5a was used to electrotransform *S. wittichii* RW1.

To obtain the plasmid pME6012-P_{Tac}-*egfp*, the P_{Tac}-*egfp* fragment from pPROBE'-P_{Tac}-*egfp* was ligated to the vector pME6012 (Heeb *et al.*, 2000) by XhoI/HindIII digestion and ligation. *E. coli* DH5α was transformed with the ligation mixture and colonies carrying the correct plasmid were selected to prepare a highly pure and concentrated plasmid preparation (around 1 µg/µl). The plasmid was introduced into strain RW1 by electroporation.

In order to potentially improve genetic stability in RW1, a 'synthetic' *egfp* gene was designed using optimal codon usage for RW1 (named *egfp*_{RW1}). The *egfp* sequence from pPROBE' and the modified *egfp*_{RW1} sequence are shown in Figure S1. The fragment P_{Tac}-*egfp*_{RW1} was produced by the company DNA 2.0 and delivered in the plasmid pJ281. A mini-transposon delivery plasmid was produced with *egfp*_{RW1} under control of P_{Tac} (pCK218::miniTn5-P_{Tac}-*egfp*_{RW1}) by ligating a NotI-digested pCK218 (Kristensen *et al.*, 1995) with the NotI-digested P_{Tac}-*egfp*_{RW1} fragment from plasmid pJ281. Both conjugation and electrotransformation were attempted to introduce the miniTn5 into RW1.

The possibility of obtaining transconjugants of RW1 using the miniTn7 delivery system was tested as well. Conjugations involved *E. coli* DH5 α (pME3280::miniTn7- P_{Tac} -*egfp*) or (pME3280::miniTn7- P_{Tac} -*mche*) as donor, *E. coli* SM1 (pUX-BF13) as transposase donor, *E. coli* HB101 (pRK2013) as helper for transfer and RW1 as recipient. Conjugations were performed by mixing stationary phase cultures of the strains in round bottom centrifuge tubes, centrifuging the cell suspension at 8,000 rpm during 2 minutes, discarding the supernatant and resuspending the cell pellet in 50 μ l of saline solution (NaCl 0.9%). The cell suspension droplet was placed on the surface of an LB agar plate and incubated at 30°C for 16 h. The cell layer was then taken with a loop from the agar plate, resuspended in 1 ml of saline solution and 150 μ l aliquots or dilutions thereof were spread on MM+SAL agar plates with the corresponding antibiotic. Petri dishes were incubated at 30°C until colonies were visible.

3. Electrotransformation of *S. wittichii* RW1 and *Sphingomonas* sp. LH128

E. coli strains were used to prepare a highly concentrated plasmid fraction (Jetstar 2.0, Genomed). Plasmids were introduced into strains RW1 or LH128 by electroporation using a slightly modified protocol from Masai *et al.* (1999). Briefly, a 20 ml exponential culture (OD₆₀₀ 0.4) of RW1 cells growing on MM+SAL was centrifuged at 8,000 rpm during 5 min at 4°C, after which the supernatant was discarded and the cell pellet washed with 5 ml of ice-cold sucrose solution (300 mM). This procedure was repeated three times, after which the cell pellet was again resuspended in 1 ml sucrose solution, and 100 μ l aliquots were transferred to ice-cold electroporation cuvettes and used immediately. Two to 5 μ g of purified plasmid DNA (from *E. coli*) were added to 100 μ l of competent cell suspension. The settings for electroporation were 25 μ F, 800 Ω , and 2.5 kV (GenePulser, Biorad). 1 ml liquid

LB medium was added directly after electroporation to resuspend the cells. This cell suspension was incubated for 16 h at 30°C in the absence of any antibiotics, after which 150 µl aliquots were plated on selective plates (MM+SAL plus Km or Tc). Transformants were allowed to form colonies for up to 4 days at 30°C, after which they were screened for the presence of the appropriate genetic construct by PCR. Colonies were purified, rescreened by PCR, and if positive, regrown in liquid culture to purify plasmid (from RW1 or LH128) using a Qiaprep kit (Qiagen). Purified plasmids from transformants were digested and verified for proper fragment patterns using agarose gel electrophoresis, and promoter inserts were sequenced to ensure that no modifications had taken place.

4. Transformation of *S. wittichii* RW1 with plasmids purified from different hosts

The transformation efficiency of *S. wittichii* RW1 or *Sphingomonas* sp. LH128 was tested with pME6012- P_{Tac} -*egfp* purified from either *E. coli* DH5 α , RW1 or *Sphingomonas* sp. LH128. 100 ng of plasmid DNA were added to the RW1 or LH128 electrocompetent cell suspension, cells were electrotransformed and plated on selective agar media (MM+SAL+Tc or R₂A+Tc, respectively). The total number of transformants was calculated per µg of plasmid DNA.

5. MiniTn5-based bioreporter construction

Based on the transcriptome data (chapter 2), two genes were targeted for the construction of bioreporters responding to DBF, Swit_4925 and Swit_5102. The upstream region Swit_4925 was amplified using the primers PSwit4925-fw and PSwit4925-rev, containing PstI and BamHI restriction sequences. The 249 bp product was digested and ligated to PstI/BamHI-digested pJAMA23 (Jaspers *et al.*, 2001). *E. coli* DH5 α was

transformed with the ligation mixture and one colony carrying pJAMA23-P₄₉₂₅-*egfp* was selected. The upstream region of gene Swit_5102 was amplified using the primers PSwit5102-fw and PSwit5102-rev. The 256 bp fragment was PstI/BamHI digested and inserted into pJAMA23 as for the Swit_4925 promoter (producing pJAMA23-P₅₁₀₂-*egfp*). The NotI fragments of pJAMA23-P₄₉₂₅-*egfp* and pJAMA23-P₅₁₀₂-*egfp* were recovered and ligated to NotI-digested pBAM1 (Martínez-García *et al.*, 2011). Ligation mixtures were used to transform *E. coli* CC118 λ pir. Concentrated plasmid preparation was purified from *E. coli* CC118 λ pir (pBAM-P₄₉₂₅-*egfp*) and (pBAM-P₅₁₀₂-*egfp*) and 2 μ g of plasmid DNA was used to electrotransform RW1 cells. The optical density (O.D.) and the eGFP fluorescence intensity of cultures of RW1 (Tn5-P₄₉₂₅-*egfp*) and RW1 (Tn5-P₅₁₀₂-*egfp*) were measured with an Ultrospec spectrometer (GE) and a FLUOstar Omega fluorimeter (BMG Labtech).

6. Transformation of *S. wittichii* RW1 with linear DNA fragments

Linear DNA fragments comprising the upstream region of gene Swit_4897 (initial DBF dioxygenase, *dxnA1*) fused to an *egfp* gene plus a Km resistance gene, were obtained by digesting the plasmid pPROBE-P_{*dxnA1*}-*egfp* with BglII and SalI, and purifying the resulting 3.1 kb fragment from gel using a Qiaquick gel extraction kit (Qiagen). *S. wittichii* RW1 was electrotransformed with 500 ng of purified DNA fragment and 150 μ l aliquots of the transformed cell mix were plated on selective plates (MM+SAL+Km). Some 170 transformants/ μ g DNA were obtained with this procedure. 96 colonies were picked and resuspended in 20 μ l of H₂O in a microtiter plate. DNA was liberated by heating to 96°C, after which the clones were screened by PCR for the presence of the expected recombination event. PCR amplifications were carried out using the primers PdxnA1-fw and *egfp*-out (386 bp amplicon), and *npt*-fw and *npt*-rev (457 bp amplicon).

To test the recombination of a double-homologous DNA fragment in RW1, linear DNA containing a Gm resistance gene flanked by two sequences of RW1 was prepared. Fragments of 531 and 541 bp, respectively, corresponding to the upstream and downstream regions of Swit_3836 linked to a Gm^R gene was obtained by SmaI/KpnI digestion of the plasmid pJP5603ISceIv2-up-Gm-down. The resulting fragment of 1.9 kb was purified from gel and an aliquot of 1.7 µg of DNA was used to electrotransform RW1 cells. Some 140 Gm^R-resistant cells/µg DNA were obtained and 19 colonies were picked for PCR screening for the presence of the linear DNA fragment. To amplify the recombined introduced DNA, primers RW4210751 and RW4212785 were used, giving a product of 2 kb in case no integration occurred and of 2.4 kb if the DNA fragment recombined into the expected chromosome target. The absence of gene Swit_3836 was further verified by PCR amplification of gene Swit_3836 using the primers Swit_3836 fw and Swit_3836 rev, obtaining a product of 420 bp in case the gene is present, and no amplification if the gene was successfully replaced by the Gm^R gene.

7. Gene deletion in *S. wittichii* RW1 using the I-SceI recombination system

The genes Swit_3836 and Swit_3924, coding for a putative alternative ECF sigma24-factor in RW1, were 2.6 and 7-fold, respectively, higher expressed in response to salt stress as compared to regular medium (Johnson *et al.*, 2011). To evaluate their role in low water potential conditions, a strategy was designed to delete these genes via homologous recombination. Hereto, we followed a protocol developed by Pósfai *et al.* (1999) and adapted by Martínez-García and de Lorenzo (2011). The upstream region of gene Swit_3836 was amplified with primers up-Swit_3836fw and up-Swit_3836rev, using RW1 as template and obtaining a 640 bp fragment. The PCR product was ligated to pGEM-T-easy (Promega) to obtain pGEM-upSwit_3836. Due to numerous difficulties in amplifying the downstream

region of Swit_3836 (such as unspecific amplifications), the fragment was synthesized by the company Mr. Gene (Regensburg, Germany) and delivered in the plasmid pMK-RQ-Swit_3837. The gene for resistance to gentamicin was amplified with primers gm-fw and gm-rev, using as template pUC18-miniTn7-Gm (Choi *et al.*, 2005), and the 822 bp product was ligated to pGEM-T-easy to obtain pGEM-gm. The SmaI/SpeI fragment of pGEM-upSwit_3836 (upstream), the SpeI/KpnI fragment of pMK-RQ-Swit_3837 (downstream), the SpeI fragment of pGEM-gm (Gm resistance) and the SmaI/KpnI digested pJP5603ISceIv2 (Wong and Mekalanos, 2000) were ligated and the ligation mixed was used to transform *E. coli* DH5 α λ pir. Gm resistant colonies were picked and grown on LB+Gm to extract the plasmid. After a restriction pattern screening, one colony carrying the correct plasmid pJP5603ISceIv2-up-Gm-down was selected. Once the construct was verified by sequencing, the plasmid was introduced in *E. coli* S17-1 λ pir (de Lorenzo and Timmis, 1994), and one colony carrying the plasmid pJP5603ISceIv2-up-Gm-down was selected to perform a conjugation procedure with *S. wittichii* RW1 as recipient. Stationary phase cultures of the RW1 (recipient) and *E. coli* S17-1 λ pir (pJP5603ISceIv2-up-Gm-down) were mixed in a 2/1 ratio (v/v). Strain S17-1 λ pir has chromosomally integrated conjugal transfer functions (RP4 transfer functions), and carries the *pir* gene for replication of R6K origin vectors. The mixture was centrifuged at 8,000 rpm during 2 minutes, the supernatant discarded and the cell pellet resuspended in 50 μ l of saline solution (NaCl 0.9%). The droplet was placed on the surface of an LB agar plate and incubated at 30°C overnight. The cell layer was then taken with a loop from the agar plate, resuspended in 1 ml of saline solution and 150 μ l aliquots were spread on MM+SAL+Km+Gm agar plates. Petri dishes were incubated at 30°C until colonies were visible, which took around 8 days.

8. Transposon mutagenesis

Transposon mutagenesis in strain RW1 was performed using two plasmid systems containing miniTn5-derived transposable elements. The first one involved the plasmid pRL27 (Larsen *et al.*, 2002) and the second the plasmid pBAM. Both plasmids code for hyperactive transposases that increase the transposition efficiency.

In the first case *S. wittichii* RW1 and *E. coli* BW20767 (pRL27) overnight cultures were mixed in different proportions and centrifuged for 2 min at 8,000 rpm. The supernatant was discarded and the cell pellet resuspended in 50 µl of saline solution (NaCl 0.9%). The 50 µl droplet was placed on an LB plate and incubated at 30°C overnight. After incubation, the cell layer was taken with a sterile loop, resuspended in 1 ml saline solution and 150 µl aliquots were plated on selective media (MM+SAL+Km). The plates were incubated at 30°C during several days until colonies were visible. For the second system, strain RW1 and *E. coli* S17-1 λpir (pBAM) overnight cultures were mixed following an identical procedure as for pRL27.

Results

Transformation and conjugation efficiencies of *S. wittichii* RW1

Existing electrotransformation protocols developed for *E. coli*, spingomonads or *P. putida* were slightly modified to improve the transformation efficiencies in RW1. The SOC medium was substituted for LB medium, since RW1 failed to grow when resuspended in SOC. The incubation period after electroporation of RW1 was extended from 1 h (for *E. coli*) to overnight, to increase the transformation efficiency. The amount of DNA used to electrotransform RW1 cells was at least 1 µg per reaction. Even with the adaptations made to the protocol, the number of electrotransformants obtained was very low. The efficiency of transformation with pPROBE-based constructs was around 60 CFU/µg DNA and around 30 CFU/µg DNA in the case of the pME6012-based constructs (Table 2). In the case of the miniTn5-based constructs, the efficiency of electrotransformation was higher, resulting in more than 100 transformants/µg DNA (Table 2). MiniTn5-constructs carrying *egfp*_{RW1}, which has a codon optimized *egfp* gene for RW1, showed a similar fluorescence intensity as RW1 carrying pME6012-*P*_{Tac}-*egfp* (non optimized).

No Km^R-RW1 transconjugants were obtained in triparental conjugation with RW1 as recipient, *E. coli* CC118 λpir (pCK218::miniTn5-*P*_{Tac}-*egfp*_{RW1}) as donor and *E. coli* HB101 (pRK2013) as helper strain. Similarly, no Gm^R-RW1 colonies were obtained by fourparental conjugation involving RW1 and *E. coli* DH5α (pME3280::miniTn7-*P*_{Tac}-*egfp*) or (pME3280::miniTn7-*P*_{Tac}-*mche*). Only with biparental conjugation using e.g., *E. coli* S17-1 λpir, we were able to obtain RW1 transconjugants. In the general transposon mutagenesis procedure using RW1 as recipient and *E. coli* BW20767 (pRL27) as donor around 2×10⁴

independent RW1 transconjugants were obtained, which was the highest number observed for any of the systems evaluated (Table 2). In contrast, in transposon mutagenesis with pBAM we did not obtain more than 1000 independent transconjugants following the same procedure.

Table 2. Transformation and conjugation efficiencies of *S. wittichii* RW1

Construct			
<u>Transformation</u>	<u>Host</u>	<u>Avg No. transformants per µg DNA</u>	
pPROBE-based	<i>E. coli</i> DH5α	60	
pME6012-based	<i>E. coli</i> DH5α	30	
pBAM1	<i>E. coli</i> S17-1 λpir	200	
pCK218::Tn5-gfp _{RW1}	<i>E. coli</i> CC118 λpir	100	
<u>Conjugation</u>	<u>Donor</u>	<u>Ratio</u>	<u>Avg No. transconjugants per CFU</u>
		<u>Recipient/Donor</u>	<u>recipient</u>
pRL27	<i>E. coli</i> BW20767	1/1	1×10 ⁻⁵
		2/1	4×10 ⁻⁵
		3/1	2×10 ⁻⁶
pBAM1	<i>E. coli</i> S17-1 λpir	1/1	3×10 ⁻⁷
		2/1	2×10 ⁻⁷
		3/1	2×10 ⁻⁷

Effect of host for plasmid extraction on transformation efficiency of *S. wittichii* RW1

In order to better understand why such low transformation efficiencies occurred for RW1, the influence of the host employed to replicate the plasmids for transformation was evaluated. Hereto we used plasmid pME6012-P_{Tac}-egfp, which constitutively expresses eGFP fluorescence. RW1 and a second strain, *Sphingomonas sp.* LH128 were electrotransformed using identical protocols with the same amount of pME6012-P_{Tac}-egfp, extracted and purified either from *E. coli* DH5α, from LH128 or from RW1. The transformation efficiency as well as the percentage of colonies showing green fluorescence was measured. Interestingly, both RW1 and LH128 showed a much higher transformation efficiency when the plasmid was extracted from the same strain, than in the case of an *E. coli* DH5α-extracted plasmid (Table 3). For RW1, 45 times more transformants were obtained with RW1-extracted plasmid than

with DH5 α -extracted. For LH128, this difference was around 12 fold higher for LH128- than for DH5 α -extracted plasmid. Moreover, the percentage of fluorescent colonies obtained in each case was surprisingly different, with more than 80% green fluorescent colonies when the plasmid was extracted from the same strain, compared to only 2-10% green fluorescent colonies for transformants with DH5 α -extracted plasmid. Electrotransformation in *Sphingomonas sp.* LH128 produced a much higher number of transformants than in RW1, and also the proportion of fluorescent colonies among transformants was higher. Interestingly, plasmid isolated from LH128 and transformed into RW1 resulted in better efficiencies than with *E. coli*-plasmid, but not as high as with host-homologous plasmid DNA (Table 3). Plasmid isolated from RW1 and delivered into LH128 was less efficient in producing transformants than *E. coli*-DNA, but showed a higher proportion of fluorescent colonies (Table 3). Collectively, these data suggest that both LH128 and RW1 have strong and strain-specific restriction-modification systems, and that both strains in addition frequently rearrange incoming DNA (concluded from the high proportion of non-fluorescent colonies).

Table 3. Transformation efficiency of *S. wittichii* RW1 and *Sphingomonas sp.* LH128 with pME6012-P_{Tac}-*egfp* extracted from different hosts.

Host for plasmid extract	RW1 Transf/ μ g DNA	Fluorescent colonies (%)	LH128 Transf/ μ g DNA	Fluorescent colonies (%)
<i>E. coli</i> DH5 α	120	1	2.9×10^4	11
LH128	850	2	3.5×10^5	81
RW1	5.5×10^3	100	9×10^3	98

MiniTn5-based bioreporter construction

S. wittichii RW1 electrotransformed with pBAM::*Tn5*-P₄₉₂₅-*egfp* or pBAM::*Tn5*-P₅₁₀₂-*egfp* produced 60 and 80 Km^R-resistant colonies/ μ g plasmid DNA, respectively. A total

of 46 colonies for Tn5-P₄₉₂₅-*egfp* and 20 colonies for Tn5-P₅₁₀₂-*egfp* were picked from MM+SAL+Km agar plates and screened by PCR amplification for the presence of *egfp* using primers *gfp-fw* and *gfp-rev*, producing a 400 bp amplicon. Only one colony gave a positive PCR amplification for miniTn5-P₄₉₂₅-*egfp* (Figure 1A), while 10 colonies for miniTn5-P₅₁₀₂-*egfp* amplified the correctly sized product (not shown).

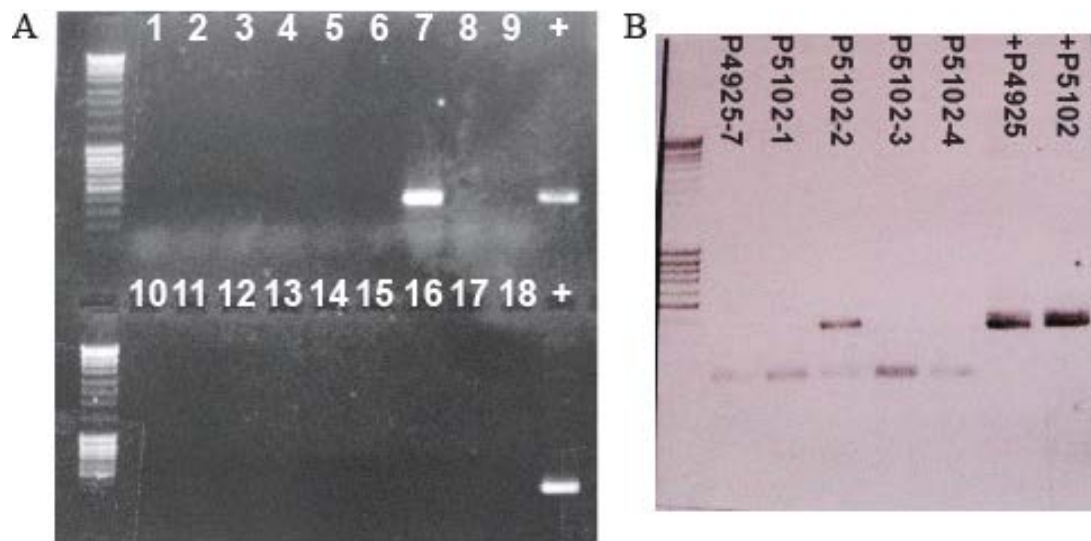


Figure 1. Genetic rearrangements in RW1 Km^R-transconjugants carrying miniTn5-derivatives. (A) PCR amplification of the *egfp* gene in DNA from RW1 Km^R-colonies transformed with the miniTn5-P₄₉₂₅-*egfp*. + represents the positive control with plasmid pBAM::miniTn5-P₄₉₂₅-*egfp*. (B) PCR amplification of the *egfp* gene in DNA from RW1 Km^R-colonies transformed with miniTn5-P₄₉₂₅-*egfp* (P4925) and miniTn5-P₅₁₀₂-*egfp* (P5102). +4925 and +5102 represent the positive controls.

RW1 Km^R-colonies that amplified correctly the *egfp* gene, one for miniTn5-P₄₉₂₅-*egfp* (P4925-7) and four for miniTn5-P₅₁₀₂-*egfp* (P5102-1 to P5102-4) were selected to characterize the *egfp* induction in response to carbon source. RW1 (P4925-7) and (P5102-1 to P5102-4) were hereto grown on MM+PHE, MM+SAL or MM+DBF, and the optical density and fluorescence were determined during growth. RW1 (P4925-7) and (P5102-2, 3 and 4)

showed no *egfp* induction, with fluorescence values being very similar to the RW1-WT without miniTn5 (Figure 2). Only strain RW1 (P5102-1) had a higher eGFP fluorescence when it was growing on SAL compared to PHE, but this strain had unfortunately lost the ability to grow on DBF. All five clones, plus RW1 (pME6012-P_{*dxnA1*}-*egfp*) and WT were analyzed by PCR for a 350 bp fragment of the *dxnA1* gene, and for each of the promoter-*egfp* construct (around 400 bp). Strains RW1 (P5102-4) and RW1 (pME6012-P_{*dxnA1*}-*egfp*) did not amplify the *dxnA1* gene, and P5102-1 showed a *dxnA1*-PCR product pattern very different from the WT (Figure 3). None of the strains correctly amplified the promoter-*egfp* fragment, indicating that the construct was either modified or deleted (Figure 3).

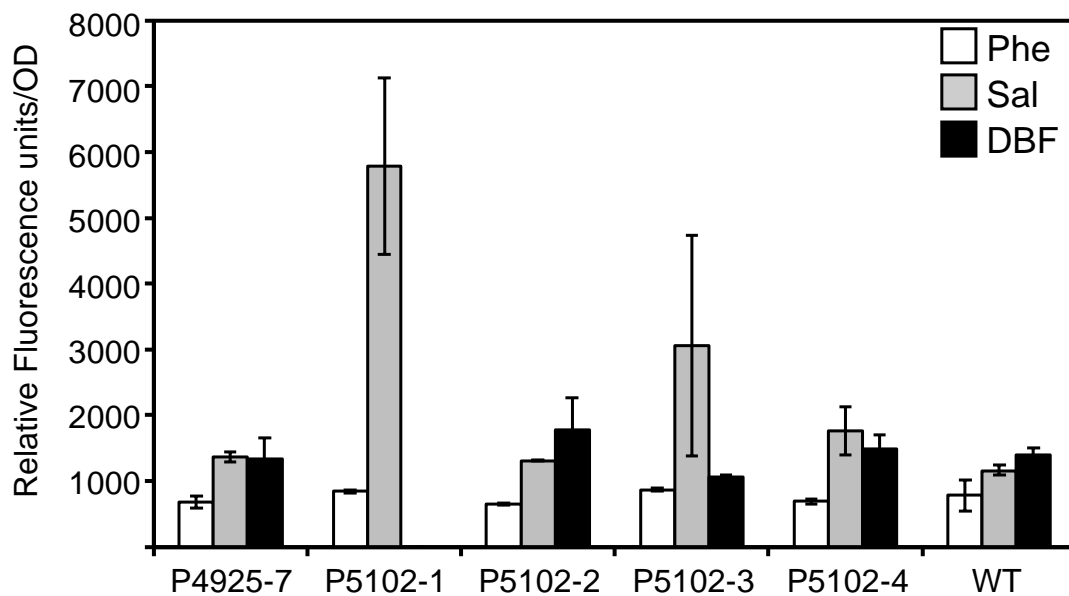


Figure 2. eGFP induction of RW1 strains in response to the carbon source. Relative fluorescence units normalized by optical density of *S. wittichii* RW1 strains carrying miniTn5-based insertions containing the promoter region of Swit_4925 or Swit_5102 plus *egfp*. WT is the RW1 strain with no transposon insertion. The carbon sources used were phenylalanine (Phe), Salicylate (Sal) and Dibenzofuran (DBF).

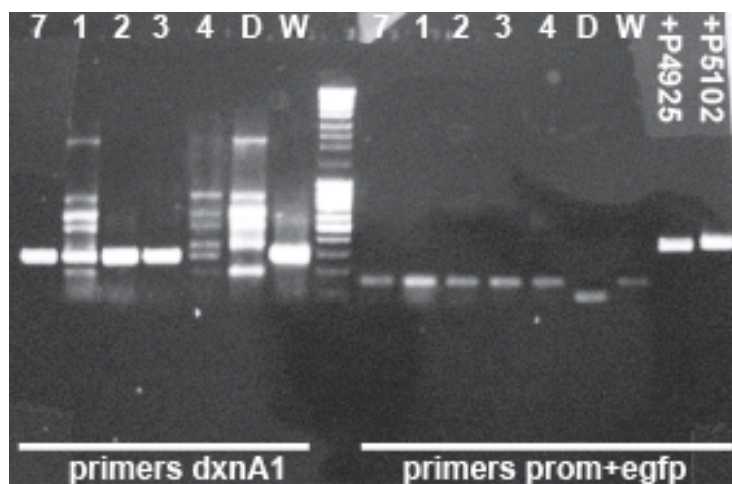


Figure 3. PCR verifications of miniTn5-carrying RW1 strains. The primers used amplified the *dxnA1* gene, and a fragment containing the promoter region P₄₉₂₅ or P₅₁₀₂ and a fraction of the *egfp* gene. Lanes: 7, RW1 miniTn5-P₄₉₂₅-*egfp* (7); 1-4, RW1 miniTn5-P₅₁₀₂-*egfp* (clones 1,2,3,and 4); D , RW1 pME6012-P_{*dxnA1*}-*egfp* and W, RW1 with no transposon insertion (wild type). Positive controls: plasmids purified from *E. coli*.

Homologous recombination in *S.wittichii* RW1

As an alternative to the introduction of gene constructs in RW1 using plasmids or miniTn5-based systems, attempts were made to use homologous recombination as a mean to deliver gene fragments on the chromosome. We noticed that RW1 can take up linear DNA during transformation. A DNA fragment with a single-ended homology and antibiotic resistance marker, namely, P_{*dxnA1*}-*egfp*-Km^R (Figure 4) was prepared and introduced in RW1 cells by electroporation. Interestingly, 170 Km^R-resistant cells/μg DNA were obtained, whereas none were obtained in a mock control. 96 Colonies were picked for screening by PCR for the presence of the introduced DNA (relevant results in Figure 5). Whereas in 18 out of 22 colonies a correctly-sized fragment was amplified with primers for the Km-resistance gene (Figure 5A), in none of them an amplification of the *dxnA1-egfp* fragment of the correct size occurred. Promoter+*egfp* amplifications produced either a larger or a smaller band than expected (Figure 5B) which was 386 bp. Clones 4, 5 and 18 (Figure 5B) showed

amplification of a band with a similar size of the expected product, however, a second amplification trial showed that the band was in fact bigger in the positive control (not shown). A second PCR screening was performed using specific primers to check whether the *dxnA1*-fragment had inserted next to the gene Swit_4898. However, in this case no PCR amplification products at all were detected for any of the 22 clones evaluated, indicating that the DNA fragment had not inserted in this area.

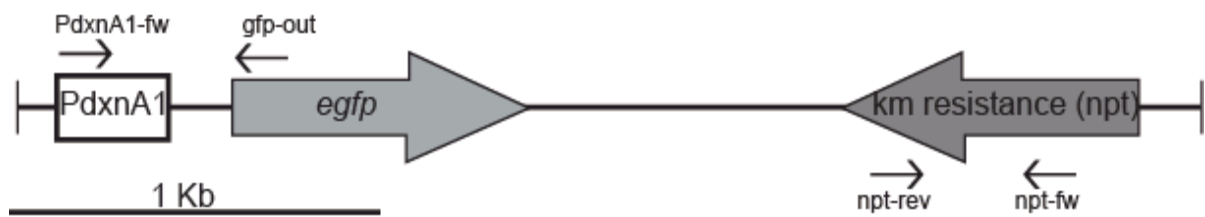


Figure 4. Linear fragment used to electrotransform *S. wittichii* RW1 cells. The primers used for PCR screening of clones are shown.

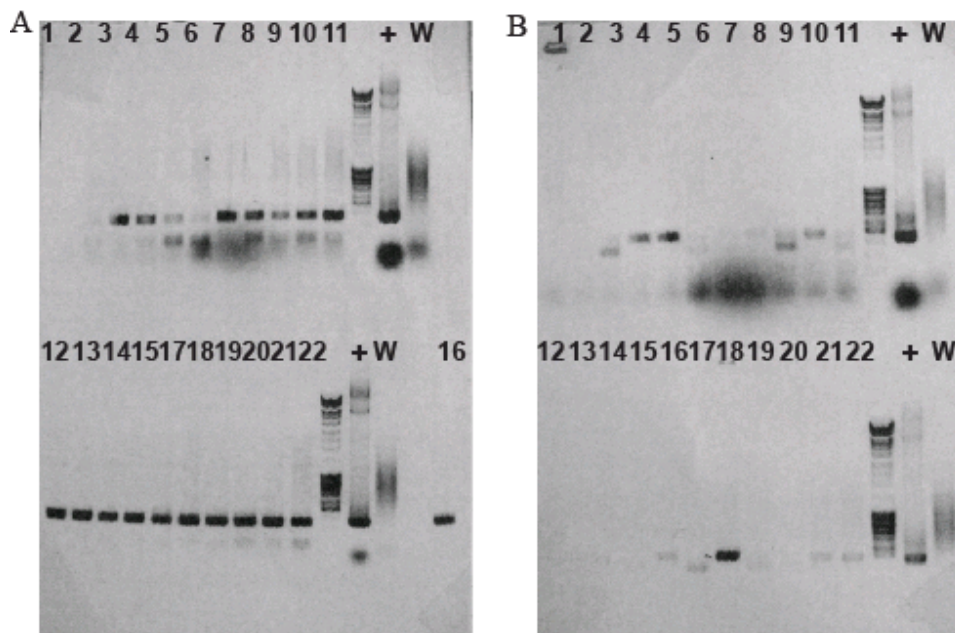


Figure 5. PCR verification of 22 transformants of RW1 with linear DNA of Figure 4. (A) Amplifications of the kanamycin resistance gene. (B) Amplifications for the fragment including P_{dxnA} plus a fraction of *egfp*. Lanes 1 to 22 represent PCR results from different Km^R -resistant colonies picked from agar plates. Lane: W, wild type RW1; +, pure plasmid pPROBE- P_{dxnA1} -*egfp* used to retrieve the linear DNA fragment (positive control).

Introduction of a double-homologous fragment in RW1 was also attempted. Linear DNA containing a Gm resistance gene flanked by two sequences of RW1, corresponding to the up- and downstream regions of Swit_3836 (Figure 6A) was prepared. Some 140 Gm^R-resistant cells/ μ g DNA were obtained by electrotransformation with the linear DNA. Nineteen colonies were picked for PCR screening for the cointegration of the insert using the primers RW4210751 and RW4212785. If the linear DNA recombined with the region in the vicinity of gene Swit_3836 (Figure 6B), an amplification product of 2.4 kb was expected, while it would be of 2 kb in the absence of cointegration (relevant results in Figure 7A). The 19 clones screened produced the same PCR fragment of around 2.2 kb, but the same as in the WT. Next, the clones were screened for the presence/absence of gene Swit_3836. In case a true recombination had taken place, the gene would be absent. PCR with primers Swit_3836 fw and Swit_3836 rev produced a fragment of 420 bp for all clones, similar as for the WT (Figure 7B). This indicated that the gene Swit_3836 is still present. Surprisingly, a second band, of around 1.2 kb was amplified in the transformants, which was absent in the WT strain. This suggested that the linear Gm^R-containing fragment was indeed inserted and perhaps within Swit_3836, but that somehow during recombination a duplication occurred preventing proper deletion of the gene Swit_3836.

Therefore, despite the (fascinating) finding that RW1 is able to take up and integrate linear DNA fragments containing single or double homologous sequences via electroporation, it is not clear where in the chromosome the insertion will take place. PCR results also indicate that rearrangements in the integrated DNA fragment occur. Better interpretation of these results may only be possible by resequencing the genomes in the transformants.

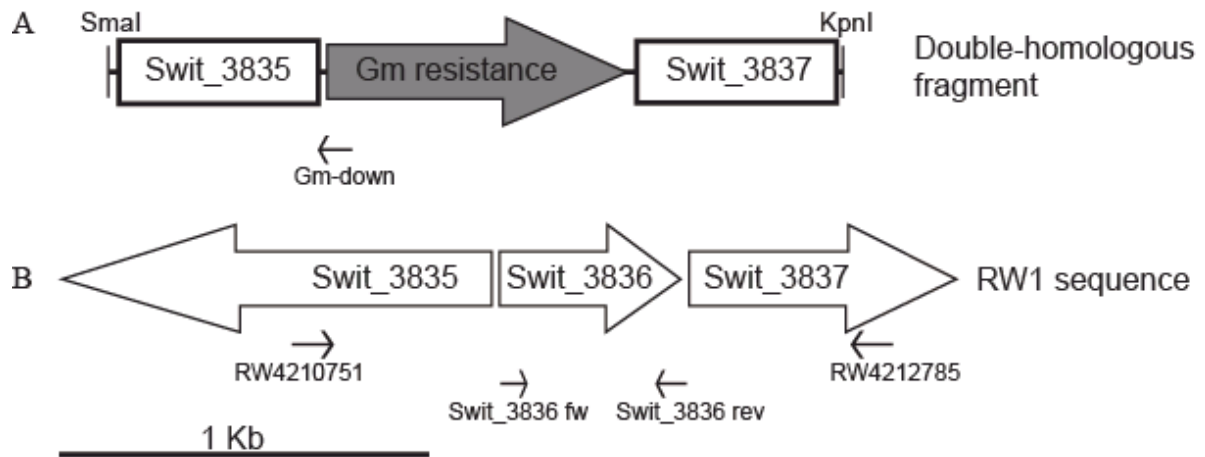


Figure 6. Strategy for deletion of Swit_3836 by double-homologous recombination and marker exchange with a linear fragment transformed into RW1. The linear fragment prepared by *SmaI/KpnI* digestion of pJP5603ISceIv2-up-Gm-down, had a size of 1.9 kb and consisted of the upstream and downstream region of gene Swit_3836, both linked to a Gm resistance gene (A). Scheme of the expected site of integration of the linear DNA fragment, in the chromosome of RW1 (B).

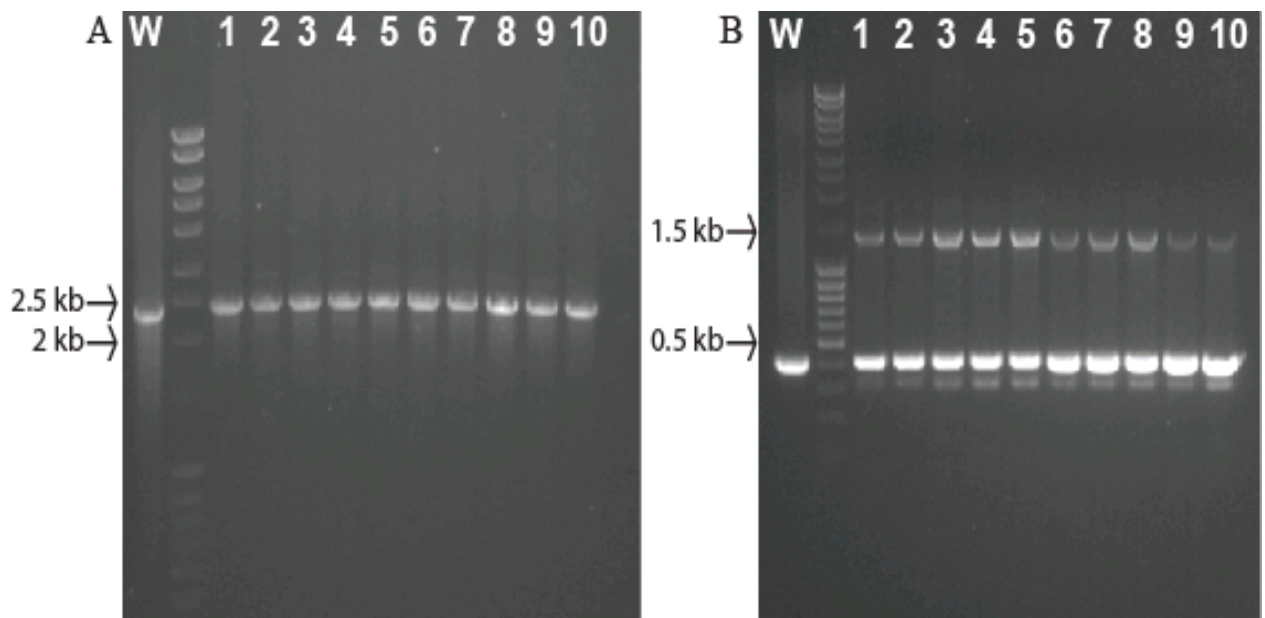


Figure 7. PCR verification of 10 mutants obtained by insertion of a double-flanked homologous fragment in RW1 cells. The primers RW4210751 and RW4212785 to detect the cointegration of the linear fragment (A) and primers Swit_3836 fw and Swit_3836 rev for the amplification of gene Swit_3836 (B), were used. W, wild type RW1; Lanes 1 to 10, different Gm^R mutants evaluated.

Gene replacement in *S. wittichii* RW1

Finally, we tried to use the technique of gene replacement by homologous recombination and marker insertion introduced on a circular plasmid to inactivate two genes on the RW1 chromosome that were reported to be induced when cells are exposed to solute stress: Swit_3836 and Swit_3924, (Johnson *et al.*, 2011). Both genes putatively code for ECF sigma24 factors (Johnson *et al.*, 2011). The strategy was to recombine a homologous DNA with an antibiotic resistance marker gene, which could then be removed in a second step of recombination. The plasmid pJP5603ISceIv2-up-Gm-down, carrying the flanking regions of Swit_3836, was introduced in RW1 cells by conjugation. A total of 36 colonies were obtained on MM+SAL+Km+Gm agar plates, which might have inserted the plasmid via recombination. All of the clones were screened by PCR for the cointegration of the *up-Gm-down* fragment within the gene Swit_3836. We first used primers annealing within the Gm-resistance gene and within the gene Swit_3837, downstream of Swit_3836. Unfortunately, no amplification was obtained in any of the Km^R-Gm^R-resistant colonies. This again indicated that an insertion seemed to have taken place, but at an improper location. Several more attempts were launched to recover clones that carried the *up-Gm-down* insertion, but no single recombinants could ever be detected by PCR.

Discussion

Various genetic tools were tried here for introducing DNA in RW1 cells, including regularly used techniques such as plasmid delivery, mini-transposon delivery, homologous recombination and transposon mutagenesis. Of the techniques that resulted in stable maintenance of genetic constructs in RW1, only the plasmid pME6012 worked satisfactorily. Transposons and mini-transposons were delivering DNA onto the RW1 genome, but their stability seemed to depend on whether RW1-homologous DNA was present or not. We found that transformation in RW1 has a very low efficiency, around 10^2 transformants/ μg DNA, compared to other gram-negative bacteria, where 10^4 - 10^{10} transformants/ μg DNA can be easily obtained (Dower *et al.*, 1988; Jacobs *et al.*, 1990; Gilchrist and Smit, 1991; and Wang *et al.*, 2010). To obtain sufficient transformant colonies, therefore, more than 1 μg of DNA had to be used. Interestingly, the poor transformation efficiency is partly the result of the source of DNA. By transforming RW1 with RW1-derived DNA instead of *E. coli*-isolated plasmid DNA we could obtain an increase in transformation efficiency of 45 times. Similar results were obtained with *Sphingomonas sp.* LH128 and LH128-derived plasmid DNA. We also noted that the transformation efficiency was higher for strain LH128. Unfortunately, it would not have helped much to use LH128 as an intermediate host for plasmid DNA production to transform into RW1, because also LH128-derived plasmid DNA transformed poorer into RW1 than RW1-derived DNA. In addition, we noticed that the proportion of fluorescent colonies among antibiotic-resistant colonies with *E. coli*-derived plasmid DNA transformed into RW1 or LH128 was extremely low. This suggests that incoming DNA is also rearranged when there is no specific selection pressure to maintain it. The proportion of fluorescent colonies among antibiotic resistant transformants also increased dramatically when the plasmid used to transform RW1 and LH128 originated from the same strain.

Basta *et al.* (2004) suggested that the sphingoglycolipids in *Sphingomonas* outer membrane could have a role in the low conjugation frequencies observed in strain RW1. Our results here strongly indicate that restriction-modification (R-M) systems must have a large influence on the transformation and (perhaps) conjugation efficiencies. R-M systems are typically comprised of an endodeoxyribonuclease (R) and a DNA-methylase (M) that recognize specific sequences of 4 to 8 nucleotides, with the methylase adding a methyl group in the restriction sequence, and the ribonuclease cleaving the non-methylated DNA, acting as a barrier against foreign DNA (Wilson, 1991). Several microorganisms possess multiple R-M systems, but in *S. wittichii* RW1 up to eight different R-M systems were proposed (REBASE-Roberts, 2010). For a number of bacterial strains it was shown that low transformation efficiencies can be improved by several orders of magnitude by inactivating their restriction system (Veiga and Pinho, 2009; Ferri *et al.*, 2010), by transformation with plasmids extracted of the same strain (Veiga and Pinho, 2009; Ferri *et al.*, 2010) or by inducing the R-M genes of the target organism in *E. coli*, thereby obtaining plasmids with the methylation pattern of the target (Yasui *et al.*, 2009). However, in those cases the bacteria only possessed one or two R-M systems, whereas *S. wittichii* RW1 genome seems to code for 8 different R-M clusters. Therefore, this seemed like a hopeless task to perform.

As mentioned above, transposon delivery into the RW1 genome was possible and the resistance marker could reproducibly be found. In fact, also transposon mutagenesis was a workable technology and no particular important instability was detected with pRL27-based transposon mutants (delivering only a Km^R-gene). However, RW1 transconjugants carrying miniTn5-P₄₉₂₅-*egfp* and miniTn5-P₅₁₀₂-*egfp* insertions were again unstable, and after a few generations displayed rearrangements in the gene constructs. One of them even lost the ability to grow on DBF as sole carbon source. This instability may be due to a large number

of native transposable elements in the genome, or must be due to rearrangements by a particular efficient recombination system in the absence of direct selection on the marker.

Interestingly, even linear DNA could be transformed into RW1 and, given the antibiotic resistance of the transformants, must have been introduced successfully by in the genome. Yet, by PCR we could not establish the exact insertion site(s). This only seems doable by marker recovery from genomic library, or by whole genome resequencing. It is also not known if such insertions are stably maintained. This type of recombination seems reminiscent of recombinations in plants or algae, where targeted homologous recombination is not (directly) possible. Essentially the same result occurred when using a gene inactivation approach with a double-homologous fragment carrying an antibiotic resistance marker gene. RW1 antibiotic resistant colonies were detected, which carried the expected double antibiotic marker resistances for 'single recombination' of the plasmid DNA. However, such colonies did not carry the construct at the expected location, as far as PCR screening could tell. We could not further invest the time here to analyze the outcome of such transformations at the genetic level, nor further optimize genetic delivery techniques.

In conclusion, it shows that RW1 is actually a very fascinating bacterium in terms of its genetic capabilities, which may actually point to evolutionary advantages when it comes down to integrating DNA. On the other hand, much more time would need to be invested to bring other genetic techniques up to speed in RW1. For the time being, however, plasmid delivery using pME6012 seems the only possibility for introducing genetic constructs. Precise gene inactivation so far was not possible and gene knockouts can only be searched from transposon insertion libraries.

References

- Armengaud J and Timmis KN** (1998) The reductase RedA2 of the multi-component dioxin dioxygenase system of *Sphingomonas sp.* RW1 is related to class-I cytochrome P450-type reductases. *European Journal of Biochemistry* 253: 437-444.
- Armengaud J, Happe B and Timmis KN** (1998) Genetic analysis of dioxin dioxygenase of *Sphingomonas sp.* strain RW1: catabolic genes dispersed on the genome. *Journal of Bacteriology* 180: 3954-3966.
- Armengaud J, Timmis KN and Wittich R-M** (1999) A functional 4-hydroxysalicylate/hydroxyquinol degradative pathway gene cluster is linked to the initial Dibenzo-*p*-dioxin pathway genes in *Sphingomonas sp.* strain RW1. *Journal of Bacteriology* 181: 3452-3461.
- Armengaud J, Gaillard J and Timmis KN** (2000) A second [2Fe-2S] ferredoxin from *Sphingomonas sp.* strain RW1 can function as an electron donor for the dioxin dioxygenase. *Journal of Bacteriology* 182: 2238-2244.
- Basta T, Buerger S and Stolz A** (2005) Structural and replicative diversity of large plasmids from sphingomonads that degrade polycyclic aromatic compounds and xenobiotics. *Microbiology* 151: 2025-2037.
- Basta T, Keck A, Klein J and Stolz A** (2004) detection and characterization of conjugative degradative plasmids in xenobiotic-degrading *Sphingomonas* Strains. *Journal of Bacteriology*. 186: 3862-3872.
- Bastiaens L, Springael D, Wattiau P, Harms H, deWachter R, Verachtert H and Diels L** (2000) Isolation of adherent Polycyclic Aromatic Hydrocarbon (PAH)-degrading bacteria using PAH-sorbing carriers. *Applied and Environmental Microbiology* 66: 1834-1843.
- Bunz PV and Cook AM** (1993) Dibenzofuran 4,4a-dioxygenase from *Sphingomonas sp.* strain RW1: angular dioxygenation by a three-component enzyme system. *Journal of Bacteriology* 175: 6467-6475.
- Bünz PV, Falchetto R and Cook AM** (1993) Purification of two isofunctional hydrolases (EC 3.7.1.8) in the degradative pathway for dibenzofuran in *Sphingomonas sp.* strain RW1. *Biodegradation* 4: 171-178.
- Cai M and Xun L** (2002) Organization and regulation of pentachlorophenol-degrading genes in *Sphingobium chlorophenicum* ATCC 39723. *Journal of Bacteriology* 184: 4672-4680.
- Choi K-H, Gaynor JB, White KG, Lopez C, Bosio CM, Karkhoff-Schweizer RR and Schweizer HP** (2005) A Tn7-based broad-range bacterial cloning and expression system. *Nature Methods* 2: 443-448.
- Coronado E, Roggo C, Johnson DR and van der Meer JR** (2012) Genome-wide analysis of salicylate and dibenzofuran metabolism in *Sphingomonas wittichii* RW1. *Frontiers in Microbiology* 3.

- de Boer HA, Comstock LJ and Vasser M** (1983) The tac promoter: a functional hybrid derived from the trp and lac promoters. *Proceedings of the National Academy of Sciences* 80: 21-25.
- de Lorenzo V and Timmis KN** (1994) Analysis and construction of stable phenotypes in gram-negative bacteria with Tn5- and Tn10-derived minitransposons. *Methods in Enzymology*, 235: 386-405.
- Dogra C, Raina V, Pal R, Suar M, Lal S, Gartemann K-H, Holliger C, van der Meer JR and Lal R** (2004) Organization of lin genes and IS6100 among different strains of hexachlorocyclohexane-degrading *Sphingomonas paucimobilis*: evidence for horizontal gene transfer. *Journal of Bacteriology* 186: 2225-2235.
- Dower WJ, Miller JF and Ragsdale CW** (1988) High efficiency transformation of *E. coli* by high voltage electroporation. *Nucleic Acids Research* 16: 6127-6145.
- Ferri L, Gori A, Biondi EG, Mengoni A and Bazzicalupo M** (2010) Plasmid electroporation of *Sinorhizobium* strains: The role of the restriction gene hsdR in type strain Rm1021. *Plasmid* 63: 128-135.
- Gai Z, Wang X, Liu X, Tai C, Tang H, He X, Wu G, Deng Z and Xu P** (2010) The genes coding for the conversion of carbazole to catechol are flanked by IS6100 elements in *Sphingomonas* strain XLDN2-5. *PLoS ONE* 5: e10018.
- Gilchrist A and Smit J** (1991) Transformation of freshwater and marine caulobacters by electroporation. *Journal of Bacteriology* 173: 921-925.
- Halden RU, Halden BG and Dwyer DF** (1999) Removal of Dibenzofuran, Dibenzo-*p*-dioxin, and 2-Chlorodibenzo-*p*-dioxin from soils inoculated with *Sphingomonas sp.* strain RW1. *Applied and Environmental Microbiology* 65: 2246-2249.
- Hanahan D** (1985) Techniques for transformation of *E. coli*. *DNA cloning: A practical approach*, (DM G, ed.) 109–135. IRL Press, Washington, DC.
- Heeb S, Itoh Y, Nishijyo T, Nishijyo T, Schnider Ur, Keel C, Wade J, Walsh U, O'Gara F and Haas D** (2000) Small, stable shuttle vectors based on the minimal pVS1 replicon for use in gram-negative, plant-associated bacteria. *Molecular Plant-Microbe Interactions* 13: 232-237.
- Herrero M, de Lorenzo V and Timmis KN** (1990) Transposon vectors containing non-antibiotic resistance selection markers for cloning and stable chromosomal insertion of foreign genes in gram-negative bacteria. *Journal of Bacteriology* 172: 6557-6567.
- Jacobs M, Wnendt S and Stahl U** (1990) High-efficiency electro-transformation of *Escherichia coli* with DNA from ligation mixtures. *Nucleic Acids Research* 18: 1653.

- Jaspers M, Meier C, Zehnder A, Harms H and van der Meer JR** (2001) Measuring mass transfer processes of octane with the help of an alkSalkB::gfp tagged *Escherichia coli*. *Environmental Microbiology* 3: 512-524.
- Johnson D, Coronado E, Moreno-Forero S, Heipieper H and van der Meer J** (2011) Transcriptome and membrane fatty acid analyses reveal different strategies for responding to permeating and non-permeating solutes in the bacterium *Sphingomonas wittichii*. *BMC Microbiology* 11: 250.
- Kristensen CS, Eberl L, Sanchez-Romero JM, Givskov M, Molin S and De Lorenzo V** (1995) Site-specific deletions of chromosomally located DNA segments with the multimer resolution system of broad-host-range plasmid RP4. *Journal of Bacteriology* 177: 52-58.
- Larsen R, Wilson M, Guss A and Metcalf W** (2002) Genetic analysis of pigment biosynthesis in *Xanthobacter autotrophicus* Py2 using a new, highly efficient transposon mutagenesis system that is functional in a wide variety of bacteria. *Archives of Microbiology* 178: 193-201.
- Martínez-García E, Calles B., Arévalo-Rodríguez M. and de Lorenzo V** (2011) pBAM1: an all-synthetic genetic tool for analysis and construction of complex bacterial phenotypes. *BMC Microbiology* 11: 38.
- Martínez-García E and de Lorenzo V** (2011) Engineering multiple genomic deletions in Gram-negative bacteria: analysis of the multi-resistant antibiotic profile of *Pseudomonas putida* KT2440. *Environmental Microbiology* 13: 2702-2716.
- Masai E, Shinohara S, Hara H, Nishikawa S, Katayama Y and Fukuda M** (1999) Genetic and biochemical characterization of a 2-pyrone-4,6-dicarboxylic acid hydrolase involved in the protocatechuate 4,5-cleavage pathway of *Sphingomonas paucimobilis* SYK-6. *Journal of Bacteriology* 181: 55-62.
- Miller WG, Leveau JHJ and Lindow SE** (2000) Improved gfp and inaZ broad-host-range promoter-probe vectors. *Molecular Plant-Microbe Interactions* 13: 1243-1250.
- Müller TA, Byrde SM, Werlen C, van der Meer JR and Kohler H-PE** (2004) Genetic analysis of phenoxyalkanoic acid degradation in *Sphingomonas herbicidovorans* MH. *Applied and Environmental Microbiology* 70: 6066-6075.
- Nam I-H, Hong H-B, Kim Y-M, Kim B-H, Murugesan K and Chang Y-S** (2005) Biological removal of polychlorinated dibenzo-*p*-dioxins from incinerator fly ash by *Sphingomonas wittichii* RW1. *Water Research* 39: 4651-4660.
- Pósfai G, Kolisnychenko V, Bereczki Z and Blattner FR** (1999) Markerless gene replacement in *Escherichia coli* stimulated by a double-strand break in the chromosome. *Nucleic Acids Research* 27: 4409-4415.

Reasoner DJ and Geldreich EE (1985) A new medium for the enumeration and subculture of bacteria from potable water. *Applied and Environmental Microbiology* 49: 1-7.

Roberts RJ, Vincze T, Posfai J and Macelis D (2010) REBASE-a database for DNA restriction and modification: enzymes, genes and genomes. *Nucleic Acids Research* 38: D234-D236.

Rochat L, Péchy-Tarr M, Baehler E, Maurhofer M and Keel C (2010) Combination of fluorescent reporters for simultaneous monitoring of root colonization and antifungal gene expression by a biocontrol *Pseudomonad* on cereals with Flow Cytometry. *Molecular Plant-Microbe Interactions* 23: 949-961.

Veiga H and Pinho MG (2009) Inactivation of the *SauI* Type I Restriction-Modification System is not sufficient to generate *Staphylococcus aureus* strains capable of efficiently accepting foreign DNA. *Applied and Environmental Microbiology* 75: 3034-3038.

Wang Q, Mueller AP, Leong CR, Matsumoto Ki, Taguchi S and Nomura CT (2010) Quick and efficient method for genetic transformation of biopolymer-producing bacteria. *Journal of Chemical Technology and Biotechnology* 85: 775-778.

Wattiau P, Bastiaens L, van Herwijnen R, Daal L, Parsons JR, Renard M-E, Springael D and Cornelis GR (2001) Fluorene degradation by *Sphingomonas sp.* LB126 proceeds through protocatechuic acid: a genetic analysis. *Research in Microbiology* 152: 861-872.

Wilkes H, Wittich R, Timmis KN, Fortnagel P and Francke W (1996) Degradation of chlorinated Dibenzofurans and Dibenzo-*p*-dioxins by *Sphingomonas sp.* strain RW1. *Applied and Environmental Microbiology* 62: 367-371.

Wilson GG (1991) Organization of restriction-modification systems. *Nucleic Acids Research* 19: 2539-2566.

Wittich RM, Wilkes H, Sinnwell V, Francke W and Fortnagel P (1992) Metabolism of dibenzo-*p*-dioxin by *Sphingomonas sp.* strain RW1. *Applied and Environmental Microbiology* 58: 1005-1010.

Wong SM and Mekalanos JJ (2000) Genetic footprinting with mariner-based transposition in *Pseudomonas aeruginosa*. *Proceedings of the National Academy of Sciences* 97: 10191-10196.

Yasui K, Kano Y, Tanaka K, Watanabe K, Shimizu-Kadota M, Yoshikawa H and Suzuki T (2009) Improvement of bacterial transformation efficiency using plasmid artificial modification. *Nucleic Acids Research* 37: e3.

Supplementary information

Figure S1. Change in codon sequence of *egfp* to obtain *egfp_{RW1}*, which favors the codon usage of *S. wittichii*

RW1.

Original sequence of *egfp* in pPROBE'

atg agt aaa gga gaa gaa ctt ttc act gga gtt gtc cca att ctt gtt gaa tta gat ggt gat gtt aat ggg cac
aaa ttt tct gtc agt gga gag ggt gaa ggt gat gca aca tac gga aaa ctt acc ctt aaa ttt att tgc act act
gga aaa cta cct gtt cca tgg cca aca ctt gtc act act ttg act tat ggt gtt caa tgc ttt tca aga tac cca gat
cat atg aaa cgg cat gac ttt ttc aag agt gcc atg ccc gaa ggt tat gta cag gaa aga act ata ttt ttc aaa
gat gac ggg aac tac aag aca cgt gct gaa gtc aag ttt gaa ggt gat acc ctt gtt aat aga atc gag tta aaa
ggt att gat ttt aaa gaa gat gga aac att ctt gga cac aaa ttg gaa tac aac tat aac tca cac aat gta tac
atc atg gca gac aaa caa aag aat gga atc aaa gtt aac ttc aaa att aga cac aac att gaa gat gga agc
ggt caa cta gca gac cat tat caa caa aat act cca att ggc gat ggc cct gtc ctt tta cca gac aac cat tac
ctg tcc aca caa tct gcc ctt teg aaa gat ccc aac gaa aag aga gac cac atg gtc ctt ctt gag ttt gta aca
gct gct ggg att aca cat ggc atg gat gaa cta tac aaa taa

Sequence of *egfp_{RW1}*

atg agc aag ggg gaa gag ctg ttc act ggc gtt gtc cca atc ctt gtt gag tta gac ggc gac gtt aat ggc cat
aag ttc tcg gtc agt ggg gag ggc gaa ggc gac gcc acc tac ggc aag ctg acc ctg aag ttc atc tgc acc
act ggc aag cta cct gtt cgg tgg cgg aca ctc gtc acc acc ttg acc tat ggc gtt caa tgc ttc tca cgc tat
cca gat cac atg aag cgc cat gac ttc ttc aag agt gcg atg cgg gag ggg tat gta cag gag aga acc ata
ttc ttc aag gac gac ggg aac tat aag acc cgt gcg gag gtc aag ttc gag ggc gac acc ctt gtt aat cgc
atc gag tta aag ggc atc gac ttc aag gaa gac ggc aac atc ctt ggg cat aag ctg gag tat aac tat aac
tca cat aat gtc tat atc atg gcg gac aag cag aag aac ggc atc aag gtt aac ttc aag atc aga cat aac atc
gag gac ggc agc gtt caa ctg gcg gac cat tat cag cag aac acc cca atc ggc gac ggc cct gtc ctt tta
cca gac aac cat tat ctg tcc aca cag tct gcc ctg teg aag gac cgg aac gag aag aga gac cac atg gtc
ctg ctg gag ttc gtc aca gcg gcg ggg atc aca cat ggc atg gac gag cta tac aag taa

CHAPTER 4

Fluorescently tagged *Sphingomonas wittichii* RW1 for the detection of dibenzofuran in liquid cultures and soil

Edith Coronado, Tekle Tafesa, Dirk Springael, and Jan Roelof van der Meer

Abstract

Bioreporters are organisms that can give an easily measurable signal in response to a compound or condition of interest. The expression of a gene involved in a catabolic pathway can be coupled to the expression of a reporter gene. This allows interrogation of the bioavailability of xenobiotic compounds in contaminated sites by the degrader bacteria themselves. In the present work we constructed *S. wittichii* RW1-based bioreporters. Three representative promoters for DBF degradation were targeted, fused to a promoterless *egfp* gene, and inserted in the broad host plasmid pME6012. The bioreporter constructs carried the sequence upstream of genes Swit_4925 (putative oxalocrotonate decarboxylase), Swit_5102 (gentisate dioxygenase) or Swit_4897 (*dxnA1*, dibenzofuran-4,4a-dioxygenase). The inducibility of the three promoters (P_{4925} , P_{5102} and P_{dxnA1}) was tested first in liquid cultures under a variety of conditions. While P_{5102} showed no eGFP induction using PHE, SAL or DBF as carbon, P_{dxnA1} produced eGFP constitutively regardless of the carbon source used. The construct P_{4925} showed an increase of eGFP production when DBF was added to the growth media, compared to SAL or PHE. P_{4925} was thus selected to apply in microcosms containing PAH-contaminated and DBF-spiked soils. Strain RW1 (pME6012- P_{4925} -*egfp*) could grow the DBF-amended microcosms, but not in the absence of supplemented DBF. An

increase in eGFP signal 2 days after inoculation in the microcosms with added DBF was observed, but no significant eGFP induction was detected in the other microcosm combinations. RW1 (*P₄₉₂₅-egfp*) was compared to two other PAH-bioreporter strains, *Sphingomonas sp.* LH128 and *Burkholderia sartisoli* RP037. We find evidence for both largely limiting PAH availability as well as strong competition of native bacteria that seem to scavenge PAH-intermediates from the primary introduced degrader population.

Introduction

Bioremediation refers to the process of controlled biological transformation of organic pollutants into harmless metabolites or mineralization into CO₂ and H₂O (Seo *et al.*, 2009). Process control can be exerted by specific stimulation of catabolic activity of native bacteria at a contaminated site, e.g., by the addition of nutrients, electron acceptors, or by mixing (Bosma *et al.*, 1996; Ahn *et al.*, 2008; Chen *et al.*, 2008). Alternatively, addition of specific biocatalysts has been considered, such as pre-enriched bacteria, which successfully degrade one or more of the target compounds present at a site (Ahn *et al.*, 2008; Zhou *et al.*, 2008; Kumar *et al.*, 2009). Unfortunately, the process of strain inoculation (bioaugmentation), does not very consistently result in increased compound degradation rates or yields, which has been related to either a poor catalytic performance or poor survival of the introduced strains. Several explanations have been proposed for this, such as the accumulation of metabolic dead-end products (Coppotelli *et al.*, 2008, 2010) or adverse environmental conditions (Megharaj *et al.*, 1997; Chen *et al.*, 2008). In addition, introduced strains may not compete well with native microorganisms (Shi *et al.*, 2001; Kumar *et al.*, 2009). Finally, the target contaminants may not be readily bioavailable, in which case the introduced bacteria cannot fully deploy their catalytic activity (Bosma *et al.*, 1996; Halden *et al.*, 1999; Johnsen and Karlson, 2004; Wammer and Peters, 2005; Aso *et al.*, 2006; Das *et al.*, 2008; Rehmann *et al.*, 2008). Many frequently found organic pollutants such as polycyclic aromatic hydrocarbons or oil constituents have a low water solubility and high hydrophobicity. This favors their sorption to the organic matrix in soil, gradually leading to the process of *aging* by which the contaminants become less and less available for biota (Harms and Bosma, 1997).

The processes outlined above are most often inferred from macro-level measurements, such as compound degradation rates or population growth, which may confound the actual cause of bioaugmentation failure. One possible alternative method deploys bacterial bioreporters, by which the bacteria themselves can be directly interrogated for their response to the contaminated material at a site. In order to do so, the bacterial catalyst in question has to be equipped with a gene reporter construct, consisting of a promoter whose expression is representative for the catabolic pathway or other, that drives expression of an easily detectable reporter protein (Leveau and Lindow, 2002; Tecon and van der Meer, 2008). Many reporter constructs have been developed (Sticher *et al.*, 1997; Stiner and Halverson, 2002; Werlen *et al.*, 2004; Tecon *et al.*, 2009; 2010; Kumari *et al.*, 2011; de las Heras and de Lorenzo, 2011), but these are mostly applied in bulk assays with aqueous samples and rarely applied to interrogate the specific environment the cells enter into once the cell encounters the target compound (Leveau and Lindow, 2001). Application of strains as bioreporters is also somewhat limited to the genetic accessibility of a wild-type strain to the genetic reporter construct. As a consequence, many bioreporters occur in strains that are useful in a simple assay (e.g., *Escherichia coli*), but which are not the bacteria of choice for bioremediation.

Here we report the construction of three bioreporters in *Sphingomonas wittichii* RW1, a bacterium of interest for bioremediation because it degrades dibenzofurans (DBF) and dibenzodioxins, two common PAHs found in contaminated areas and after incineration processes (Safe, 1990). Representative promoters for DBF degradation were selected from a previously carried out transcriptome study (Coronado *et al.*, 2012), and from previous work by others (Bunz and Cook, 1993; Bunz *et al.*, 1993; Armengaud and Timmis, 1998; Armengaud *et al.*, 1998; 1999; 2000; Basta *et al.*, 2004). Selected promoter regions were

fused to promoterless *egfp* on broad-host range plasmids introduced into RW1. Primarily we focused on a promoter upstream of the gene Swit_4925 with 12-fold higher expression during growth of RW1 on DBF compared to phenylalanine, and another one upstream of Swit_5102, with 19-fold higher expression (Coronado *et al.*, 2012). Swit_4925 is putatively involved in the transformation of 2-OH-2,4-pentadienoate, an intermediate from DBF metabolism, whereas Swit_5102 is predicted to code for a gentisate dioxygenase (Coronado *et al.*, 2012). In addition, we selected the promoter upstream of the gene Swit_4897 (*dxnA1*), which codes for the dibenzofuran-4,4a-dioxygenase, catalyzing the initial step in DBF degradation (Armengaud *et al.*, 1998). The genetic stability of the constructs and the activity of the three promoters (P_{4925} , P_{5102} and P_{dxnA1}) were tested first in liquid cultures under a variety of conditions. The best performing construct (P_{4925}) was selected and tested in PAH-contaminated and DBF-spiked soils for population growth and reporter induction. Behavior of RW1 (P_{4925} -*egfp*) was then compared to two other PAH-bioreporter strains, *Sphingomonas* sp. LH128 and *Burkholderia sartisoli* RP037-*mche* (Tecon *et al.*, 2009). Interestingly, we find evidence for both largely limiting PAH availability as well as strong competition of native bacteria that seem to scavenge PAH-intermediates from the primary introduced degrader.

Materials and methods

1. Bacteria cultivation

A stock of *S. wittichii* RW1 (Wittich *et al.*, 1992) was kept at -80°C and a small aliquot was plated on agar with 5 mM salicylate (SAL). Liquid minimal medium (MM) was based on DSM457 amended with 5 mM salicylate (MM+SAL) as reported elsewhere (Johnson *et al.*, 2011). Other carbon sources employed for RW1 culturing were phenylalanine (PHE) at 5 mM or dibenzofuran (DBF), which was dosed at 5 µmol per ml in form of crystals (DBF aqueous solubility is 5 mg per L). *Sphingomonas sp.* LH128 (pME6012-*phnA1-egfp*) is a phenanthrene (PHN) degrader with a plasmid reporter construct in which the promoter of the PHN dioxygenase is fused to *egfp* (Bastiaens *et al.*, 2000; Tekle Tafese, in preparation). LH128 was grown on R₂A media (Reasoner and Geldreich, 1985) agar plates, and in MM liquid cultures with PHN crystals dosed at 5 µmol per ml (PHN aqueous solubility is 1.6 mg per L). *B. sartisoli* RP037-*mche* (pPROBE-P_{*phnS*}-*egfp*) is a PHN degrader carrying a reporter plasmid responding to naphthalene and phenanthrene (Tecon *et al.*, 2009). It was cultured in Tryptone Yeast (TY) agar plates with 50 mM NaCl (Tecon *et al.*, 2006). For liquid cultures we used the type 21C mineral medium (Gerhardt *et al.*, 1981) to which PHN crystals were added in a dosage of 5 µmol per ml (21C+PHN). Strains RW1, LH128 and RP037 were all incubated at 30°C; when in liquid medium, they were cultured in a rotary shaker at 180 rpm. Cultures were inoculated at a turbidity (optical density, OD₆₀₀) of 0.005 and grown until stationary phase (OD of around 1). *E. coli* strains were grown in Luria Broth (LB) at 37°C. Antibiotic usage included kanamycin (Km, at 50 µg per ml), gentamicin (Gm, at 8 µg per ml) and tetracycline (Tc, at 20 µg per ml) to select for the presence of plasmids, and

cycloheximide (Cyc, at 100 µg per ml) to select against fungal growth. All strains used are listed in Table 1.

Table 1. Strains, plasmids and primers used in this study. P02- One of the native RW1 plasmids, Chromosome. Bold letters in the sequences represent the restriction sites introduced.

	Description		Ref.
Strains			
<i>Sphingomonas wittichii</i> RW1	Dibenzofuran degrader		Wittich <i>et al.</i> , 1992
<i>Escherichia coli</i> DH5α	Host for propagation of plasmids		Hanahan <i>et al.</i> , 1985
<i>Sphingomonas sp.</i> LH128	Phenanthrene degrader		Bastiaens <i>et al.</i> , 2000
<i>Burkholderia sartisoli</i> RP037-mche	Phenanthrene degrader		Tecon <i>et al.</i> , 2009
Plasmids			
pME6012	Shuttle vector		Heeb <i>et al.</i> , 2000
pME3280::miniTn7-P _{Tac} -gfp	Plasmid containing a miniTn7 coding for an <i>egfp</i> gene under the control of the constitutive promoter P _{Tac}		Rochat <i>et al.</i> , 2010
pME6012-P _{dxnA1} - <i>egfp</i>	DBF bioreporter, <i>dxnA1</i> promoter		This study
pJAMA23	Vector coding for a promoterless <i>egfp</i> gene		Jaspers <i>et al.</i> , 2001
pJAMA23-P ₄₉₂₅	Plasmid pJAMA23 with promotor region of gene Swit ₄₉₂₅ and <i>egfp</i>		This study
pJAMA23::P ₅₁₀₂	Plasmid pJAMA23 with promotor region of gene Swit ₅₁₀₂ and <i>egfp</i>		This study
pME6012-P ₄₉₂₅ - <i>egfp</i>	DBF bioreporter, Swit ₄₉₂₅ promoter and the <i>egfp</i> gene		This study
pME6012-P ₅₁₀₂ - <i>egfp</i>	DBF bioreporter, Swit ₅₁₀₂ promoter and the <i>egfp</i> gene		This study
pPROBE'-gfp-tagless	Broad-host range promoter probe vector with <i>egfp</i>		Miller <i>et al.</i> , 2000
pCK218	Mini-Tn5 delivery vector		Kristensen <i>et al.</i> , 1995
Primers			
<u>Primers</u>	<u>Position in sequence (nt)</u>	<u>Sequence</u>	
PdxnA1-rev	P02-12447	gccttcagcacac ccggg tcgcatca	Amplification of upstream region of gene <i>dxnA1</i> in RW1 (SmaI)
PdxnA1-fw	P02-12742	ggggtcgcac atgcctgtctcc	Amplification of upstream region of gene <i>dxnA1</i> in RW1 (SalI)
PSwit4925-rev	P02-38303	caattgt ggatcc atgagcgc	Amplification of the upstream region of gene Swit ₄₉₂₅ (BamHI)
PSwit4925-fw	P02-38532	cggtgtg ctgcag caagcgg	Amplification of the upstream region of gene Swit ₄₉₂₅ (PstI)
PSwit5102-rev	P02-213036	tacgcgc ggatcc gcctttt	Amplification of the upstream region of gene Swit ₅₁₀₂ (BamHI)

PSwit5102-fw	P02- 213291	gagtgat ctgcag agccggg	Amplification of the upstream region of gene Swit_5102 (PstI)
PSwit1848-rev	Ch- 2067652	cgtgc gggtacc gcatcgcc	Amplification of the upstream region of gene Swit_1848 (KpnI)
PuspA3-fw	Ch- 278862	ggccatccggaattctgctcc	Amplification of the upstream region of gene Swit_0266 (EcoRI)
PuspA-rev	Ch- 279129	cagcaacagcatatgcttcaccgc agg	Amplification of the upstream region of gene Swit_0266 (NdeI)
PSwit1848-fw	Ch- 2067856	cctcgggc agatct tcggcaa	Amplification of the upstream region of gene Swit_1848 (BglII)
PSwit2634-rev	Ch- 2917309	ccaccgc gtacc ggatggac	Amplification of the upstream region of gene Swit_2634 (KpnI)
PSwit2634-fw	Ch- 2917103	ctggcgc agatct ataaaata	Amplification of the upstream region of gene Swit_2634 (BglII)

2. Genetic stability

To test genetic delivery and stability in strain RW1 we used either the broad host plasmid pPROBE'-gfp-tagless (Miller *et al.*, 2000), and pME6012 (Heeb *et al.*, 2000), or the mini-Tn5 (Kristensen *et al.*, 1995) and mini-Tn7 delivery systems (Rochat *et al.*, 2010). Plasmid pPROBE'-tagless was equipped with the constitutive promoter P_{Tac} , by placing a SmaI-EcoRI restriction fragment of pME3280::miniTn7- P_{Tac} -*mche* (Rochat *et al.*, 2010) upstream of the promoterless *egfp*. The P_{Tac} -*egfp* fragment was recovered by XhoI-HindIII digestion and ligated into the alternative broad host range vector pME6012, producing pME6012- P_{Tac} -*egfp*. For mini-Tn5 delivery, a codon optimized *egfp* for RW1, named *egfp_{RW1}* (Figure S1), was synthesized together with P_{Tac} (DNA 2.0, Inc., USA). This fragment was ligated into the NotI-digested mini-transposon delivery vector pCK218 (Kristensen *et al.*, 1995), producing the plasmid pCK218::miniTn5- P_{Tac} -*egfp_{RW1}*.

Plasmids were purified to high concentration (around 1 μ g per μ l) from *E. coli* hosts by using a Jetstar 2.0 kit, according to the manufacturer's instructions (Genomed). Plasmids were then introduced into strain RW1 by electroporation using a slightly modified protocol from Masai *et al.* (1999). Briefly, cells were recovered from a 20 ml RW1 culture

exponentially growing on MM+SAL (OD₆₀₀ 0.4) by centrifugation at 8,000 rpm during 2 min at 4°C, after which the supernatant was discarded and the cells were resuspended in 5 ml of ice-cold sucrose solution (300 mM). The procedure of centrifugation and resuspension was repeated three times, after which cells were used immediately for electroporation. Hereto, 100 µl cell suspension in sucrose solution was transferred to an ice-cold electroporation cuvette, and mixed with 1 to 3 µg of purified plasmid DNA in a maximum of 10 µl volume. Cells were electroporated at 25 µF, 800 Ω, and 2.5 kV (GenePulser, Biorad), after which they were immediately mixed with 1 ml LB medium. This cell suspension was transferred to a 5 ml glass vial and incubated for 16 h at 30°C in the absence of any antibiotics, after which 150 µl were plated on selective plates (MM+SAL plus Km or Tc). RW1 transformants were allowed to form colonies for up to 7 days at 30°C, after which they were screened for the presence of the appropriate genetic construct by PCR. Colonies were purified on the same medium, rescreened by PCR, and if positive, regrown in liquid MM+SAL culture with the appropriate antibiotics. Plasmids were purified from such RW1 cultures using a standard Qiaprep kit according to manufacturer's instructions (Qiagen). Purified plasmids from RW1 were digested and verified for proper restriction fragment patterns using standard agarose gel electrophoresis, and the regions containing promoter inserts were sequenced to ensure that no modifications had taken place.

pCK218::miniTn5-P_{Tac}-*egfp*_{RW1} (Km^R) was maintained in *E. coli* CC118 λpir, from where it was purified (QIAprep, Qiagen). An aliquot of 500 ng of purified plasmid was used to electrotransform *S. wittichii* RW1 cells and a colony carrying the correct construct was selected by PCR screening. The plasmid pME3280::miniTn7-P_{Tac}-*egfp* (Gm^R) was introduced into RW1 by conjugation using *E. coli* DH5α as plasmid donor, *E. coli* SM1(pUX-BF13) as Tn7 transposase donor and *E. coli* HB101 (pRK2013) as helper for transfer, as described by

Lambertsen *et al.* (2004). Potential RW1 transconjugants/transposon mutants were selected on MM+SAL in the presence of the appropriate antibiotic. Colonies were purified and verified by PCR for the presence of the appropriate construct.

The genetic stability of plasmid and transposon-based constructs in RW1 was tested across five subsequent passages of liquid culturing (approximately 50 generations) and plating. Stationary phase cultures of RW1 (pPROBE- P_{Tac} -*egfp*), (pME6012- P_{Tac} -*egfp*) or RW1 (miniTn5- P_{Tac} -*egfp*_{RW1}) were inoculated 200-fold diluted in MM+SAL medium, with or without the addition of the respective antibiotic (Km or Tc). After culturing for 24 h a sample was taken for serial dilutions, which were plated on MM+SAL solid media with or without antibiotics. The rest of the cell suspension was diluted to initiate a new series of cultures. This procedure was repeated four times. The number of antibiotic resistant colonies and of colonies that showed eGFP fluorescence after each cycle were counted, and compared to the number of colonies on plates without antibiotics.

3. Construction of DBF bioreporter strains

A 296-bp region upstream of the gene *dxnA1* was amplified from the RW1 genome using the PCR with primers P_{dnxA1}-fw and P_{dnxA1}-rev (Table 1). The amplicon was digested at primer internal SalI and SmaI sites, purified, and ligated with the KpnI-XhoI pME6012 vector fragment and the KpnI-SmaI *egfp* fragment from plasmid pME3280::miniTn7- P_{Tac} -*egfp*. Tc-resistant *E. coli* DH5 α transformants were verified by PCR and restriction digestion of purified plasmid for correctness of the cloning (pME6012-P_{*dxnA1*}-*egfp*). A 249-bp region upstream of Swit_4925 was amplified using the primers P_{Swit4925}-fw and P_{Swit4925}-rev, containing PstI and BamHI restriction sites. The amplicon was digested and ligated to the PstI-BamHI-digested *egfp*-promoter probe vector pJAMA23

(Jaspers *et al.*, 2001). After transformation into *E. coli* DH5 α this resulted in plasmid pJAMA23-P_{4925-egfp}. This plasmid was digested with KpnI and HindIII to recover the 1 kb P_{4925-egfp} fragment, which was ligated to KpnI-HindIII-digested pME6012. After transformation into *E. coli* DH5 α this resulted in plasmid pME6012-P_{4925-egfp}. Similarly, a 256 bp upstream region of gene Swit_5102 was amplified using the primers PSwit5102-fw and PSwit5102-rev, and cloned in pME6012 to produce plasmid pME6012-P_{5102-egfp}. As a control for general response to stress growth conditions we used a 270 bp region upstream of the gene Swit_0266, which codes for an UspA-like general stress protein. This region was PCR amplified (primers PuspA3-fw and PuspA-rev) and equally cloned in pME6012 to produce plasmid pME6012-P_{uspA-egfp}.

4. Bioreporter tests

eGFP induction in *S. wittichii* RW1 from the reporter plasmids (pME6012-P_{4925-egfp}), (pME6012-P_{5102-egfp}) and (pME6012-P_{dxnA1-egfp}), was calibrated in liquid culture as function of carbon source and growth rate. RW1 reporter precultures were grown until stationary phase (OD~1.0) on MM+SAL+Tc. Cultures were subsequently 200-fold diluted in 50 ml flasks containing 15 ml of MM with PHE, SAL or DBF as carbon sources, and regrown. Cultures were regularly sampled for turbidity (Ultrospec, GE) and eGFP fluorescence measurements (FLUOstar Omega, BMG Labtech, or Zeiss epifluorescence microscopy - see below). To test the effect of water potential decrease, cultures were amended with increasing amounts NaCl or polyethylene glycol 8000, as specified by Johnson *et al.* (2011).

RW1, LH128 and RP037 bioreporters were then applied directly to a set of contaminated and non-sterile sandy soil microcosms, to assess PAH availability from the

contamination and competition from indigenous microorganisms. We used sand recovered from a beach near the shore of Lake Geneva close to St. Sulpice (Switzerland) as basis for the microcosms, in order to facilitate recovery of the reporter cells and subsequent epifluorescence microscopy analysis. Sand was used as such (S, see below), amended with DBF (S+DBF) or PHN (S+PHN), with additional loamy soil (Ter Munck [van Gestel *et al.*, 2012], S+TM), or with contaminated soil from a former gas manufacturing plant near Jonction, Geneva (S+J). The Jonction soil contains among others the PAHs anthracene (260 mg per kg soil), naphthalene (150 mg per kg soil) and fluorene (150 mg per kg soil), and further benzene (40 mg per kg soil) and toluene (70 mg per kg soil). For amendment with DBF or PHN, 200 g of sand contained in a glass vial were supplemented with 34.5 mg DBF or 44.5 mg PHN dissolved in 5 ml of dichloromethane (final dosage 2.5 μmol per g soil). The sand was vigorously shaken for several minutes after which it was spread out on aluminum foil under a fume hood. The sand-DBF or sand-PHN mixture was dried overnight to allow the solvent to evaporate. For the 'sand alone' treatment (S) 200 g material was supplemented with 5 ml dichloromethane and treated similarly as for S+DBF or S+PHN. For the 'S+TM' treatment air-dry TM loamy soil was added to the sand at 10% *w/w* and thoroughly mixed. For 'S+J', we mixed the Jonction PAH-contaminated material with the sand in 10% *w/w*. Individual microcosms were then prepared in triplicate for each sampling time point, which consisted of 1 g material in a 2 ml microcentrifuge tube, to which the reporter cells were added.

Reporter strains *S. wittichii* (pME6012-P₄₉₂₅-*egfp*) and (pME6012-P_{dxnA1}-*egfp*) were grown until stationary phase on MM+DBF. *Sphingomonas* LH128 (pME6012-*phnA1-egfp*) and *B. sartisoli* RP037-*mche* (pPROBE-P_{phnS}-*egfp*) were grown on MM+PHN and 21C+PHN, respectively. Precultures were diluted in saline solution (NaCl 0.9%) to reach an

approximate cell density of 1×10^5 CFU in a volume of 250 μ l. 250 μ l of cell suspension was inoculated per individual microcosm, which leads to approximately 50% water holding capacity, and the vials were vigorously shaken. For non-inoculated series 250 μ l saline solution was added to each of the microcosms. To recover cells, 1 ml of saline solution was added to a microcentrifuge tube, which was vigorously mixed for 10 sec and then sedimented for a few seconds. Approximately 0.9 ml of supernatant was transferred to a clean 2 ml tube. The extraction was repeated once more with 1 ml sterile 0.9% NaCl-solution, and both supernatants were pooled. From the approximately 2 ml of soil extracted liquid, an aliquot was used to prepare serial dilutions, which were plated on MM+SAL+Tc+Cyc-agar to count for colony-forming units (CFU) of the RW1 bioreporters, on R2A+Tc+Cyc for LH128 and on TY+Gm+Km+Cyc for *B. sartisoli*. The rest of the soil extract was centrifuged for 1 min at 2000 rpm to separate soil particles, and the supernatant (around 1.9 ml) was transferred to a new microcentrifuge tube. The transferred mixture was centrifuged during 30 min at 13,000 rpm, and the supernatant was discarded, except for the last ~ 20 μ l. This droplet was used to resuspend the cell pellet and was then used for microscope visualizations.

An assay was performed to test the scavenging of DBF metabolites by native bacteria present in the soil, which would affect the growth of the inoculated RW1 strain. A non-inoculated microcosm containing S+J+DBF and incubated at 30°C during 5 days was used to extract the native bacteria by saline solution washing, as described above. Aliquots of 200 μ l of the soil-extracted bacterial suspension were plated on MM agar plates with *meta*-toluate as carbon source (5 mM). The plates were incubated at 30°C and colonies (after 2 days) were washed of the plates and kept as a mixture. An aliquot of 500 μ l of this mixture was used to start a culture in 15 ml MM+*meta*-toluate. The culture was incubated overnight at 30°C on a rotary shaker until an $OD_{600}=0.2$ was reached, then it was centrifuged to remove the growth

media (8000 rpm for 5 min) and resuspended in 1.5 ml of saline solution. In parallel overnight liquid cultures of strains RW1 (pME6012-P₄₉₂₅-*egfp*) and (pME6012-P₅₁₀₂-*egfp*) (MM+DBF) were used to inoculate six Erlenmeyer flasks for each strain, containing 15 ml of MM+DBF, at an initial OD₆₀₀ of 0.005. The cultures were incubated in a rotary shaker (180 rpm) at 30°C until they reached an OD₆₀₀ of 0.2. At this point, half of the flasks were inoculated with 1.5 ml of the suspension of soil-extracted bacteria and the other half with 1.5 ml of saline solution. The cell cultures were continued to grow to stationary phase while measuring regularly the number of cells per ml and the eGFP intensity of RW1 reporter cells using flow cytometry (LSRFortessa, BD Biosciences). The settings for the flow cytometer measurements were as follows: Sample flow 2 µl/sec, Sample volume 200 µl, Voltage FSC 50, SSC 200 FITC 500/ Threshold FSC 500.

5. Epifluorescence microscope

A volume of 5 µl of cell suspension was transferred to a regular microscope slide, covered with a 20x40 mm cover slip. Cells were imaged at 1000 x magnification using a Zeiss Axioscop 2 epifluorescence microscope (EFM), first in phase contrast and then at eGFP illumination conditions (excitation filter: BP470/40; dichromatic mirror 500; emission filter: BP 525/50). Images were recorded as 16-bit TIFF files using a SPOT camera operated by the VisiScope cell explorer (Visitron Systems, Germany). Fluorescence intensity of individual cells was quantified on the TIFF-images using a previously described subroutine and masking in MetaMorph (7.0r3) (Tecon *et al.*, 2006). The data are presented as average of fluorescence intensity for strain RW1 and *B. sartisoli*, and as boosted average corresponding to the 3% of the cell population with the highest signal intensity for LH128. To test the differences in fluorescence intensities in the soil inoculated cells, an ANOVA ($p \leq 0.05$) was performed followed by a Tukey's post hoc test using the R software.

Results

Genetic stability of reporter constructs in *S. wittichii* RW1

The efficiency of transformation of *S. wittichii* RW1 for plasmid-based constructs (purified from *E. coli*) was around 10-70 transformants per μg plasmid DNA. Antibiotic-resistant and fluorescent RW1 colonies with verified correctness of the reporter construct were successively cultured in liquid medium for four transfers (~ 28 generations) in presence or absence of the antibiotic selecting for the plasmid marker. On average 60% of colonies of RW1 (pPROBE'-P_{Tac}-*egfp*) was Km-resistant after the first growth passage without antibiotic selection pressure, whereas close to 100% of the colonies were Km-resistant when the cells had been grown on medium with Km (Figure 1A). After the fourth passage, the proportions of Km^R-colonies decreased to 50 and 75%, respectively, for cells that had been growing on medium without or with Km. Astonishingly, only around 1% of the Km^R-colonies after the fourth transfer were fluorescent, regardless of the addition of Km to the liquid growth medium. Close to 100% of RW1 (pME6012-P_{Tac}-*egfp*) colonies were Tc^R after the first transfer, irrespective of Tc addition to the liquid growth medium (Figure 1B). During the subsequent transfers, the proportion of Tc^R-colonies decreased to 25% in the case of growth without Tc-addition to the culture medium, whereas it remained close to 100% for colonies in the Tc-supplemented liquid culture. Around 75% of the Tc^R-colonies were no longer fluorescent after the second transfer in medium without Tc, but almost 100% remained fluorescent as long as Tc had been added. Plasmids based on pME6012 were thus better maintained in RW1 than those based on pPROBE.

As an alternative to the plasmid system, two transposons were tested for maintenance in RW1, a miniTn7 and a miniTn5-based construct. Unfortunately, no RW1 transconjugants with mini-Tn7 insertion (pME3280::miniTn7- P_{Tac} -*egfp*) could be obtained, despite different attempts of conjugation or electrotransformation. In contrast, RW1 electrotransformants with the mini-Tn5:: P_{Tac} -*egfp*_{RW1} were obtained at an estimated frequency of 100 transformants per μ g DNA. After four passages in liquid medium without Km, close to 60% of all colonies were still Km^R and fluorescent. This percentage was close to 90% when Km had been added to the liquid growth medium (Figure 1C). Unfortunately, mini-Tn5-based constructs carrying RW1 homologous DNA for unknown reasons were not stable in RW1, but after several passages in MM+SAL+Km liquid growth medium produced false PCR amplicons despite conferring Km^R (data not shown). We therefore chose to work with pME6012-based reporter constructs in RW1 from thereon.

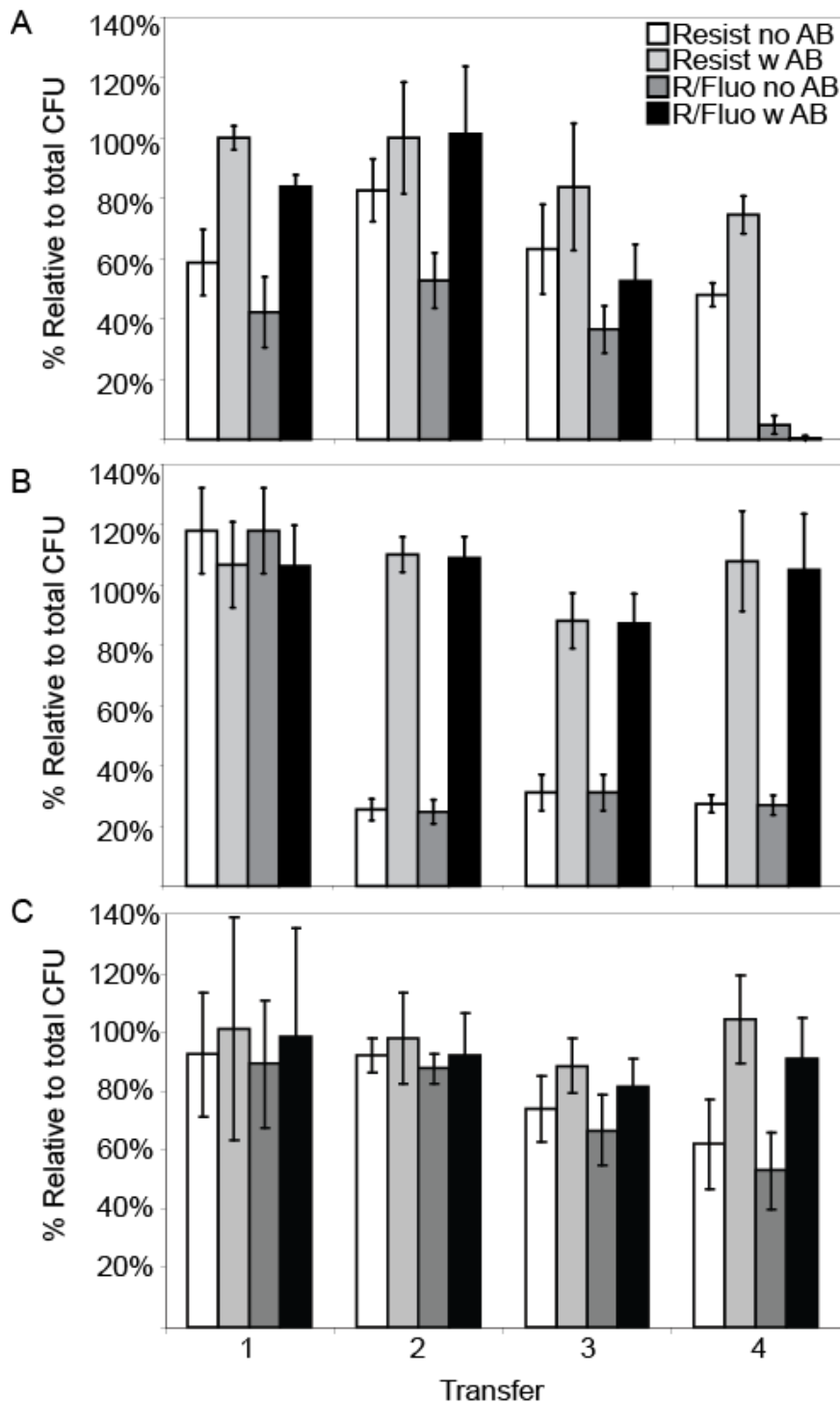


Figure 1. Plasmid maintenance of pPROBE- P_{Tac} -*egfp* (A), pME6012- P_{Tac} -*egfp* (B) and miniTn5:: P_{Tac} -*egfp* (C) in *Sphingomonas wittichii* RW1 over four successive culture transfers (~28 generations) in liquid medium with SAL as sole carbon source without (no AB) or with (AB) addition of antibiotic selecting for the plasmid or transposon insertion. Proportions show the number of antibiotic resistant colonies (Resist) divided by the number of colonies on non-selective media, or the number of fluorescent colonies amidst all resistant colonies (R/Fluo). For pPROBE and mini-Tn5, Km was used as antibiotic, whereas Tc was used for pME6012.

Calibration of the eGFP response of RW1 bioreporters under standard conditions

Two putative RW1 promoter regions, selected from microarray data from a previous study (Coronado *et al.*, 2012), plus the upstream region of the previously described *dxnA1*-gene (Armengaud *et al.*, 1998), were evaluated for their inducibility in the presence of DBF, SAL and PHE. Strain RW1 (pME6012- P₄₉₂₅-*egfp*) displayed higher fluorescence when growing on DBF than on SAL or PHE, measured either by fluorimeter (not shown) or by EFM (Figure 2A and 2D). In contrast, RW1 (pME6012-P_{*dxnA1*}-*egfp*) produced a slightly higher eGFP fluorescence when grown with SAL compared to PHE or DBF (Figure 2B and 2D). Contrary to our expectations from microarray data (19-fold higher signal in DBF-grown compared to PHE-grown cells), strain RW1 (pME6012-P₅₁₀₂-*egfp*) did not produce more eGFP fluorescence when grown with DBF compared to PHE or SAL (Figure 2C and 2D).

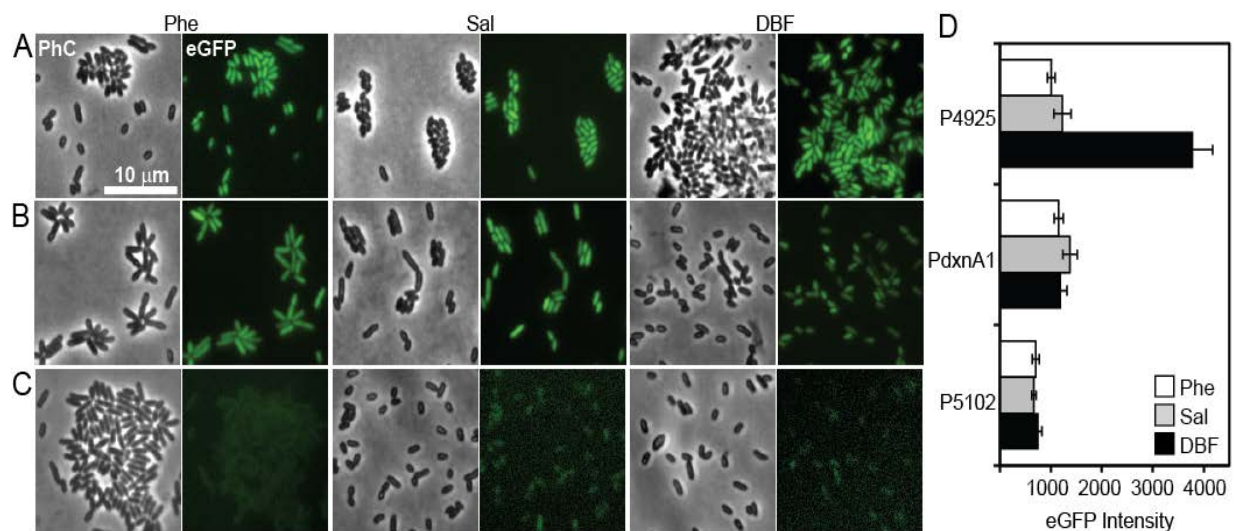


Figure 2. Microscope images (phase contrast, PhC and the corresponding eGFP fluorescence image) of RW1 carrying the constructs (A) pME6012-P₄₉₂₅-*egfp*, (B) pME6012-P_{*dxnA1*}-*egfp* and (C) pME6012-P₅₁₀₂-*egfp*, grown with PHE, SAL or DBF as carbon sources. (D) Average eGFP intensity of the RW1 clones grown with PHE, SAL and DBF, measured from EFM images of early stationary phase cultures.

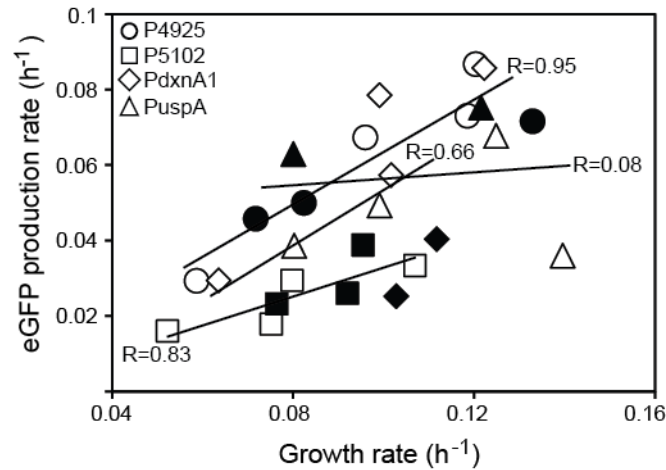


Figure 3. eGFP production rate as a function of growth rate of RW1 carrying the construct pME6012- P_{4925} -*egfp* (○/●), pME6012- P_{5102} -*egfp* (□/■), pME6012- P_{dxnA1} -*egfp* (◇/◆) and pME6012- P_{uspA} -*egfp* (△/▲). Rates were calculated from linear regression of ln-transformed eGFP or culture turbidity values versus time. Decrease of exponential growth rate was achieved by decreasing water potential in the medium through the addition of NaCl (open symbols) or PEG (closed symbols).

All three RW1 strains were next tested for activity of the promoter fragments as a function of growth rate on SAL, which was modulated by increasing concentrations of NaCl or PEG. Addition of NaCl or PEG decreases the water potential in the medium, which has been suggested to mimic the conditions in a dry soil (Halverson and Firestone, 2000). eGFP production rates from the catabolic promoters P_{4925} and P_{5102} were linearly dependent on the growth rate ($R=0.95$ and $R=0.83$, respectively, Figure 3), suggesting they are insensitive to lowered water potential by either NaCl or PEG. However, the increase in eGFP production rate from P_{5102} as function of growth rate was smaller than from P_{4925} (i.e., slope in Figure 3). In contrast, the eGFP production rate from P_{dxnA1} was correlated less well to the growth rate ($R=0.66$, Figure 3), which was mainly due to the difference in reaction of the promoter upon addition of NaCl or PEG. This suggests that *dxnA1* expression is dependent on the type of water stress. As a control, we used RW1 (pME6012- P_{uspA} -*egfp*), in which case there was no

apparent correlation between the growth rate and the eGFP production rate ($R=0.08$, Figure 3). This indicates that expression of the *uspA*-like gene in RW1 remains upright when cells grow slower.

Bioreporter response in contaminated material

Due to its specific *egfp* induction in liquid cultures in the presence of DBF compared to PHE, RW1 (pME6012-P₄₉₂₅-*egfp*) was selected to interrogate contaminant availability in sandy soil microcosms. Hereto cells were inoculated at relatively low density in the microcosms (10^5 per g material) and followed during 8 days for population size development and single cell eGFP fluorescence. RW1 (pME6012-P₄₉₂₅-*egfp*) could be detected by plating on MM+SAL+Tc during the 8 days of the experiment in all microcosms except for the uninoculated control. All colonies growing on MM+SAL+Tc agar plates showed green fluorescence. RW1 population growth was observed in S+DBF microcosms with an increase from 6×10^5 to 8×10^7 CFU/g five days after inoculation, which decreased to 3×10^7 CFU/g at day 8 (Figure 4A). RW1 cells also multiplied with approximately similar growth rates in sand mixed with the highly contaminated material from Jonction to which DBF was added (S+J+DBF), but yielding a smaller maximum population size (4×10^7 CFU/g after 4 d). In S+TM the population increased during the first day after inoculation from 1×10^6 to 8×10^6 CFU/g, after which it decreased until around 1×10^6 CFU/g at day 8. Similarly, in the S+J microcosms, a small increase from 3×10^4 to 1×10^6 CFU/g was observed after 1 d. After this time the population remained at around 10^5 CFU/g soil (Figure 4A). Population developments were similar for microcosms inoculated with RW1 (pME6012-P_{dxnA1}-*egfp*, Figure S2).

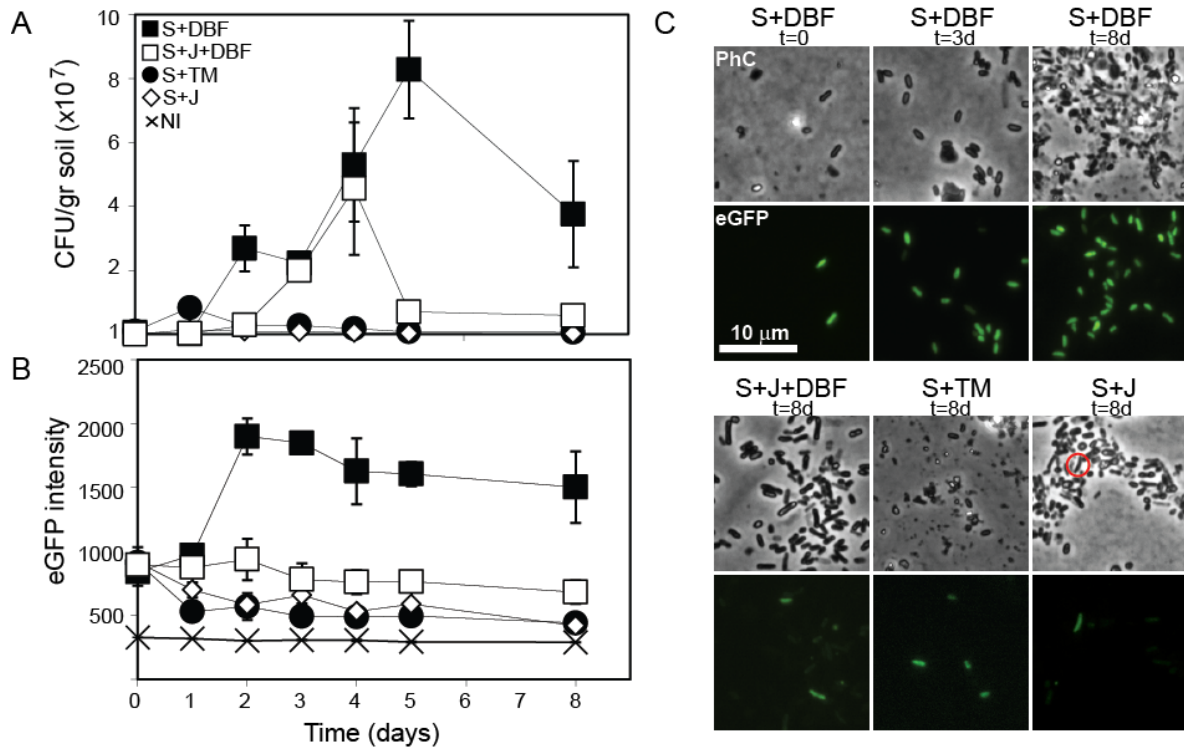


Figure 4. Population size development and reporter gene expression of RW1 (pME6012-*P*₄₉₂₅-*egfp*) inoculated in different microcosms. (A) Number of Tc^R-RW1 CFU/g soil over time and (B) average eGFP levels. Microcosms included S+DBF (■), S+J+DBF (□), S+TM (●) S+J (◇) and non-inoculated S microcosms, NI (×). (C) Illustrations of microscope images (phase contrast, PhC and the corresponding eGFP image) of RW1 (pME6012-*P*₄₉₂₅-*egfp*) at the moment of inoculation (t=0), 3 (t=3d), 8 days (t=8d) after inoculation in S+DBF (upper panels), and 8 days after inoculation in S+J+DBF, S+J and S+TM (lower panels).

Interestingly, average eGFP levels of RW1 (pME6012-*P*₄₉₂₅-*egfp*) cells inoculated in S+DBF increased two-fold after inoculation until day 2, after which it remained constant until the end of the experiment (Figure 4B). In contrast, average eGFP levels remained constant in cells inoculated in S+J+DBF. In all the microcosms supplemented with either pristine (S+TM) or contaminated soil (S+J), the eGFP signals decreased from the day of inoculation and were lower than in microcosm S+DBF (Figure 4B). Even if the signals in cells from microcosm S+J were slightly higher than in cells from S+TM, this difference was not significant. Microscope images at different time points clearly show an increase in the

overall number of cells in microcosm S+J+DBF or S+J, many of which were not RW1 (Figure 4C). The lower eGFP signal from RW1 cells in microcosms S+J+DBF compared to S+DBF therefore suggests that indigenous bacteria compete with RW1 for DBF. Since the P_{4925} -promoter responds to a metabolic intermediate the lower eGFP signal in S+J+DBF may indicate that indigenous bacteria scavenge (temporarily) released metabolic intermediates from DBF by RW1. eGFP signals from inoculated cells of RW1 (pME6012- P_{dxnA1} -*egfp*) were no different in S+DBF or S+TM microcosms, whereas its population increased from 7×10^5 to 2×10^7 in S+DBF (Figure S2), indicating that the *dxnA1*-promoter is constitutively on and does not react to DBF.

PAH-availability in the Junction material was further evaluated by inoculations with the *Sphingomonas sp.* LH128 (pME6012- P_{phnA1} -*egfp*) and *B. sartisoli* RP037-*mche* bioreporters. The population of LH128 increased in S+PHN microcosms from 1×10^4 to 7×10^5 CFU/g at day 8, but not in S+J+PHN or S+J (Figure 5). Microscope images indicated again a high number of cells from indigenous bacteria besides the LH128 reporter cells (Figure 5C). Only around 3% of the LH128 cells in the S+PHN microcosms showed eGFP signal, which increased over time until day 5 (Figure 5B). A similar proportion of fluorescent cells was observed when LH128 was grown in pure liquid cultures with PHN as carbon source. The rest of the cells had a low signal comparable to background. No eGFP-expressing LH128 reporter cells were detected in the S+J+PHN or the S+J microcosms. This may have been the result of the competition for PHN by indigenous microorganisms present in the Junction material (Figure 5C). In contrast to LH128, the *B. sartisoli* PHN reporters did not grow in any of the microcosms (not shown) and there was no difference in eGFP intensity in the different samples during the whole duration of the experiment (Figure S3), but these results will have to be further repeated and verified.

To test whether the lower eGFP levels in RW1 reporter cells in S+J+DBF compared to S+DBF microcosms were due to scavenging of substrate (DBF) or metabolites, we co-cultured RW1 (pME6012-*P*₄₉₂₅-*egfp*) or RW1 (pME6015-*P*₅₀₁₂-*egfp*) in MM+DBF with or without a mix of *meta*-toluate degrading strains isolated from Junction. Indeed, RW1 populations in co-cultures yielded only about half of the size attained in pure culture (Figure 6A and 6C) similar to what was observed in soil microcosms (Figure 4A). In contrast, eGFP intensities of RW1 reporter cells were indistinguishable in pure or co-culture (Figure 6B and 6D).

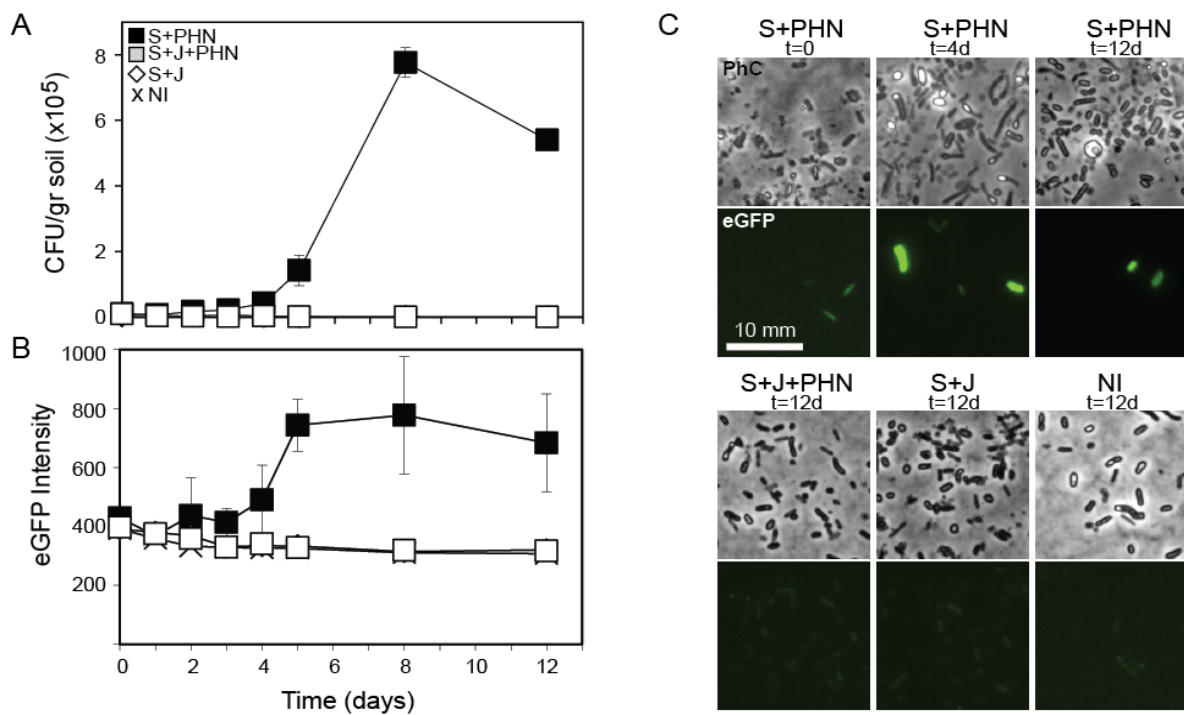


Figure 5. Population size development and reporter gene expression of LH128 (pME6012-*P*_{phnA1}-*egfp*) inoculated in microcosms. (A) Number of Tc^R-CFU/g soil and (B) boosted average eGFP level. Microcosms included, S+PHN (■), S+J+PHN (□), S+J (◇) and non-inoculated S microcosms, NI (×). (C) Illustrative microscope images (phase contrast, PhC and the corresponding eGFP image) of LH128 (pME6012-*P*_{phnA1}-*egfp*) at the moment of inoculation (t=0), 4 (t=4d), 12 days (t=12d) after inoculation in S+PHN (upper panels), and 12 days after inoculation in S+J+PHN, S+J and without inoculation, NI (lower panels).

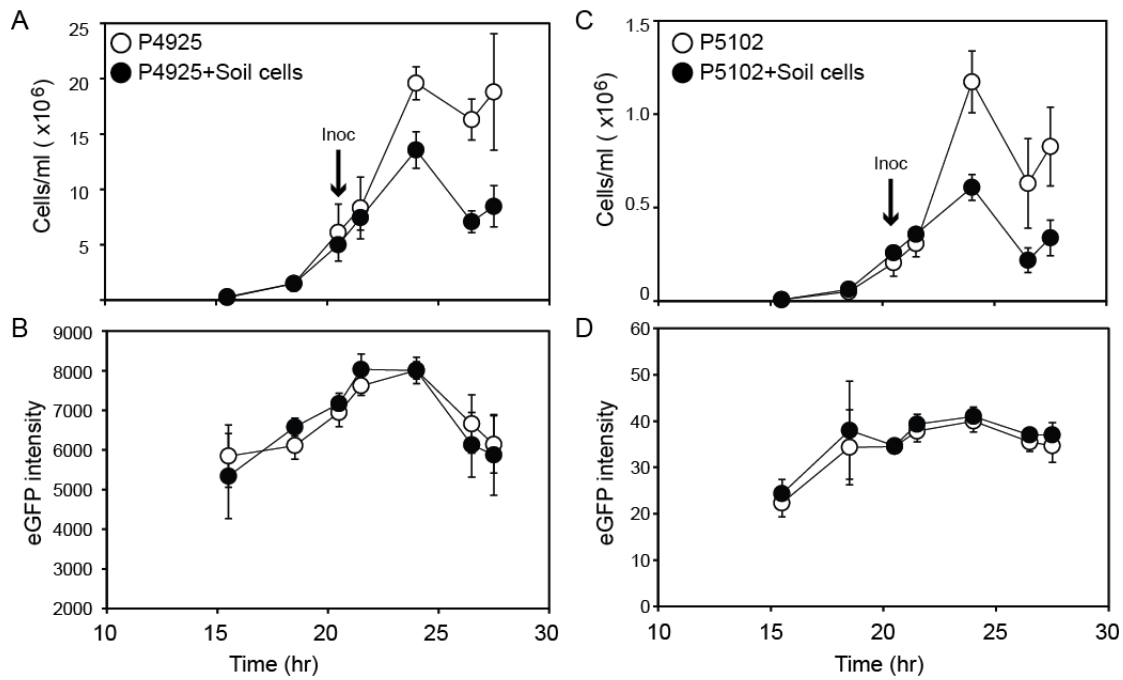


Figure 6. Population development and reporter gene expression of RW1 (pME6012-P₄₉₂₅-*egfp*) or (pME6012-P₅₁₀₂-*egfp*) growing in MM+DBF in pure or co-culture (+Soil cells) with three *m*-toluate degrading strains isolated from Jonction. (A, C) Number of RW1 cells per ml culture volume over time (flow cytometry data). (B, D) Average eGFP levels of individual RW1 reporter cells. Arrows indicate the point when the cultures were coinoculated with the *m*-toluate degrading strains.

Discussion

Bacterial bioreporters have been shown to be useful for probing the physical or chemical nature of the immediate environment surrounding the reporter cells (Leveau and Lindow, 2002; Tecon *et al.*, 2006). For example, a *proU-gfp* fusion in *Pantoea agglomerans* or *Pseudomonas syringae* was useful to document water potential differences in soils, on plant leaves and around plant roots (Axtell and Beattie 2002; Herron *et al.*, 2010). In other work, cells of *E. herbivora* carrying a *fruB-egfp* fusion probed the available fructose content leaking from plant leaves (Leveau and Lindow, 2001), whereas others used an *E. coli*-based GFP reporter to gauge tetracycline presence in the rat intestine (Bahl *et al.*, 2004). Bioreporters have also been used to measure the availability of hydrophobic contaminants such as PAHs (Tecon *et al.*, 2006; 2010) PAH bioreporters respond with rather low signals, which is thought to be due to the low aqueous solubility of the PAH (Tecon *et al.*, 2009; 2010). In addition, they have to be constructed in the strain which metabolizes the PAH, because it is often a metabolite which leads to induction from PAH-responsive promoters rather than the parent PAH-compound itself (Tecon *et al.*, 2006; Werlen *et al.*, 2004). The goal of the underlying work was to develop PAH-bioreporters based on *S. wittichii* RW1 and use those to better understand the fate of bioaugmented strains in contaminated material (here: PAHs). RW1 is not a standard laboratory bacterium for which genetic tools are easily available, and previous studies have reported difficulties in performing genetic studies in RW1 (Armengaud *et al.*, 1998), and plasmid instabilities (Basta *et al.*, 2004). Our results demonstrated that promoter-*egfp* fusions could be introduced into RW1 and relatively stably maintained using the broad-host range vector pME6012 (Heeb *et al.*, 2000). In contrast, similar constructions in pPROBE-type plasmids were not very well maintained and must have undergone genetic rearrangements, since many RW1 transformant colonies displayed

antibiotic resistance of the plasmid but no longer carried *egfp*. Systems like the mini-Tn5, known for their stability in numerous gram-negative bacteria (de Lorenzo and Timmis, 1994), were not stable to the same extent in RW1. Although RW1 transformants carrying mini-Tn5 insertions (Kristensen *et al*, 1995) were obtained, we detected genetic rearrangements by PCR after several generations of growth in liquid media even in the presence of the corresponding antibiotic. Despite several attempts, no transformants carrying a mini-Tn7 insertion were obtained using the system of Rochat *et al*. (2010), perhaps due to an inappropriate insertion site (McKknown *et al.*, 1988) in the RW1 chromosome.

Based on transcriptome data obtained from a previous study (Coronado *et al.*, 2012) three loci involved in DBF degradation were selected as target for DBF bioreporter construction. The first consisted in an upstream region of *dxnA1*, which codes for part of the dibenzofuran dioxygenase (P_{dxnA1}), the second in a region upstream of the cluster Swit_4925-4921, which encodes the downstream part of a *meta*-cleavage pathway (P_{4925}), and the third in a region upstream of the genes Swit_5102-5101, with Swit_5102 putatively coding for the enzyme gentisate dioxygenase that transforms gentisate to 3-maleyl pyruvate (P_{5102}). As expected, strain RW1 (pME6012- P_{dxnA1} -*egfp*) detectably expressed eGFP, but independent of its growth substrate (DBF, SAL or PHE), confirming that this region contains a constitutive promoter (Bunz and Cook, 1993; Armengaud *et al.*, 1998; Coronado *et al.*, 2012). Good eGFP inducibility on DBF compared to PHE- or SAL-grown cells was found for RW1 (pME6012- P_{4925} -*egfp*), which is in agreement with the transcriptome data (Coronado *et al.*, 2012). In contrast, RW1 (pME6012- P_{5102} -*egfp*) expressed *egfp* very poorly and showed no sign of specific induction either in liquid cultures or soil microcosms regardless of DBF addition. Therefore, even though global expression analysis had indicated up to 19-fold increased expression of the cluster Swit_5102-5101 in DBF- compared to PHE-grown cells

and more than 50-fold in SAL- versus PHE-grown cells (Coronado *et al.*, 2012), the P₅₁₀₂-reporter construct remained mostly uninduced. This could indicate that the 256-bp fragment used for cloning may not contain the promoter sequence, or that the plasmid again displayed some sort of rearrangement (see e.g., Chapter 3 for P₅₁₀₂-reporter induction of a mini-Tn5 insertion). More tests should be done in order to find the promoter location in this area.

The RW1 (pME6012-P₄₉₂₅-*egfp*) appeared to be useful to monitor DBF degradation activity not only in liquid cultures but also in soil microcosms. Interestingly, inoculated RW1 reporter cells multiplied in DBF-amended soil microcosms and were still detected 8 days after inoculation. This positive result was in contrast to previous studies by Megharaj *et al.* (1997) and Halden *et al.* (1999), who inoculated RW1 to soil microcosms spiked with DBF and dibenzodioxin, but found a constant decrease in cell numbers from the moment of the inoculation. This may be explained by the high inoculation cell density (10⁸ CFU per g soil), which cannot be sustained by the amount of DBF, whereas we started from a low inoculation density (10⁵ CFU/g), in which case population growth can occur. RW1 reporter cells grown in soil microcosms with DBF also increased eGFP reporter signal, indicating they were actively metabolizing DBF. Interestingly, however, when a small fraction of highly PAH-contaminated material from Jonction was added to the microcosms with DBF, RW1 reporter cells multiplied to a much lower population yield and displayed lower eGFP expression (Figure 4B). Since the material in those microcosms is not sterilized, a large proportion of endogenous bacteria from Jonction developed, which likely competed with RW1 for carbon. The lower eGFP expression of the RW1 reporter cells is intriguing and suggests that one particular type of metabolite, possibly 2-OH-2,4-penta-dienoate that is cleaved from DBF in yielding salicylate, is scavenged by the endogenous cells. We attempted to demonstrate this directly in liquid culture by using competition experiments with three strains isolated from

Jonction on the basis to metabolize *m*-toluate, and therefore, theoretically capable of metabolizing 2-OH-2,4-penta-dienoate. Unfortunately, RW1 reporter cells in co-culture on DBF did not decrease eGFP expression, although their yield was indeed again lower than in pure culture. This confirms that interspecies interactions and resource competition is a common trait in nature, as has been reported by others authors (Møller *et al.*, 1998; Pelz *et al.*, 1999; Wintermute and Silver, 2010; McGenity *et al.*, 2012) and a key trait to manipulate when enhancing the efficacy of bioaugmentation. More studies should be performed in order to determine the nature of the interaction of RW1 strain with native soil organisms to degrade the xenobiotic compounds.

The population size of inoculated RW1 reporter cells also increased in microcosms with Jonction material only (and without added DBF), but to a much lower level than in microcosms with added DBF. In addition, their eGFP expression was barely detectable suggesting that RW1 cannot find sufficient specific carbon substrate in Jonction to multiply, or is outcompeted entirely by endogenous cells for usage of PAHs. Similar results were obtained with the PHN-reporter strain *Sphingomonas sp.* LH128 (pME6012-*phnA1-egfp*). Although the LH128 PHN-reporter multiplied and expressed eGFP in sandy microcosms with PHN but without Jonction material, it failed entirely to do so when Jonction material was present (Figure 5). Again, microscopy data suggested abundant growth of other endogenous bacteria from the Jonction material, which effectively competed for PHN present in Jonction and/or added externally. Even less than RW1, the LH128 PHN-reporter was not capable of sustaining sufficiently long in microcosms with Jonction material to 'report' on its PAH-availability.

Bioavailability has been pointed as the main constraint for the success of bioremediation (Harms and Bosma, 1997; Bosma *et al.*, 1996; Wammer and Peters, 2005). The results presented here show that RW1 could survive in the soil supplemented with DBF, and thus has no inherent 'incapacity' to survive in such environments. However, the bacterium did not react to the compounds present in Jonction material, and even with subsequent addition of DBF, developed less well than in sand plus DBF alone. Since the Jonction soil comes from an old contaminated site (close to 100 years), the PAHs present may be no longer available for degradation, or have insufficient DBF to support RW1 population growth. Screening of compound availability and competition by the use of bioreporter strains, therefore, makes sense as a strategy to assess the possible outcome of bioaugmentation before starting in large-scale.

References

- Ahn Y-B, Liu F, Fennell DE and Häggblom MM** (2008) Biostimulation and bioaugmentation to enhance dechlorination of polychlorinated dibenzo-*p*-dioxins in contaminated sediments. *FEMS Microbiology Ecology* 66: 271-281.
- Armengaud J and Timmis KN** (1998) The reductase RedA2 of the multi-component dioxin dioxygenase system of *Sphingomonas sp.* RW1 is related to class-I cytochrome P450-type reductases. *European Journal of Biochemistry* 253: 437-444.
- Armengaud J, Gaillard J and Timmis KN** (2000) A second [2Fe-2S] ferredoxin from *Sphingomonas sp.* strain RW1 can function as an electron donor for the dioxin dioxygenase. *Journal of Bacteriology* 182: 2238-2244.
- Armengaud J, Happe B and Timmis KN** (1998) Genetic analysis of dioxin dioxygenase of *Sphingomonas sp.* strain RW1: catabolic genes dispersed on the genome. *Journal of Bacteriology* 180: 3954-3966.
- Armengaud J, Timmis KN and Wittich R-M** (1999) A functional 4-hydroxysalicylate/hydroxyquinol degradative pathway gene cluster is linked to the initial Dibenzo-*p*-dioxin pathway genes in *Sphingomonas sp.* strain RW1. *Journal of Bacteriology* 181: 3452-3461.
- Aso Y, Miyamoto Y, Mine Harada K, Momma, K, Kawai S, Hashimoto W, Mikami B, Murata K** (2006) Engineered membrane superchannel improves bioremediation potential of dioxin-degrading bacteria. *Nature Biotechnology* 24: 188-189.
- Axtell CA and Beattie GA** (2002) Construction and characterization of a proU-gfp transcriptional fusion that measures water availability in a microbial Habitat. *Applied and Environmental Microbiology* 68: 4604-4612.
- Bahl MI, Hansen LH, Licht TR and Sørensen SJ** (2004) In vivo detection and quantification of tetracycline by use of a whole-cell biosensor in the rat intestine. *Antimicrobial Agents and Chemotherapy* 48: 1112-1117.
- Basta T, Keck A, Klein J and Stolz A** (2004) detection and characterization of conjugative degradative plasmids in xenobiotic-degrading *Sphingomonas* Strains. *Journal of Bacteriology*. 186: 3862-3872.
- Bastiaens L, Springael D, Wattiau P, Harms H, deWachter R, Verachtert H and Diels L** (2000) Isolation of adherent Polycyclic Aromatic Hydrocarbon (PAH)-degrading bacteria using PAH-sorbing carriers. *Applied and Environmental Microbiology* 66: 1834-1843.
- Bosma TNP, Middeldorp PJM, Schraa G and Zehnder AJB** (1996) Mass transfer limitation of biotransformation: quantifying bioavailability. *Environmental Science and Technology* 31: 248-252.

- Bunz PV and Cook AM** (1993) Dibenzofuran 4,4a-dioxygenase from *Sphingomonas sp.* strain RW1: angular dioxygenation by a three-component enzyme system. *Journal of Bacteriology* 175: 6467-6475.
- Bünz PV, Falchetto R and Cook AM** (1993) Purification of two isofunctional hydrolases (EC 3.7.1.8) in the degradative pathway for dibenzofuran in *Sphingomonas sp.* strain RW1. *Biodegradation* 4: 171-178.
- Chen J, Wong MH, Wong YS and Tam NFY** (2008) Multi-factors on biodegradation kinetics of polycyclic aromatic hydrocarbons (PAHs) by *Sphingomonas sp.* a bacterial strain isolated from mangrove sediment. *Marine Pollution Bulletin* 57: 695-702.
- Coppotelli B, Ibarrolaza A, Del Panno M and Morelli I** (2008) Effects of the inoculant strain *Sphingomonas paucimobilis* 20006FA on soil bacterial community and biodegradation in phenanthrene-contaminated soil. *Microbial Ecology* 55: 173-183.
- Coppotelli B, Ibarrolaza A, Dias R, Panno M, Berthe-Corti L and Morelli I** (2010) Study of the degradation activity and the strategies to promote the bioavailability of phenanthrene by *Sphingomonas paucimobilis* strain 20006FA. *Microbial Ecology* 59: 266-276.
- Coronado E, Roggo C, Johnson DR and van der Meer JR** (2012) Genome-wide analysis of salicylate and dibenzofuran metabolism in *Sphingomonas wittichii* RW1. *Frontiers in Microbiology* 3.
- Das P, Mukherjee S and Sen R** (2008) Improved bioavailability and biodegradation of a model polyaromatic hydrocarbon by a biosurfactant producing bacterium of marine origin. *Chemosphere* 72: 1229-1234.
- de las Heras A and de Lorenzo V** (2011) In situ detection of aromatic compounds with biosensor *Pseudomonas putida* cells preserved and delivered to soil in water-soluble gelatin capsules. *Analytical and Bioanalytical Chemistry* 400: 1093-1104.
- de Lorenzo V and Timmis KN** (1994) Analysis and construction of stable phenotypes in gram-negative bacteria with Tn5- and Tn10-derived minitransposons. *Methods in Enzymology*, 235: 386-405.
- Gerhardt, P, Murray, RGE, Costilow, RN, Nester, EW, Wood, WA, Krieg, NR, and Briggs Philipps, G.** (1981) *Manual of methods for general bacteriology*. Washington, DC, USA: American Society for Microbiology.
- Halden RU, Halden BG and Dwyer DF** (1999) Removal of Dibenzofuran, Dibenzo-*p*-dioxin, and 2-Chlorodibenzo-*p*-dioxin from soils inoculated with *Sphingomonas sp.* strain RW1. *Applied and Environmental Microbiology* 65: 2246-2249.
- Halverson LJ and Firestone MK** (2000) Differential effects of permeating and nonpermeating solutes on the fatty acid composition of *Pseudomonas putida*. *Applied and Environmental Microbiology* 66: 2414-2421.

- Hanahan D** (1985) Techniques for transformation of *E. coli*. DNA cloning: A practical approach, (DM G, ed.) 109–135. IRL Press, Washington, DC.
- Harms H and Bosma TNP** (1997) Mass transfer limitation of microbial growth and pollutant degradation. *Journal of Industrial Microbiology and Biotechnology* 18: 97-105.
- Heeb S, Itoh Y, Nishijyo T, Schnider Ur, Keel C, Wade J, Walsh U, O'Gara F and Haas D** (2000) Small, stable shuttle vectors based on the minimal pVS1 replicon for use in gram-negative, plant-associated bacteria. *Molecular Plant-Microbe Interactions* 13: 232-237.
- Herron PM, Gage DJ and Cardon ZG** (2010) Micro-scale water potential gradients visualized in soil around plant root tips using microbiosensors. *Plant, Cell and Environment* 33: 199-210.
- Jaspers M, Meier C, Zehnder A, Harms H and van der Meer JR** (2001) Measuring mass transfer processes of octane with the help of an alkSalkB::gfp tagged *Escherichia coli*. *Environmental Microbiology* 3: 512-524.
- Johnsen AR and Karlson U** (2004) Evaluation of bacterial strategies to promote the bioavailability of polycyclic aromatic hydrocarbons. *Applied Microbiology and Biotechnology* 63: 452-459.
- Johnson D, Coronado E, Moreno-Forero S, Heipieper H and van der Meer J** (2011) Transcriptome and membrane fatty acid analyses reveal different strategies for responding to permeating and non-permeating solutes in the bacterium *Sphingomonas wittichii*. *BMC Microbiology* 11: 250.
- Kristensen CS, Eberl L, Sanchez-Romero JM, Givskov M, Molin S and De Lorenzo V** (1995) Site-specific deletions of chromosomally located DNA segments with the multimer resolution system of broad-host-range plasmid RP4. *Journal of Bacteriology* 177: 52-58.
- Kumari R, Tecon R, Beggah S, Rutler R, Arey JS and van der Meer JR** (2011) Development of bioreporter assays for the detection of bioavailability of long-chain alkanes based on the marine bacterium *Alcanivorax borkumensis* strain SK2. *Environmental Microbiology* 13: 2808-2819.
- Kumar M, Wu P-C, Tsai J-C and Lin J-G** (2009) Biodegradation of soil-applied polycyclic aromatic hydrocarbons by sulfate-reducing bacterial consortium. *Journal of Environmental Science and Health, Part A* 44: 12 - 20.
- Lambertsen L, Sternberg C and Molin S** (2004) Mini-Tn7 transposons for site-specific tagging of bacteria with fluorescent proteins. *Environmental Microbiology* 6: 726-732.
- Leveau JHJ and Lindow SE** (2001) Appetite of an epiphyte: Quantitative monitoring of bacterial sugar consumption in the phyllosphere. *Proceedings of the National Academy of Sciences* 98: 3446-3453.

- Leveau JHJ and Lindow SE** (2002) Bioreporters in microbial ecology. *Current Opinion in Microbiology* 5: 259-265.
- Masai E, Shinohara S, Hara H, Nishikawa S, Katayama Y and Fukuda M** (1999) Genetic and biochemical characterization of a 2-pyrone-4,6-dicarboxylic acid hydrolase involved in the protocatechuate 4,5-cleavage pathway of *Sphingomonas paucimobilis* SYK-6. *Journal of Bacteriology* 181: 55-62.
- McGenity TJ, Folwell BD, McKew BA and Sanni GO** (2012) Marine crude-oil biodegradation: a central role for interspecies interactions. *Aquatic Biosystems* 8: 10-29.
- McKown RL, Orle KA, Chen T and Craig NL** (1988) Sequence requirements of *Escherichia coli* attTn7, a specific site of transposon Tn7 insertion. *Journal of Bacteriology* 170: 352-358.
- Megharaj M, Wittich RM, Blasco R, Pieper DH and Timmis KN** (1997) Superior survival and degradation of dibenzo-*p*-dioxin and dibenzofuran in soil by soil-adapted *Sphingomonas sp.* strain RW1. *Applied Microbiology and Biotechnology* 48: 109-114.
- Miller WG, Leveau JHJ and Lindow SE** (2000) Improved gfp and inaZ broad-host-range promoter-probe vectors. *Molecular Plant-Microbe Interactions* 13: 1243-1250.
- Møller S, Sternberg C, Andersen JB, Christensen BB, Ramos JL, Givskov M and Molin S** (1998) In situ gene expression in mixed-culture biofilms: evidence of metabolic interactions between community members. *Applied and Environmental Microbiology* 64: 721-732.
- Pelz O, Tesar M, Wittich R-M, Moore ERB, Timmis KN and Abraham W-R** (1999) Towards elucidation of microbial community metabolic pathways: unravelling the network of carbon sharing in a pollutant-degrading bacterial consortium by immunocapture and isotopic ratio mass spectrometry. *Environmental Microbiology* 1: 167-174.
- Reasoner DJ and Geldreich EE** (1985) A new medium for the enumeration and subculture of bacteria from potable water. *Applied and Environmental Microbiology* 49: 1-7.
- Rehmann L, Prpich GP and Daugulis AJ** (2008) Remediation of PAH contaminated soils: Application of a solid-liquid two-phase partitioning bioreactor. *Chemosphere* 73: 798-804.
- Rochat L, Péchy-Tarr M, Baehler E, Maurhofer M and Keel C** (2010) Combination of fluorescent reporters for simultaneous monitoring of root colonization and antifungal gene expression by a biocontrol *Pseudomonad* on cereals with Flow Cytometry. *Molecular Plant-Microbe Interactions* 23: 949-961.

Safe S (1990) Polychlorinated Biphenyls (PCBs), Dibenzo-*p*-dioxins (PCDDs), dibenzofurans (PCDFs), and related compounds: environmental and mechanistic considerations which support the development of toxic equivalency factors (TEFs). *Critical Reviews in Toxicology* 21: 51-88.

Seo J-S, Keum Y-S and Li Q (2009) Bacterial degradation of aromatic compounds. *International Journal of Environmental Research and Public Health* 6: 278-309.

Shi T, Fredrickson JK and Balkwill DL (2001) Biodegradation of polycyclic aromatic hydrocarbons by *Sphingomonas* strains isolated from the terrestrial subsurface. *Journal of Industrial Microbiology and Biotechnology* 26: 283-289.

Sticher P, Jaspers MC, Stemmler K, Harms H, Zehnder AJ and van der Meer JR (1997) Development and characterization of a whole-cell bioluminescent sensor for bioavailable middle-chain alkanes in contaminated groundwater samples. *Applied and Environmental Microbiology* 63: 4053-4060.

Stiner L and Halverson LJ (2002) Development and characterization of a green fluorescent protein-based bacterial biosensor for bioavailable toluene and related compounds. *Applied and Environmental Microbiology* 68: 1962-1971.

Tecon R and Van der Meer JR (2008) Bacterial biosensors for measuring availability of environmental pollutants. *Sensors* 8: 4062-4080.

Tecon R, Beggah S, Czechowska K, Sentchilo V, Chronopoulou P-M, McGenity TJ and van der Meer JR (2010) Development of a multistrain bacterial bioreporter platform for the monitoring of hydrocarbon contaminants in marine environments. *Environmental Science and Technology* 44: 1049-1055.

Tecon R, Binggeli O and van der Meer JR (2009) Double-tagged fluorescent bacterial bioreporter for the study of polycyclic aromatic hydrocarbon diffusion and bioavailability. *Environmental Microbiology* 11: 2271-2283.

Tecon R, Wells M and Van Der Meer JR (2006) A new green fluorescent protein-based bacterial biosensor for analysing phenanthrene fluxes. *Environmental Microbiology* 8: 697-708.

van Gestel CAM, McGrath SP, Smolders E, Ortiz MD, Borgman E, Verweij RA, Buekers J and Oorts K (2012) Effect of long-term equilibration on the toxicity of molybdenum to soil organisms. *Environmental Pollution* 162: 1-7.

Wammer KH and Peters CA (2005) Polycyclic Aromatic Hydrocarbon biodegradation rates: a structure-based study. *Environmental Science and Technology* 39: 2571-2578.

Werlen C, Jaspers MCM and van der Meer JR (2004) Measurement of biologically available naphthalene in gas and aqueous phases by use of a *Pseudomonas putida* biosensor. *Applied and Environmental Microbiology* 70: 43-51.

Wintermute EH and Silver PA (2010) Emergent cooperation in microbial metabolism. *Molecular Systems Biology* 6:407.

Wittich RM, Wilkes H, Sinnwell V, Francke W and Fortnagel P (1992) Metabolism of dibenzo-*p*-dioxin by *Sphingomonas sp.* strain RW1. *Applied and Environmental Microbiology* 58: 1005-1010.

Zhou HW, Luan TG, Zou F and Tam NFY (2008) Different bacterial groups for biodegradation of three- and four-ring PAHs isolated from a Hong Kong mangrove sediment. *Journal of Hazardous Materials* 152: 1179-1185.

Supplementary information

Figure S1. Change in codon sequence of *egfp* to obtain *egfp_{RW1}*, which favors the codon usage of *S. wittichii*

RW1.

Original sequence of *egfp* in pPROBE'

atg agt aaa gga gaa gaa ctt ttc act gga gtt gtc cca att ctt gtt gaa tta gat ggt gat gtt aat ggg cac
aaa ttt tct gtc agt gga gag ggt gaa ggt gat gca aca tac gga aaa ctt acc ctt aaa ttt att tgc act act
gga aaa cta cct gtt cca tgg cca aca ctt gtc act act ttg act tat ggt gtt caa tgc ttt tca aga tac cca gat
cat atg aaa cgg cat gac ttt ttc aag agt gcc atg ccc gaa ggt tat gta cag gaa aga act ata ttt ttc aaa
gat gac ggg aac tac aag aca cgt gct gaa gtc aag ttt gaa ggt gat acc ctt gtt aat aga atc gag tta aaa
ggt att gat ttt aaa gaa gat gga aac att ctt gga cac aaa ttg gaa tac aac tat aac tca cac aat gta tac
atc atg gca gac aaa caa aag aat gga atc aaa gtt aac ttc aaa att aga cac aac att gaa gat gga agc
ggt caa cta gca gac cat tat caa caa aat act cca att ggc gat ggc cct gtc ctt tta cca gac aac cat tac
ctg tcc aca caa tct gcc ctt tgg aaa gat ccc aac gaa aag aga gac cac atg gtc ctt ctt gag ttt gta aca
gct gct ggg att aca cat ggc atg gat gaa cta tac aaa taa

Sequence of *egfp_{RW1}*

atg agc aag ggg gaa gag ctg ttc act ggc gtt gtc cca atc ctt gtt gag tta gac ggc gac gtt aat ggc cat
aag ttc tgg gtc agt ggg gag ggc gaa ggc gac gcc acc tac ggc aag ctg acc ctg aag ttc atc tgc acc
act ggc aag cta cct gtt cgg tgg cgg aca ctc gtc acc acc ttg acc tat ggc gtt caa tgc ttc tca cgc tat
cca gat cac atg aag cgc cat gac ttc ttc aag agt gcg atg cgg gag ggg tat gta cag gag aga acc ata
ttc ttc aag gac gac ggg aac tat aag acc cgt gcg gag gtc aag ttc gag ggc gac acc ctt gtt aat cgc
atc gag tta aag ggc atc gac ttc aag gaa gac ggc aac atc ctt ggg cat aag ctg gag tat aac tat aac
tca cat aat gtc tat atc atg gcg gac aag cag aag aac ggc atc aag gtt aac ttc aag atc aga cat aac atc
gag gac ggc agc gtt caa ctg gcg gac cat tat cag cag aac acc cca atc ggc gac ggc cct gtc ctt tta
cca gac aac cat tat ctg tcc aca cag tct gcc ctg tgg aag gac cgg aac gag aag aga gac cac atg gtc
ctg ctg gag ttc gtc aca gcg gcg ggg atc aca cat ggc atg gac gag cta tac aag taa

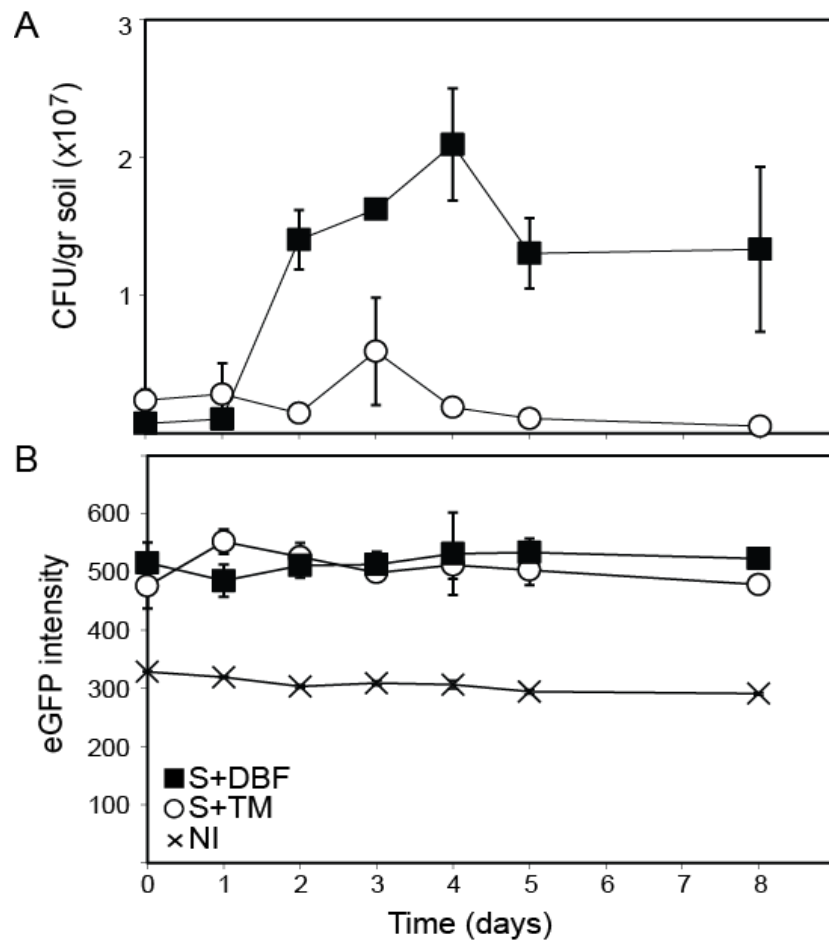


Figure S2. Population development and reporter gene expression of RW1 ($pME6012-P_{P_{dvnA1}}-egfp$) inoculated in the microcosms. (A) Number of Tc^R -CFU/g soil over time. (B) Average eGFP level. Different microcosms, S+DBF (■), S+TM (○) and non-inoculated microcosms, NI (×).

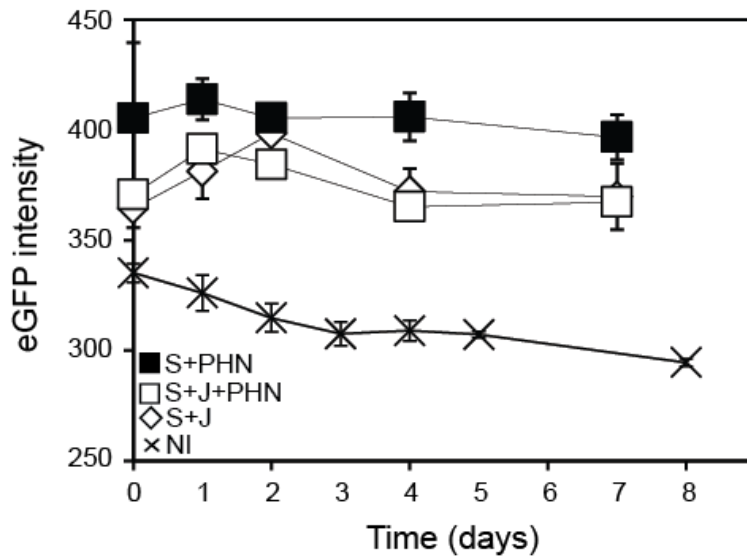


Figure S3. Reporter gene expression of *B. sartisoli* RP0037-*mche* (pPROBE- P_{phnS} -*egfp*) inoculated in the microcosms. (A) Number of Tc^R -CFU/g soil over time and (B) average eGFP level. Different microcosms, S+PHN (■), S+J+PHN (□), S+J (◇) and non-inoculated microcosms, NI (×).

CHAPTER 5

Identification of water stress promoters in *Sphingomonas*

wittichii RW1

Edith Coronado, Clémence Roggo, Marc Jordi.

Abstract

The term water stress refers to the low availability of water for microorganisms to grow and perform basic metabolic functions. Water availability has been proposed as a major constraint for the use of microorganisms in contaminated sites with the purpose of bioremediation. *Sphingomonas wittichii* RW1 is a bacterium capable of degrading the xenobiotic compounds dibenzofuran and dibenzo-*p*-dioxin, and has potential to be used as a microorganism for targeted bioremediation. The aim of the current work was to understand the influence of water stress on the catabolic activity of RW1. We explored, by means of transposon mutagenesis, the genes involved in the cell's resistance to water stress. Conditions of low water potential were mimicked by adding NaCl or PEG8000 to the growth media. When using selection for solute stress (NaCl addition), we recovered transposon mutants unable to grow with insertions in genes involved in proline and glutamate biosynthesis, and further in a gene putatively involved in aromatic compound catabolism. Transposon mutants growing poorer on medium with lowered water potential also included ones that had insertions in genes involved in more general functions such as transcriptional regulator, elongation factor, cell division protein, RNA polymerase β or an aconitase were also isolated.

The three transposon mutant screening methods used here allowed the isolation of different transposon mutants, with the screening based on differential production of eGFP in salt conditions being the more efficient.

Clémence Roggo contributed to the transposon mutant encapsulation, selection in agarose beads and sequencing. Marc Jordi contributed to the transposon mutant selection by replica plating and subsequent sequencing of selected clones.

Introduction

Several studies describe the selection and use of specific microbial strains for bioremediation purposes (Vogel, 1996; Shi *et al.*, 2001; Ahn *et al.*, 2008; Chen *et al.*, 2008; Das *et al.*, 2008; Rehmann *et al.*, 2008; Kumar *et al.*, 2009). However, for a success of bioaugmentation it is not only the strain itself that counts, and various factors in the environment in which the microbes are introduced can have profound impact on their biodegradation activities and therefore in their bioremediation efficiency (Leahy and Colwell, 1990; Holden *et al.*, 1997). One of the main important factors is thought to be the availability of water (water *activity* or water *potential*) (Holden *et al.*, 1997).

The water activity depends on the concentration of solutes in a given solution; the higher the solute concentration the lower the water activity. A decrease in water activity is equivalent to a lowered water potential and this translates in an increase of the osmotic pressure (Potts, 1994). The osmotic potential is numerically equal to osmotic pressure but has a negative sign (the units used here are MPa) and is the pressure necessary to prevent a flow of solvent through a membrane (Brown, 1976). The osmotic potential has two components, the solute potential (SP) and matric potential (MP) with the SP increasing linearly with increasing concentration of solutes and the MP describing the interaction of water with surfaces and interfaces (colloidal particles and solid particles from 0.002 to 1 μm diameter) (Potts, 1994). Water stress is then a consequence of the lowering of water potential, with less water available to enter the cell or available to maintain regular biochemical processes in the cell (Brown, 1976). Cells under osmotic (solute) stress will face diminished water activity as a consequence of high concentrations of solutes outside the cell and will experience a net flux of water towards the extracellular environment. Matric stress is a consequence of the net flux

of water from the inside to the outside as a result of capillary forces of non-permeating solutes (Potts, 1994).

Microorganisms are known to be able to defend themselves against changes in water potential, by changing their membrane fatty acid composition, synthesizing compatible intracellular solutes like trehalose or sucrose, producing exopolysaccharides or overproducing transmembrane transporters (Boch *et al.*, 1994; Lucht and Bremer, 1994; Ogahara *et al.*, 1995; Halverson and Firestone, 2000; Hallsworth *et al.*, 2003; Mutnuri *et al.*, 2005; Singh *et al.*, 2005; Reva *et al.*, 2006; LeBlanc *et al.*, 2008; Brill *et al.*, 2011; Gülez *et al.*, 2011; Johnson *et al.*, 2011). It is also known that solute and matric stress result in different effects on cells (Halverson and Firestone, 2000; Axtell and Beattie, 2002; Hallsworth *et al.*, 2003; Reva *et al.*, 2006; Cytryn *et al.*, 2007; Johnson *et al.*, 2011). For example, Johnson *et al.* (2011) observed an increased expression of a gene for an extracellular sigma24 factor when exposing *S. wittichii* RW1 to solute stress but not to matric stress. In contrast, several genes involved in protein turnover and repair were differentially expressed as a response to matric but not to solute stress. Commonly differentially expressed genes in both solute and matric stress compared to no stress conditions included genes involved in trehalose, exopolysaccharide or flagella biosynthesis.

Genome-wide transcription analysis of RW1 exposed or not to solute or matric stress has helped to identify the genes differentially responding to such conditions (Johnson *et al.*, 2011). To try and find out whether such differentially expressed genes are important or essential for the cell to resist water stress, we used transposon mutagenesis followed by mutant screening for growth. In the present work, two mini-Tn5 mutant libraries were created, one using the pRL27 system (Larsen *et al.*, 2002), and the second one with a

modified version, pRL27::miniTn5-*egfp*, coding for a promoterless *egfp* gene. The resulting libraries were screened for the absence of growth on NaCl-amended agar plates, for smaller microcolonies inside agarose beads upon exposure to NaCl-amended medium (pRL27), or by higher production of eGFP (miniTn5-*egfp*) following NaCl exposure using flow cytometry. The insertion sites of the transposon mutants were then recovered and determined by DNA sequencing, and compared to the RW1 genome.

Materials and methods

1. Bacteria cultivation

A stock of *Sphingomonas wittichii* RW1 was kept at -80°C and a small aliquot was plated on agar with 5 mM salicylate (SAL). Minimal media was based on DSM457 amended with 5 mM salicylate (MM+SAL). Agar plates consisted on MM+SAL supplemented with 1.5% of bacteriological agar No.1 (Oxoid). All RW1 cultures were incubated at 30°C. For selection and maintenance of the transposon insertions, kanamycin (Km, at 50 µg per ml) was added to MM+SAL. *Escherichia coli* strains were grown in Lysogeny Broth (LB) adding Km to maintain the selective pressure for the plasposon vectors. *E. coli* was incubated at 37°C according to standard procedures. Table 1 shows a list of strains, plasmids and primers used here.

Table 1. Strains, plasmids and primers used.

	Description	Reference	
Strains			
<i>Sphingomonas wittichii</i> RW1	Dibenzofuran degrader	Wittich <i>et al.</i> , 1992	
<i>E. coli</i> BW20767	For conjugative transfer of oriR6K oriTRP4 plasmids. Has <i>pir</i> / inserted into the chromosome. Donor of pRL27 plasposon.	Metcalf <i>et al.</i> , 1996; Larsen <i>et al.</i> , 2002.	
<i>E. coli</i> CC118 λ <i>pir</i>	For replication of <i>pir</i> -dependent plasmids	Herrero <i>et al.</i> , 1990	
<i>E. coli</i> S17-1 λ <i>pir</i>	For replication and mobilization of plasmids with oriR6K.	de Lorenzo <i>et al.</i> , 1990	
Plasmids			
pRL27	Codes for a hyperactive transposase and contains a miniTn5 - <i>ori</i> transposable element. Used for mutant library creation.	Larsen <i>et al.</i> , 2002	
pRL27-gfp	For transposon mutant library creation, codes for a promoterless <i>egfp</i> gene in a miniTn5 transposable element	This study	
pBAM1	All synthetic plasmid bearing R6K <i>oriV</i> , <i>oriT</i> sequence, coding for a hyperactive transposase and a miniTn5 transposable element. Used for mutant library creation.	Martínez-García <i>et al.</i> , 2011	
Primers			
tnpRL17-1	aacaagcaggatgtaacg	Sequencing of miniTn5 insertion sites (pRL27)	Larsen <i>et al.</i> , 2002
tnpRL13-2	cagcaacaccttctcacga	Sequencing of miniTn5 insertion sites (pRL27- <i>egfp</i>)	Larsen <i>et al.</i> , 2002
GFPout	tcaacaagaattgggacaactccag	Anealing in <i>egfp</i> 70 nucleotides towards start	van der Meer group
npt-fw	atcgtggctggccacgacggg	Forward primer for the amplification of the Km resistance gene	van der Meer group
npt-rev	ctgatagcggctccgccacacc	Reverse primer for the amplification of the Km resistance gene	van der Meer group

2. Reduced water potential conditions

Liquid and solid media with altered water activities (potentials) were prepared following the method described by Halverson and Firestone (2000). Briefly, increasing amounts of NaCl or PEG 8000 were added to liquid MM+ SAL to mimic a decrease in SP and MP, respectively (Table 2). A stationary phase culture ($OD_{600} \sim 1.0$) of *S. wittichii* RW1 was used to inoculate 50 ml flasks containing 15 ml of MM+SAL (control) and flasks containing NaCl-amended or PEG-amended MM+SAL. Amendments corresponded to a

decrease in water potential of -0.5, -1.0, -1.5, -2.0 and -2.5 MPa with respect to the control (the control media has a water potential of around -0.23 MPa). Three replica flasks were prepared for each condition. Cultures were inoculated to an initial optical density of $OD_{600}=0.005$, and incubated on a rotary shaker at 30°C until stationary phase was reached. OD_{600} was measured regularly (Ultrospec, GE) and the maximum specific growth rate (μ_{max} , h^{-1}) as a function of water potential was calculated by linear regression on ln-transformed OD-values versus time.

Table 2. Reduction in water potential by NaCl (SP) and PEG8000 (MP) addition.

Water potential reduction (MPa)	NaCl (g/L)	mM	PEG 8000 (g/L)	mM
- 0.5	2.9	50	27.6	3.2
-1.0	5.8	100	40.6	5
-1.5	11.6	200	59.6	7.5
-2.0	17.4	300	73.6	9.2
-2.5	28.9	510	95.4	12

3. Transposon mutant libraries

Two different transposon mutant libraries of *S. wittichii* RW1 were created in order to identify genes important for solute stress survival. The first involved the plasmid pRL27::miniTn5 (Larsen *et al.*, 2002) and the second a modified version, the plasmid pRL27::miniTn5-*egfp*.

To produce the first library, *S. wittichii* RW1 and *E. coli* BW20767 (pRL27::miniTn5) overnight cultures were mixed in a 2/1 ratio (2 ml/1 ml) and centrifuged for 2 min at 8,000 rpm. The supernatant was discarded and the cell pellet resuspended in 50 μ l of saline solution (NaCl 0.9%). The 50 μ l droplet was placed on the surface of an LB plate and incubated at 30°C overnight. After incubation, the cell layer was recovered with a sterile loop,

resuspended in 1 ml saline solution and 150 µl aliquots were plated on selective media (MM+SAL+Km). The plates were incubated at 30°C during several days and when colonies were visible they were picked individually for replicate screening.

Plasmid pRL27::miniTn5-*egfp* was constructed by ligating an Asp718-digested and 5' end Klenow filled pRL27-DNA to the SmaI-EcoRV *egfp* fragment of pPROBE (Miller *et al.*, 2000). The ligation mixture was used to transform *E. coli* BW20767 (Metcalf *et al.*, 1996). A colony of *E. coli* carrying pRL27::miniTn5-*egfp* was selected and used to perform a conjugation with *S. wittichii* RW1. Overnight cultures of RW1 and *E. coli* BW20767 (pRL27::miniTn5-*egfp*) were mixed in a 2/1 ratio (2 ml/1 ml) as described above. Colonies growing on MM+SAL+Km plates were washed off with saline solution and kept as mutant library mix. The library was divided in 1 ml aliquots which were stored at -80°C.

4. Transposon library screening

The *S. wittichii* RW1 pRL27-miniTn5-generated library (library 1) was screened for growth impairment by replica plating on medium with NaCl (-1.5 MPa decrease). Individual colonies were picked from MM+SAL+Km plates and replica plated in parallel on control plates (MM+SAL+Km) and NaCl-amended MM+SAL+Km agar plates, which contained a NaCl concentration of 11.6 g/L, equivalent to a SP of -1.5 MPa. Colonies that failed to grow on MM+SAL+Km-NaCl but grew on control plates were selected for further characterization.

The pRL27-miniTn5 library 1 was also used for growth deficient clones in a flow cytometric (FC) procedure in which individual cells were encapsulated in agarose beads. (FC). Encapsulated cell mixtures were prepared as follows: a single frozen Tn5 mutant

library aliquot was grown until stationary phase in MM+SAL and subsequently diluted to an OD₆₀₀ of 0.1, which allowed the encapsulation of approximately one single cell per bead. Empty beads and beads carrying a high number of cells (initial cell culture OD ~1.4) were prepared as FC controls. All the material to be used (tubes, tips, pluronic acid) was preheated at 42°C and the procedure was carried out at 37°C. Fresh 2.5% agarose solution was prepared in deionized water and stored at 55°C, and transferred at 42°C only 20 min before starting the protocol. One ml of preheated 2.5% agarose solution was mixed with 30 µl of pluronic acid (Pluronic F-68 solution 10%, Sigma-Aldrich) by vortexing for one minute. After that 200 µl of cell suspension were added to the agarose solution and vortexed during one additional minute. A total of 500 µl of this agarose-cell mixture were transferred drop by drop into 15 ml of silicone oil (dimethylpolysiloxane, Sigma-Aldrich) preheated at 37°C while vortexing simultaneously (2 min). The tube was immediately plunged into crushed ice and left for 10 min, after which it was centrifuged for 10 min at 2'000 rpm. The oil was decanted, the beads were resuspended with 15 ml of PBS solution (phosphate buffered saline) and the residual oil was removed. The bead suspension was passed through a sieve of 70 µm pore size and both filtrate (<70 µm fraction) and beads remaining on the sieve (>70 µm fraction) were retained. The filtrate was then passed through a 40 µm-pore sieve, resulting in a 70-40 µm (filter cake fraction) and <40 µm fraction (filtrate from second sieving). After preliminary tests on FC, the beads with a size lower than 40 µm were kept for further microcolony growth screening.

Agarose beads containing (miniTn5 mutant library) cells were analyzed by flow cytometry (FACSAria, BD Biosciences) and using the BD FACSDiva software (version 6.1.3). An aliquot containing the cells-beads solution was stained by adding 1/1000 volume of SYTO®9 solution (Invitrogen) and incubated in the dark for 15 min. Stained cell-bead mix

was aspirated at approximately 50-100 $\mu\text{l}/\text{min}$ and FSC, SSC and Green Fluorescence (FITC-channel) were recorded.

Gates were set using the free RW1 cell suspension (Figure 4A), a suspension of empty beads (Figure 4B), or beads prepared with RW1 cultures with an OD_{600} of 1.4 (Figure 4C) and 0.07 (Figure 4D). Gate P4 corresponds then to the beads carrying a high cell number of cells while P5 includes beads with a low cell density. The presence of cells in beads from gates P4 and P5 was confirmed by sorting and subsequent epifluorescence/phase-contrast microscopy. After setting an accurate drop delay value (Accudrop protocol, BD FACSAria), P5 beads were sorted and recovered in a tube (Settings: Voltage FSC 25, SSC 383, FITC 429 / Threshold FSC 1000). Approximately 900'000 events were recovered in 1.4 ml of media. The P5 subpopulation was then divided in three fractions, adding to one of them MM+Km (no carbon), to the second MM+Km+SAL (0.5 mM) and to the last one MM+Km+SAL+NaCl (-1.5 MPa). The salicylate concentration (0.5 mM) was lower in this experiment to avoid microcolonies developing too large and exploding the beads. Bead suspensions were incubated at 30°C and 100 rpm for 3 days. A bead sample was analysed for microcolony growth every day by staining, FC and epifluorescence microscopy. Gates were adjusted with FITC versus SSC signals: Gate P1 corresponding to beads containing developed microcolonies (high fluorescence) and gate P2 corresponding to beads containing non-developed microcolonies (low fluorescence). Beads, which after 3 days of incubation entered in the P2-gate, were again sorted out individually and placed as microdroplets directly on MM+SAL+Km agar plates. Plates were incubated at 30°C until regular RW1 colonies were visible (~7 days). Transposon mutant colonies were then rescreened in liquid cultures to determine growth rates and biomass yields in presence or absence of NaCl at -1.5 MPa.

The RW1 miniTn5-*egfp* library (library 2) was screened for cells producing a higher eGFP signal under growth conditions with decreased SP compared to the signal in control media. The assumption here was that an increased eGFP production under lower water potential would indicate that the insertion of the transposable element is within or close to a gene higher expressed under solute stress, and thus perhaps implicated in resisting this stress. A 1 ml aliquot of the library mix was taken out of the -80° storage, slowly thawed, diluted in 50 ml of fresh media (MM+SAL+Km) and incubated overnight at 30°C on a rotary shaker at 180 rpm. Single cell eGFP intensities in the library mutant cultures were determined by flow cytometry (FACS Aria, BD Biosciences). Pure cultures of RW1 and *E. coli* BW20767 were employed to define the fluorescence level of cells not expressing eGFP (Figure 7A and 7B, P1 gate). An RW1 transposon mutant recovered from plate showing a constitutive eGFP was selected to define the high fluorescence gate (Figure 7C, P2 gate).

To screen the mutant library we first wished to discard the P2 subpopulation of cells expressing high eGFP fluorescence since it would contain constitutively eGFP-producing clones. Thus the P1 subpopulation was recovered by cell sorting (Settings: Voltage FSC 200, SSC 300, FITC 300 / Threshold FSC 1000), transferred to an Erlenmeyer flask containing 20 ml of MM+SAL+Km and again incubated overnight with rotary shaking. This depleted mutant culture was then divided in two fractions. To one of them 1 ml of a NaCl solution (116 g/L) was added to achieve a decrease in water potential of -1.5 MPa, whereas to the other we added 1 ml of sterile water (control). The cultures were incubated in a rotary shaker and after 2 and 6 hours of incubation, a 5 ml aliquot was taken from each flask to measure the fluorescence level of individual cells by FC. In this case, we focused on the cells having high eGFP fluorescence (P2 gate), assuming they might contain mutants with insertions near NaCl-inducible promoters. Cells in the P2-gate were sorted, transferred to new Erlenmeyer

flasks containing 20 ml of MM+SAL+Km and grown until an OD₆₀₀ of around 0.6. NaCl exposure was repeated once more and the cells falling into the P2 gate from the NaCl exposed cultures (both after 2 and 6 h) were again sorted. The recovered P2 cells were now directly plated on MM+SAL+Km agar plates and incubated at 30°C until colonies developed. Individual colonies were picked up and transferred to 96-well microtiter plates containing 200 µl of MM+SAL+Km per well. In total 768 individual colonies in 8 microtiter plates were picked and kept as master plates. The master plates were used to inoculate two series of new microtiter plates, 8 plates containing control media (MM+SAL+Km) and 8 plates with NaCl-amended media (MM+SAL+Km+NaCl -1.5 MPa). The eGFP intensity and OD₆₀₀ of NaCl-exposed plates were measured after 2, 4, 8 and 20 h using a FLUOstar Omega plate reader (BMG Labtech), and compared to those in the control plates (without NaCl addition). eGFP intensities were then normalized by the culture density.

The growth rates of the different transposon mutant selected on NaCl-exposed conditions were calculated in MM+SAL+KM+NaCl media and compared to the growth in MM+SAL+Km control media. The growth rate was determined as a linear regression of the ln-transformed OD-values as a function of time.

5. Identification of miniTn5 insertion sites

Total DNA of RW1 transposon mutants was extracted with the Xanthogenate method by Tillett and Neilan (2000). Briefly, overnight cell cultures were pelleted, resuspended in Xanthogenate lysis buffer (0.5 g Potassium Ethyl Xanthogenate, 10 ml 4M Ammonium Acetate, 5 ml 1M Tris-HCl pH 7.4, 2 ml 0.45M EDTA, 2.5 ml 20% SDS in 50 ml of H₂O) and incubated at 65°C during 2 h. Cell debris was removed by centrifugation and the supernatant was transferred to a new tube into which one volume of

phenol:chloroform:isoamyl alcohol (25:24:1) was added and mixed until emulsion formed. After centrifugation, the DNA in the aqueous phase was recovered, precipitated with isopropanol, then washed once with 70% ethanol, dried and finally resuspended in 200 μ l of H₂O. DNA was digested overnight in 20 μ l with SacII (which does not cut inside the transposon), diluted to 100 μ l, and treated with T4 DNA ligase to produce self-circularized fragments. This ligation mixture was transformed into *E. coli* DH5 α pir and plated on agar medium containing Km. Circularized fragments containing the transposon replicate as plasmids because of the existing origin of replication, and were purified from the *E. coli* transformants. Plasmid DNA was then used as template for BigDye® terminator sequencing according to the protocol of the supplier (Applied Biosystems), and using primers tnpRL17-1 for miniTn5 and tnpRL17-2 or GFPout for miniTn5-*egfp*.

6. Southern blot hybridization

The presence of unique transposon insertions in six randomly picked RW1 transposon mutants was analyzed by Southern blot hybridization. Total DNA of transposon mutants was extracted by the Xanthogenate method described above. 2 μ g of DNA were digested with SacII in a volume of 20 μ l. The digested DNA was loaded on a 200 ml agarose gel (1.5%) and run slowly overnight at 4°C. The DNA was depurinated by soaking the agarose gel in 0.25 M HCl during 15 min with agitation. The gel was then placed on a vacuum blotter and the DNA denatured by adding a solution of 0.5 M NaOH plus 1.5 M NaCl. Next the gel was neutralized with a solution of 1 M Tris-HCl plus 1.5 M NaCl at pH 7.6, and the DNA was transferred to an N-bond membrane (Whatman) on a vacuum blotter (Amersham) using 20 x SSC buffer (SSC is 3 M NaCl plus 0.3 M Sodium Citrate at pH 7.6). The DNA on the membrane was then again denatured by rinsing with the NaOH/NaCl solution, and

neutralized with the Tris-HCl/NaCl solution. DNA in the membrane was crosslinked in a UV Stratalinker (UVP) at 1800 J, and afterwards washed with 2x SSC buffer. The membrane was placed in a hybridization bottle and 15 ml of hybridization buffer (5x SSC buffer, 2x blocking reagent [Roche], 0.1% N-Lauroylsarcosine, and 0.02% SDS) were added. A DIG-labeled probe was prepared by PCR amplification of the Km resistance gene using the primers npt-fw and npt-rev (457 bp amplicon) on pRL27, with a mixture of deoxyribonucleotides containing DIG-11-dUTP (Roche). The DIG-probe was denatured for 10 min at 95°C and then chilled at 4°C. 10 µl of the DIG-probe were added to the hybridization buffer contained in the bottle and the membrane was incubated 16 h at 65°C in the hybridization oven. The membrane was next removed from the oven and washed twice with a solution of 2 x SSC/ 0.2% SDS, and, finally, with a solution of 0.1 x SSC/ 0.1% SDS. Detection of the DIG-marker was performed using anti-DIG antibody and CSPD chemiluminescent substrate according to the recommendations of the supplier (Roche). The membrane was then exposed to an X-ray film in a cassette at 37°C during 15 min and the film was developed in an X-ray film processor (Curix60, AGFA).

Results

Effect of decrease in solute and matric potential on growth rate of *S. wittichii* RW1

The effect of decreasing water potential on the growth rate of *S. wittichii* RW1 in control media (with a water potential of -0.23 MPa) was tested by addition of increasing amounts of NaCl or PEG8000. Growth rates of RW1 diminished in a similar manner with decreasing water potential below -0.5 MPa upon NaCl or PEG addition (Figure 1A and 1B, respectively). At a water potential of -1.5 MPa the growth rate of the strain RW1 decreased to 40% and 60% (for SP and MP respectively) of the control. When the water potential decreased to -2.5 MPa below the control medium, the growth rate decreased by 80% (SP) and 70% (MP). Interestingly, a small consistent increase in growth rate was observed at salt concentrations invoking a water potential decrease of -0.25 and -0.5 MPa, suggesting the cells need slightly more salt than provided in the basal growth medium. A water potential of -1.5 MPa was selected as the condition for mutant library screening, since it clearly decreased growth rates of RW1, but did not arrest growth completely.

MiniTn5 transposon mutant screening

A library of around 13,000 RW1 transconjugants was obtained in the conjugation procedure between *S. wittichii* RW1 and *E. coli* BW20767 (pRL27::miniTn5) as donor. Six clones were picked randomly, the total DNA was isolated, digested and hybridized against a probe targeting the Km resistance gene. Southern blot hybridization results showed that a single transposon insertion had occurred in every mutant, and at a different genomic position (Figure 2), suggesting that a true transposition event had taken place.

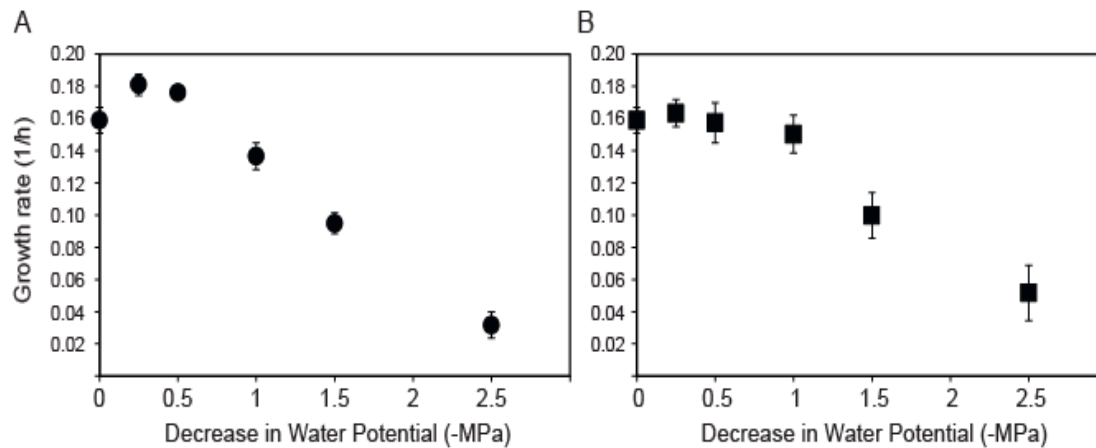


Figure 1. Growth rate of *S. wittichii* RW1 in MM+SAL as a function of water potential decrease by NaCl (A) or PEG (B). Redrawn from Johnson *et al.* (2011).

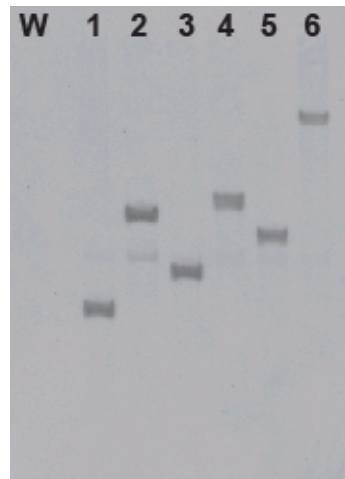


Figure 2. Southern blot showing the transposon insertions in *SacII*-digested DNA from six randomly chosen RW1 transposon mutants. The DIG-labeled probe used was a fragment from the Km resistance gene. W, wild type RW1; 1-6, RW1 transposon mutants.

To screen for mutants carrying a transposon insertion in essential genes for NaCl stress resistance, 600 colonies were replica streaked on control medium plates and plates supplemented with NaCl to a calculated (additional) water potential decrease of -1.5 MPa. Three clones were detected, which no longer grew on NaCl-amended plates. The transposon insertions were located in genes Swit_2730, Swit_2731 and Swit_3468. The gene Swit_2730

is annotated as a hypothetical protein, gene Swit_2731 codes for an aconitase-domain protein and gene Swit_3468 codes for an RNA polymerase β subunit. The growth rate of the mutants was determined by growth on MM+SAL+Km media and NaCl-supplemented media.

Unfortunately, only clone 355, carrying the insertion in gene Swit_3468 was able to regrow in liquid cultures. The growth rate of clone 355 (Table 3) was indeed lower than the growth rate of the WT strain, both in control media and NaCl-supplemented media.

A second library of approximately 22,000 transconjugants was obtained and some 2000 colonies were streaked in parallel in control agar and NaCl-amended plates. Eight colonies were found to be impaired in growth in the presence of NaCl and the insertion sites of the transposons were determined (Table 3). Two clones had an insertion in Swit_2710, coding for a pseudouridine synthase C (clones 1-G3 and 3-G2), one clone in Swit_2958, coding for a BadM/Rrf2 family transcriptional regulator (clone 6-D11), and one with an insertion in the intergenic region between Swit_3114 and Swit_3115, which code for a hypothetical protein and ribosomal protein L36, respectively (clone 6-E3). We found one insertion in Swit_3770, coding for an AMP-dependent synthetase / ligase (clone 6-G5), one insertion in Swit_4693, coding for a protein-disulfide isomerase-like protein (clone 7-D4), and finally, two clones with insertions in the intergenic region between Swit_5333 and Swit_5334 (clones 5 and 10-G5). These open reading frames code for a hypothetical protein and cell division FtsK/SpoIIIE, respectively.

The growth rates of the transposon mutants in NaCl-supplemented media compared to control media were generally lower (Table 3). However, when comparing their growth curves with that of the WT, we observed various differences. A group of four mutants (6-G5, 3-G2, 6-E3 and 1-G3) grew slower both in control and NaCl medium, reaching a low final OD₆₀₀

compared to WT grown in both media. These we considered as salt-sensitive mutants. Four other mutants (10-G5, 7-D4, 6-D11 and clone 5) showed a growth lag of 24 h in salt medium compared to WT and a random control Tn5-mutant. However, these mutants reached the same final OD₆₀₀ on salt medium as the WT, but only after a longer time period. These mutants were characterized as slower growers in presence of NaCl.

This same mutant library was also screened by agarose beads encapsulation and by FC analysis and sorting, following a procedure illustrated schematically in Figure 3. Agarose beads of a size lower than 40 µm and mostly containing single cells were prepared. Then the different samples were passed through the flow cytometer. The free cell suspension (Figure 4A), empty agarose beads (Figure 4B) and agarose beads prepared with high (Figure 4C) and low density cultures (Figure 4D) allowed the definition of gates corresponding to the beads containing a high number of cells (P4) and beads with only one or two cells per bead (P5). Microscope images taken immediately after sorting out the different populations confirmed that the settings in gating were correct (Figures 4E to 4H).

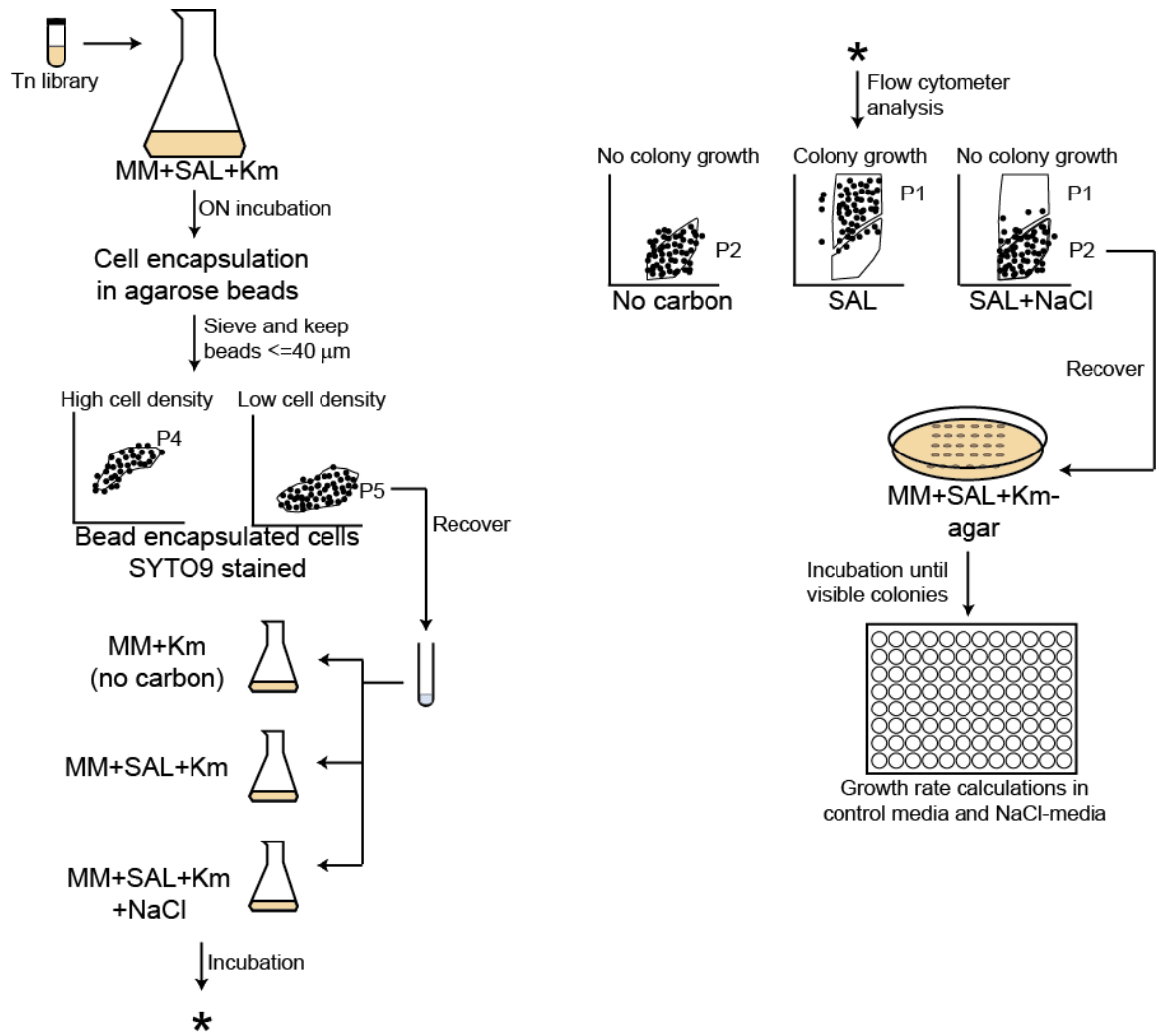


Figure 3. Schematic diagram of the agarose encapsulation-flow cytometry screening procedure followed to detect NaCl sensitive transposon mutants.

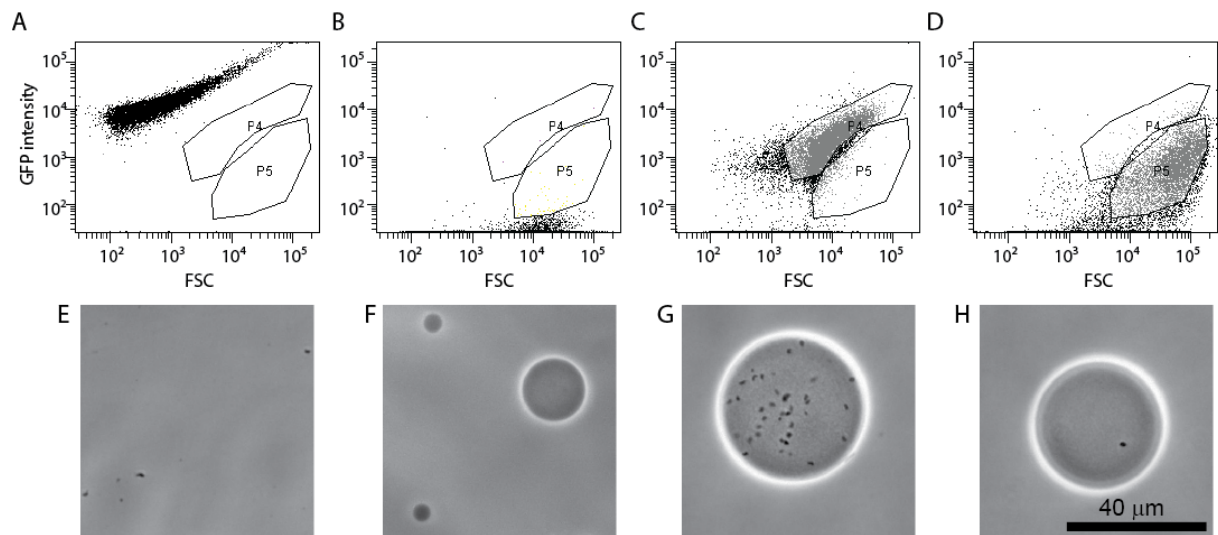


Figure 4. Flow cytometer diagrams and corresponding microscope images of green fluorescence versus forward scatter (FSC) of *S. wittichii* RW1 miniTn5 mutant cells embedded or not in agarose beads and stained with SYTO[®]9. MiniTn5 mutant library as free cells (A, E), empty agarose beads (B, F), agarose beads prepared with a highly concentrated cell culture $OD_{600} \sim 1.4$ (C, G), or with a diluted cell culture $OD_{600} \sim 0.07$ (D, H). P4, gate with beads with high cell density; P5, beads with low cell density.

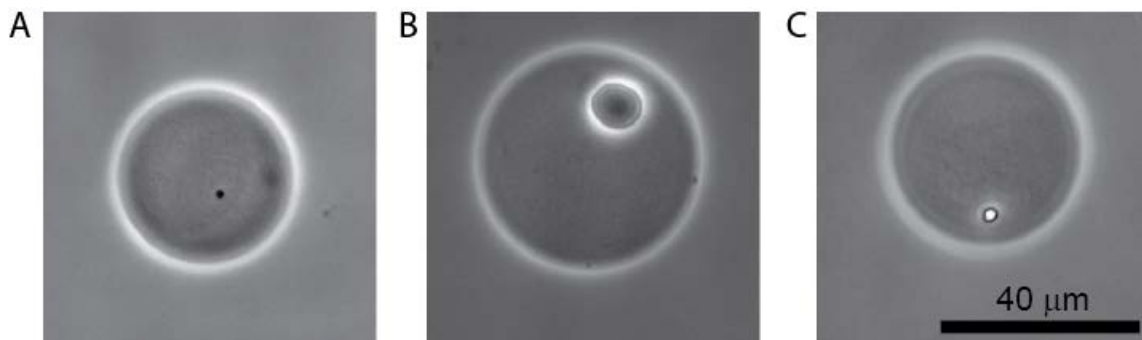


Figure 5. Microcolony growth inside agarose beads exposed to different media. Bead with cells on MM with no carbon added (A), in MM+SAL 0.5 mM (B), or in MM+SAL 0.5 mM supplemented with NaCl. Images show phase-contrast at 400 x magnification.

Around 7200 beads were recovered from P5 gate, which corresponds to the beads containing a low cell density, ideally one or two cells. These beads were further exposed to conditions of no carbon, MM+SAL or MM+SAL supplemented with NaCl.

This FC screening protocol allowed the selection of 400 clones which formed small microcolonies within beads in salt conditions (Figure 5C), comparable to those formed in media without any added carbon (Figure 5A). In contrast, much larger microcolonies formed in regular medium with SAL (Figure 5B). The clones were individually recovered on MM+SAL+Km agar plates. Thirty mutants developed into colonies on plate after sorting, and their growth rate was re-examined in MM+SAL+Km compared to MM+SAL+NaCl+Km. Unfortunately, from the 30 recovered mutants, only one clone displayed repeatedly slower growth under salt conditions (Table 3, clone FACS26). The transposon insertion site was sequenced and this clone carries a mutation in the gene *Swit_5337* (GreA/GreB family elongation factor), which is thought to interact with RNA polymerase for an efficient transcription. The mutant FACS 26 showed a small growth delay in salt liquid medium and the growth rate was lower in both control and salt media, compared to the WT strain in both growth conditions (Table 3). This mutant was thus characterized as a slower grower in salt conditions.

As an alternative to the traditional replica plating screening, which is a rather long and tedious process, and to the agarose beads screening, which gave us a very low recovery (only one clone consistently had a lower growth in salt media), a third screening method was developed by creating a new transposon mutant library using the *miniTn5-egfp* construct. A library of around 22,000 mutants was obtained by conjugation of RW1 and *E. coli* BW20767 (*pRL27::miniTn5-egfp*). In this case, the mutant library was screened for an increased eGFP signal in single cells when exposed to media with decreased SP (-1.5 MPa). The procedure followed is depicted in Figure 6.

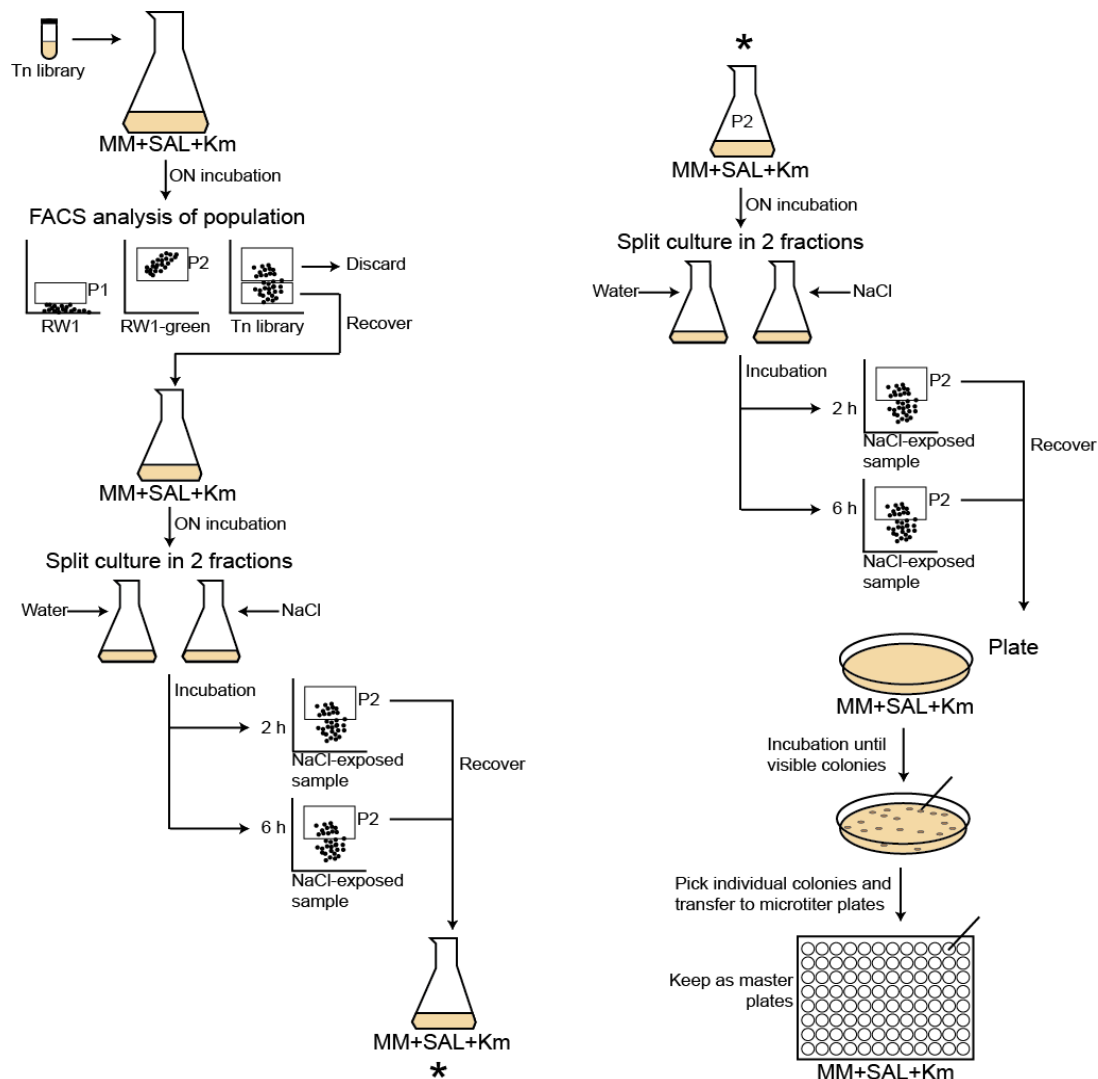


Figure 6. Diagram of the *egfp*-flow cytometry screening of transposon mutants followed to detect genes with a higher expression in the presence of NaCl.

Cells of RW1 WT (Figure 7A) and BW20767 (pRL27::miniTn5-*egfp*) (Figure 7B) were used to define a low fluorescence gate, P1. One particular RW1 (miniTn5-*egfp*) clone showing a constitutive high green fluorescence and retrieved from plate, was used to set the high fluorescence gate, P2 (Figure 7C). The FC dot plot of the RW1 mutant library showed that the library contains both cells with a low and a high fluorescence (Figure 7D). The cells falling into the P2 gate were discarded since we assumed they include mostly constitutively eGFP-producing clones. The cells in the P1 gate were sorted out and used to expose to NaCl.

After two rounds of NaCl exposure and fluorescence assisted sorting of potentially induced cells from P2, some 7000 cells were recovered from P2 and deposited on agar plates for culturing. 768 Colonies were picked and rescreened in 96-well microtiter plate format for growth and fluorescence in the presence of NaCl compared to control growth conditions. A total of 45 mutant strains displayed a culture-density normalized eGFP signal 1.3 to 2 times higher when exposed to NaCl than in control media. After repeated verification, 16 of the 45 clones showed consistent higher normalized eGFP fluorescence when exposed to NaCl compared to the control (Figure 8). In some of clones the signals developed only after 4 h and in others after 8 h of NaCl-exposure. On average, normalized GFP signals in NaCl-induced cultures were between 1.3 to 1.6 times higher than in the control (Table 3).

Regarding their growth rates in salt media, one group of mutants (A1, B1, C3, F3, B12, G1, G8 and F1) showed a higher growth rate than the WT grown in the same NaCl-amended media. A second group of clones (H12, H5, A8 and A9) had a diminished growth rate in salt media when compared to the WT strain. A third set of mutants (D6, H10, C7 and F8) had a growth rate similar to the one observed in WT in salt exposure-conditions.

The miniTn5 insertion sites of 14 of the 16 clones were determined. Clone H12 was not able to regrow and the sequence of clone A8 could never be recovered, despite numerous attempts (Table 3). Ten out of the 14 recovered insertion sites were identical and had occurred within the gene Swit_3298, which codes for a protein from the family of glyoxalase/bleomycin resistance/dioxygenase. Two further clones were identical but had an insertion in the gene Swit_4143. This gene codes for a 5-oxoprolinase, which is involved in proline metabolism, catalyzing the interconversion of L-glutamate to 5-oxo-L-proline. One transposon insertion localized in Swit_0265, which is annotated as a glutamate synthase,

involved in conversion of 2-oxoglutarate and L-glutamine into L-glutamate. The last clone identified carries an insertion in Swit_3912, which is annotated as an iron-sulfur cluster assembly protein.

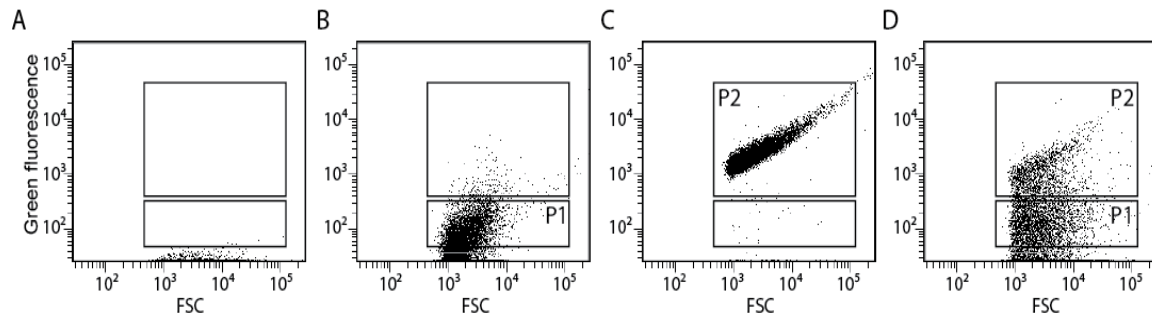


Figure 7. Flow cytometer diagrams of green fluorescence versus forward scatter (FSC) of *S. wittichii* RW1 wild-type cells (A), *E. coli* BW20767 (pRL27-*egfp*) (B), RW1 (miniTn5-*egfp*) with constitutively high eGFP production (C), and the uninduced RW1Tn5-*egfp* library (D). P1 was used as gate for low fluorescence whereas P2 was used to differentiate cells with high green fluorescence.

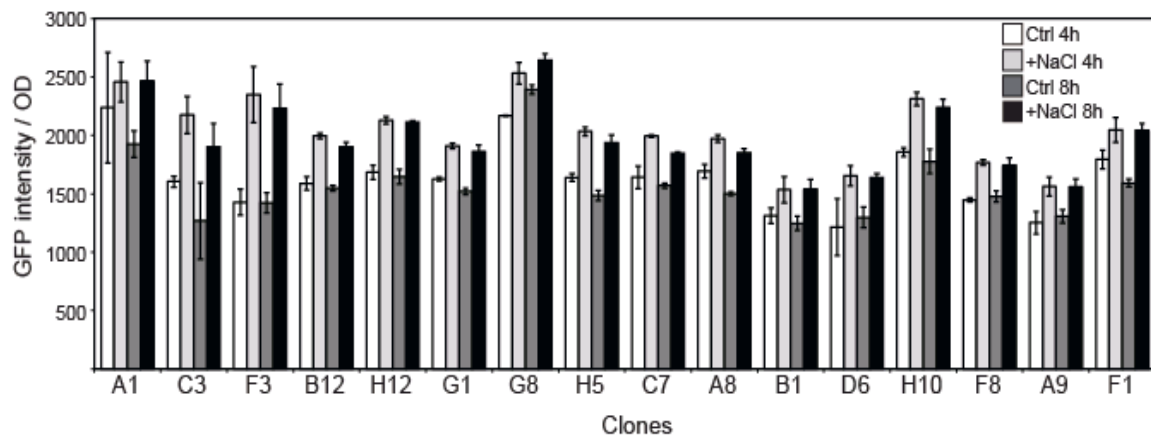


Figure 8. Culture-density normalized eGFP values in selected RW1 mutants, which showed consistent increase in NaCl-amended compared to control conditions. Measurements show values after 4 and 8 h of exposure.

Table 3. Summary of insertion sites, gene names, growth rates (μ , h^{-1}) in control media (Ctrl), NaCl-supplemented media (NaCl) of RW1 WT and miniTn5 mutant strains. The mutants obtained with the miniTn5 were screened by replica plating and agarose bead encapsulation. The mutants obtained with the miniTn5-*egfp* procedure were selected basis of a higher eGFP production after NaCl exposure. A transposon mutant with no observed growth impairment is included (Positive).

Clone	Insertion site	Gene annotation	μ Ctrl (1/h)	μ NaC (1/h)	Ctrl Ratio	NaCl Ratio	Ratio	Ratio	
					μ_{WT}/μ_{Mut}	μ_{WT}/μ_{Mut}	μ_{Ctrl}/μ_{NaCl}	eGFP _{Ctrl} /GFP _{NaCl}	4h
Tn5									
WT avg			0.060±0.01	0.027±0.004	1	1	2.2		
Positive avg			0.043±0.01	0.026±0.004	1.4	1	1.6		
355	Swit_3468	RNA polymerase β subunit	0.044±0.002	0.029±0.001	1.1	0.8	1.5		
6-E3	Intergenic Swit_3114- Swit_3115	Hypothetical protein Ribosomal protein L36, rpmJ	0.021 ± 0.0009	0.011 ± 0.0007	2.6	1.8	1.9		
7-D4	Swit_4693	Protein-disulfide isomerase- like protein	0.053±0.005	0.027±0.001	1.3	1.1	1.9		
3-G2	Swit_2710	Pseudouridine synthase C, RluA family	0.024±0.0003	0.007±0.0008	2.3	2.8	3.3		
1-G3	Swit_2710	Pseudouridine synthase C, RluA family	0.028±0.002	0.011±0.001	2.6	2.4	2.5		
6-G5	Swit_3770	AMP-dependent synthetase and ligase	0.033±0.001	0.017±0.0009	1.5	1.5	2		
5	Intergenic Swit_5333- Swit_5334	Hypothetical protein Cell division FtsK/SpoIIIE	0.035±0.0003	0.024±0.0003	1.4	1	1.4		
10-G5	Intergenic Swit_5333- Swit_5334	Hypothetical protein Cell division FtsK/SpoIIIE	0.064±0.005	0.023±0.0009	1	1.4	2.7		
6-D11	Swit_2958	BadM/Rrf2 family transcriptional regulator	0.057±0.0009	0.026±0.0005	0.9	1	2.2		
FACS26	Swit_5337	GreA/GreB family elongation factor	0.043±0.002	0.015±0.0004	1.4	1.7	2.8		

Tn5-gfp									
A1	Swit_3298	Glyoxalase/bleomycin resistance/dioxygenase	0.047±0.001	0.037±0.004	1.3	0.7	1.2	1.1	1.3
B1	Swit_3298	Glyoxalase/bleomycin resistance/dioxygenase	0.043±0.003	0.034±0.007	1.4	0.8	1.2	1.1	1.2
C3	Swit_3298	Glyoxalase/bleomycin resistance/dioxygenase	0.040±0.009	0.047±0.001	1.5	0.5	1	1.3	1.5
F3	Swit_3298	Glyoxalase/bleomycin resistance/dioxygenase	0.021±0.005	0.043±0.003	2.8	0.6	0.5	1.6	1.6
B12	Swit_3298	Glyoxalase/bleomycin resistance/dioxygenase	0.049±0.006	0.037±0.004	1.2	0.7	1.3	1.2	1.2
H12	ND		0.025±0.006	0.007±0.0008	2.3	3.8	3.6	1.2	1.3
G1	Swit_3298	Glyoxalase/bleomycin resistance/dioxygenase	0.040±0.003	0.032±0.003	1.5	0.8	1.2	1.1	1.2
G8	Swit_4143	Hydantoinase/oxoprolinase domain protein	0.042±0.004	0.039±0.004	1.4	0.6	1	1.1	1.1
H5	Swit_3298	Glyoxalase/bleomycin resistance/dioxygenase	0.047±0.007	0.016±0.0007	1.3	1.7	3	1.2	1.3
D6	Swit_0265	Glutamine amidotransferase	0.041±0.003	0.025±0.002	1.4	1	1.6	1.3	1.2
H10	Swit_4143	Hydantoinase/oxoprolinase domain protein	0.040±0.004	0.027±0.0005	1.4	1	1.4	1.2	1.2
C7	Swit_3298	Glyoxalase/bleomycin resistance/dioxygenase	0.042±0.0004	0.026±0.0003	1.4	1	1.6	1.2	1.1
A8	ND		0.046±0.002	0.022±0.0014	1.3	1.2	2.1	1.1	1.2
F8	Swit_3298	Glyoxalase/bleomycin resistance/dioxygenase	0.044±0.0004	0.025±0.0017	1.3	1	1.7	1.2	1.2
A9	Swit_3298	Glyoxalase/bleomycin resistance/dioxygenase	0.046±0.0002	0.024±0.001	1.3	1.1	1.9	1.2	1.2
F1	Swit_3912	Iron-sulfur cluster assembly accessory protein	0.046±9E-05	0.039±0.002	1.3	0.6	1.1	1.1	1.3

Discussion

Water stress has been considered as a major constraint in the survival of bacteria in the environment. We confirmed that exposing RW1 to media with decreasing solute or matrix potential provoked a decrease in its growth rate compared to control conditions.

One way to obtain a closer understanding of the genes involved in the resistance to water stress is to create a transposon mutant library and to screen for mutants with altered phenotypes. Three strategies were used here: in the first case we tested for reduced growth of mutants on agar plates with decreased water potential in comparison to control plates. In the second case, we screened for small-sized microcolonies embedded in agarose beads grown in NaCl-supplemented media. In the third strategy, we tested for increased expression of *egfp* in cells exposed to medium with lower water potential, with the idea that when the *egfp* transposon inserts in a gene that is higher expressed under lower water potential, it may be detected in the screen. Two types of mutant libraries were thus developed, the first using pRL27::miniTn5 and the second pRL27::miniTn5-*egfp*. With the first type of mutant library, 11 clones were identified that could no longer grow on NaCl-amended agar plates (-1.5 MPa). The insertion sites (Table 3) were localized in genes Swit_2730, Swit_2731 and Swit_3468, Swit_2710 (two clones), Swit_2958, the intergenic region between Swit_3114 and Swit_3115, Swit_3770, Swit_4693 and the intergenic region between Swit_5333 and Swit_5334 (two clones) .

Swit_2730 (coding for a hypothetical protein) is located upstream of Swit_2731 (aconitase-domain containing protein). It has no similarity with other known genes, except for two hypothetical proteins from *Sphingobium chlorophenolicus* L1 and *Sphingobium*

japonicum UT26S. Interestingly, the two hypothetical proteins in the *Sphingobium* species and the one of *S. wittichii* RW1 have similar genes in their vicinity: *folC* (for dihydrofolate synthase), *trpAB* (for tryptophan synthase α and β) and *accD* (for acetyl-CoA carboxylase transferase β), all of which are involved in central metabolism. Johnson *et al.* (2011) found 10-fold lower expression of Swit_2730 in *S. wittichii* RW1 cultures grown on media amended with PEG to mimic matric stress compared to non-stressed medium.

The downstream gene, Swit_2731 (aconitase-domain containing protein) could be involved in the TCA cycle catalyzing the reaction of isomerization of citrate into isocitrate via the intermediate *cis*-aconitate. In other organisms, the aconitase gene has been implicated in multiple functions other than TCA cycle. In *E. coli*, an aconitase gene is activated by the SoxRS oxidative stress regulatory system (Gruer and Guest, 1994; Cunningham *et al.*, 1997) while a second aconitase is activated by the ferric uptake regulator (Gruer and Guest, 1994). In *Caulobacter crescentus*, an aconitase gene product was found to be part of a degradosome (Hardwick *et al.*, 2010). In *Bacillus subtilis*, the CitB aconitase is both an enzyme and an RNA binding protein, and *citB* mutants are defective in sporulation, suggesting that the aconitase acts as an RNA binding regulatory protein (Serio *et al.*, 2006). The interruption of genes Swit_2730 and Swit_2731, putatively involved in the TCA cycle, reduce the ability of RW1 to resist salt induced stress, suggesting that the metabolic activities in which they are involved, contribute to the resistance process.

The third gene, Swit_3468 codes for a RNA polymerase β subunit, with a gene size of 4368 bp. The miniTn5 insertion is located 480 bp before the end of the gene. The RNA polymerase β could thus still be functional, but perhaps with a lower activity than the wild-

type polymerase. An extra stress imposed to the cells by means of NaCl exposure could affect to a higher degree the growth of the mutant clone.

Two mutants carried the transposon in Swit_2710, but with slightly different insertion position of the transposon (~500 bp). Swit_2710 codes for a pseudouridine synthase C that belongs to the four-membered RluA family (RluA, RluC, RluD and TruC). These enzymes are involved in the modification of uridine to pseudouridine (the C₅-glycoside isomer of uridine) in RNA (Hamma and Ferré-D'Amaré, 2006). Interestingly, an *E. coli* mutant with a truncated version of *rluD* could not form pseudouridine and showed poor growth (Gutgsell *et al.*, 2001). The growth deficit was independent of pseudouridine depletion, which suggests that pseudouridine synthase possesses an additional function in growth regulation (Gutgsell *et al.*, 2001). RluA has been found to be induced in conditions of high salinity in *Yersinia pestis* (Han *et al.*, 2005) and Qiao *et al.*, (2013) related the gene pseudouridine synthase to a stress response function. This suggest that pseudouridine synthase has a role in the cells resistance to stress conditions.

One transposon insertion localized in gene Swit_2958. This gene encodes for a BadM/Rrf2 family transcriptional regulator. Interestingly, transposon insertions in Swit_2958 were also underrepresented in the mutant library cultured for 50 generations on salt medium (Roggo *et al.*, submitted). Since this gene encodes a transcriptional regulator, it could perhaps modulate the expression of neighboring genes or of other genes important for water stress response. Directly upstream of Swit_2958 is a gene (Swit_2957) coding for an OsmC family protein. OsmC is induced by elevated osmolarity in *E. coli* and was speculated to have a peroxiredoxin activity working as scavenger for reactive oxygen species (Gutierrez and Devedjian, 1991; Shin *et al.*, 2004). Although Swit_2957 itself was not identified as being

differentially represented in the mutant libraries, another gene for an OsmC family protein (Swit_3232) was indeed underrepresented in the library grown for 50 generations on NaCl medium (Roggo *et al.*, submitted).

One transposon inserted in the intergenic region between Swit_3114 and Swit_3115. Swit_3115 encodes a ribosomal protein L36 that constitutes the large subunit of the ribosome, which was shown as non-essential for protein synthesis or ribosome integrity in *E. coli* (Ikegami *et al.*, 2005). Swit_3114 codes for a hypothetical protein and had already been identified as being 2.4 times up-regulated in a genome-wide transcription analysis of RW1 cells under a short-term perturbation with NaCl (-0.25 MPa) (Johnson *et al.*, 2011). Interestingly, the gene was also up-regulated in *S. wittichii* RW1 cells inoculated in sand for 30 minutes (Silvia Moreno, unpublished data). In addition, mutants in this intergenic region were underrepresented in the mutant library sequences after 50 generations growth on salt medium (Roggo *et al.*, submitted). All these results suggest that Swit_3114 plays a role when the cells have to deal with water stress. In contrast, both Swit_3114 and Swit_3115 were differentially regulated when *S. wittichii* RW1 was growing on dibenzofuran compared to cells growing on phenylalanine (Coronado *et al.*, 2012). This suggests that it is also involved in other types of stress, such as exposition to a toxic compound.

Swit_3770 is annotated as an AMP-dependent synthetase and ligase, but its function is not known. This gene has a similarity to the long-chain acyl CoA-synthetase from *Amycolatopsis mediterranei* (361 bp overlap) by BLAST comparison, thus could be putatively involved in fatty acid biosynthesis.

One mutant contained a transposon in a gene coding for a protein-disulfide isomerase-like protein (Swit_4693). Protein-disulfide isomerases catalyze the structural change of disulfide bonds in proteins and play a role in proper protein folding. Therefore, Swit_4693 may have a role in maintaining folding of damaged proteins in cells exposed to salt stress. The gene was also differentially regulated in RW1 cells exposed during 6 hours to dibenzofuran compared to phenylalanine-grown cells (Coronado *et al.*, 2012).

Two clones were recovered with a transposon inserted in another intergenic region (between the genes Swit_5333 and Swit_5334), but this insertion is unlikely to disrupt a promoter, because the genes are facing inwards. Swit_5333 and Swit_5334 encode, respectively, a hypothetical protein and the cell division protein FtsK/SpoIIE. This last one is a member of the division machinery that participates in the cell fission. A differential expression of an *ftsK* gene was demonstrated in *P. putida* KT2440 after exposure to 0.8 M urea, which was used to create a negative matrix potential (Reva *et al.*, 2006). However, since this gene has a general role in cell division, its function does not seem specific to water stress. Perhaps it is likely that the phenotype of growth delay in liquid cultures supplemented with NaCl is caused by the transposon insertion in an uncharacterized gene within the 680-bp long intergenic region. This intergenic region contains a dozen of predicted ORFs, none of which has significant amino acid similarities with other sequences in the NCBI database.

Using the replica plating procedure around 2600 individual colonies were screened for a growth deficit in NaCl-supplemented plates. Eleven clones showed a lower growth in salt conditions (11 per 2600 screened). One disadvantage of this method is that only clones that can grow on SAL plates will grow, and clones that have lost the ability to use this carbon source or to grow in agar plates will be omitted.

When performing a screening of library 1 by agarose bead encapsulation, exposure to NaCl and sorting by FACS, 400 clones were recovered with an apparent deficit of growth in the presence of NaCl. Of these, only 30 grew to form microcolonies in agar plates. This suggests that either cells cannot escape very well from the agarose beads deposited on the agar surface, or were already damaged in the beads and could not regrow. When re-evaluating the growth of those 30 in control and NaCl-amended liquid cultures, only one clone showed consistent poor growth in salt-conditions. This further indicates that too many false-negative clones were picked up in the FACS procedure. This clone (FACS 26) had a transposon insertion in a gene for a GreA/GreB family elongation factor (Swit_5337), which interacts with RNA polymerase and stimulates the transcription elongation (Opalka *et al.*, 2003). However, not this gene itself but a gene coding for another GreA/GreB family elongation factor (Swit_2490) was under-represented in salt-incubated samples screened by library sequencing (Roggo *et al.*, submitted).

The very low number of interesting mutants identified by FACS screening (1 per 7200 screened) suggests that the sorted beads contained a large number of false negatives, for example clones whose poor growth was just a consequence of the sorting procedure, and not as a result of a decrease in solute potential. However, due to the large number of beads that is possible to screen using FACS (up to 10^3 events/second), it could be worth to optimize the selection procedure. For example, the gates could be set more conservatively or several rounds of regrowing and sorting could be performed.

A second type of library (library 2) was created with the insertion of the miniTn5-*egfp* transposon. A screening protocol using FACS technology allowed the recovery of 768 clones that produced a higher eGFP intensity when exposed to NaCl. After two further rounds of

rescreened NaCl exposure and eGFP measurement 14 mutants were recovered that consistently displayed higher normalized eGFP signals in the presence of NaCl-amended media (14 per 7000 screened). Interestingly, ten clones carried the same insertion in gene Swit_3298, a protein from the broad family named glyoxalase/bleomycin resistance/dioxygenase, suggesting this mutant was abundant in the selected flow cytometry gates. The function of Swit_3298 is not known and the protein family comprises proteins with very broad activities. Swit_3298 has an amino acid similarity of 43% over the whole length to BphC (biphenyl-2,3-diol-1,2-dioxygenase) of several other organisms such as *Rhodococcus* sp. RHA1, *Rhodococcus globerulus* or *Mycobacterium tuberculosis*. On the other hand, the glyoxalase proteins are related to salt stress resistance factors in plants (Sairam and Tyagi, 2004; Lin *et al.*, 2010).

Two transposon insertions were located in Swit_4143 (putative 5-oxoprolinase) and Swit_0265 (putative glutamate synthase). Such enzymes are involved in the synthesis of proline and glutamate, which are known compatible solutes. As a consequence of hyperosmotic shock, the primary response in bacteria is to stimulate the uptake of potassium and synthesize glutamate (Sleator and Hill, 2002). The secondary response is the accumulation of neutral osmoprotectants (compatible solutes), which in contrast to the ionic osmolytes of the primary response, can be accumulated to high intracellular concentration to counteract the outflow of water, without adversely affecting cellular processes (Sleator and Hill, 2002). Compatible solutes can reach high intracellular concentrations without disturbing cellular functions since they are highly soluble molecules and do not carry a net charge at physiological pH. Compatible solutes also serve as stabilizers of proteins and cell components against the denaturing effects of high ionic strength (Kempf and Bremer, 1998; Sleator and Hill, 2002). Molecules such as glycine betaine, trehalose, glycerol,

glucosylglycerol, proline, glutamate, ectoine, carnitine and choline, can be accumulated through synthesis or uptake from the environment following exposure to osmotic stress (Kempf and Bremer, 1998) with different microorganisms having a preference for one or more compatible solutes (Lucht and Bremer, 1994; Ogahara *et al.*, 1995; Brill *et al.*, 2011). In many microorganisms, proline biosynthesis proceeds from the precursor glutamate (Brill *et al.*, 2011; Moses *et al.*, 2012). In *B. subtilis* the accumulation of proline in osmotically stressed cells is followed by a decrease in glutamate level suggesting that *B. subtilis* prefers proline over glutamate as an osmolyte and begins to convert glutamate into proline as soon as is exposed to osmotic stress (Brill *et al.*, 2011). The results of our transposon mutant screening suggest that proline and glutamate are compatible solutes produced by RW1, important for the response of the cell to solute stress.

The last transposon insertion identified is in Swit_3912, which belongs to the super family of iron-sulfur cluster assembly proteins. Proteins containing iron-sulfur clusters participate in a diversity of functions such as electron transport, substrate binding, regulation of gene expression and enzymatic activities (Johnson *et al.*, 2005). It is not clear what the function of gene Swit_3912 is in resistance to salt stress so further characterization of this mutant should be performed.

In this study, three mutant screening methods were used to detect genes putatively involved in the water stress resistance induced by NaCl exposure by *S. wittichii* RW1. The three methods showed different efficiencies of relevant mutant recovery. The classical replica plating screening allowed recovering a higher proportion of mutants from the total of colonies screened. However this method requires to pick several thousands of colonies in order to be exhaustive and long incubation times (up to 7 days for colonies to appear on agar

plates). The screening involving FACS technology had a lower proportion of recovered mutants, however it permitted to screen a higher number of mutants in a shorter time period (up to 10^3 per second), which makes it an interesting technique that needs further optimization. All three screening protocols resulted in a number of clones that can give us an indication of the genes involved in the water stress resistance process. However, several of these genes are either hypothetical genes, or genes with unknown function. The screening techniques can also recover mutants that have a better growth on salt conditions, which may have a survival advantage during bioaugmentation of contaminated soils.

In a recent study (Roggo *et al.*, submitted), ultra high throughput sequencing technology permitted the identification of 357 genes involved in the survival of *S. wittichii* RW1 to similar salt conditions. This is a very promising technique that can further complement the results obtained by mutant isolation, replicate screening and gene identification.

References

- Ahn Y-B, Liu F, Fennell DE and Häggblom MM** (2008) Biostimulation and bioaugmentation to enhance dechlorination of polychlorinated dibenzo-*p*-dioxins in contaminated sediments. *FEMS Microbiology Ecology* 66: 271-281.
- Axtell CA and Beattie GA** (2002) Construction and characterization of a proU-gfp transcriptional fusion that measures water availability in a microbial habitat. *Applied and Environmental Microbiology* 68: 4604-4612.
- Boch J, Kempf B and Bremer E** (1994) Osmoregulation in *Bacillus subtilis*: synthesis of the osmoprotectant glycine betaine from exogenously provided choline. *Journal of Bacteriology* 176: 5364-5371.
- Brill J, Hoffmann T, Bleisteiner M and Bremer E** (2011) Osmotically controlled synthesis of the compatible solute proline is critical for cellular defense of *Bacillus subtilis* against high osmolarity. *Journal of Bacteriology* 193: 5335-5346.
- Brown AD** (1976) Microbial water stress. *Bacteriological Reviews* 40: 803-846.
- Chen J, Wong MH, Wong YS and Tam NFY** (2008) Multi-factors on biodegradation kinetics of polycyclic aromatic hydrocarbons (PAHs) by *Sphingomonas sp.* a bacterial strain isolated from mangrove sediment. *Marine Pollution Bulletin* 57: 695-702.
- Coronado E, Roggo C, Johnson DR and van der Meer JR** (2012) Genome-wide analysis of salicylate and dibenzofuran metabolism in *Sphingomonas wittichii* RW1. *Frontiers in Microbiology* 3.
- Cunningham L, Gruer MJ and Guest JR** (1997) Transcriptional regulation of the aconitase genes (acnA and acnB) of *Escherichia coli*. *Microbiology* 143: 3795-3805.
- Cytryn EJ, Sangurdekar DP, Streeter JG, Franck WL, Chang W-S, Stacey G, Emerich DW, Joshi T, Xu D and Sadowsky MJ** (2007) Transcriptional and physiological responses of *Bradyrhizobium japonicum* to desiccation-induced stress. *Journal of Bacteriology* 189: 6751-6762.
- Das P, Mukherjee S and Sen R** (2008) Improved bioavailability and biodegradation of a model polyaromatic hydrocarbon by a biosurfactant producing bacterium of marine origin. *Chemosphere* 72: 1229-1234.
- de Lorenzo V, Herrero M, Jakubzik U and Timmis KN** (1990) Mini-Tn5 transposon derivatives for insertion mutagenesis, promoter probing, and chromosomal insertion of cloned DNA in gram-negative eubacteria. *Journal of Bacteriology* 172: 6568-6572.
- Gruer MJ and Guest JR** (1994) Two genetically-distinct and differentially-regulated aconitases (AcnA and AcnB) in *Escherichia coli*. *Microbiology* 140: 2531-2541.

- Gülez G, Dechesne A, Workman CT and Smets BF** (2012) Transcriptome dynamics of *Pseudomonas putida* KT2440 under water stress. *Applied and Environmental Microbiology* 78: 676-683.
- Gutgsell NS, Del Campo M, Raychaudhuri S and Ofengand J** (2001) A second function for pseudouridine synthases: A point mutant of RluD unable to form pseudouridines 1911, 1915, and 1917 in *Escherichia coli* 23S ribosomal RNA restores normal growth to an RluD-minus strain. *RNA* 7: 990-998.
- Gutierrez C and Devedjian JC** (1991) Osmotic induction of gene *osmC* expression in *Escherichia coli* K12. *Journal of Molecular Biology* 220: 959-973.
- Hallsworth J, Heim S and Timmis KN** (2003) Chaotropic solutes cause water stress in *Pseudomonas putida*. *Environmental Microbiology* 5: 1270-1280.
- Halverson LJ and Firestone MK** (2000) Differential effects of permeating and nonpermeating solutes on the fatty acid composition of *Pseudomonas putida*. *Applied and Environmental Microbiology* 66: 2414-2421.
- Hamma T and Ferré-D'Amaré AR** (2006) Pseudouridine Synthases. *Chemistry and biology* 13: 1125-1135.
- Han Y, Zhou D, Pang X, Zhang L, Song Y, Tong Z, Bao J, Dai E, Wang J, Guo Z, Zhai J, Du Z, Wang X, Wang J, Huang P and Yang R** (2005). Comparative transcriptome analysis of *Yersinia pestis* in response to hyperosmotic and high-salinity stress. *Research in Microbiology* 156, 403-415.
- Hardwick SW, Chan VSY, Broadhurst RW and Luisi BF** (2010) An RNA degradosome assembly in *Caulobacter crescentus*. *Nucleic Acids Research* 39: 1449-1459.
- Herrero M, de Lorenzo V and Timmis KN** (1990) Transposon vectors containing non-antibiotic resistance selection markers for cloning and stable chromosomal insertion of foreign genes in gram-negative bacteria. *Journal of Bacteriology* 172: 6557-6567.
- Holden PA, Halverson LJ and Firestone MK** (1997) Water stress effects on toluene biodegradation by *Pseudomonas putida*. *Biodegradation* 8: 143-151.
- Ikegami A, Nishiyama K-I, Matsuyama S-I and Tokuda H** (2005) Disruption of *rpmJ* encoding ribosomal protein L36 decreases the expression of *secY* upstream of the *spc* Operon and inhibits protein translocation in *Escherichia coli*. *Bioscience, Biotechnology, and Biochemistry* 69: 1595-1602.
- Johnson DC, Dean DR, Smith AD and Johnson MK** (2005) Structure, function, and formation of biological iron-sulfur clusters. *Annual Review of Biochemistry* 74: 247-281.
- Johnson D, Coronado E, Moreno-Forero S, Heipieper H and van der Meer J** (2011) Transcriptome and membrane fatty acid analyses reveal different strategies for responding to permeating and non-permeating solutes in the bacterium *Sphingomonas wittichii*. *BMC Microbiology* 11: 250.

- Kempf B and Bremer E** (1998) Uptake and synthesis of compatible solutes as microbial stress responses to high-osmolality environments. *Archives of Microbiology* 170: 319-330.
- Kumar M, Wu P-C, Tsai J-C and Lin J-G** (2009) Biodegradation of soil-applied polycyclic aromatic hydrocarbons by sulfate-reducing bacterial consortium. *Journal of Environmental Science and Health, Part A* 44: 12 - 20.
- Larsen R, Wilson M, Guss A and Metcalf W** (2002) Genetic analysis of pigment biosynthesis in *Xanthobacter autotrophicus* Py2 using a new, highly efficient transposon mutagenesis system that is functional in a wide variety of bacteria. *Archives of Microbiology* 178: 193-201.
- Leahy JG and Colwell RR** (1990) Microbial degradation of hydrocarbons in the environment. *Microbiological Reviews* 54: 305-315.
- LeBlanc JC, Gonçalves ER and Mohn WW** (2008) Global response to desiccation stress in the soil actinomycete *Rhodococcus jostii* RHA1. *Applied and Environmental Microbiology* 74: 2627-2636.
- Lin F, Xu J, Shi J, Li H and Li B** (2010) Molecular cloning and characterization of a novel glyoxalase I gene *TaGly I* in wheat (*Triticum aestivum* L.). *Molecular Biology Reports* 37: 729-735.
- Lucht JM and Bremer E** (1994) Adaptation of *Escherichia coli* to high osmolarity environments: Osmoregulation of the high-affinity glycine betaine transport system ProU. *FEMS Microbiology Reviews* 14: 3-20.
- Martínez-García E, Calles B., Arévalo-Rodríguez M. and de Lorenzo V** (2011) pBAM1: an all-synthetic genetic tool for analysis and construction of complex bacterial phenotypes. *BMC Microbiology* 11: 38.
- Metcalf WW, Jiang W, Daniels LL, Kim S-K, Haldimann A and Wanner BL** (1996) Conditionally replicative and conjugative plasmids carrying lacZ for cloning, mutagenesis, and allele replacement in bacteria. *Plasmid* 35: 1-13.
- Miller WG, Leveau JHJ and Lindow SE** (2000) Improved gfp and inaZ broad-host-range promoter-probe vectors. *Molecular Plant-Microbe Interactions* 13: 1243-1250.
- Moses S, Sinner T, Zapras A, Stoveken N, Hoffmann T, Belitsky BR, Sonenshein AL and Bremer E** (2012) Proline utilization by *Bacillus subtilis*: uptake and catabolism. *Journal of Bacteriology* 194: 745-758.
- Mutnuri S, Vasudevan N, Kastner M and Heipieper H** (2005) Changes in fatty acid composition of *Chromohalobacter israelensis* with varying salt concentrations. *Current Microbiology* 50: 151-154.
- Ogahara T, Ohno M, Takayama M, Igarashi K and Kobayashi H** (1995) Accumulation of glutamate by osmotically stressed *Escherichia coli* is dependent on pH. *Journal of Bacteriology* 177: 5987-5990.

- Opalka N, Chlenov M, Chacon P, Rice WJ, Wriggers W and Darst SA** (2003) Structure and function of the transcription elongation factor GreB bound to bacterial RNA Polymerase. *Cell* 114: 335-345.
- Potts M** (1994) Desiccation tolerance of prokaryotes. *Microbiology and Molecular Biology Reviews* 58: 755-805.
- Qiao J, Shao M, Chen L, Wang J, Wu G, Tian X, Liu J, Huang S and Zhang W** (2013). Systematic characterization of hypothetical proteins in *Synechocystis sp.* PCC 6803 reveals proteins functionally relevant to stress responses. *Gene* 512, 6-15.
- Rehmann L, Prpich GP and Daugulis AJ** (2008) Remediation of PAH contaminated soils: Application of a solid-liquid two-phase partitioning bioreactor. *Chemosphere* 73: 798-804.
- Reva ON, Weinel C, Weinel M, Bohm K, Stjepandic D, Hoheisel JD and Tummeler B** (2006) Functional genomics of stress response in *Pseudomonas putida* KT2440. *Journal of Bacteriology* 188: 4079-4092.
- Sairam RK and Tyagi A** (2004) Physiology and molecular biology of salinity stress tolerance in plants. *Current Science* 86: 407-421
- Serio AW, Pechter KB and Sonenshein AL** (2006) *Bacillus subtilis* aconitase is required for efficient late-sporulation gene expression. *Journal of Bacteriology* 188: 6396-6405.
- Shi T, Fredrickson JK and Balkwill DL** (2001) Biodegradation of polycyclic aromatic hydrocarbons by *Sphingomonas* strains isolated from the terrestrial subsurface. *Journal of Industrial Microbiology and Biotechnology* 26: 283-289.
- Shin DH, Choi I-G, Busso D, Jancarik J, Yokota H, Kim R and Kim S-H** (2004) Structure of OsmC from *Escherichia coli*: a salt-shock-induced protein. *Acta Crystallographica Section D* 60: 903-911.
- Singh J, Kumar D, Ramakrishnan N, Singhal V, Jervis J, Garst JF, Slaughter SM, DeSantis AM, Potts M and Helm RF** (2005) Transcriptional response of *Saccharomyces cerevisiae* to desiccation and rehydration. *Applied and Environmental Microbiology* 71: 8752-8763.
- Sleator RD and Hill C** (2002) Bacterial osmoadaptation: the role of osmolytes in bacterial stress and virulence. *FEMS Microbiology Reviews* 26: 49-71.
- Tillett D and Neilan BA** (2000) Xanthogenate nucleic acid isolation from cultured and environmental cyanobacteria. *Journal of Phycology* 36: 251-258.
- Vogel TM** (1996) Bioaugmentation as a soil bioremediation approach. *Current Opinion in Biotechnology* 7: 311-316.

Wittich RM, Wilkes H, Sinnwell V, Francke W and Fortnagel P (1992) Metabolism of dibenzo-*p*-dioxin by *Sphingomonas sp.* strain RW1. Applied and Environmental Microbiology 58: 1005-1010.

CHAPTER 6

General discussion

Genetic manipulation of *S. wittichii* RW1

In the present study several techniques were tried for the introduction of recombinant DNA into RW1 cells, such as plasmid delivery, mini transposon delivery, homologous recombination and transposon mutagenesis. The plasmid delivery system proved to be the most stable in this strain, even though part of the population lost the plasmids when the strain is grown without an antibiotic pressure. When attempting to transform RW1 cells, very low transformation efficiencies were observed and amounts around 1 µg of DNA had to be used in order to obtain enough transformants. The transformation efficiency improved up to 45 times when the DNA was of RW1-origin. This suggests that the restriction/modification system of strain RW1 has an influence on the low efficiencies observed. Furthermore, when introducing miniTn5-based constructs in strain RW1, rearrangements of the constructs were observed, which is consistent with observations by Basta *et al.* (2004). Quite interestingly, RW1 took up and integrated linear DNA fragments, which may be a process that can be exploited in the future. However, genome resequencing will have to be used in order to understand where this DNA is integrating and how this process could be further harvested to make recombinant constructs or gene knockouts in RW1.

Environmental bacterial isolates are more difficult to manipulate with the available molecular biology tools, in comparison to the strains commonly used in laboratory. In this

cases, techniques such as Ultra High Throughput Sequencing (Roggo *et al.*, submitted), which are culture independent, seem a more practical alternative to screen for gene functions needed for a certain condition, for example.

***S.wittichii* RW1 transposon mutant screening**

To identify genes implicated in water stress resistance by strain RW1, a mutant library was created and screened on the basis of growth impairment in NaCl-supplemented media or by the increased production of eGFP fluorescence in response to NaCl exposure. The three methods used to select relevant mutants showed different recovery efficiencies. While the classical replica plating showed a recovery of 11 mutants out of 2600 screened, the FACS-based mutant analysis had a recovery of 1 per 7200 screened for the bead encapsulated-mutants and 14 per 7000 screened for the eGFP production-based selection. Even though with the replica plating the recovery ratio seems higher, the FACS-based screening allows the analysis of a higher number of mutants in a shorter time (around 10^3 mutants per second). All three screening protocols allowed us to recover a number of clones that can give us an indication of the genes involved in the water stress resistance process. The transposon insertions directed us to gene functions related to compatible solute synthesis (glutamate and proline) and to cell membrane modification. Other gene functions, such as transcriptional regulators, RNA polymerase β subunit, a cell division protein or an aconitase, were also found with the mutant screening, but can less easily be interpreted as to their function in salt stress resistance.

Nowadays with the great advances in sequencing technology and the drop of sequencing costs, techniques such as ultra high throughput sequencing seem a more feasible

screening option. This very promising technique eliminates the need of culturing the mutants, measuring the growth impairment and the gene identification. In a recent study (Roggo *et al.*, submitted), ultra high throughput sequencing technology permitted the identification of 357 genes involved in the survival of *S. wittichii* RW1 to similar salt conditions.

Degradation and monitoring of DBF by RW1-based bioreporters

As part of the major objectives of this work, the global response of *S. wittichii* to exposure to DBF was studied. Two different techniques were used here, a genome-wide gene expression microarray analysis and genome-wide transposon screening. We designed three different types of exposure of cells to DBF: in the first, named short exposure in batch, RW1 was grown on phenylalanine (PHE) until reaching exponential phase, when cells were harvested and resuspended in the same medium with PHE or with DBF. The second type of exposure, named transient exposure in chemostat, consisted of RW1 cells grown continuously under carbon limiting conditions with PHE, while a new carbon source (DBF) was instantaneously added. In the third induction, long exposure in batch, RW1 cells were grown in batch either on PHE, SAL or on DBF as sole carbon source, and cells were harvested in exponential phase.

This extensive analysis allowed us to identify the response of RW1 to a short exposure to DBF, which includes the repression of genes for central metabolic pathways, such as the TCA cycle, amino acid metabolism, ribosomal proteins, elongation factors, tRNA-synthetases and cell division proteins. This suggests that the cells experienced a condition of starvation and stress response. In the transient exposure in chemostat, RW1 cells perceived DBF not just as a new carbon substrate but rather as a stress factor, requiring the

regulation of specific stress-response genes. Genes for catalases, peroxiredoxins and glutathione-s-transferases, genes implicated in DNA repair, chaperones and OmpA-domain containing proteins, the RpoD sigma factor and of alternative ECF sigma 24 factors had an increased expression. It was only in the long exposure in batch that RW1 cells seem to metabolize DBF since an induction of DBF degrading genes was observed. An interesting finding is that several catabolic pathways for DBF degradation were active at the same time, suggesting important genetic redundancy in the RW1 genome. This was further verified with the transposon mutant sequencing which showed that actually only a few transposon insertions completely abolished growth on DBF.

In order to detect and monitor DBF in the environment, bacterial bioreporters were constructed targeting three genes involved in DBF degradation, selected based on the transcriptome data. The first consisted in an upstream region of *dxnA1*, which codes for part of the dibenzofuran dioxygenase (P_{dxnA1}), the second in a region upstream of the cluster Swit_4925-4921, which encodes the downstream part of a *meta*-cleavage pathway (P_{4925}), and the third in a region upstream of the genes Swit_5102-5101, with Swit_5102 putatively coding for the enzyme gentisate dioxygenase that transforms gentisate to 3-maleyl pyruvate (P_{5102}). The construct carrying the promoter P_{dxnA1} showed a detectable eGFP signal, but its intensity was independent on the carbon source used. In contrast, the construct with the P_{5102} had almost no eGFP production regardless of DBF addition. However, a construct carrying the promoter region in a miniTn5, showed an eGFP induction in the presence of salicylate, but failed to grow with DBF as carbon source (Chapter 3, clone P5102-1). This could indicate that the plasmid based construct carrying the region P5102 could have suffered a genetic rearrangement or modification. This would have to be verified in the future. The construct

carrying the P₄₉₂₅ region showed a good *egfp* induction in the presence of DBF both in liquid cultures and in soil microcosms, what makes it an attractive tool for DBF monitoring.

The inoculation of RW1 bioreporters in soil microcosms containing polluted material or pristine sand provided further direct evidence for the hypothesis formulated by other authors (Harms and Bosma, 1997; Bosma *et al.*, 1996; Wammer and Peters, 2005) that the bioavailability of the carbon sources is a major constraint in the bioremediation process. Even if RW1 could survive and grow in the soil supplemented with DBF, the bacterium could not grow in PAH contaminated material from an ancient gas factory, nor induced the DBF bioreporter. Thus, when attempting to bioaugment aged contaminated sites, it would be worth to use the bioreporter tests to examine under which conditions bioavailability of the compounds present can be ameliorated.

References

- Basta T, Keck A, Klein J and Stolz A** (2004) detection and characterization of conjugative degradative plasmids in xenobiotic-degrading *Sphingomonas* Strains. *Journal of Bacteriology*. 186: 3862-3872.
- Bosma TNP, Middeldorp PJM, Schraa G and Zehnder AJB** (1996) Mass transfer limitation of biotransformation: quantifying bioavailability. *Environmental Science and Technology* 31: 248-252.
- Harms H and Bosma TNP** (1997) Mass transfer limitation of microbial growth and pollutant degradation. *Journal of Industrial Microbiology and Biotechnology* 18: 97-105.
- Wammer KH and Peters CA** (2005) Polycyclic Aromatic Hydrocarbon biodegradation rates: a structure-based study. *Environmental Science and Technology* 39: 2571-2578.

CURRICULUM VITAE

Edith Aimée Coronado Martinez

Born in Sinaloa, Mexico, June 19th 1978

Nationality: Mexican

- 1996-2001** Bachelor Studies
Biochemistry Engineering
Universidad Autonoma de Sinaloa, México
- 2001-2004** Master Studies in Biotechnology
Thesis: “Participation of Alginate in the Agregation of *Azotobacter vinelandii* in liquid culture”
Institute of Biotechnology-Department of Bioengineering
National Autonomous University of México (UNAM)
Director: Dr. Carlos Pena
- 2004-2007** Teacher of Chemistry, Biology and Physics
Secondary School Level, Sinaloa, México
- 2007-2012** PhD student, Department of Fundamental Microbiology
Faculty of Biology and Medicine, University of Lausanne
Director: Prof. Jan Roelof van der Meer

LIST OF PUBLICATIONS

Coronado, E. Roggo, C., Johnson DR and van der Meer, JR (2012) Genome-Wide Analysis of Salicylate and Dibenzofuran Metabolism in *Sphingomonas wittichii* RW1. *Frontiers in Microbiology*. 3.

Johnson, D., Coronado, E., Moreno-Forero, S., Herman J Heipeiper and van der Meer, J (2011) Transcriptome and membrane fatty acid analyses reveal different strategies for responding to permeating and non-permeating solutes in the bacterium *Sphingomonas wittichii*. *BMC Microbiology* 11(1):250.

Tafese FT, Breugelmans P, Lavigne R, Coronado E, Johnson, D, van der Meer JR, Mayer A, Heipeiper H, Hofkens J and Springael D (2012) Exposure to solute stress affects genome-wide expression but not the PAH-degrading activity of *Sphingomonas sp.* LH128 in biofilms. *Applied and Environmental Microbiology*. 78: 8311-8320

Roggo C, Coronado E, Moreno S, Harshman K, Weber J and and van der Meer, JR (2013) Genome-Wide transposon insertion scanning of environmental survival functions in the polycyclic aromatic hydrocarbon degrading bacterium *Sphingomonas wittichii* RW1. Submitted



UNIL | Université de Lausanne

Unicentre

CH-1015 Lausanne

<http://serval.unil.ch>

personal use within the meaning of LDA (art. 19, para. 1 letter a). Failure to do so will expose offenders to the sanctions laid down by this law. We accept no liability in this respect.